MSC.Nastran Version 70

Advanced Dynamic Analysis
User's Guide

C O N T E N T S

MSC.Nastran Advanced Dynamic Analysis User's Guide

3

System Matrix Formulations

4

Boundary Conditions and Coupling to Other Disciplines

5

Dynamic Solution Techniques

6

Data Recovery

A

Theory of Eigenvalue Extraction Methods

B

SSSALTER Library For MSC.Nastran

C
Set Notations

D
Selected Bibliography

INDEX

Preface

- About this Book

- List of MSC.Nastran Books

- Technical Support

- Internet Resources

- Permission to Copy and Distribute MSC Documentation

About this Book

The *MSC.Nastran Advanced Dynamic Analysis User's Guide* extends many of the topics covered in the *MSC.Nastran Basic Dynamic Analysis User's Guide* and serves as a starting point for other dynamics-related topics. Basically, it is a compendium of new material as well as material from many sources, including internal reports and other existing MSC documentation. The purpose of this guide is to aid the experienced dynamics user in modeling and solving general problems in dynamics using MSC.Nastran. Of particular interest are the topics dealing with non-structural interactions such as control systems or fluids. Other useful topics cover model checkout procedures and dynamics data recovery options.

Notes to the Reader

This book is not intended to be a stand-alone document. Because this guide has very little overlap with the *MSC.Nastran Basic Dynamic Analysis User's Guide* or the *MSC.Nastran Quick Reference Guide,* it does not cover basic MSC.Nastran dynamics input data and usage. You are encouraged to keep these other texts handy when using this document.

Given the wide range of subject matter, it was difficult to organize the flow of this guide into a meaningful sequence. As a compromise, the chosen sequence of topics roughly adheres to the typical sequence of tasks performed by an engineer who builds a model and performs an analysis. These five tasks are as follows:

1. Building the model.
2. Reducing the matrices.
3. Applying boundary conditions.
4. Solving for results.
5. Data recovery and postprocessing.

The contents in each chapter corresponding to these steps can be summarized as follows:

Modeling. The modeling chapter covers special modeling inputs used only by the dynamics solutions. Discussions of the various mass and damping options are followed by instructions on the use of direct input matrices, transfer functions, and nonlinear loads. A section on model debugging describes the special checks often employed by dynamics specialists.

Matrices. The matrix formulation chapter focuses on matrix reduction methods and modeling special effects with matrices. Here the type of analysis determines the matrix reduction options. The formulations of cyclic symmetry and aeroelastic matrices are also included. Unfortunately, the topics of superelements and modal synthesis were not available for this edition. For information on Version 68 and earlier, the reader is referred to the *MSC.Nastran Superelement User's Guide.* Version 70 contains many changes and will require a new user guide.

Boundary Conditions. The chapter on boundary conditions describes methods of enforcing known boundary motions as well as coupled boundaries between structural and fluid models. Unlike static analysis, enforced motions in dynamics are not processed directly, but must be input indirectly through the dynamic loads. The other sections in this chapter describe the three major methods of modeling fluids and their interfaces.

Dynamic Solutions. The chapter on dynamic solutions focuses on the advanced dynamic options for the numerical computations. Options such as complex eigenvalues, nonlinear transient response, and Fourier transformations are additions to the solutions described in the *MSC.Nastran Basic Dynamic Analysis User's Guide*. Aeroelastic solutions and dynamic design optimization are related topics that require special solutions.

Data Recovery. The final chapter deals with dynamic data recovery and postprocessing options. Several methods are available for recovering modal responses. Spectrum and random analysis are tools which provide additional information on the expected structural response.

Acknowledgements

I wish to express my appreciation to all of the MSC staff and others who contributed to this book. New material was contributed by Michael Gockel, William Rodden, and David Bella.   Adapted material from other sources was provided by Erwin Johnson, Ted Rose, Dean Bellinger, and Ken Blakely. Wendy Webb worked closely with me to refine the content and prepare the book for publication. My hearty thanks to all.

David N. Herting

List of MSC.Nastran Books

Below is a list of some of the MSC.Nastran documents. You may order any of these documents from the MSC.Software BooksMart site at www.engineering-e.com.

Installation and Release Guides

❏ Installation and Operations Guide

❏ Release Guide

Reference Books

❏ Quick Reference Guide

❏ DMAP Programmer's Guide

❏ Reference Manual

User's Guides

❏ Getting Started

❏ Linear Static Analysis

❏ Basic Dynamic Analysis

❏ Advanced Dynamic Analysis

❏ Design Sensitivity and Optimization

❏ Thermal Analysis

❏ Numerical Methods

❏ Aeroelastic Analysis

❏ User Modifiable

❏ Toolkit

Technical Support

For help with installing or using an MSC.Software product, contact your local technical support services. Our technical support provides the following services:

- Resolution of installation problems
- Advice on specific analysis capabilities
- Advice on modeling techniques
- Resolution of specific analysis problems (e.g., fatal messages)
- Verification of code error.

If you have concerns about an analysis, we suggest that you contact us at an early stage.

You can reach technical support services on the web, by telephone, or e-mail:

Web Go to the MSC Mechanical Solutions website at **www.mechsolutions.com**, and click on **Support**. Here, you can find a wide variety of support resources including application examples, technical application notes, available training courses, and documentation updates at the MSC.Software Training, Technical Support, and Documentation web page.

Phone and Fax

United States
MSC.Patran Support
Telephone: (800) 732-7284
Fax: (714) 784-4343

MSC.Nastran Support
Telephone: (800) 732-7284

Munich, Germany
Telephone: (49) (89) 43 19 87 0
Fax: (49) (89) 43 61 71 6

Rome, Italy
Telephone: (390) (6) 5 91 64 50
Fax: (390) (6) 5 91 25 05

Moscow, Russia
Telephone: (7) (095) 236 6177
Fax: (7) (095) 236 9762

**Frimley, Camberley
Surrey, United Kingdom**
Telephone: (44) (1276) 67 10 00
Fax: (44) (1276) 69 11 11

Tokyo, Japan
Telephone: (81) (3) 3505 02 66
Fax: (81) (3) 3505 09 14

Paris, France
Telephone: (33) (1) 69 36 69 36
Fax: (33) (1) 69 36 45 17

Gouda, The Netherlands
Telephone: (31) (18) 2543700
Fax: (31) (18) 2543707

Madrid, Spain
Telephone: (34) (91) 5560919
Fax: (34) (91) 5567280

Email Send a detailed description of the problem to the email address below that corresponds to the product you are using. You should receive an acknowledgement that your message was received, followed by an email from one of our Technical Support Engineers.

MSC.Patran Support	mscpatran.support@mscsoftware.com
MSC.Nastran Support	mscnastran.support@mscsoftware.com
MSC.Nastran for Windows Support	mn4w.support@mscsoftware.com
MSC.Dytran Support	mscdytran.support@mscsoftware.com
MSC.Mvision Support	mscmvision.support@mscsoftware.com
MSC.Fatigue Support	mscfatigue.support@mscsoftware.com
MSC.SuperForge Support	mscsuperforge.support@mscsoftware.com
MSC Institute Course Information	msctraining.support@mscsoftware.com

Training

The MSC Institute of Technology provides basic and specialized training in the use of MSC's MCAE software products, as well as in general analysis subjects, such as thermal analysis, finite element modeling, and fatigue-life prediction. We offer the world's largest selection of engineering analysis and design training courses, comprising more than 50 different courses. More than 5,000 engineers attend classes offered by the MSC Institute annually.

The MSC Institute of Technology is located at:

> 2 MacArthur Place
> Santa Ana, CA 92707
> Phone: (800) 732-7211
> Fax: (714) 784-4028

The Institute maintains state-of-the-art classroom facilities and individual computer graphics laboratories at training centers throughout the US. All of our courses emphasize hands-on computer laboratory work to facilitate skills development.

Courses can be taught on-site, and can even be customized to meet your business' specific needs. We also offer video courses, interactive multimedia training, and a specialized instructor's program.

Course Information and Registration. For detailed course descriptions, schedule information, and registration call the Training Specialist at (800) 732-7211 or visit www.mscsoftware.com.

Internet Resources

MSC.Software (www.mscsoftware.com)

MSC.Software corporate site with information on the latest events, products and services for the CAD/CAE/CAM marketplace.

Simulation Center (simulate.engineering-e.com)

Simulate Online. The Simulation Center provides all your simulation, FEA, and other engineering tools over the Internet.

Engineering-e.com (www.engineering-e.com)

Engineering-e.com is the first virtual marketplace where clients can find engineering expertise, and engineers can find the goods and services they need to do their job

MSC.Linux (www.mscsoftware.com/hpc)

Now with almost 40-years of unparalleled experience in scientific and technical computing, MSC.Software is leveraging this knowledge to deliver its customers state-of-the-art, high performance computing solutions based on clustered computing for running engineering and life sciences applications.

CATIASOURCE (plm.mscsoftware.com)

Your SOURCE for Total Product Lifecycle Management Solutions.

Process Architecture Lab (PAL) (pal.mscsoftware.com/services/pal)

PAL is a virtual product development environment that enables PAL participants and customers to define, validate, and demonstrate advanced tools, processes, and e-business solutions.

Permission to Copy and Distribute MSC Documentation

If you wish to make copies of this documentation for distribution to co-workers, complete this form and send it to MSC.Software Corporation. MSC will grant written permission if the following conditions are met:

- All copyright notices must be included on all copies.
- Copies may be made only for fellow employees.
- No copies of this manual, or excerpts thereof, will be given to anyone who is not an employee of the requesting company.

Please complete and mail to MSC for approval:

MSC.Software Corporation
Attention: Legal Department
2 MacArthur Place
Santa Ana, CA 92707

Name: _____

Title: _____

Company: _____

Address:_____

_____

Telephone:_____Email: _____

Signature:_____ Date: _____

Please do not write below this line.

APPROVED: MSC.Software Corporation

Name: _____

Title: _____

Signature:_____ Date: _____

Fold here

_____

_____

_____

Place
Stamp
Here

MSC.Software Corporation

Attention: Legal Department

2 MacArthur Place

Santa Ana, CA 92707

Fold here

Introduction

- Overview
- Purpose of this Guide
- Range of Readers
- Summary

1.1 Overview

MSC support personnel are frequently asked whether MSC.Nastran will solve a particular unusual problem. The standard answer is "of course we can solve this problem." However, they add that the correct question is, "How much time and effort can you afford to spend on the analysis?" They are usually guided by their conception of MSC.Nastran as a toolkit, with the ability to be molded by the user into a custom system to solve a special class of structural problems. The limitations of dynamic analysis in MSC.Nastran are governed more by the conveniences of the code than by its capabilities.

From its original designs, MSC.Nastran has provided a comprehensive set of capabilities for structural dynamics analysis. Although the designers were skilled in the methods used by the aerospace industry, the capabilities have been applicable to many other problems, such as earthquakes, automobiles, nuclear power plants, and many consumer products. Because of these broad capabilities in the product, it has been difficult to document an instruction document that explains how to use the system.

1.2   Purpose of this Guide

The purpose of this document is to guide the user into the recommended procedures for solving the difficult problems with structural dynamics. Its predecessor is the *MSC.Nastran Basic Dynamic Analysis User's Guide,* which is recommended for instructions on the typical dynamics problems and use of the basic input data. This follow-on document covers many aspects that would not accomodate the scope of the basic guide as well as new topics related to other MSC.Nastran capabilities (such as aeroelasticity, optimization, or random analysis). The basic principles also apply to related applications such as cyclic symmetry.

1.3 Range of Readers

The target audience for this document covers a range of engineers bounded by two skill levels. On one side we have the knowledgeable MSC.Nastran user who is familiar with MSC.Nastran and the use of basic dynamics, but needs to learn more about the other available dynamic techniques, including some of the advanced theory. On the other side we have the dynamics specialist who is familiar with the advanced methods, or has experience with other FE codes, but needs some instructions in the input formats and the procedures. Many readers may only be interested in a few specialized topics and will only be interested in a few chapters.

Most of the intended readers fit somewhere between these extremes. Because this guide covers many disjoint topics, it is not intended to be casual reading material. This manual does not overlap the *MSC.Nastran Basic Dynamic Analysis User's Guide* and is not intended for beginners in both MSC.Nastran and dynamics solutions.

This guide covers all of the dynamics capabilities not covered completely in the *MSC.Nastran Basic Dynamic Analysis User's Guide*. This includes advanced structural dynamics topics such as random analysis as well as related nonstructural dynamics subjects such as transfer functions and acoustics. The treatment of each topic depends on the availability of other available documentation.

Topics such as aeroelasticity or nonlinear analysis are well-documented in separate user's guides, and their dynamics interfaces will only be introduced here. On the other hand, this guide will be the sole source for topics such as hydroelasticity, which will be covered in detail. Equations are included only when required to clarify an explanation; this guide will not be a substitute for a theoretical manual. The goal is to provide sufficient detail for a basic understanding of the use of each topic.

1.4   Summary

The chapters of this guide are divided into three groups: modeling practices, solution options, and data recovery processes. The appendices contain reference material such as eigenvalue theories, alter libraries, and set descriptions.

"**Dynamic Modeling Options**" on page 7, "**System Matrix Formulations**" on page 61, and "**Boundary Conditions and Coupling to Other Disciplines**" on page 85 cover the processes of building the matrices that represent the physical problems. The topics include the finite elements, the special dynamic modeling options, and the available matrix operations. Of special interest are the fluid boundary options such as acoustics.

"**Dynamic Solution Techniques**" on page 139 covers the methods of solving a set of dynamics matrices. These include complex eigenvalues, transient analysis, frequency response, and other variations such as aeroelastic flutter. Also included is a brief discussion of design optimization in dynamics.

"**Data Recovery**" on page 213 covers the special aspects of data recovery in dynamics analysis. Special topics include random vibrations and response spectrum analyses.

Dynamic Modeling Options

- ■ Overview

- ■ Mass Modeling

- ■ Modeling Damping Effects

- ■ DMIGs, Extra Points, and Transfer Functions

- ■ Nonlinear Load Functions (NOLINi)

- ■ Debugging Dynamic Models

2.1   Overview

In general, the practice of building MSC.Nastran models for dynamic analysis is similar to building statics or normal modes models. However, in dynamics the higher costs of running detailed large order models usually results in a different approach. For instance, a frequency response analysis using SOL 108 may require solutions at more than 100 frequencies. Each frequency will require an unsymmetric matrix solution using complex variables, which will cost four to ten times more than a single static solution. If memory is sufficient, the total result is a running time larger by a factor of 400 to 1000. If the required memory (four times more is needed) is insufficient, the solution will spill, and even longer run times will result. In addition, the database and scratch file space requirements will be much larger and the size of the output data becomes unwieldy. The result is that many users who simply take fine mesh static models directly into a dynamic analysis find this process is very costly and may give up completely.

Strategies for Dynamic Analysis. The two major approaches to avoid the problems described above are to use the *matrix reduction* methods available in MSC.Nastran or to simply build another *dynamic model* with fewer points and elements. The matrix reduction methods use sophisticated approximations to reduce the cost of the dynamic solutions. However, they add complexity to the system and may also cost processing time overhead. Instead of making decisions about the element mesh size, the user must consider the frequency band and loading characteristics of the actual structure.

Although building a separate dynamic model will require extra work, it has several advantages. The requirements for precise stress results for statics are usually not as important for dynamics, thereby allowing the use of larger elements. The requirements for accurate dynamic results are not as dependent on small elements since loads tend to be distributed over wider areas by the inertial and damping effects. The actual accuracy criteria for dynamic models is related to wavelength size relative to the mesh size. Also, in a smaller dynamic model the job of interpreting outputs with plotters and other methods becomes much easier.

It should also be noted that the process of changing finite element meshes is becoming easier with modern geometry-based modeling systems and automated mesh generation.

Plan the Analysis. The following steps are recommended before starting a dynamic analysis:

1. Estimate the frequency range of the structure. The first mode frequency can usually be estimated by a simple equivalent beam calculation. A normal modes analysis is highly recommended for dynamics regardless of the approach.

2. Consider the type and frequency content of the loads. Localized high frequency sources such as brake squeal require different approaches from low frequency distributed loads such as wind forces on a bridge.

3. Use expected wavelengths to estimate required mesh size. A wavelength can be estimated from the frequency and sound speed. Six elements per wave for approximately 10% accuracy is a general rule-of-thumb. Also, this method may be used to evaluate the quality of the calculated eigenvectors.

4. Always use SETs for output requests as a general practice. The use of Case Control requests such as STRESS = ALL for a large transient analysis could possibly exceed the size limits of your postprocessor.

5. Estimate the computer resources (CPU time, database size, output requirements) for large problems before production runs are made. A good method is to run the model with only a few time steps or frequencies, and examine the major time and size messages in the F04 output file. The actual costs can then be extrapolated with reasonable accuracy.

The basic modeling, constraints, and loading functions for dynamics are described in the *MSC.Nastran Basic Dynamic Analysis User's Guide*. The following sections discuss some of the more difficult and obscure topics.

2.2 Mass Modeling

Basic Definitions of Mass. The mass matrix in MSC.Nastran may contain much more information than simple structural mass and inertia terms. In fact, it may contain control system terms, fluid compressibility, or electromagnetic capacitance. One basic definition is that any term which contributes to the generalized kinetic energy must create a coefficient in the mass matrix. Another definition is that any generalized force, F, proportional to an acceleration term $\ddot{u}$ produces a mass term M, i.e.,

$$\{F\} = [M]\{\ddot{u}\} \qquad \text{Eq. 2-1}$$

where each component of the acceleration vector $\{\ddot{u}\}$ represents a generalized degree-of-freedom.

The mass matrix is required for nearly all dynamic solution sequences. It is also used for generating gravity and centrifugal loads for static solutions. Inertia relief solutions require the mass matrix to balance the unbalanced forces on a free body. All solutions may calculate the total mass and center of gravity (CG) information for printout.

Note that mass is not required for heat transfer dynamics.

Mass Data Input Options

MSC.Nastran provides the following means to specify the mass properties of the finite element model:

1. The density (mass per unit volume) of the structural materials, which comprises the finite element (RHO on the MATi Bulk Data entries).

2. Nonstructural mass per unit length of line elements or mass per unit area of surface elements (NSM on the property Bulk Data entry). Examples of this feature are coatings and thermal insulating materials.

3. Concentrated mass and inertia terms at a grid point via a CONM2 Bulk Data entry. The provisions of the CONM2 entry are the mass, the offset of the center of mass from the grid point, and the moments and products of inertia about the center of mass. As an option, the center of mass may be measured from the origin of the basic coordinate system rather than as an offset from the grid point.

4. A full 6×6 symmetric matrix of mass coefficients at a grid point via the CONM1 Bulk Data entry.

5. Mass coupling between any two degrees-of-freedom via the CMASSi (i = 1,2,3,4) Bulk Data entries. The form of the relationship is

$$\begin{Bmatrix} f_1 \\ f_2 \end{Bmatrix} = -\begin{bmatrix} M & -M \\ -M & M \end{bmatrix} \begin{Bmatrix} \ddot{u}_1 \\ \ddot{u}_2 \end{Bmatrix} \qquad \text{Eq. 2-2}$$

where f_1 and f_2 are the inertia forces acting at degrees-of-freedom 1 and 2, respectively, and M is the mass coefficient, specified on the CMASSi entry (or on the PMASS entry if i = 2 or 4). In most applications, the second degree-of-freedom is not specified. In this case, the entry generates the inertia force $f_1 = -M\ddot{u}_1$, and M is added to the mass matrix in the diagonal position corresponding to u_1. An important application of the CMASSi entry occurs in the recommended method for specifying enforced motion at grid points (see "**Enforced Motion with Loads**" on page 87).

6. Transfer functions defined on the TF Bulk Data entry may contribute terms to the mass matrix.

7. Direct Matrix inputs may be added to the mass matrix via DMIG Bulk Data and M2GG = or M2PP = Case Control commands.

Three Related Parameters. The bulk data input also includes three parameters which relate to the specification of mass properties. They are:

1. PARAM,WTMASS,V1 – Specifies a factor by which to multiply the mass of the structure to obtain dimensionally correct mass. For example, if the ft-lb-sec system is used, and the mass input unit is pounds, then V1 = 1/32.174 = .031081. This factor operates on all mass terms (except those defined on DMIG entries; PARAM,CM2,V1 may be used for these instead).

2. PARAM,COUPMASS,1 – Requests that the coupled mass option be used rather than the lumped mass option for all elements which support the coupled mass option. In the lumped mass option, the distributed mass of an element is simply divided up and the parts are located at the connected grid points. In the coupled mass option, the distributed mass is replaced by a nondiagonal mass matrix which couples the connected grid points. The latter method is sometimes more accurate, but it uses more computer time. See the *MSC.Nastran Reference Manual* for descriptions of the elements.

3. PARAM,GRDPNT,V1 – Causes the Grid Point Weight Generator to be executed. The value of the parameter, V1, is an integer which identifies a grid point at which the rigid body mass properties of the structure will be computed. See the *Getting Started with MSC.Nastran User's Guide* for an example of the output format which is provided. This capability can be used as a check on mass and geometric input data.

Coupled Mass Matrix Terms

A common difficulty for finite element beginners is to comprehend the generation of off-diagonal or coupled terms in the mass matrix. These are caused by the following actions.

1. With PARAM,COUPMASS, the finite elements themselves generate coupled terms to represent the distributed element mass more accurately than simple lumped masses on the grid points. The total kinetic energy of the element is represented by shape functions, which in turn, are coupled functions of displacement and rotation.

2. The internal matrix operations in the solution sequences produce coupled mass terms. MPCs and RBE-type elements cause the mass to be redistributed from the dependent degrees-of-freedom to the remaining independent points. The ASET, OMIT, and Superelement reduction operations may automatically fill the entire mass matrix. These operations will maintain exact total mass and CG properties and provide a good approximation to the inertia effects of the eliminated points, but they can be costly.

3. Direct user inputs such as CMASSi scalar elements and CONMi mass elements may produce off-diagonal mass terms. Other inputs that cause coupling are direct matrix inputs (DMIG), and transfer functions (TF).

An example of a coupled scalar mass is illustrated in the example below:
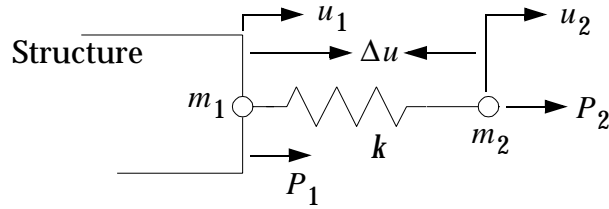
A spring, k, and two masses, m_1 and m_2, are attached to a structural model. However, when modeling fluids or other special connections, the user may wish to use the difference in displacements, $\Delta u = u_1 - u_2$, instead of u_2 as the primary degree-of-freedom.

We may find the equivalent coupled mass matrix by the use of energy methods. The potential energy, V, and the kinetic energy, T, for this part of the system are:

$$V = k\Delta u^2 / 2$$

$$T = m_1 \ddot{u}_1^2 + m_2(\ddot{u}_1 - \Delta \ddot{u})^2 \qquad \text{Eq. 2-3}$$

From basic energy principles, the resulting equilibrium equations are

$$\ldots + m_1 \ddot{u}_1 + m_2(\ddot{u}_1 - \Delta \ddot{u}) = P_1 + P_2 \qquad \text{Eq. 2-4}$$

and

$$k\Delta u - m_2(\ddot{u}_1 - \Delta \ddot{u}) = -P_2$$

The mass matrix for the two degrees-of-freedom becomes

$$[m] = \begin{bmatrix} m_1 + m_2 & -m_2 \\ -m_2 & m_2 \end{bmatrix}$$

Eq. 2-5

where $\lfloor u \rfloor = \lfloor u_1, \Delta u \rfloor$ are the active degrees-of-freedom. Two CMASSi elements may be used; one will be coupled to two points. Note that the spring, k, is now connected to Δu only.

An alternate method would be to use the MPC constraints to produce the same effect. Simply include all three DOFs in the model and use conventional lumped masses and a connected spring. Choose $u_2 - u_1 + \Delta u = 0$ as the MPC equation, and the reduced mass and stiffness matrices will be identical to the system above.

Mass Effects in Moving Coordinate Systems

In most cases the motions of the grid points in MSC.Nastran are measured in a set of fixed coordinate systems. Even large displacement nonlinear analysis uses displacements measured in fixed directions. However, there are several cases in which it is more convenient to use a moving coordinate system. Examples follow:

Spinning Bodies

If the entire structure is spinning at a constant angular velocity, both static centrifugal forces and coupled dynamic inertial terms may be needed. An example is a high speed turbine wheel that exhibits gyroscopic stability problems.

For dynamic analysis of rotating bodies, a special solution will be provided in the DMAP alter library for the generation of extra matrix terms caused by the rotating coordinates. For a body rotation defined by the angular velocity vector, $\vec{\Omega}$, and for a location vector of a point, $\vec{r}$, the absolute velocity vector of the point, $\vec{V}$, in fixed coordinates is

$$\vec{V} = \vec{\Omega} \times (\vec{r} + \vec{u}) + \dot{\vec{u}}$$

Eq. 2-6

The acceleration vector is

$$\ddot{\vec{r}} = \vec{\Omega} \times \left(\vec{\Omega} \times \vec{r} \right) + \vec{\Omega} \times \left(\vec{\Omega} \times \vec{u} \right) + 2 \left(\vec{\Omega} \times \dot{\vec{u}} \right) + \ddot{\vec{u}}$$

Eq. 2-7

The first term on the right-hand side of **Eq. 2-7** is the static centrifugal force; the second term is the centripetal stiffness; the third term is the Coriolis force; the last term, $\ddot{\vec{u}}$, is the relative acceleration vector.

Another term that is calculated for spinning bodies is the so-called differential stiffness matrix. It is proportional to the steady centrifugal preloads in the elements. These are the terms that would stiffen a string if a weight on the string were swung in a circular motion. These terms are important because they are approximately the same magnitude as the Coriolis and centripetal stiffness terms defined in **Eq. 2-7**. (Centrifugal stiffness and differential stiffness terms are of the same magnitude.)

The basic matrix equation for the forces in the moving system is

$$[M]\{A\} + [B]\{V\} + [K]\{u\} = \{P\} \qquad \text{Eq. 2-8}$$

The special MSC.Nastran process assembles the terms in **Eq. 2-7** into matrices, that when substituted into **Eq. 2-8**, result in

$$[M]\{\ddot{u}\} + [B + B^c]\{\dot{u}\} + [K + K^c + K^d]\{u\} = \{P(t)\} \qquad \text{Eq. 2-9}$$

where:

$[B^c]$ = generates the velocity-dependent Coriolis forces. Note that B^c is not symmetric!

$[K^c]$ = the centripetal stiffness matrix

$[K^d]$ = the differential stiffness matrix

The system defined by **Eq. 2-9** may be solved with a transient analysis, a frequency response, or a complex eigenvalue calculation. The complex eigenvalues may be obtained for a series of spin rates to determine the critical angular speeds. At each angular velocity the complex roots are obtained in the form $p_n = \sigma_n \pm i\omega_n$. Unstable conditions usually occur when $\omega_n \sim P\Omega$, where P is a positive integer. By definition, the system is unstable if σ_n is a positive number.

Inertia Relief

If a free body is accelerating due to constant unbalanced loads, the inertia relief solution provides the ability to obtain static deflections relative to a set of reference points attached to the moving coordinate system. An example is an airplane in a steady turn or accelerating dive. Although this capability is a static solution, it is obtained from the dynamics theory.

The basic matrix equation for the inertia relief method is

$$[K]\{u\} = \{P\} - [M]\{a_o\} \qquad \text{Eq. 2-10}$$

where $\{u\}$ are displacements relative to the moving system and $\{a_o\}$ are the steady accelerations to be determined from the mass and loads. If $[D]$ is a matrix whose columns define the rigid body motions of the structure, then for a free body,

$$[D]^T[K]\{u\} = \{0\} = [D]^T\{P\} - [D]^T[M]\{a_o\} \qquad \text{Eq. 2-11}$$

where $[D]$ is called the rigid body tranformation matrix. However, since the full-sized vector, $\{a_o\}$, is a rigid body motion, it may be defined in terms of accelerations at a set of reference coordinates, $\{a_r\}$, by the equation

$$\{a_o\} = [D]\{a_r\} \qquad \text{Eq. 2-12}$$

Combining **Eq. 2-12** into **Eq. 2-11** and eliminating $\{a_r\}$, we obtain

$$\{a_o\} \ = \ [D][m]^{-1}[D]^T\{P\} \qquad\qquad \text{Eq. 2-13}$$

where the total mass matrix for the reference coordinates is

$$[m] \ = \ [D]^T[M]\{D\} \qquad\qquad \text{Eq. 2-14}$$

The resulting set of equations defined in **Eq. 2-10** may now be arbitrarily constrained since the total load is balanced by the inertia forces.

Two different methods are used in MSC.Nastran to calculate the rigid body matrix $[D]$. In SOL 24 the SUPORT Bulk Data entry define the reference degrees-of-freedom. Any number of u_r degrees-of-freedom that provide a nonredundant set of supports may be used. This option allows partially free bodies and extra mechanisms. In SOLs 61 and 101 the grid point geometry is used (PARAM,GRDPNT) to define six rigid body displacement vectors. In these cases, only six free motions are allowed.

Base Excitations

One of several methods to solve problems with enforced motion is to constrain the point of motion and solve the problem in the accelerating system. This method is related to inertia relief but uses entirely different inputs. It is easy to use for earthquake analysis of buildings, in which the base is accelerating uniformly.

If a structure is attached to a semi-rigid base that causes a known stress-free motion, $\{u_0\}$, the total structural motion, $\{u_A\}$, is

$$\{u_A\} \ = \ \{u_0\} + \{u_g\} \qquad\qquad \text{Eq. 2-15}$$

where $\{u_g\}$ are displacements relative to the base motion. If the structure is not constrained elsewhere, we may assume that the $\{u_0\}$ base displacements produce no force and

$$[M]\{\ddot{u}_g + \ddot{u}_0\} + [K]\{u_g\} \ = \ \{P_g\} \qquad\qquad \text{Eq. 2-16}$$

If we move the known base motion $\{\ddot{u}_0\}$ to the right hand side it looks almost identical to a gravity load:

$$[M]\{\ddot{u}_g\} + [K]\{u_g\} \ = \ \{P_g\} - [M]\{\ddot{u}_0(t)\} \qquad\qquad \text{Eq. 2-17}$$

Acceleration Method. If the acceleration is uniform over the structure, a time-dependent gravity load has exactly the same form as the last term of **Eq. 2-17**, and the GRAV input load data may be used.

An example data input for a dynamic acceleration load is shown below. For more details on these input formats, see the "**MSC.Nastran Basic Dynamic Analysis User's Guide**" on page iii.

Case Control	
LOADSET = 20	$ Requests LSEQ Id. 20 Process
DLOAD = 200	$ Requests Dynamic Load #200
Bulk Data	
GRAV, 386, , 386.4, -1.0	$ Defines Gravity Load in -x direction
LSEQ, 20, 201, 386	$ Assembles GRAV load vector $ Added to DAREA Id. 201
TLOAD1, 200, 201, etc.	$ Dynamic Load using DAREA Id. 201

The net result is that the time-dependent inertia loads are applied to all points on the structure in the –x direction in proportion to the time-dependent function specified on the TLOADi or RLOADi Bulk Data entry. The base points should be constrained and the displacements will be calculated relative to the moving base. However, note that the accelerations output from the solution will also be relative to the base motion and should be corrected before being compared with accelerometer data.

A simpler alternative to base motion is the large mass approach, described in "**Enforced Motion with Loads**" on page 87.

2.3   Modeling Damping Effects

The physical causes of damping in dynamic analysis are any processes which dissipate energy or reduce the structural response through internal friction. Furthermore, the internal velocities or displacements cause reactive damping forces which are irreversible and nonconservative. Examples are mechanical devices such as shock absorbers, the internal hysteresis that occurs in materials such as rubber, friction in joints, and other nonlinear effects such as plastic strains in metals.

The four types of damping in MSC.Nastran are viscous, structural, modal, and nonlinear. The basic input formats and applications for the damping coefficients in MSC.Nastran are explained in "**Mass Input**" on page 17 of the *MSC.Nastran Basic Dynamic Analysis User's Guide*. The following discussions are directed to advanced applications and the special problems of damping.

Viscous Damping

The primary method for modeling viscous damping is through the CVISC and CDAMPi Bulk Data entries. These produce forces which are linearly proportional to the velocities of the connected grid points. Another source of viscous damping is structural damping that must be converted to viscous damping in the transient response solutions. The *MSC.Nastran Basic Dynamic Analysis User's Guide* covers this topic. Some additional details are included below.

Structural Damping

Structural damping is intended to simulate the effects of linear material energy loss proportional to the strains. In other words, this method approximates effects similar to hysteresis. It is specified in the material definition input, MATi, and on the parameter, G. Note that in the frequency response and complex eigenvalue solutions, the structural damping produces imaginary numbers in the complex stiffness matrix. In the transient solutions, the matrix terms are converted to equivalent viscous damping; i.e., the forces will be proportional to the derivative of strain with respect to time.

The physical basis for the phenomenon of imaginary stiffness is explained by **Figure 2-1**. Shown is the force due to a stiffness matrix term, K, plotted against the displacement of the point. As the displacements cycle sinusoidally, the imaginary stiffness, G, causes a phase lag in the force response resulting in an elliptical path. The area enclosed by the curve is equal to the dissipated energy.
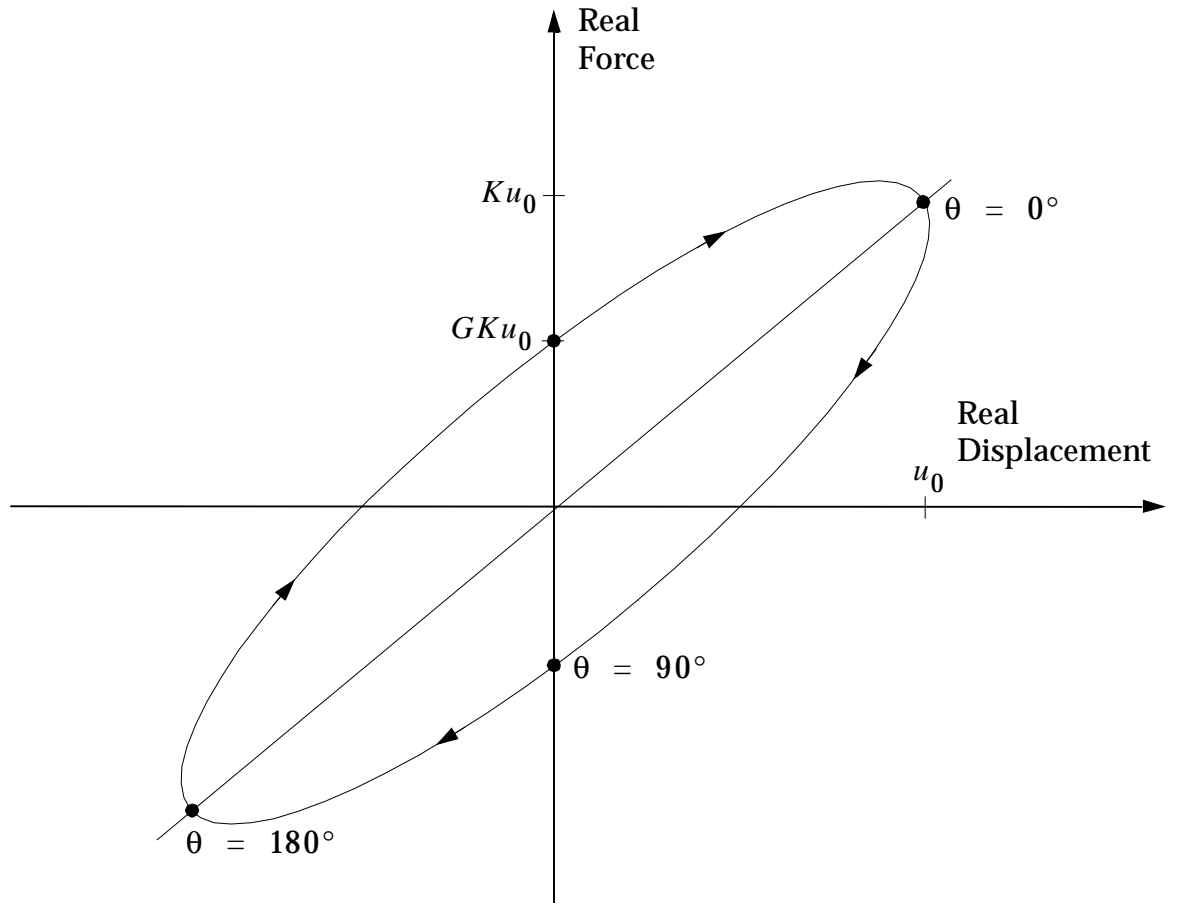
Figure 2-1 Equivalent Hysteresis Path for Imaginary Stiffness Damping

The basic definition for the steady-state actual displacements, in terms of the complex displacements is

$$u_r(t) = Re(u_0(\omega)e^{i\omega t}) \qquad \text{Eq. 2-18}$$

where u_r is the actual real displacement, u_0 is normally a complex variable that we will set to a real number, ω is the steady state frequency, and $e^{ix} = \cos(x) + i\sin(x)$. If a structural damping coefficient, G, is added to the stiffness matrix, the resulting complex forces are in the following form:

$$F(\omega) = (1 + iG)Ku_0e^{i\omega t} \qquad \text{Eq. 2-19}$$

The real part of the forces are

$$F_r = Re(F) = Ku_0(\cos\omega t - G\sin\omega t) \qquad \text{Eq. 2-20}$$

The incremental work done over a period of time is

$$dW = F_r du_r \qquad \text{Eq. 2-21}$$

where, from **Eq. 2-18**

$$du_r = -(u_0\sin\omega t)\omega dt \qquad \text{Eq. 2-22}$$

Combining **Eq. 2-20** through **Eq. 2-22** and integrating over a full cycle, results in the work

$$= \int_{0}^{2\pi/\omega} -Ku_0^2 \sin \omega t (\cos \omega t - G \sin \omega t) \omega dt \qquad \text{Eq. 2-23}$$

Evaluating the integral, we obtain work loss per cycle

$$W = \pi G K u_0^2 \qquad \text{Eq. 2-24}$$

Note that the elastic energy terms average zero over the interval, but the energy dissipated by the structural damping exists. The area inside the curve in **Figure 2-1** is equivalent to the damping energy loss, w.

This damping method is a reasonable linear approximation to the classical hysteresis effect. It may also be used to approximate other similar cyclic energy losses such as the effects of loose joints and fasteners. (Hint: construct a similar trajectory curve and estimate the area.)

The main disadvantage of structural damping is that complex numbers must be converted to real numbers in transient analysis; i.e., structural damping is converted to linear viscous damping. This is good only when the response is dominated by a single known frequency.

Modal Damping

For the modal solution formulations, a special damping input is provided in addition to the other damping terms described above. It is used primarily for efficiency and when test results or contract specifications provide damping factors. These terms are applied only to the uncoupled modal equations. When coupling effects are absent, the method avoids expensive matrix calculations.

A second reason for using modal damping is that modal testing may provide accurate damping inputs on a mode-by-mode basis. These damping factors may be converted to a frequency-dependent table, TABDMP. If the MSC.Nastran normal mode frequencies are close and the damping factors are small. The third reason—when damping factors are specified by a third party—is frequently meant to keep the analyst more conservative. By restricting the solutions to artificially low damping, this will force the staff to solve their design problems for the worst case.

Modal damping is available only for the modal solutions method. The matrix terms generated for modal analysis, and added to any direct matrix inputs, are

$$m_i \ddot{\xi}_i + b_i \dot{\xi}_i + k_i \xi_i = P_i \qquad \text{Eq. 2-25}$$

In this equation, ξ_i is the generalized coordinate of the i-th mode.

In accordance with modal definitions, the modal viscous damping coefficient b_i may be expressed as

$$b_i = g_i \omega_i m_i \qquad \text{Eq. 2-26}$$

where ω_i is the undamped vibration frequency (equal to $\sqrt{k_i/m_i}$), expressed in radians per unit time. The dimensionless input coefficient, g_i, is equal to twice the critical damping ratio of the mode. It is evaluated by linear interpolation of a user-specified function of frequency, $g(f)$.

The physical meaning of modal damping is somewhat clouded. Its effect is viscous damping, but it is proportional to the stiffness matrix, and varies with modal frequency. The damping effects are distributed to the structure depending on the energy distribution in each mode shape.

Another aspect of modal damping to remember is that the damping coefficient, b, is constant for each mode. If the mode is forcibly excited at a different frequency the initial damping factor still applies. In other words, the damping at any particular frequency is a function of several modal damping factors. This may cause unexpected results for frequencies where a mode is not dominant.

The user specifies pairs of values f, g on a TABDMP1 Bulk Data entry, which is selected by the SDAMPING Case Control command. There are also provisions for expressing damping as a fraction of critical damping (C/C_c) or amplification quality factor (Q). If accurate test results are available, the user can specify different damping coefficients, obtained from modal tests, for the different frequency ranges. The user can ensure that the desired damping has been obtained for a set of modes whose frequencies are known from a previous run by providing the desired f, g pairs on the TABDMP1 entry.

The complete damping matrix for modal transient analysis, $[B]$, is

$$[B] \ = \ [b_i] + [\phi]^T [B^v][\phi] \qquad \qquad \text{Eq. 2-27}$$

where $[b_i]$ is a diagonal matrix whose elements are given by **Eq. 2-26**, $[\phi]$ is the matrix of eigenvectors, and $[B^v]$ is the matrix of nonmodal damping terms. Note that the damping effects which enter $[B^v]$ may well be duplicated by the effects included in $[b_i]$ so that, in general, the user should be careful when using both forms simultaneously.

Note: In frequency response and complex eigenvalue analysis, the complete damping matrix is similar, except that structural damping is treated as a complex stiffness matrix.

Also, the matrix $[\phi]^T[B^v][\phi]$ in **Eq. 2-27**, or the equivalent complex stiffness matrix, is generally coupled so that the efficient uncoupled methods of analysis cannot be used when $[B^v]$ is present.

It is the accepted practice in many industries to express viscous damping as a fraction of critical damping. Critical damping is defined as the value at which the homogenous solution of **Eq. 2-25** transitions from a damped sinusoid to a nonoscillating, decaying exponential. A solution for the modal equation shows the value of critical damping, C_c, to be

$$C_c \ = \ 2 \sqrt{k_i m_i} \qquad \qquad \text{Eq. 2-28}$$

The fraction of critical damping, ζ_i, is calculated from the equation

$$\zeta_i \equiv \frac{b_i}{C_c} = \frac{b_i}{2\sqrt{k_i m_i}}$$

Eq. 2-29

Another form of damping specification is the amplification quality factor, Q_i, with the definition

$$Q_i = \frac{1}{2\zeta_i} = \frac{1}{g_i}$$

Eq. 2-30

All three forms of damping specification are available for modal damping.

An illustration of the comparison between modal damping and an equivalent function of structural damping is shown in **Figure 2-2**, showing the different options for modal damping tables. With unit modal masses, a constant modal damping table actually corresponds to a viscous damping that increases with modal frequency. This method falls between the two extremes (constant viscous damping and equivalent structural damping) and serves as a general purpose compromise.
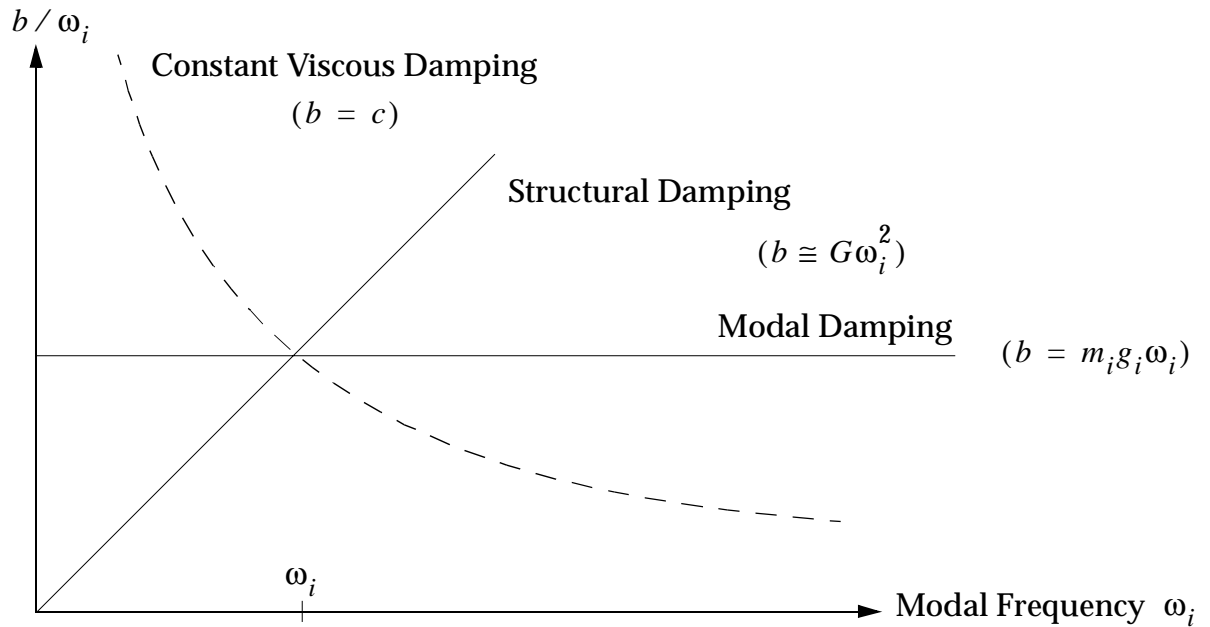
Figure 2-2 Damping Coefficients Versus Modal Frequency

Nonlinear Damping

This discussion explains the limitations in damping caused by the nonlinear transient solution algorithms (SOL 129). Frequency response and complex eigenvalue solutions are not available in nonlinear analysis. For specialized nonlinear dynamics topics, see "**Nonlinear Transient Response Analysis**" on page 161. For basic information on the MSC.Nastran nonlinear solutions, see the *MSC.Nastran Handbook for Nonlinear Analysis* or the *MSC.Nastran Reference Manual*.

Finite elements may be either linear or nonlinear in the nonlinear formulations, and the damping effects will be treated differently for each type. The basic rules for nonlinear transient analysis are as follows:

1. Plastic yield in the nonlinear materials automatically absorbs energy when the structure follows a loading and unloading cycle. This is an actual hysteresis effect that produces an accurate form of damping. However, note that strain rate effects are not calculated directly. Strain rate effects must be modeled with structural damping parameters, which are converted internally to viscous damping.

2. Viscous damping elements are always linear and will participate as constant matrix terms.

3. Structural damping, defined with parameters and material bulk data inputs (the GE field on the MATi entries), is recognized for both linear and nonlinear elements. The damping matrix terms are calculated for the current material stiffness moduli and geometry. Note, however, that the tangent matrices are only updated periodically. The actual damping on nonlinear elements is unpredictable and can change answers for different runs on the same problem—depending on the convergence rate and iteration strategy. It is recommended that the matrix update strategy forces an update on the tangent matrix at every time step.

4. A modal formulation (and therefore modal damping) is not available in a nonlinear solution.

5. Superelements may be used to reduce the size of a nonlinear problem by separating the linear elements into an upstream component. Component modal synthesis may then be used to maintain accuracy. Structural damping is allowed on superelements.

2.4   DMIGs, Extra Points, and Transfer Functions

In dynamics modeling, we frequently need to include special nonfinite element effects such as mechanical devices, servomechanisms, smart structures, and matrices from external structures. These effects can usually be included as extra terms in the system matrices along with extra degrees-of-freedom in the generalized displacement vectors.

The major difference between extra points (EPOINT data) and normal scalar points (SPOINT data) is that the extra points are added to the system after the finite element matrix assembly and real eigenvalue solution. Therefore, structural elements, constraints, and static loads may not be connected to EPOINTs. Also, as with scalar points, they are processed only in the residual superelement in SE formulations.

The EPOINT Set

Using standard set notation (see "**Set Notations**" on page 281), the extra point set merges with the structural degrees-of-freedom according to the following diagram:

For Direct Formulations:
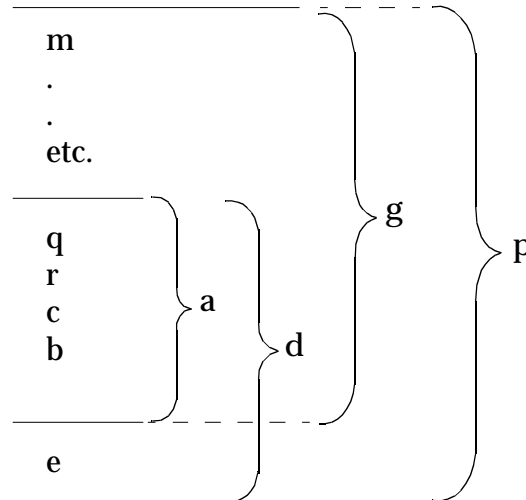
In direct solutions, the system matrices are formed by merging structural points and e-points into the p-set. The actual solution matrices are assembled and added together at the reduced, d-set level.

The set logic for modal formulations is as follows:
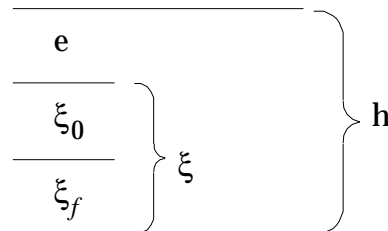
In modal solutions the system matrices are transformed to the modal coordinates and merged with the extra point degrees-of-freedom. The modal coordinates include free body modes, ξ_0, and flexible modes, ξ_f. Note that the coupling between the structural motions

Modal Transformations

When extra points are included in the modal formulation, a transformation is needed between the physical displacements and the modal coordinates. The displacements, u_p, are defined by the transformation

$$\{u_p\} = \left\{\frac{u_g}{u_e}\right\} = [\phi_{ph}]\left\{\frac{\xi}{u_e}\right\}$$

Eq. 2-31

where:

$$[\phi_{ph}] = \begin{bmatrix} \phi_g & 0 \\ 0 & I \end{bmatrix}$$

and ϕ_g are the real eigenvectors. The loads and direct input matrices are transformed consistently with the displacements. For the applied loads, P,

$$\{P_h\} = [\phi_{ph}]^T\{P_p\}$$

Eq. 2-32

Direct input matrices, K2PP, are transformed similarly in the form

$$[K_{hh}^2] = [\phi_{ph}]^T[K_{pp}^2][\phi_{ph}]$$

Eq. 2-33

Mass and damping matrices are also transformed similarly.

Note that the extra points remain in the modal formulation. These are useful for modeling transfer functions, initial conditions, and simple nonlinear functions.

Because these matrix terms couple the modal coordinates, this option is more expensive than solving the simple uncoupled modal equations of motion. The coupled solution requires the same type of matrix operations as the direct method.

Direct Matrix Inputs

Since direct matrix input (DMIG) data is covered in the *MSC.Nastran Linear Static Analysis User's Guide* and the *MSC.Nastran Basic Dynamic Analysis User's Guide*, this section will be brief.

Note: DMIG matrices are selected by the K2PP =, B2PP =, and the M2PP = Case Control commands.

For dynamics modeling, the direct input matrices are defined for the p-set of degrees-of-freedom for mass, damping, and stiffness matrices. The actual values are defined by the user and may represent any type of linear solution, including fluids, electrical circuits, and external structures. However, some practical recommendations are as follows:

1. Use the double field bulk data format (DMIG*) if more than three significant digits of the input values are desired. Note that these solutions are sensitive to the precision of the matrix terms. Use DMAP modules, INPUTi, for full double-precision input.

2. Use the automatic selection of single- or double-precision data for the system. The program sets the size depending on the word size of the computer.

3. Use the symmetric matrix option if possible. The unsymmetric flag will force all operations into the unsymmetric mode, costing time and storage space.

An example problem that uses DMIG data for generating friction forces is given in "**Complex Eigensolutions**" on page 146.

Transfer Functions

The MSC.Nastran transfer functions (TF inputs) are actually a convenient method for generating special unsymmetric matrix input. When used with extra points they can define second order operators with one output and multiple inputs. The basic equation defining individual TF input is

$$(B_0 + B_1 p + B_2 p^2)u_d + \sum_i (A_{oi} + A_{1i}p + A_{2i}p^2)u_i = 0 \qquad \text{Eq. 2-34}$$

Here u_d is the dependent degree-of-freedom, u_i are the selected input degrees-of-freedom, and the coefficients A and B are user-specified.

Internally, these coefficients are simply added to a single row in the matrix equation:

$$[Mp^2 + Bp + K]\{u\} = \{P\} \qquad \text{Eq. 2-35}$$

The terms are added to the matrices in the following positions:

1. All terms in a single function are added to the row of the matrices corresponding to u_d.

2. B_0 is added to the diagonal term of $[K]$. B_1 is added to the $[B]$ matrix, and B_2 is added to the $[M]$ matrix on the diagonals, respectively.

3. For each independent point , u_i, A_{0i}, A_{1i} , and A_{2i} are added to the column corresponding to u_i, and the row corresponding to u_d, of the stiffness, damping, and mass matrices, respectively.

Limitations

If the TF terms are the only occupants of the u_d row of the matrix equation, the dynamic solution will include the basic equation. However, no internal checks are made for additional terms in the TF row in the matrices or loads. To avoid conflicts, the following rules apply:

1. u_d should be the dependent variable for only one TF.

2. u_d should not be a component of a structural grid point unless the transfer function defines a load (see the discussion of transfer functions below).

3. External excitation signals, dynamic loads (DLOAD), and nonlinear functions (NOLINi) may be applied to the u_d point.

4. Unlike the multipoint constraints, the TF equations do not conserve energy. The matrix terms are not symmetric, and no reciprocity forces are generated.

Pickups and Transducers

Connections to the structure may be needed for both inputs and outputs from the transfer functions. To specify inputs, the structural displacements, velocities, or accelerations may be referenced on the A_i and u_i input fields. The u_d may be an extra point defining the pickup voltage. This signal may then be processed by a series of transfer functions (including feedback loops) until a servo generates a load on the structure.

It is recommended that the transfer function results applied to the structure be represented by a force or moment. An enforced displacement, velocity, or acceleration is difficult to model within the limitations described above.

To generate a force, F_j on a structural point, u_j, with a transfer function,

$$F_j = (A_0 + A_1 p + A_2 p^2) u_e$$

define a TF function of the form

$$(0) u_j - (A_0 + A_1 p + A_2 p^2) u_e = 0 \qquad \text{Eq. 2-36}$$

The B_j coefficients must be zero since the structural point u_j is already connected to the finite elements. This transfer function is equivalent to adding a positive force on the right-hand side of the matrix equation.

If the force or moment is acting on an actuator with a feedback loop, include the feedback as another transfer function.

Higher-Order Transfer Functions

In many cases the control system includes a polynomial transfer function of order greater than two and cannot be modeled directly. Since the TF inputs are limited to second-order polynomials, the larger polynomials must be subdivided into several TF inputs with intermediate extra points. For instance, if a point, u_a, is defined by the polynomial

$$(A + Bp + Cp^2 + Dp^3 + Ep^4) u_b = G(p) u_a \qquad \text{Eq. 2-37}$$

this may be subdivided into two equations suitable for the TF format:

$$(A + Bp + Cp^2) u_b + p^2 u_{e1} - G(p) u_a = 0 \qquad \text{Eq. 2-38}$$

and

$$u_{e1} - (Dp + Ep^2)u_b = 0 \qquad\qquad \text{Eq. 2-39}$$

Here, u_{e1} is an intermediate extra point which is coupled to the u_b degree-of-freedom in both equations.

Note that this method may produce a singular mass matrix that causes problems for certain complex eigenvalue options. This would occur in the example above if $E = 0$. A solution is discussed in "**Complex Eigensolutions**" on page 146.

Alternate Method. If the polynomial is available in factored form, i.e., $G_1(p) \cdot G_2(p) \cdot G_3(p)...$, a series of TF transfer functions can be used as illustrated in the following sketch.
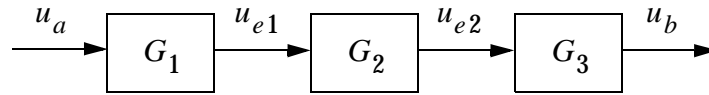
If u_b is the dependent degree-of-freedom, the TF equations will be in the following form:

$$u_{e1} - G_1 u_a = 0$$

$$u_{e2} - G_2 u_{e1} = 0$$

$$u_b - G_3 u_{e2} = 0$$

For polynomials in the denominator of a transfer function, use a feedback loop or coupled equations as shown in the previous example. See the example below for a realistic application.

Example

As an example of the general approach, consider the control system shown in **Figure 2-3**, which might represent a simplified model of an optical device. It contains many of the components found in control systems including attitude and rate sensors, signal conditioners, and a nonlinear mechanical actuator with local feedback. The structure is represented in **Figure 2-3** by the displacement components, which are sensed by the control system, or to which loads are applied.

The transfer functions (TFs) of the control system are listed in **Table 2-1**. The first five transfer functions give the outputs of the devices labeled 1 to 5 in **Figure 2-3** in terms of their inputs. TF 6 defines the force on the structure, at point u_{11}, which is a function of the input to the mechanical actuator.

In the analysis, an extra point is assigned to each of the new variables, u_4, ..., u_{10}. The coefficients of the transfer functions, expressed by TFs 1 to 6, are listed in **Table 2-2**. Note the coefficient of 0.0 for the structural degree-of-freedom, u_{11}, on TF 6. The existing structure provides the stiffness and mass for this displacement.
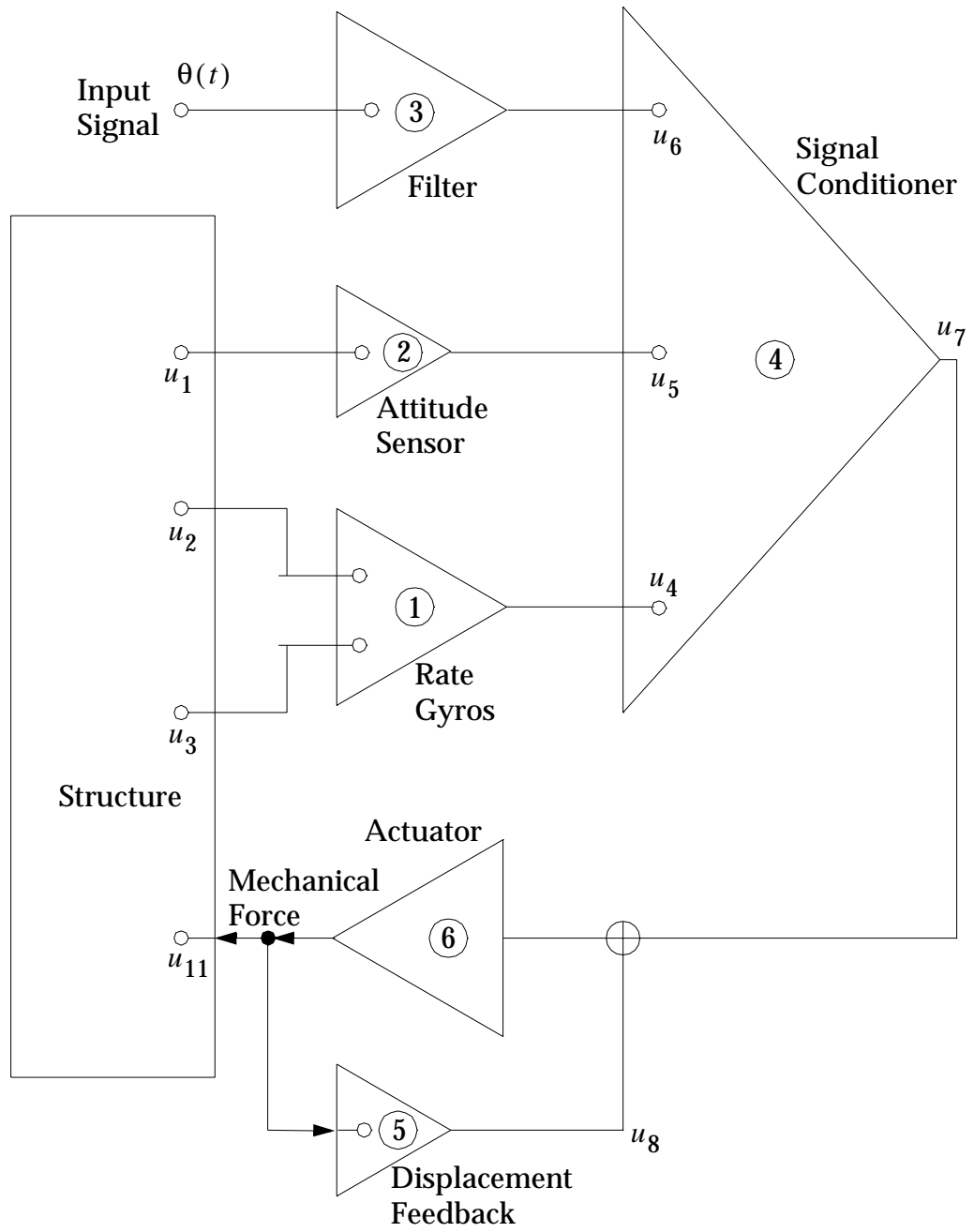
Figure 2-3 Example Control System

Table 2-1 Equations of Example Control System

Equation	TF Number
$u_4 = \dfrac{1}{1 + \tau_1 p}(Apu_2 + Bpu_3)$	1
$u_5 = \dfrac{1}{1 + \tau_2 p}Ru_1$	2
$u_6 = \dfrac{1}{1 + \tau_3 p}u_{10}$	3

Table 2-1 Equations of Example Control System (continued)

Equation	TF Number
$u_7 = \dfrac{A_0 + A_1 p}{B_0 + B_1 p + B_2 p^2}(Cu_4 + Du_5 + Eu_6)$	④
$u_8 = \dfrac{Gu_{11}}{1 + \tau_4 p}$	⑤
$(0)u_{11} = -k(u_7 - u_8)$	⑥

Table 2-2 Transfer Function Table

Transfer Function No.	u_d	b_0	b_1	b_2	u_i	a_0	a_1	a_2
1	u_4	1	τ_1		u_2		$-A$	
					u_3		$-B$	
2	u_5	1	τ_2		u_1	$-R$		
3	u_6	1	τ_3		u_{10}	-1		
4	u_7	B_0	B_1	B_2	u_4	$-CA_0$	$-CA_1$	
					u_5	$-DA_0$	$-DA_1$	
					u_6	$-EA_0$	$-EA_1$	
5	u_8	1	τ_4		u_{11}	$-G$		
6	u_{11}	0.0			u_7	$-k$		
					u_8	$+k$		

Input Data File

The actual structure is a beam-like optical pointing device pivoting on the center. The data file for a complex eigenvalue analysis is shown in **Listing 2-1**. The attitude sensor ($u_5 = \theta_z$), the first rate gyro ($u_2 = u_y$), and a lumped mass are located on the right end (GRID 1). The second rate gyro is attached to the next point (GRID 3). The actuator is connected to the left end (GRID 11) in the y direction. The units for the mechanical model are millimeters, kilograms, seconds, milliNewtons, and radians. The units for the control system variables (EPOINTs 4,5,6,7,8,10) are volts.

Listing 2-1 Data Listing for Optical Device Control System

```
ID ADUG,TFANDE
DIAG 8
SOL 107
TIME 5
CEND
TITLE = CONTROL SYSTEM EXAMPLE FOR ADUG
SUBTITLE = TRANSFER FUNCTIONS AND EXTRA POINTS
LABEL = COMPLEX MODES
SPC = 10
TFL = 6
CMETHOD = 200
SDISP=ALL
BEGIN BULK
$
EIGC,200,INV,MAX,,,,,,+EIG1
+EIG1,0.0,-1.0,0.0,1200.,20.0,10
$
$ STRUCTURE IS A BOX BEAM PIVOTING AT THE CENTER
GRDSET,,,,,,,1345
GRID,1,,500.0
GRID,3,,250.0
GRID,14,,0.0
GRID,15,,-250.0
GRID,11,,-500.0
CBEAM,1,1,1,3,,,1.0
CBEAM,2,1,3,14,,,1.0
CBEAM,3,1,14,15,,,1.0
CBEAM,4,1,15,11,,,1.0
PBEAM,1,1,1000.,125+6,125+6,,250.+6
MAT1,1,69.0+6,,0.3,5.0-6
$ OPTICAL DEVICE ON THE END
CONM2,6,1,,10.0,,,,,+CNM2
+CNM2,8.0+5,,4.0+5,,,4.0+5
$                     PIVOT ON THE CENTER
SPC,10,14,12
$                      EXTRA POINTS ARE VOLTAGES
EPOINT,4,5,6,7,8,10
$          TRANSFER FUNCTIONS IN ORDER
$                  RATE GYROS PICK UP VELOCITIES
TF,6,4,,1.0,0.015,,,,+TF101
+TF101,1,2,,-0.25,,,,,+TF102
+TF102,3,2,,-0.5
$                  ATTITUDE SENSOR MEASURES ROTATION RZ
TF,6,5,,1.0,0.02,,,,+TF201
+TF201,1,6,-1.2
$                  INPUT SIGNAL, E10, IS FILTERED
TF,6,6,,1.0,0.001,,,,+TF301
+TF301,10,,-1.0
$                  SIGNAL CONDITIONER COMBINES THE VOLTAGES
TF,6,7,,39.48,8.885-2,1.0-4,,,+TF401
+TF401,4,,-20.0,-0.4,,,,,+TF402
+TF402,5,,-200.0,-4.0,,,,,+TF403
+TF403,6,,100.,-20.0
$                  DISPLACEMENT FEEDBACK TO THE ACTUATOR
TF,6,8,,1.0,0.005,,,,+TF501
+TF501,11,2,-1.0
$               ACTUATOR FORCES ARE ADDED TO ROW OF STRUCTURAL MATRICES
TF,6,11,2,0.0,,,,,+TF601
+TF601,7,,-1.0+5,,,,,,+TF602
+TF602,8,,1.0+5
$                  TEMPORARILY GROUND POINT 10 WITH A DIAGONAL TERM
TF,6,10,,1.0
ENDDATA
```

2.5   Nonlinear Load Functions (NOLINi)

The nonlinear load functions (NOLINi) are available in all of the transient solutions for the purpose of generating direct forces from simple displacement and velocity functions. This is a mature capability in MSC.Nastran that preceded the development of the material and geometric nonlinear capabilities. It was intended to provide a direct method for modeling certain mechanisms and special effects at the local level where only a few degrees-of-freedom are coupled. It is not intended for general nonlinear analysis since the logic cannot detect geometric changes and has no means of using element stresses or forces.

The main applications for the NOLINi functions are for local devices such as contact problems, joints, and nonlinear dampers. For each nonlinear force component, the dependencies with displacement and velocity degrees-of-freedom are explicitly defined on one or more bulk data entries.

The limitations on the use of these functions are caused primarily by their simplicity. These limitations are:

1. They have no memory or other path dependencies. Specifically, they provide no direct means for including data from previous states.

2. Each input function only applies loads to a single degree-of-freedom, which requires a great deal of effort to describe complex models.

3. The system treats these functions as simple forces rather than finite elements. Therefore, the lack of a tangent matrix results in potential stability problems.

4. In the linear solutions, all degrees-of-freedom in the NOLIN functions must be in the dynamic solution set.

The input data is simply a case control request: NONLINEAR, with one or more NOLINi Bulk Data entries to define the set. The four basic options to define a scalar nonlinear force, N_i, in terms of the degrees-of-freedom, u_j, are summarized in the table below.

Option	Function	Comments
NOLIN1	$N_i = SF(u_j)$	$F(u_j)$ is a TABLEDi input
NOLIN2	$N_i = Su_j u_k$	Product of two variables
NOLIN3	$N_i = S(u_j)^A,\ u_j > 0$	A is an input exponent
NOLIN4	$N_i = -S(-u_j)^A,\ u_j < 0$	Same except for negative u

The variables, u, may be displacement or velocity components of grid, scalar, or extra points in the solution set. In the DIRECT TRANSIENT solutions, the connected degrees-of-freedom, u_i and u_j, etc., must remain in the solution set, u_d. In the modal

transient solutions, only extra points are available for use by the NOLINi entries. In nonlinear transient solutions all degrees-of-freedom are available, but unfortunately, extra points are not supported.

Note that these functions mimic the basic nonlinear function generators used in passive analog computers (MSC.Software's original business). They may be added together and combined with other functions such as MPCs and scalar elements to handle a variety of problems.

Theory for the Standard Transient Solutions

The basic linear transient solution integrates the matrix equation

$$[M]\{a\} + [B]\{v\} + [K]\{u\} = \{P\} + \{N\} \qquad \text{Eq. 2-40}$$

where $\{N\}$ are the nonlinear forces which are dependent on variable displacements, $\{u\}$, and velocities, $\{v\}$, of the unknowns. Note that if these functions were used to replace a stiffness term, the proper definition of N would be $N = -Ku$.

There are several options in MSC.Nastran for transient integration. For the basic purposes of this introduction, we will discuss the simplest form, the three-point method which performs a step-by-step calculation. At time step t_n, the solution is $\{u_n\}$ and the step size is h. Dropping the brackets, the averaged values of displacement, u, velocity, v, acceleration, a, and load, P, in terms of the three discrete steps are as follows:

$$u = \beta u_{n+1} + (1 - 2\beta)u_n + \beta u_{n-1} \qquad \text{Eq. 2-41}$$

$$v = \{u_{n+1} - u_{n-1}\} / 2h \qquad \text{Eq. 2-42}$$

$$a = (u_{n+1} - 2u_n + u_{n+1}) / h^2 \qquad \text{Eq. 2-43}$$

$$P = \beta P_{n+1} + (1 - 2\beta)P_n + \beta P_n \qquad \text{Eq. 2-44}$$

In the solution, the vectors at step $n+1$ are obtained by substituting **Eq. 2-2** through **Eq. 2-5** in **Eq. 2-40**. This method is actually a variation of the Newmark-Beta method and is guaranteed to be stable if $\beta > 0.25$. For consistency and stability, it would be desirable to have the N vector also in this form. Ideally, the nonlinear loads would be consistent with the the linear displacements and loads, i.e.,

$$N = \beta N_{n+1} + (1 - 2\beta)N_n + \beta N_{n-1} \qquad \text{Eq. 2-45}$$

However, $N_{n+1} = N(u_{n+1}, v_{n+1})$ is not available and can only be approximated by extrapolating the equation:

$$N_{n+1} \sim 2N_n - N_{n-1} \qquad \text{Eq. 2-46}$$

Substituting this approximation into **Eq. 2-45** we obtain the term used in MSC.Nastran:

$$N \sim N \qquad \text{Eq. 2-47}$$

In other words, calculating the nonlinear function at the center step is a valid approximation to the value averaged over three steps. Unfortunately, when u is rapidly changing, N will lag behind and create unstable oscillations. The results of an unstable integration usually grow with a period of two or three time steps per cycle. An alternate option for averaging nonlinear loads is available with DIAG 10, although it is *not* recommended.

Example of a Nonlinear Spring

An example of an unstable system can be illustrated with a single variable example. Attach a nonlinear spring function to a mass as shown in the sketch below.
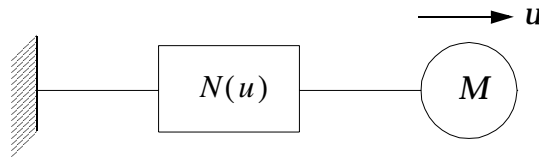
For small motions, if we define the function as an equivalent spring with $N = ku$, the integration equation for u_{n+1} is

$$M(u_{n+1} - 2u_n + u_{n-1})/h^2 = N = -ku_n \qquad \text{Eq. 2-48}$$

For stability analysis, we will assume a uniform growth rate, r, where $u_n = ru_{n-1}$ and $u_{n+1} = ru_n$. Substituting into **Eq. 2-48** we obtain a quadratic equation for r:

$$r^2 + 2\left(\frac{kh^2}{2M} - 1\right)r + 1 = 0 \qquad \text{Eq. 2-49}$$

If the magnitude of r is greater than 1, the solution will potentially diverge (r may be complex). It is easy to show that if $kh^2 > 4M$ the system will have a real root $r < -1$, which is an unstable oscillation that changes sign every step.

In other words, the stability limit for the nonlinear stiffness for this case is

$$-\frac{\partial N}{\partial u} = k \leq \frac{4M}{h^2} \qquad \text{Eq. 2-50}$$

The cure for divergence is to either reduce the time step, h, add linear stiffness to replace some of the nonlinear portion, or add enough mass, M, in parallel to the nonlinear function to satisfy the criteria for every possible value of k. Scalar mass elements CMASSi may be added to couple two scalar points, in parallel with the nonlinear spring, without affecting the total mass of the structure.

Velocity-Dependent Nonlinear Forces

When a NOLINi function references a velocity of a grid, scalar, or extra point component as an input, the nonlinear force must be calculated from the existing displacements. However, for consistency with the linear damping terms in **Eq. 2-40**, the nonlinear force should be:

$$N_v = -B(u,v) \cdot (u_{n+1} - u_{n-1}) / 2h \qquad \text{Eq. 2-51}$$

However, the current displacements u_{n+1} have not been calculated at this stage, so we again use the assumption of **Eq. 2-46** and obtain the approximation:

$$N_v \sim -B(u,v)(u_n - u_{n-1}) / h \sim N[(u_n - u_{n-1}) / h] \qquad \text{Eq. 2-52}$$

The stability of velocity-dependent NOLINi systems is very marginal for most applications. Replacing the nonlinear spring (k) in the example problem above with a nonlinear damper, b, we obtain the following system equation:

$$M(u_{n+1} - 2u_n + u_{n-1}) / h^2 = N = -b \cdot (u_n - u_{n-1}) / h \qquad \text{Eq. 2-53}$$

For stability analysis we may substitute ru_n and $r^2 u_n$ as in the stiffness example above, to obtain a quadratic equation:

$$r^2 + \left(\frac{bh}{M} - 2\right)r + \left(1 - \frac{bh}{M}\right) = 0 \qquad \text{Eq. 2-54}$$

Unstable roots ($|r| > 1$) will occur when

$$b > 2M / h \qquad \text{Eq. 2-55}$$

Again, the problem will show up as a spurious diverging oscillation. Divergence may be cured by decreasing the time step size, h, by changing part of the nonlinear function, b, into a linear damper, or by adding mass in parallel with the nonlinear function. SOL 129 is better suited than SOL 109 for unstable or badly conditioned problems.

Nonlinear Transient Solution Sequences

The general nonlinear transient solutions described in "**Nonlinear Transient Response Analysis**" on page 161 will also process the NOLINi functions. They provide an advantage in that they will give the same stability as a linear solution, and will control the diverging solutions. These methods make an attempt to calculate, for time step $n+1$, the displacements and velocities by iterating on **Eq. 2-40** through **Eq. 2-45** in a loop. This will provide more consistency with the linear terms. When the advanced methods such as line search and quasi-Newton options are activated, the adverse effects of the nonlinear forces are corrected effectively, but at the cost of additional solution steps.

However, the nonlinear methods may also attempt to change the tangent stiffness matrix when errors become too large in the solution search. Unfortunately, the NOLINi functions only provide forces on the right side and do not contribute their changes to the matrices. Not only will results not be improved, cost will be increased as well. Furthermore, since new self-adaptive method modifies the time step size based on the current values of the critical nonlinear matrix terms, the NOLINi terms will be ignored and the process may still diverge.

In summary, the nonlinear transient solutions may be adapted for severe cases of NOLINi-caused instabilities but will need careful changes to the default control parameters on the TSTEPNL inputs.

Recommendations for Using NOLIN1 Input

The following suggestions may be useful if problems occur because of nonlinear forces:

1. Use the nonlinear solution (SOL 129) for potentially better error controls and stability. This approach may use more time and disk storage space and require additional effort to select the proper control parameters. We recommend starting with the following approximate TSTEPNL Bulk Data parameters:

   Method = "TSTEP"
   KSTEP > NDT
   MAXITER = 2
   MAXLS = 6
   MAXDIV = 10
   LSTOL = 0.1

2. Avoid functions that will overwhelm the linear elements attached to the same points. See the discussions on stability above. Most nonlinear functions can be defined as the sum of linear elements and a nonlinear correction using NOLINi inputs. If the slope of the nonlinear correction function is smaller in magnitude than the linear coefficients, the problem will be stable. Also, added mass in parallel with the function always helps.

3. Never set up nonlinear functions in series, i.e., using the output of one NOLINi as an input to a second NOLINi function. Each stage in effect causes a time delay of one or more time steps for the resulting forces. If the results are a corrective force, they will act much like a control system with a bad feedback loop. At a critical frequency the corrective forces will be applied with a delay that causes them to have the wrong sign.

4. The forces, N, must have the same sign and direction as an externally applied load on the structure. Note that this will have the opposite sign as the forces applied to the GRID points by the finite elements. (The N force for a spring element will have a negative value for a positive displacement.) This frequently causes some difficulty in debugging the input data.

5. Use MPC or TF data to simplify the NOLINi inputs. A single nonlinear spring in three dimensions connecting two points could require up to $6 \cdot 6 = 36$ nonlinear functions. Alternatively, one MPC equation could be used to define the strain as an added scalar point, and one nonlinear function would define the generalized force (force times length) on the scalar point. Because the MPC constraints are consistent, the force will automatically be distributed to all six degrees-of-freedom.

6. Plan ahead to retain the nonlinear points in the solution set. Remember that in SOLs 109 and 112 the NOLINi functions may not reference any dependent or eliminated degree-of-freedom. Note that in a modal analysis, this leaves only extra points.

7. Use the full nonlinear solution (SOL129) for small to medium-sized problems.

Application Example – Coupling of Rotating Structures

An advanced use for the NOLINi functions is the connection between a rotating structure and a flexible supporting structure. The example below shows how to connect two grid points, with one rotating at a constant rate relative to the other. This method could be used to analyze sudden transients in rotating machinery. However, cost considerations would limit the analysis to a finite number of cycles.

As shown in the sketch, GRID 101 (u_r) is attached to the rotating structure. The rate of rotation is known, but the actual angle is a function of time. GRID 201 (u_f) represents the fixed bearing point coincident with point 101. It would typically be defined with an RBE3 as the average motion of the points on the bearing race.
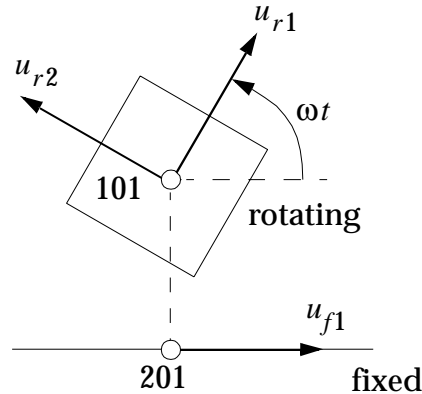
The definition of the connection, as shown in the sketch is:

$$u_{r1} = u_{f1} \cos(\omega t) + u_{f2} \sin(\omega t)$$

$$u_{r2} = -u_{f1} \sin(\omega t) + u_{f2} \cos(\omega t)$$

A simple MPC equation may be used to connect the axial coordinates u_3. The rotations may have similar definitions but are not shown. A similar equation defines the forces on the fixed point N_f in terms of the rotating forces Q_r.

For the actual connection, we will use the Lagrange Multiplier technique (see "**Lagrange Multiplier Technique**" on page 92 for details) by defining another GRID Q_r which defines the constraint forces on point 101. The resulting matrix partition equation for the three points is

$$
\begin{bmatrix} M_{ff} & 0 & 0 \\ 0 & m_{rr} & 0 \\ 0 & 0 & 0 \end{bmatrix} \begin{Bmatrix} \ddot{u} \\ \ddot{u} \\ \ddot{Q}_r \end{Bmatrix} + \begin{bmatrix} K_{ff} & 0 & 0 \\ 0 & K_{rr} & I \\ 0 & I & 0 \end{bmatrix} \begin{Bmatrix} U_f \\ u_r \\ Q_r \end{Bmatrix} = \begin{Bmatrix} P_f + N_f \\ P_r \\ N_q \end{Bmatrix} \qquad \text{Eq. 2-56}
$$

where:

$$
\{N_f\} = \begin{Bmatrix} P_{r1}\cos(\omega t) - P_{r2}\sin(\omega t) \\ P_{r1}\sin(\omega t) + P_{r2}\cos(\omega t) \end{Bmatrix}
$$

$$
\{N_Q\} = \begin{Bmatrix} u_{f1}\cos(\omega t) - u_{r2}\sin(\omega t) \\ -u_{f1}\sin(\omega t) + u_{r2}\cos(\omega t) \end{Bmatrix}
$$

In order to generate the sine and cosine terms, we will add two scalar points and connect unit masses and springs $k = \omega^2$. Using initial conditions, these are the sine and cosine functions defined as scalar displacements. The following input data will solve the connection:

In Case Control

```
IC = 100 $ For sine and cosine
K2PP = RCOUP  $ For matrix terms
NONLINEAR=10 $ For NOLIN2
```

In Bulk Data

```
$ 50 radian/sec oscillators ( Note: Don't use PARAM,G)
SPOINT,2001,2002  $ sine and cosine
CMASS4,2001,1.0,2001
CMASS4,2002,1.0,2002
CELAS4,2003,2500.0,2001
CELAS4,2004,2500.0,2002
TIC,100,2001,,,50.0   $ sine
TIC,100,2002,,1.0        $ cosine

$ Lagrange Multiplier Grid and unit Matrix Terms.
GRID,3001, , , , , ,3456
DMIG,RCOUP,0,6,1,2
DMIG,RCOUP,101,1,,3001,1,1.0
DMIG,RCOUP,101,2,,3001,2,1.0
$ Note that other half is generated when using the SYM option

$ Nonlinear Functions = Products of Two Dof., Q_r and sine/cosine
NOLIN2,10,201,1,1.0,3001,1,2002
NOLIN2,10,201,1,-1.0,3001,2,2001
NOLIN2,10,201,2,1.0,3001,1,2001
NOLIN2,10,201,2,1.0,3001,2,2002
$
$ Products of U_1 and sine/cosine
NOLIN2,10,3001,1,1.0,201,1,2002
NOLIN2,10,3001,1,1.0,201,2,2001
NOLIN2,10,3001,2,-1.0,201,1,2001
NOLIN2,10,3001,2,1.0,201,2,2002
$ end for one pair of points
```

Any type of structure may be connected to the axis points. However, for best stability place all of the mass at the axis on the active side, GRID 201, where the nonlinear force is applied. For inertia effects such as centripetal and Coriolis forces, the rotating body may require matrix inputs described in the section on moving coordinates. In order to keep these terms from affecting the fixed structure, superelement partitioning is recommended.

2.6   Debugging Dynamic Models

This section outlines a procedure for systematically checking and documenting a finite element model. Currently many models are generated by one organization and transmitted to other groups for subsequent analysis. Since these models have had various levels of analytical validation and documentation, checkout procedures are needed to ensure that the models will be consistent and mathematically well-conditioned. These procedures, however, are not substitutes for the independent verification phase of analysis. They are intended to remove modeling errors in the design process, rather than during the test updating phase, which occurs well after the hardware is built.

Modeling Hints

There is no single checklist that will ensure a complete check of a comprehensive finite element model. Also, there is no substitute for actual test correlation with the model, nor is there a substitute for the analyst's engineering interpretation of the output and one's intuition. A results prediction, which is determining gross results before the analysis, can be used to good advantage. Simple load paths or natural frequencies of equivalent simple beam/mass systems, etc., can be used to remove redundancies and predict the results. In fact, this must be accomplished to some degree to size the model initially. This will also provide baseline data, and the effects of finer modeling will then be known.

Relative to preparation of the pilot model, the following are a few suggestions for eliminating or reducing modeling problems.

- Start construction of a simple pilot model in which the user should:
    - Use beams and plates instead of solids.
    - Use RBE2s and RBE3s where they will simplify.
    - Simplify modeling offsets and local modeling details.
    - Ignore minor discontinuities such as holes and fillets.

Further refinement after this initial modeling should yield acceptable changes in the results.

- Do not rely on bending capability of thin plates and long, thin axial members to render the model kinematically stable.
- Make an initial run with membrane-only properties and pinned ended bars, and check for irregularities.
- Avoid use of AUTOSPC in the final model.
- For shells, use the parameters K6ROT or SNORM.

The post-analysis assessment should include a check of the physical significance of the loads and of the load path. Offsets whose moments are not properly accounted for may overly weaken a very stiff load path. Also, large moments in relatively weak bending members or plates may indicate modeling problems.

Stress analysis should be performed at the detailed part level with the loads from the model. The use of element stresses directly from the output of the model requires detailed review in most cases. In fact, model properties may be intentionally different from the actual hardware to obtain correct load distributions, and to match test data or dynamic characteristics. Effective thicknesses or reduced bending properties may have been used to reflect panel cutouts or partial beam and fixity. In this event, the finite element model loads should be used with the actual drawing or as-built dimensions for detail stress analysis. This piece-part assessment ensures a check and balance of the finite element model and the stress distributions visualized and treated by the element selection. Also, the source of the components of stress are known, that is, whether the predominant stress component is due to bending or axial loads. Load transformation matrices are useful for isolating critical design conditions but are not necessarily a sufficient basis for computing the margin of safety.

One area in which an underestimation of load could occur is the local response of small masses during a dynamic analysis. These should be addressed in the detailed stress analysis with both the model predictions and an alternate loading such as a specified loading condition. For the model to give correct loads for the local response of a mass, one needs all of the following:

- Mass must be represented by enough points to characterize the energy of the critical local mode (a single-point mass may not be sufficient).

- Mass must be supported by proper elastic elements to represent the local mode (RBE2 or RBE3 may not be sufficient).

- Mass must be in the ASET.

- Model and all analysis (input spectra, etc.) must be carried beyond this local critical mode (as far as frequency is concerned).

Testing Dynamic Models

Once the finite element model is completed and all documentation (such as model schematics (road maps) as well as material and geometric property calculations) are updated to the final model version, the following series of tests should be performed in order to validate the model. It is recommended that these tests be run on the model and subsystem models during the development stages as well.

Geometry Plots

The MSC.Nastran plotting package MSC.Patran, or another preprocessor graphics package should be used to obtain visual images of the finite element model from many views in such a way as to provide a clear representation of each element in at least one view and to verify overall geometry and placement of elements. Figure 2-4 shows the Galileo spacecraft finite element model and Figure 2-5 shows the Wide Field/Planetary Camera finite element model. A shrink option should be used if possible to make sure all elements are present (see Figure 2-6). This is particularly helpful when bars or beams are used to model stringers along the edges of plate elements. Discontinuities show up only when the
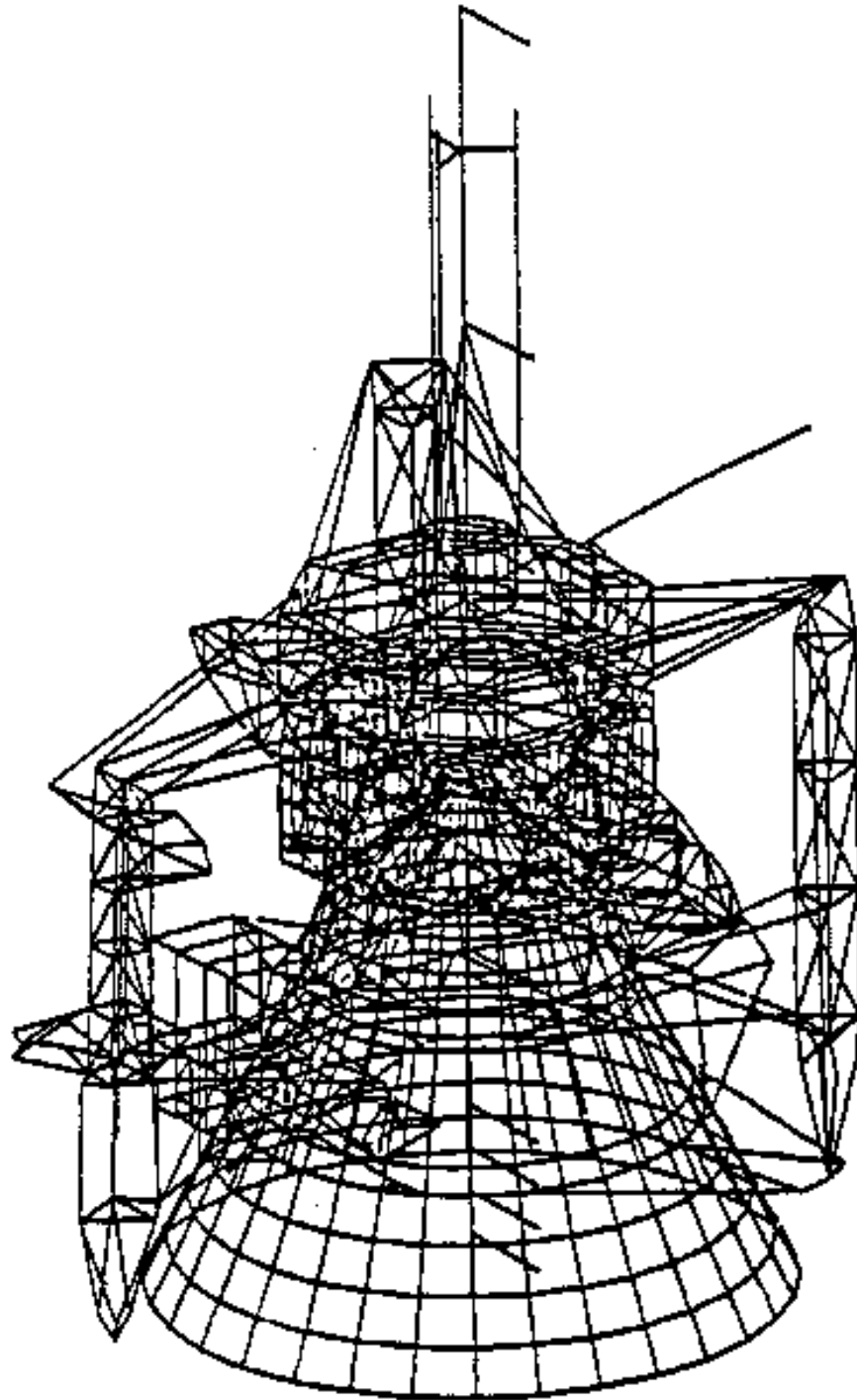
Figure 2-4 Galileo Finite Element Model
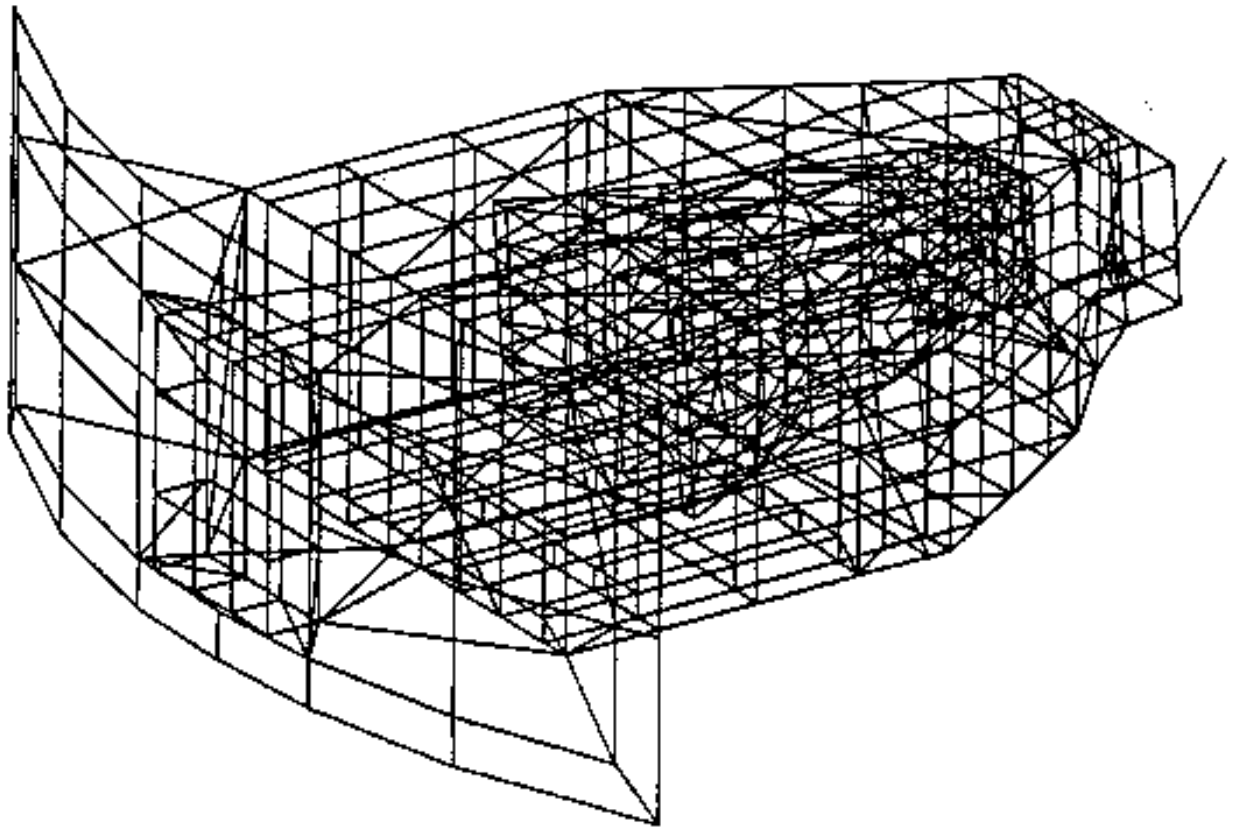
Figure 2-5 Galileo Wide Field Planetary Camera Finite Element Model
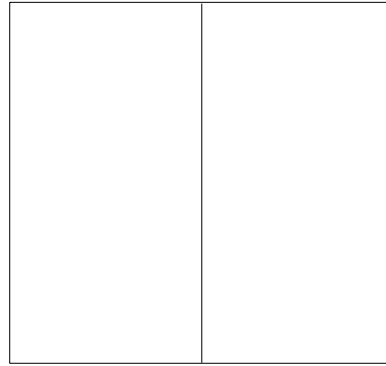
a) Shears and Bars, No Shrink
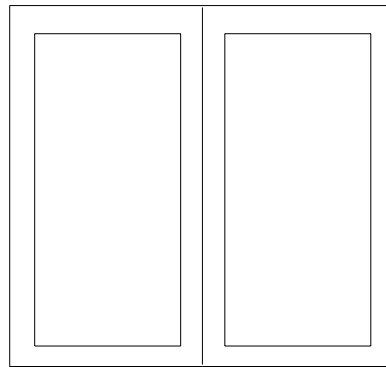
b) Bars Regular Size, Shears Shrunk
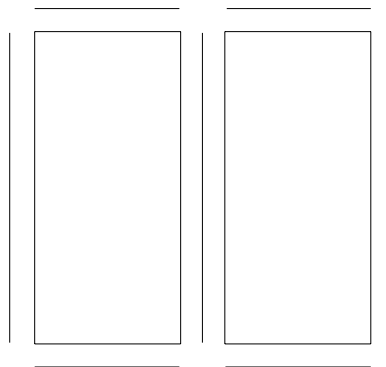
c) Bars and Shears Both Shrunk

Figure 2-6 Shrink Option

Checkout Run RF24D32

A checkout run using the rigid format alter RF24D32 should be used to check connectivity and duplicate element numbering. Any duplicate numbering should be corrected so that errors with plot sets will not occur. The connectivity table does not include MPCs or rigid elements (RBE2, RBE3, or RBAR). The checkout run also supplies all grid locations in basic coordinates and lists the lengths, areas, and volumes of all elements. **Listing 2-2** gives a listing of the parameters used and **Listing 2-3** through **Listing 2-10** give examples of the

Listing 2-2 Checkout Run

```
$ BEGINNING OF RF ALTER 24$32
$
$  CHECK INPUT DATA
$                    R I G I D   F O R M A T   24
$
$  CHECK CONTROL INPUT
$       CASE CONTROL DECK THAT WILL BE USED IN PRODUCTION RUN.
$
$       UNDEFORMED PLOTS MAY BE REQUESTED INCLUDING PROPERTY IDS
$             AND SPC POINTS
$
$  BULK DATA INPUT
$       COMPLETE BULK DATA DECK TO BE SUBMITTED FOR PRODUCTION RUN
$ THE FOLLOWING PARAMETERS MUST BE SET TO THE INDICATED VALUES TO OBTAIN
$       OUTPUT FOR-
$         1. GPL     . SET PARAMETER GPL TO GPL
$         2. EQEXIN - SET PARAMETER EQEXIN TO EQEXIN
$         3. GPDT   - SET PARAMETER GPDT TO GPDT
$         4. CSTM    . SET PARAMETER CSTM TO CSTM
$         5. BGPDT  - SET PARAMETER BGPDT TO BGPDT
$         6. MGG     - SET PARAMETER PRTMGG TO +1
$         7. ETT    - SET PARAMETER GPTT TO GPTT
$         8. GPECT  - SET PARAMETER GPECT TO +1 TO OBTAIN LIST OF ELEMENTS
$            CONNECTED TO GRIDS.
$         9. PROUT -- SET TO POSITIVE VALUE TO OBTAIN SORTED LIST OF
$            ELEMENT IDS.
$        10. EST   - SET TO POSITIVE VALUE TO OBTAIN LENGTHS, AREAS,
$            OR VOLUMES OF ELEMENTS.
$        11. PG     -- SET PRTPG=+1 TO PRINT THE LOAD VECTOR MATRIX
$        12. A SUMMATION OF LOAD IN BASIC WILL AUTOMATICALLY BE PRINTED
$
$  THE ITEMS CHECKED INCLUDE - GRID CONNECTION AND PROPERTY CARDS, MASS
$      PROPERTIES OF STRUCTURE, LOADS, TEMPERATURES AND CONSTRAINTS
$      AS WELL AS SOME GEOMETRY AND MATERIAL PROPERTIES
$      FOR EACH SUBCASE IN ALL BOUNDARY CONDITIONS.
$
$  THE ITEMS NOT CHECKED INCLUDE - GEOMETRY, MATERIAL PROPERTIES AND
$      GRID POINT SINGULARITIES
$-----------------------------------------------------------
```

Output from the Grid Point Weight Generator is recommended. Set PARAM,GRDPNT point to a positive integer. The value of the integer indicates the grid point to be used as the reference point. If the integer is zero or an undefined grid, the origin of the basic coordinate system is the reference point.

Listing 2-3 Formatted List of Table Data Block EQEXIN (Record 1)

EXTERNAL SORT ID	EXTERNAL GRID OR SCALAR ID	INTERNAL NUMBER	EXTERNAL GRID OR SCALAR ID	INTERNAL NUMBER	EXTERNAL GRID OR SCALAR ID	INTERNAL NUMBER	EXTERNAL GRID OR SCALAR ID	INTERNAL NUMBER
1	10	1	11	2	12	3	13	4
5	14	5	15	6	16	7	19	8
9	20	9	21	10	22	11	23	12
13	24	13	25	14	26	15	29	16
17	30	17	31	18	32	19	33	20

- Grid IDs as found in the Bulk Data are listed in numerical increasing order from left to right (four per row) and are listed under the column heading External Grid or Scalar ID.

- The corresponding internal ID number is given to the immediate right of the grid number under the column heading Internal Number.

- In the example above, grid point number 25 has internal sort number 14.

- The first column marked External Sort ID may be ignored (it simply increments by four because there are four External Grid/Internal Numbers per line).

- RF24D32 provides similar information in the following tables: GPL Record 1, GPL Record 2, and EQEXIN Record 2. The table shown above was chosen because its format is easier to explain.

- This output is obtained by using RF Alter RF24D32 and PARAM,EQEXIN,EQEXIN.

Listing 2-4 Formatted List of Table Data Block GPDT (Record 1)

INTERNAL ID	COORDINATE SYSTEM ID	COORDINATES IN DEFINING COORDINATE SYSTEM			DISPLACEMENT COORDINATE SYSTEM ID	CONSTRAINT CODE
		X	Y	Z		
1	10	0.00000E + 00	0.00000E + 00	4.22100E + 00	10	0
2	10	0.00000E + 00	0.00000E + 00	4.92100E + 00	10	0
3	10	0.00000E + 00	0.00000E + 00	8.30800E + 00	10	0
4	10	0.00000E + 00	0.00000E + 00	4.92100E + 00	10	0
5	10	0.00000E + 00	0.00000E + 00	8.30800E + 00	10	0
6	10	0.00000E + 00	0.00000E + 00	8.48800E + 00	10	0
7	10	0.00000E + 00	0.00000E + 00	9.25000E + 00	10	0
8	1000	1.73000E + 01	−4.11000E + 00	0.00000E + 00	0	123456
9	20	0.00000E + 00	0.00000E + 00	4.22100E + 00	20	0

Internal grid ID number as found from Table Exeqin Record 1

Coordinate system in which grid point geometry is defined

Spatial location of grid points in defining coordinate system

Coordinate system ID for grid point displacements, forces, and constraints

Permanent single-point constraints defined on GRID Bulk Data cards
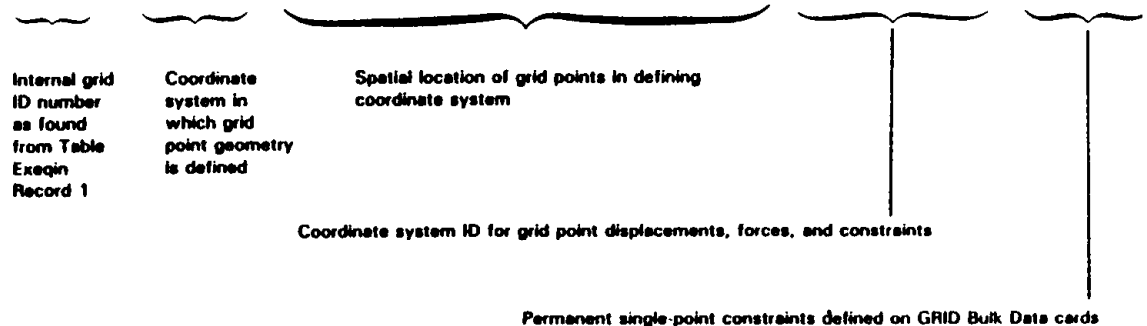
- This output is obtained by using RF Alter RF24D32 and PARAM,GPDT,GPDT.

Listing 2-5 Formatted List of Table Data Block CSTM (Record 1)

N	ID	TYPE	R(I,1)	R(I,2)	R(I,3)	T(I)
1	80	1	1.00000000E + 00	0.00000000E + 00	0.00000000E + 00	0.00000000E + 00
			0.00000000E + 00	1.00000000E + 00	0.00000000E + 00	0.00000000E + 00
			0.00000000E + 00	0.00000000E + 00	1.00000000E + 00	5.61500015E + 01
2	5	2	0.00000000E + 00	1.00000000E + 00	0.00000000E + 00	0.00000000E + 00
			0.00000000E + 00	0.00000000E + 00	1.00000000E + 00	0.00000000E + 00
			1.00000000E + 00	0.00000000E + 00	0.00000000E + 00	− 1.26000004E + 01
3	5000	2	9.99999940E − 01	4.76837192E − 09	0.00000000E + 00	0.00000000E + 00
			− 4.75675632E − 09	9.97564018E − 01	− 6.97565004E − 02	− 3.13941073E + 00
			− 3.32624928E − 10	6.97565004E − 02	9.97564018E − 01	− 4.06719875E + 00

Transformation matrix from the global (local) to the basic coordinate system. An identity matrix here indicates the coordinate system is parallel to the basic system.

The origin of the coordinate system given in the basic coordinate system

Coordinate system type is: 1 = rectangular; 2 = cylindrical; 3 = spherical

Coordinate system ID as found in Bulk Data. Not listed in numerical order.

Internal coordinate system number given in numerical order

- This output is obtained by using RF Alter RF24D32 and PARAM,CSTM,CSTM.

Listing 2-6 Formatted List of Table Data Block BGPDT (Record 1)

INTERNAL ID	COORDINATE SYSTEM ID	COORDINATES IN BASIC COORDINATE SYSTEM		
		X	Y	Z
1	10	1.35806E + 00	− 5.25850E + 00	2.43840E + 00
2	10	1.58327E + 00	− 4.73337E + 00	2.84278E + 00
3	10	2.67300E + 00	− 2.19252E + 00	4.79939E + 00
4	10	1.58327E + 00	− 4.73337E + 00	2.84278E + 00
5	10	2.67300E + 00	− 2.19252E + 00	4.79939E + 00
6	10	2.73091E + 00	− 2.05749E + 00	4.90337E + 00
7	10	2.97608E + 00	− 1.48585E + 00	5.34357E + 00

Spatial location of grid points in basic coordinate system

Internal grid ID number as found in Table Exeqin Record 1

Coordinate system ID for grid points displacements, forces, and constraints

- This output is obtained by using RF Alter RF24D32 and PARAM,BGPDT,BGPDT.

Listing 2-7 Element Type Count

THERE ARE	705 BAR	ELEMENTS FIRST EID	=	10 LAST EID	=	15408
THERE ARE	2 BEAM	ELEMENTS FIRST EID	=	100 LAST EID	=	900
THERE ARE	6 ELAS2	ELEMENTS FIRST EID	=	1040 LAST EID	=	1045
THERE ARE	117 CONM2	ELEMENTS FIRST EID	=	998 LAST EID	=	5250
THERE ARE	438 QUAD4	ELEMENTS FIRST EID	=	1019 LAST EID	=	31451
THERE ARE	101 SHEAR	ELEMENTS FIRST EID	=	1057 LAST EID	=	11657
THERE ARE	223 TRIA3	ELEMENTS FIRST EID	=	731 LAST EID	=	31071

- This output is obtained by using RF Alter RF24D32 and PARAM,PROUT,+1.
- Elements not accounted for include MPCs, RBARs, RBE1s, RBE2s, RBE3s.

Listing 2-8 Elements Listed in Numerical Order

ID	TYPE	ID	TYPE	ID	TYPE	ID	TYPE	ID	TYPE
10	BAR	11	BAR	12	BAR	13	BAR	14	BAR
15	BAR	16	BAR	20	BAR	21	BAR	22	BAR
**** 1001	BAR	DUPLICATES A CONM2							
1002	CONM2								
**** 1002	BAR	DUPLICATES A CONM2							
1003	BAR	1004	BAR	1011	BAR	1012	BAR	1014	CONM2
1015	CONM2	1016	CONM2	1017	BAR	1018	BAR	1019	CONM2

Asterisks indicate a duplicated element number

- This output is obtained by using RF Alter RF24D32 and PARAM,PROUT,+1.

Listing 2-9 Grid Point-Element Connection List

GRID POINT	CONNECTED ELEMENTS ID	TYPE	CONNECTED ELEMENTS ID	TYPE	CONNECTED ELEMENTS ID	TYPE	CONNECTED ELEMENTS ID	TYPE	CONNECTED ELEMENTS ID	TYPE
1032	11001	BAR	11022	BAR	11047	BAR	11048	BAR	1032	CONM2
1032	1744	QUAD4	1732	SHEAR	1748	SHEAR	1719	TRIA3	1720	TRIA3
1032	1721	TRIA3								
1033	11001	BAR	11002	BAR	11026	BAR	11027	BAR	1732	SHEAR
1033	1733	SHEAR	1748	SHEAR	1749	SHEAR				
1034	11002	BAR	11003	BAR	11031	BAR	11032	BAR	1733	SHEAR
1034	1734	SHEAR	1749	SHEAR	1750	SHEAR				

- This output is obtained by using RF Alter RF24D32 and PARAM,GPECT,+1.
- Elements not accounted for include MPCs, RBARs, RBE1s, RBE2s, RBE3s.

Listing 2-10 Element Length, Area, or Volume

```
ELEMENT TYPE = BAR
ELEMENT ID  LENGTH  VOLUME   ELEMENT ID  LENGTH  VOLUME   ELEMENT ID  LENGTH  VOLUME   ELEMENT ID  LENGTH  VOLUME
   1832    5.13668 0.405796    1833     5.23643 0.413678    1834     11.07   0.87453    1835     8.82    0.69678
   1836    11.07   0.87453     1837     8.82    0.69678     1838     11.07   0.87453    1839     8.82    0.69678
   1850    6.275   1.56875     1851     5.15759 1.2894      1852     6.64324 1.66081    1853     5.13666 1.28417

ELEMENT TYPE = BAR
ELEMENT ID  LENGTH  VOLUME   ELEMENT ID  LENGTH  VOLUME   ELEMENT ID  LENGTH  VOLUME   ELEMENT ID  LENGTH  VOLUME
   15302   1.33939 0.001339    15303    1.33939 0.001339    15304    1.33939 0.001339    15305    1.33939 0.001339
   15306   1.33939 0.001339    15307    1.33939 0.001339    15308    1.75    0.00175     15309    1.75    0.00175
   15400   4.73394 2.36697     15401    2.02678 1.01339     15402    2.5042  1.2521      15403    2.45211 1.22606
   15404   2.45231 1.22616     15405    5.06811 2.53406     15406    4.85001 2.425       15407    5.6528  2.8264
   15408   5.65271 2.82636

ELEMENT TYPE = BEAM
ELEMENT ID  LENGTH  VOLUME   ELEMENT ID  LENGTH  VOLUME   ELEMENT ID  LENGTH  VOLUME   ELEMENT ID  LENGTH  VOLUME
   100     7.44262 18.7905     900      7.03656 5.91071

ELEMENT TYPE = QUAD4
ELEMENT ID   AREA   VOLUME   ELEMENT ID   AREA   VOLUME   ELEMENT ID   AREA   VOLUME   ELEMENT ID   AREA   VOLUME
   1019    18.3429 1.10057     1020     18.4783 0.923918    1021     22.1611 1.32967    1022     20.6317 1.2379
   1023    21.5992 1.72794     1024     36.013  2.88104     1025     31.36   2.1952     1026     36.013  2.16078
   1027    35.3506 2.12103     1028     7.06676 0.565341    1030     2.7875  0.39025    1061     10.035  1.4049

ELEMENT TYPE = SHEAR
ELEMENT ID   AREA   VOLUME   ELEMENT ID   AREA   VOLUME   ELEMENT ID   AREA   VOLUME   ELEMENT ID   AREA   VOLUME
   1734    21.808  1.74464     1735     35.2222 2.81778     1736     29.7567 2.38054    1737     35.2222 2.81778
   1738    13.8272 1.10618     1739     11.6816 0.934528    1740     13.8272 1.10618    1741     21.1265 1.69012
   1742    19.787  1.58296     1743     21.1265 1.69012     1748     16.24   1.2992     1749     13.72   1.0976

ELEMENT TYPE = TRIA3
ELEMENT ID   AREA   VOLUME   ELEMENT ID   AREA   VOLUME   ELEMENT ID   AREA   VOLUME   ELEMENT ID   AREA   VOLUME
   731     1.08276 0.378965    732      1.08276 0.378965    733      1.08276 0.378965    734      1.08276 0.378965
   735     1.08276 0.378965    736      1.08276 0.378965    737      1.08276 0.378965    738      1.08276 0.378965
   1078    0.0725  0.019125    1079     0.0725  0.018125    1155     4.32    2.4192     1156     4.32    2.4192
```

- This is special output and is obtained by using RF Alter RF24D32 and PARAM,EST,+1.

Mass Distribution

PARAM,GRDPNT uses the Grid Point Weight Generator (GPWG), which gives the mass, the CG, the moments of inertia, and the principal moments of inertia and their direction cosines (see **Table 2-3**). Full use should be made of this diagnostic tool to correlate the model with existing hardware or mass properties calculations. The GPWG uses only the weight properties and geometry to calculate mass properties. The resultant mass properties are also called the rigid body mass properties. Note that PARAM,WTMASS does not affect the GPWG output—it is factored out of the printed results.

Table 2-3 PARAM,GRDPNT Weight Inertia Matrix

OUTPUT FROM GRID POINT WEIGHT GENERATOR

REFERENCE POINT = 1000 | — GRID POINT OR ORIGIN OF BASIC
MO   COORDINATE SYSTEM

```
·   1.562092E+00    -1.669640E-17    -1.040834E-17    -4.440692E-16     5.894034E+01    -1.359722E+01  ·
·  -1.767218E+17     1.562092E+00    -1.416518E-16    -5.894034E+01    -4.973032E-16     3.635694E-01  ·
·  -1.040834E-17    -1.419229E-16     1.562092E+00     1.359722E+01    -3.635694E-01    -4.440692E-16  ·
·   4.440692E-16    -5.894034E+01     1.359722E+01     3.191095E+03     3.648479E+00    -2.795030E+00  ·
·   5.894034E+01     2.972035E-16    -3.635694E-01     3.648479E+00     3.283023E+03    -5.082753E+02  ·
·  -1.359722E+01     3.635694E-01     2.220446E-16    -2.795030E+00    -5.082753E+02     4.852746E+02  ·
```

S

```
·   1.000000E+00        0.                0.            ·  ) TRANSFORMATION MATRIX
·   0.               1.000000E+00         0.            ·  } FROM THE BASIC SYSTEM
·   0.                  0.             1.000000E+00     ·  ) TO THE PRINCIPAL MASS AXES
```

DIRECTION
MASS AXIS SYSTEM (S)	MASS	X-C.G.	Y-C.G.	Z-C.G.
X	1.562092E+00	0.0	8.704492E+00	3.773167E+01
Y	1.562092E+00	2.327452E-01	0.0	3.773167E+01
Z	1.562092E+00	2.327452E-01	8.704492E+00	0.0

I(S)

```
·   8.488209E+02    -6.813166E+00    -1.092305E+01   ·  ) MOMENTS OF INERTIA IN THE
·  -6.813166E+00     1.059020E+03    -4.770467E+00   ·  } BASIC COORDINATE SYSTEM
·  -1.092305E+01    -4.770467E+00     3.668331E+02   ·  )
```

I(Q)

```
·   1.059279E+03                                     ·  )
·                    8.488406E+02                    ·  } PRINCIPLE MOMENTS OF INERTIA
·                                     3.665549E+02   ·  )
```

Q

```
·  -3.274377E-02    -9.992094E-01     2.254901E-02   ·  ) DIRECTION COSINES FROM
·  -9.994364E-01     3.290163E-02     6.865341E-03   ·  } BASIC COORDINATES TO
·  -7.401970E-03    -2.231805E-02    -9.997235E-01   ·  ) PRINCIPAL INERTIA AXES
```

— PRINCIPLE MASSES AND ASSOCIATED CENTERS OF GRAVITY RELATIVE TO THE REFERENCE POINT

— RIGID BODY MASS MATRIX RELATIVE TO THE REFERENCE POINT IN THE BASIC COORDINATE SYSTEM

Static Loading

Static loading, such as a simple gravity load, can be helpful in checking out various properties of finite element models. Displacements, element forces, and support reactions (SPC forces) derived from 1G loading conditions provide a first check on mass, stiffness, and determinacy of supports. Weight and CG can be calculated from SPC forces, which should also be compared to any applied loads or weight. Load paths can also be assessed using the element forces. Epsilon, Max Ratio, and SPC forces (at grids other than legitimate boundary conditions) describe the overall health of the stiffness matrix. See **Table 2-4** and **Table 2-5** for example printout data.

Table 2-4 Epsilon, Strain Energy and Max Ratio From Statics Run

··· USER INFORMATION MESSAGE 4158 – STATISTICS FOR SYMMETRIC DECOMPOSITION OF DATA BLOCK KOO FOLLOW
     MAXIMUM RATIO OF MATRIX DIAGONAL TO FACTOR DIAGONAL = 3.9E+03 AT ROW NUMBER 594

··· USER INFORMATION MESSAGE 3035 FOR DATA BLOCK KLL

LOAD SEQ. NO.	EPSILON	STRAIN ENERGY	EPSILONS LARGER THAN 0.001 ARE FLAGGED WITH ASTERISKS
1	-3.0539089E-14	8.2555099E+01	
2	1.0082989E-14	8.7870163E+01	
3	9.0509631E-16	2.3730776E+01	

··· USER INFORMATION MESSAGE 3035 FOR DATA BLOCK KOO

LOAD SEQ. NO.	EPSILON	STRAIN ENERGY	EPSILONS LARGER THAN 0.001 ARE FLAGGED WITH ASTERISKS
1	6.5035202E-15	2.2547545E-01	
2	7.3623740E-15	2.2061828E-01	
3	2.0116192E-15	1.3978869E-01	

Table 2-5 SPC Forces From Statics Run

FORCES OF SINGLE-POINT CONSTRAINT

1.0G (+X)   SUBCASE 1

POINT ID.	TYPE	T1	T2	T3	R1	R2	R3
201	G	0.0	0.0	0.0	0.0	2.797872E – 13	0.0
2811	G	0.0	1.778028E – 06	0.0	0.0	0.0	0.0
2711	G	0.0	– 3.070124E – 06	0.0	0.0	0.0	0.0
3197	G	0.0	0.0	0.0	0.0	0.0	2.731404E – 09
3198	G	0.0	0.0	0.0	0.0	0.0	3.327725E – 09
3297	G	0.0	0.0	0.0	0.0	0.0	2.494900E – 09
3298	G	0.0	0.0	0.0	0.0	0.0	– 1.839192E – 09
3397	G	0.0	0.0	0.0	0.0	0.0	– 4.187774E – 10
3398	G	0.0	0.0	0.0	0.0	0.0	– 4.716660E – 09
3497	G	0.0	0.0	0.0	0.0	0.0	1.664817E – 09
3498	G	0.0	0.0	0.0	0.0	0.0	8.814997E – 11
5602	G	0.0	0.0	0.0	0.0	0.0	6.451412E – 05
5603	G	0.0	0.0	0.0	0.0	0.0	– 8.358259E – 05
5604	G	0.0	0.0	0.0	0.0	0.0	3.047899E – 05
5605	G	0.0	0.0	0.0	0.0	0.0	– 3.166949E – 05
5606	G	0.0	0.0	0.0	0.0	0.0	2.126513E – 05
5607	G	0.0	0.0	0.0	0.0	0.0	2.643013E – 05
5608	G	0.0	0.0	0.0	0.0	0.0	– 4.914991E – 05
5609	G	0.0	0.0	0.0	0.0	0.0	4.414012E – 05
5610	G	0.0	0.0	0.0	0.0	0.0	– 3.978080E – 05
5611	G	0.0	0.0	0.0	0.0	0.0	3.061714E – 05
9999	G	– 5.640888E + 03	5.932931E – 06	– 1.097869E – 07	1.562507E – 04	4.669583E + 05	– 4.979101E + 02

MODEL WEIGHT
RECOVERED AT
THE BOUNDARY

MOMENT CONSISTENT
WITH MODEL WEIGHT
AND C.G. DATA

SPC FORCES AND MOMENTS IN THE ACCEPTABLE RANGE

Allowable values for these quantities are as follows:

Epsilon*	$\leq 1.0 \times 10^{-6}$ (large model)
	$\leq 1.0 \times 10^{-9}$ (small model)
Max Ratio	$\leq 1.0 \times 10^{+5}$
SPC Forces (at internal points)	$\leq 1.0 \times 10^{-5}$ (model weight)
SPC Moments (at internal points)	$\leq 1.0 \times 10^{-3}$ (model weight) × (unit length)

* Epsilon is machine dependent. The above data is for CDC 64-bitword. Other machines should give smaller numbers (1.0×10^{-8} and 1.0×10^{-11}). Mechanisms or symmetry conditions may require reevaluation of SPC force limits.

The 1G cases also provide a rough approximation of the frequency of the first mode. This approximation can be accomplished by using the displacement (D) at the CG in the equation $FN \sim \frac{1}{2\pi}\sqrt{G/D}$.

A 1G static load case can easily be obtained through the GRAV entry. This is preferred over the inertia relief type method.

Static forces and moments can be applied to generate displacements, element, and SPC forces. The magnitude and point of application of the forces should be representative of typical structural loading, thereby allowing the analyst a good feel for the size of displacements and forces as in the 1G cases. It is also helpful to use element strain energy and grid point force balance with these runs. For information on the details of requesting these capabilities, see Case Control Commands, "**ESE**" on page 200 and "**GPFORCE**" on page 209 of the *MSC.Nastran Quick Reference Guide.*

Free Body Equilibrium Check

Using Solution 101 and the set of CHECKA alters in the SSSALTER Library, an equilibrium check can be run to further validate the stiffness matrix. This check calculates the strain energy resulting from unit translations and rotations.

All SUPORTs and SPCs should be removed. Include the following PARAMs in the Bulk Data: AUTOSPC,YES; GPL; SEQOUT,1. The output from the AUTOSPC processor should be reviewed carefully (see **Table 2-6** for an example of AUTOSPC). This table will include all degrees-of-freedom that have no stiffness. Each degree-of-freedom should be checked and, if singular, it should be SPC'd; if it is not intended to be singular, then the model must be corrected.

Table 2-6 Grid Point Singularity Table

POINT ID	TYPE	FAILED DIRECTION	STIFFNESS RATIO	OLD USET	NEW USET
1000	G	4	0.00E + 00	O	S
1000	G	5	0.00E + 00	O	S
1000	G	6	0.00E + 00	O	S

The KRBF matrix (see **Table 2-7**) is printed out and is a measure of the force required for the rigid body displacements. All elements should be small, e.g.,

- Diagonal translations $< 1.0 \times 10^{-2}$
- Diagonal rotation $< 2.0 \times 10^{2}$
- Off-diagonal terms $< 2.0 \times 10^{2}$

Table 2-7 KRBF Matrix

MATRIX KRBF   (GINO NAME 101) IS A DB PREC   6 COLUMN X   6 ROW SQUARE MATRIX.

COLUMN   1   ROWS   1 THRU   6 ─────────────────────────────────────
ROW
     1) (5.6036D − 06)   6.2035D − 08   − 9.8440D − 08   − 8.1671D − 07   1.7130D − 04   1.1562D − 05

COLUMN   2   ROWS   1 THRU   6 ─────────────────────────────────────
ROW
     1)   6.2502D − 08   (6.3425D − 06)   8.2305D − 07   − 8.1379D − 05   1.1740D − 07   − 9.2047D − 06

COLUMN   3   ROWS   1 THRU   6 ─────────────────────────────────────
ROW
     1) − 9.7452D − 08   8.2517D − 07   (5.5577D − 06) − 1.9905D − 05   − 1.3735D − 06   1.2302D − 06

COLUMN   4   ROWS   1 THRU   6 ─────────────────────────────────────
ROW
     1) − 7.2425D − 07   − 8.2143D − 05   − 2.0377D − 05 | 2.5692D + 01 | − 3.6712D − 04   2.2372D − 04

COLUMN   5   ROWS   1 THRU   6 ─────────────────────────────────────
ROW
     1)   1.7143D − 04   7.7165D − 08   − 3.1777D − 06   − 3.7383D − 04 | 7.8407D + 00 | 4.3714D − 01

COLUMN   6   ROWS   1 THRU   6 ─────────────────────────────────────
ROW
     1)   1.1508D − 05   − 9.3303D − 06   1.1475D − 06   2.3130D − 04   4.3714D − 01 | 1.4307D + 00 |

- Forces due to translations (circled) should be less than 1.E–2.

- Moments due to rotations (rectangle) should be less than 2.0E+2.

- Off diagonal terms should be less than 2.0E+2.

Also printed in the matrix KRBFN, the forces at the grid points normalized to a maximum of 1.0 (see **Table 2-8**). As seen from **Table 2-8**, this check easily identifies which grid points and DOFs are causing problems.

Table 2-8 KRBFN Matrix

Rigid Body Check

If the model is primarily used for dynamic analysis, the CHECKA DMAP alter performs an equilibrium check in Solution 103. In this case, the unit translations and rotations are considered to be the rigid body displacements of the structure in output coordinates about the SUPORT point. Strain energy, which should be very small, is calculated and printed out.

The strain energy, the Epsilons, and the Max Ratio should also be checked at this point, as they were for the static case (see **Table 2-9**).

Table 2-9 Epsilon, Strain Energy, and Max Ratio from Rigid Body Modes Run

```
••• USER INFORMATION MESSAGE 4158—STATISTICS FOR SYMMETRIC DECOMPOSITION OF DATA BLOCK KOO
      FOLLOW MAXIMUM RATIO OF MATRIX DIAGONAL TO FACTOR DIAGONAL = 7.4E+04 AT ROW NUMBER 702

••• USER INFORMATION MESSAGE 3035 FOR DATA BLOCK KLR

SUPPORT
PT. NO.      EPSILON        STRAIN   ENERGY   EPSILONS LARGER THAN 0.001 ARE FLAGGED WITH ASTERISKS

   1      1.2895072E–16      0.0000000E+00
   2      1.2895072E–16     –7.2759576E–12
   3      1.2895072E–16     –5.4569682E–12
   4      1.2895072E–16     –2.2351742E–08
   5      1.2895072E–16     –4.4703484E–08
   6      1.2895072E–16     –7.4505806E–09
```

- The SUPORT entry is required for epsilon and strain energy.

This option requires a SUPORT entry. The DOF supported must form a determinate interface or high strain energy will result. The model displacements printed represent the displacements caused by moving a support DOF one unit while holding the other support DOFs fixed. The model displacements should be checked for unit value (see **Table 2-10**).

Table 2-10 Rigid Body Mode Shapes

```
EIGENVALUE =  0.000000E+00
    CYCLES =  0.000000E+00
                                        REAL EIGENVECTOR NO. 2

POINT ID.    TYPE        T1              T2              T3          R1       R2       R3
   2001       G       0.0             0.0            0.0          0.0      0.0      0.0
   2002       G       0.0             0.0            0.0          0.0      0.0      0.0
   2003       G       0.0             0.0            0.0          0.0      0.0      0.0
   2102       G       0.0           1.000000E+00     0.0          0.0      0.0      0.0
   2131       G       0.0           1.000000E+00     0.0          0.0      0.0      0.0
   2704       G       0.0           1.000000E+00     0.0          0.0      0.0      0.0
   2732       G       0.0           1.000000E+00     0.0          0.0      0.0      0.0
   7010       G     4.446353E–01    8.957117E–01     0.0          0.0      0.0      0.0
   7011       G    –4.446353E–01    8.957117E–01     0.0          0.0      0.0      0.0
   7012       G    –4.446353E–01    8.957117E–01     0.0          0.0      0.0      0.0

                  GRIDS 7010 THRU 7012 OUTPUT
                  IN A LOCAL COORDINATE SYSTEM


EIGENVALUE =  0.000000E+00
    CYCLES =  0.000000E+00
                                        REAL EIGENVECTOR NO. 3

POINT ID.    TYPE        T1              T2              T3          R1       R2       R3
   2001       G       0.0             0.0            0.0          0.0      0.0      0.0
   2002       G       0.0             0.0            0.0          0.0      0.0      0.0
   2003       G       0.0             0.0            0.0          0.0      0.0      0.0
   2102       G       0.0             0.0          1.000000E+00   0.0      0.0      0.0
   2131       G       0.0             0.0          1.000000E+00   0.0      0.0      0.0
   2704       G       0.0             0.0          1.000000E+00   0.0      0.0      0.0
   2732       G       0.0             0.0          1.000000E+00   0.0      0.0      0.0
   7010       G       0.0             0.0          1.000000E+00   0.0      0.0      0.0
   7011       G       0.0             0.0          1.000000E+00   0.0      0.0      0.0
   7012       G       0.0             0.0          1.000000E+00   0.0      0.0      0.0
```

- Eigenvalues and cycles are set equal to zero by the DMAP alter package.

Please note that these alters assume max normalization on the EIGR entry.

Thermal Test Case

As a further check on connectivity and the stiffness matrix, an isothermal expansion test case can be run with a statically determinate interface. This is done on SOL 101 with a TEMPD for the constant temperature load. All of the coefficients of expansion should be

set to the same value. This check will not be rigid if rigid elements or bar offsets are present. Rigid elements will not expand and may generate distortion forces and stresses unless the appropriate degrees-of-freedom are released.

Modal Analysis

There are several diagnostic tools that can be used to further assess the integrity of the model. These tools (effective mass, strain energy, kinetic energy, deformed plots) are outlined in the following paragraphs.

The two major means of reducing the number of dynamic degrees-of-freedom in the modal analysis are outlined below.

A major concern in dynamic analysis is the choice of an appropriate ASET when using the Guyan reduction. The quality of the solution depends upon the reduced mass matrix formed by this ASET. Will it retain sufficient mass in correct distribution to adequately predict mode shapes and frequencies?

The results of a GDR run can be used to select an ASET for use in future processing if desired (see the flow chart in **Figure 2-7**). See the description for CHECKA in "**SSSALTER Library For MSC.Nastran**" on page 269. A proven rule-of-thumb for ASET selection is to include all DOFs that have more than 2% of the system KE for all major modes (determined by comparing EFMASS to the system weight) and more than 5% for the other modes. One must be careful in the case of assemblies with a fine mesh; although the whole assembly may be moving in a mode, there may not be any individual DOFs with greater than 2% of the system kinetic energy. This is usually evident when a mode has a sizeable EFMASS, and either no terms with a large kinetic energy or the terms with noticeable kinetic energy do not account for the EFMASS of the mode. If this is the case, then there is no substitute for common sense determination of DOFs that describe the subsystem motion.
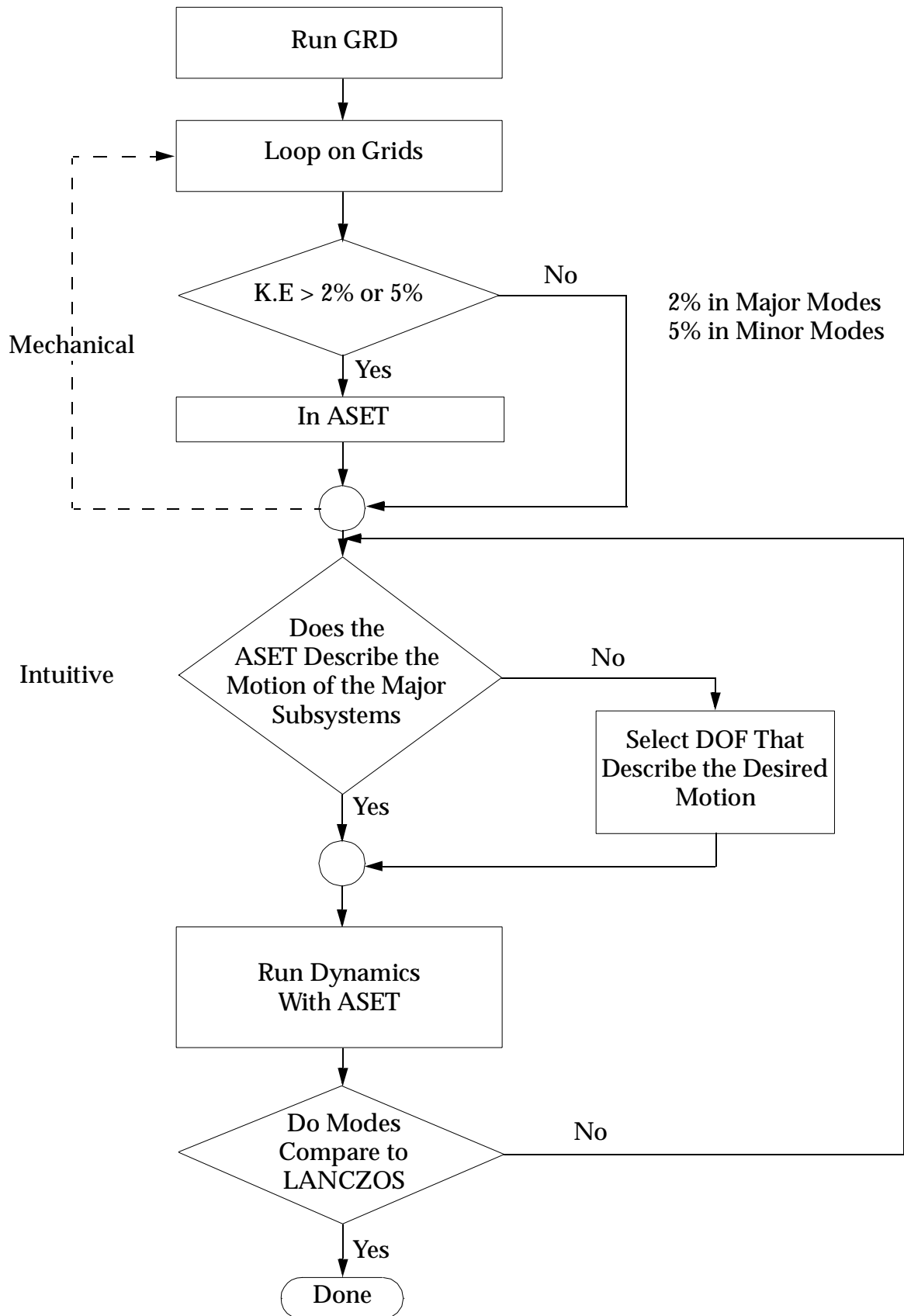
Figure 2-7 ASET Selection Flow Chart

Note also that this removes the rigid body mode check from the run, since the SUPORT entry must be removed (unless the run is a free-free run).

MER – MREMER – MR – EFMASS

An important diagnostic tool is the elastic-rigid coupling matrix (MER), a triple product of the elastic mode shape matrix, the ASET mass matrix, and the rigid body displacement matrix with respect to the interface. This $N \times 6$ matrix gives the square root of the effective mass in each retained mode so that the product of each element of this matrix will itself give the effective mass contained in that mode in the associated direction. These values are in EFMASS. This matrix can be used to determine which modes are energetic in terms of interface loading. **Table 2-11** shows a sample MER matrix taken from **Reference 3**. The elements of this matrix have been squared and units converted to give recognizable weight units.

Table 2-11 Galileo Spacecraft Baseline Model Modal Weight and Inertia
(Lb, Lb-in^2)

Mode	X	Y	Z	RX	RY	RZ
1	0	0	0	2.5E+00	2.3E+03	8.3E+01
2	0	0	1	2.3E+03	3.4E-01	5.0E-02
3	1188	479	0	7.9E+06	2.1E+07	2.2E+03
4	489	1144	0	2.0E+07	8.7E+06	6.2E+02
5	2	1888	3	8.2E+06	1.2E+04	1.0E+02
6	1097	5	0	1.7E+05	5.7E+06	9.2E+05
7	1007	10	0	3.1E+05	5.5E+06	3.2E+05
8	1	296	0	5.2E+06	8.9E+03	2.1E+05
9	45	3	0	9.4E+04	2.4E+05	1.2E+05
10	11	554	33	3.5E+06	5.3E+04	1.5E+02
11	533	0	31	2.0E+02	3.2E+06	2.8E+04
12	5	6	221	3.5E+04	2.9E+04	9.0E+05
13	41	25	770	1.1E+05	1.9E+05	4.0E+05
14	3	29	84	1.8E+05	3.5E+04	7.0E+05
15	9	0	7	7.9E+02	9.2E+04	5.2E+05
16	0	24	6	3.3E+04	3.4E+02	1.4E+04
17	2	0	63	3.9E+04	4.6E+03	3.6E+03
18	50	86	1	6.9E+04	7.7E+04	6.1E+05
19	2	0	35	2.8E+04	3.4E+03	1.1E+04
20	27	196	0	1.6E+05	3.4E+04	3.8E+05
21	55	6	1	2.4E+03	7.3E+04	7.8E+03
22	15	51	40	4.6E+04	2.9E+04	1.2E+04
23	6	19	3055	2.2E+04	2.6E+04	6.5E+04
24	100	0	479	4.3E+04	2.9E+05	1.2E+05
25	8	15	5	1.0E+04	2.5E+04	1.4E+04
26	157	7	15	3.6E+03	2.2E+05	5.2E+03
27	1	1	149	3.1E+04	1.8E+03	1.5E+04
28	21	1	30	7.0E+04	2.8E+04	1.5E+04
29	0	1	0	6.6E+03	1.6E+03	5.0E+00
30	10	1	0	1.2E+03	1.2E+04	9.0E+03
31	71	138	9	4.2E+05	1.3E+05	7.0E+03
32	67	5	0	2.6E+04	5.3E+04	1.6E+02
33	22	38	20	8.9E+04	6.7E+04	3.8E+02
34	2	47	6	1.3E+03	4.2E+04	3.1E+01
35	67	49	1	8.2E+04	2.0E+05	2.2E+02
36	0	0	0	1.5E+02	1.4E+01	1.4E+01
37	0	0	0	3.5E+02	4.1E+02	1.2E+02
38	0	10	0	5.4E+04	2.7E+04	3.0E+02
39	13	1	6	4.7E+03	8.6E+03	1.8E+03
40	6	22	0	1.5E+03	1.8E+03	1.8E+04
41	7	2	8	2.3E+01	3.4E+03	8.7E+03
42	12	11	41	4.9E+04	1.4E+04	5.6E+03
43	0	8	1	8.9E+03	3.6E+01	1.9E+04

Table 2-11 Galileo Spacecraft Baseline Model Modal Weight and Inertia
(Lb, Lb-in^2) (continued)

Mode	X	Y	Z	RX	RY	RZ
44	0	3	8	1.4E+04	1.2E+03	2.9E+04
45	0	0	49	1.3E+04	4.1E+01	6.7E+03
46	9	29	0	1.7E+04	2.2E+04	5.3E+03
47	1	0	4	1.6E+03	6.2E-01	4.9E+03
48	0	2	13	1.9E+04	5.0E+02	4.1E+03
49	4	3	66	1.2E+04	1.8E+04	1.7E+04
50	0	0	4	1.0E+03	6.7E+02	6.1E+02
51	0	18	0	1.6E+04	6.2E+03	3.7E-02
52	1	4	3	1.8E+04	8.9E+02	4.6E+02
53	2	7	1	2.6E+04	4.1E+03	4.2E+02
54	0	0	1	2.6E+02	7.5E+03	8.3E+02
55	14	3	0	1.4E+04	8.4E+04	2.5E+02
56	0	6	0	7.5E+03	9.3E+03	2.8E+03
57	9	14	1	1.1E+04	1.3E+03	3.5E+02
58	0	0	2	1.8E+03	2.6E+03	4.6E+03
59	27	15	0	3.8E+04	3.6E+04	8.4E+03
60	1	25	4	6.4E+04	6.5E+03	3.6E+03
61	42	12	3	3.7E+04	6.8E+04	9.1E+03
62	15	11	0	1.5E+04	2.6E+04	3.3E+04
63	0	1	0	1.4E+03	3.8E+03	2.8E+00
64	31	11	0	3.5E+03	6.6E+04	1.2E+05
65	3	1	1	1.0E+02	6.9E+02	2.1E+04
66	0	0	0	6.6E+02	3.4E+01	1.5E+03
67	2	0	4	4.5E+02	1.3E+04	1.4E+04
68	3	3	0	3.4E+03	9.3E+02	1.7E+03
69	0	0	2	4.1E-01	2.5E+02	8.1E+01
70	0	8	·0	4.1E+04	4.7E+01	1.0E+04
TOTAL:	5316	5355	5287	4.69E+07	4.61E+07	5.76E+06
RIGID	5591	5591	5591	4.74E+07	4.67E+07	6.19E+06
MODAL%	0.95	0.96	0.95	0.99	0.99	0.93

The product of MER with itself transposed (MREMER) gives the total effective mass retained using the ASET DOF number of modes. The diagonal of MREMER is compared with that of the rigid mass matrix (MR) to determine if sufficient mass is contained in the selected modes to consider the model valid. The generation of the MR matrix also makes use of the stiffness matrix (see the sketch below). The MR matrix should also be compared to the mass properties of the Grid Point Weight Generator. The inertias are calculated about the SUPORT grid and, unless this is the point selected with PARAM,GRDPNT, the inertias will not agree. A typical allowable is a 5% loss of mass. This comparison can then be used to modify the choice of ASET DOF or to increase the number of modes. This diagonal is shown as the TOTAL line of Table 2-11 and is compared against the full model weight.

Table 2-12 Galileo Baseline S/C Modal Frequencies

Mode	Freq	Mode Description	Kinetic Energy Distribution
1	6.3	PWS Antenna	PWS, 100%
2	6.8	PWS Antenna	PWS, 100%
3	13.7	SXA bending, X	SXA 45%, RPM 22%
4	13.7	SXA bending, Y	SXA 48%, RPM 21%
5	16.7	Probe, Y	Probe 83%
6	18.2	Sciboom X, core torsion	Sciboom 45%, SXA 20%
7	18.5	Probe X	Probe 53%
8	18.6	SXA Y	SXA 41%, Probe 9%
9	19.0	Probe X, SXA X	SXA 34%, Probe 32%
10	22.2	Sciboom Z bounce	Sciboom 57%
11	22.7	RTGs Z bounce, -phase	RTGs 61%, RPM 19%
12	23.8	Nutation damper lateral	Nutation Damper 51%
13	24.3	RTGs Z bounce, in phase	RTGs 61%
14	25.7	Nutation damper lateral	Nutation Damper 52%,
15	27.0	Nutation damper lateral	Nutation Damper 70%,
16	28.5	RRH Antenna, Y	RRH 48%, EPD 22%
17	28.7	Scan platform theta X	Scan platform 96%
18	29.7	-X RTG lateral (Y)	-X RTG 96%
19	31.9	Scan sunshade (Z)	Sunshade 92%
20	32.5	+X RTG lateral (Y)	+X RTG 93% .
21	33.7	PLS+RRH+Sciboom	PLS 31%
22	35.4	EPD+PLS+Sciboom	PLS 31%
23	38.0	S/C Z bounce	RPM 54%, Probe 10%
24	38.3	Scan platform X	Scan 73%, RPM 16%
25	38.6	PLS+EPD+Thrusters	PLS 40%, EPD 21%
26	40.4	Probe torsion, RPM	Probe 50%
27	40.8	-X Thruster, RPM	RPM 53%
28	41.3	Sciboom mag tip, box	Sciboom 47%
29	43.1	Thrusters lateral (Y)	Thrusters 89%
30	43.3	RRH antenna X	RRH 95%
31	44.9	RPM tanks, probe torsion	RPM 38%, Probe 17%
32	45.8	-X RTG X motion	-RTG 57%
33	46.1	Sciboom, misc	Sciboom 49%, Scan 20%
34	46.7	Scan platform Z, X	Scan platform 53%
35	47.7	400N engine, Probe tors	400N 13%, Probe 10%
36	48.0	-X Thruster torsion	-X Thruster 95%
37	48.1	+X Thruster torsion	+X Thruster 95%
38	48.3	400N engine X, SBA	400N 56%, SBA 27%
39	48.8	400N engine Y, SBA	400N 43%, SBA 19%
40	49.6	RPM+Despun Box Z bounce	RPM 32%, Despun box 17%

To calculate the MER and MREMER and to print them along with the MR, one should use the CHECKA DMAP alter from the SSALTER library when there is a SUPORT entry in the Bulk Data Section. The model must be cantilevered from the SUPORT; that is, the SUPORT DOFs are the only constraints preventing rigid-body motion. The G factor $385.0886 \text{ in/sec}^2$ is in the ALTER. If another value is desired, it must be substituted.

Kinetic and Strain Energy

The CHECKA alters may also be used for printing the kinetic energy distribution as a fraction of the total, in the form of eigenvectors, for each mode. This information is useful for showing the energy distribution *within a mode*, whereas the MER matrix is useful for

determining *which mode* is energetic. The various grid points within a model can be grouped together and the energy then given by subsystem. **Table 2-12** shows a sample taken from **Reference 3**. Examination of **Table 2-11** and **Table 2-12** show that for modes 1 and 2 the PWS subsystem has 100% of the KE, but in terms of effective mass it is negligible (the Plasma Wave Subsystem (PWS) is a very light antenna). In contrast, the probe in mode 5 not only has the predominant percent KE but is also an energetic mode (**Table 2-12**).

Element strain energy can also be used to determine which elastic elements are participating within a given mode. These two diagnostic tools can help isolate a weak or very flexible area of the model that may only be a modeling error.

The whole package is intended for use with SOL 3. The model must have a determinate support point without any SPCs to fix the base.

Deformed Plots

Another diagnostic tool is plotting. Deformed geometry plots, the eigenvector output, and MER help to identify mode shapes and classify them. Plots will also highlight excessive deflections that point to stiffness matrix problems.

Information from these diagnostics will feed back to both the stiffness and mass matrices and the ASET degrees-of-freedom. In only a few iterations, all mass and stiffness problems can be rectified and the model will be a realistic representation of the true structure.

The quality of the above checks depends on the quality of ASET chosen. It is good practice to make at least one run using Generalized Dynamic Reduction and to verify the model by comparing the resulting modes to those obtained using the ASET. If the two runs are not comparable, the LANCZOS run should be used to select an ASET. The inclusion of all terms with significant KE usually gives a good ASET, but since large, stiff assemblies might not have large energy at individual grid points, common sense should also be used.

References

1. *MSC.Nastran Handbook for Linear Analysis*, Version 64, The MacNeal-Schwendler Corporation, August 1985.

2. "Equivalent Spring-Mass System for Normal Modes," R. M. Bamford, B. K. Wada, and W. H. Gayman, NASA Technical Memorandum 33-380, February 1971.

3. "Galileo S/C NASTRAN Model, Descriptive Data, and Checkcase Results," R. Calvet and G. Wang, May 1985.

4. "Checks that Pay," J. C. Auker, *Proceedings*, the MSC.Nastran European User's Conference, Munich, West Germany, May 1984.

5. JSC-20545, "Simplified Design Options for STS Payloads," D. A. Hamilton, May 1985.

System Matrix Formulations

- ■ Overview

- ■ Theoretical Basis for Reduction Methods

- ■ Dynamics of Rotating Structures

- ■ Overview of Aeroelastic Analysis

3.1 Overview

The solutions used in dynamic analysis are more complicated than the solution of a simple matrix equation. Compared to linear static analysis, the running time for a dynamics problem is more costly, the required file space is more excessive, and the larger amounts of output data can be difficult to digest. Therefore, attention should be paid to reducing the number of solution equations to manageable levels.

Other special effects enter into many cases of dynamic analysis. Certain loads, such as those used in rotating structures and in aerodynamics, require special matrix formulations and solution strategies. These problems use conventional matrices to represent structural properties, but they can also require extra degrees-of-freedom and may need to account for fundamental changes such as nonlinear effects. For example, in rotating structures the connections vary with phase angles. In aeroelasticity the effects of the air flow vary with frequency.

This chapter begins with an explanation of the various options available in MSC.Nastran for reducing the size of the solution matrices in dynamic analysis. Direct methods, modal formulations, and combinations are discussed.

The next section presents methods for the analysis of finite element models in rotating coordinate systems. Applications include turbo machinery, disk drives, and flexible shafts.

The last section is an introduction to the use of aeroelasticity, which can be applied to any problem with a steady fluid flow attached to a flexible structure.

3.2 Theoretical Basis for Reduction Methods

In the following development we will start from the full-size structural matrix equations and derive the equations for Static Condensation, Guyan Reduction, Generalized Dynamic Reduction (GDR), and Component Mode Synthesis. These operations will apply to both single structures and superelement models. We will also try to explain the physical consequences of the assumptions involved in reducing the systems.

Definition

The basic dynamic equation before reduction is given in the u_f set (after SPC and MPC constraints have been applied, but before DMIGs and extra points). The standard matrix equation to be reduced is:

$$
\begin{bmatrix} \bar{M}_{aa} & M_{ao} \\ M_{oa} & M_{oo} \end{bmatrix} \begin{Bmatrix} \ddot{u}_a \\ \ddot{u}_o \end{Bmatrix} + \begin{bmatrix} \bar{B}_{aa} & B_{ao} \\ B_{oa} & B_{oo} \end{bmatrix} \begin{Bmatrix} \dot{u}_a \\ \dot{u}_o \end{Bmatrix} + \begin{bmatrix} \bar{K}_{aa} & K_{ao} \\ K_{oa} & K_{oo} \end{bmatrix} \begin{Bmatrix} u_a \\ u_o \end{Bmatrix} = \begin{Bmatrix} \bar{P}_a \\ P_o \end{Bmatrix}
$$

Eq. 3-1

where:

u_a, $\dot{u}_a$, $\ddot{u}_a$ are the displacements, velocities, and accelerations of the analysis (a) set, to be retained.

u_o, $\dot{u}_o$, $\ddot{u}_o$ are the displacements, velocities, and accelerations of the omit (o) set, to be eliminated.

    M, B, K   are the mass, damping, and stiffness matrices (assumed to be real and symmetric).

    P_a, P_o are the applied loads.

Note that all free-body motions must be included in the u_a partition. Otherwise, K_{oo} will be singular. The bar quantities ($\bar{P}$, etc.) indicate unreduced values.

Statics

For statics problems, we may ignore the mass and damping effects and solve the lower partition of **Eq. 3-1** for u_o:

$$
\{u_o\} = -[K_{oo}^{-1}]([K_{oa}]\{u_a\} + \{P_o\})
$$

Eq. 3-2

The two parts of **Eq. 3-2** become the Guyan matrix G_o and the static corrective displacement u_o^o:

$$
[G_o] = -[K_{oo}^{-1}]\{K_{oa}\}
$$

Eq. 3-3

$$
\{u_o^o\} = [K_{oo}^{-1}]\{P_o\}
$$

Eq. 3-4

The exact static solution system is obtained by substituting **Eq. 3-2** through **Eq. 3-4** into the upper partition terms of **Eq. 3-1**, resulting in the reduced equations used in the static solution

$$[K_{aa}]\{u_a\} = \{P_a\}$$

Eq. 3-5

and

$$\{u_o\} = [G_o]\{u_a\} + \{u_o^o\}$$

Eq. 3-6

where:

$$[\overline{K}_{aa}] = [K_{aa}] + [K_{ao}][G_o]$$

Eq. 3-7

$$\{P_a\} = \{\overline{P}_a\} + [G_o^T]\{P_o\}$$

Eq. 3-8

In actual practice the size of the u_a set is usually small compared to u_o, but the reduced matrices are dense, resulting in no savings in cost. The savings in solving **Eq. 3-5** are usually offset by the costs of calculating G_o and u_o^o.

However, for dynamics, we also may approximate the vectors $\ddot{u}_o$ and $\dot{u}_o$ to reduce the order of the system. A good place to start is to use the static properties. From **Eq. 3-6**, define the transformation

$$\{u_f\} = \begin{Bmatrix} u_a \\ \hline u_o \end{Bmatrix} = [H_f]\{u_f'\}$$

Eq. 3-9

where:

$$\{u_f'\} = \begin{Bmatrix} u_a \\ \hline u_o^o \end{Bmatrix}$$

Eq. 3-10

$$[H_f] = \begin{bmatrix} I & 0 \\ \hline G_o & I \end{bmatrix}$$

Eq. 3-11

Here u_o^o are the incremental displacements relative to the static shape. The system described in **Eq. 3-1** may be transformed to the new coordinates with no loss of accuracy. The stiffness matrix in the transformed system is

$$[K_{ff}'] = \begin{bmatrix} I & G_o^T \\ \hline 0 & I \end{bmatrix} \begin{bmatrix} K_{aa} & K_{ao} \\ \hline K_{oa} & K_{oo} \end{bmatrix} \begin{bmatrix} I & 0 \\ \hline G_o & I \end{bmatrix}$$

Eq. 3-12

Performing the multiplication and substituting **Eq. 3-3** results in

$$[K_{ff}'] = \begin{bmatrix} \overline{K}_{oo} & 0 \\ \hline 0 & K \end{bmatrix}$$

Eq. 3-13

Although the stiffness matrix becomes decoupled, the mass and damping matrices tend to have more coupling than the original system. Since the damping terms have the same form as the mass, we will not include them here. The exact transformed system becomes

$$
\begin{bmatrix} M'_{aa} & M'_{ao} \\ M'_{oa} & M'_{oo} \end{bmatrix} \begin{Bmatrix} \ddot{u}_a \\ \ddot{u}_o \end{Bmatrix} + \begin{bmatrix} K_{aa} & 0 \\ 0 & K_{oo} \end{bmatrix} \begin{Bmatrix} u_a \\ u_o \end{Bmatrix} = \begin{Bmatrix} P_a \\ P_o \end{Bmatrix}
$$

Eq. 3-14

where:

$$
[M'_{aa}] = [M_{aa}] + [M_{ao}][G_o] + [G_o]^T [M_{oa} + M_{oo} G_o]
$$

Eq. 3-15

$$
[M'_{ao}] = [M'^T_{oa}] = [M_{ao}] + [G_o^T M_{oo}]
$$

Eq. 3-16

$$
[M'_{oo}] = [M_{oo}]
$$

Eq. 3-17

The damping matrix terms of B'_{ff} are similar in form to the mass matrix partitions. An alternative derivation which does not rely on symmetric transformation is given below. Starting from **Eq. 3-1** through **Eq. 3-8**, we may estimate the acceleration effects of the omitted points by the equation

$$
\{\ddot{u}_o\} \cong [G_o]\{\ddot{u}_a\}
$$

Eq. 3-18

Substituting **Eq. 3-18** into the lower partition of **Eq. 3-1**, and solving for u_o, with damping neglected, we obtain the approximation

$$
\{u_o\} = [K^{-1}_{oo}](\{P_o\} - [K_{oa}]\{u_a\} - [M_{oa} + M_{oo} G_o]\{\ddot{u}_a\})
$$

Eq. 3-19

Substituting **Eq. 3-3** for K_{oa} and **Eq. 3-16** for the mass terms into **Eq. 3-19**, we obtain

$$
\{u_o\} \cong [G_o]\{u_a\} + K^{-1}_{oo}[\{P_o\} - [M'_{oa}]\{\ddot{u}_a\}]
$$

Eq. 3-20

Substituting **Eq. 3-18** and **Eq. 3-20** into the upper half of **Eq. 3-1** (ignoring damping), we obtain

$$
[\bar{M}_{aa} + M_{ao} G_o]\{\ddot{u}_a\} + [\bar{K}_{aa} + K_{ao} G_o]\{u_a\} - [K_{ao} K^{-1}_{oo}][M_{oa} + M_{oo} G_o]\{\ddot{u}_a\}
$$
$$
= \{\bar{P}_a\} - [K_{ao}][K^{-1}_{oo}]\{P_o\}
$$

Eq. 3-21

Combining the terms, we obtain the same results as **Eq. 3-14** through **Eq. 3-17**.

The significance of this exercise is to show that the Guyan transformation has very interesting properties, namely:

1. The approximation occurs only on the acceleration terms (**Eq. 3-18**).
2. The stiffness portion of the reduced system is exact.
3. The interior displacements defined by **Eq. 3-20** and **Eq. 3-14** are nearly identical.

The significant aspects of the partially decoupled system described by **Eq. 3-9** through **Eq. 3-21** are that most of the MSC.Nastran reduction methods are easily developed from this form and the approximations are conveniently explained in these terms. The Guyan reduction, the GDR process, and the modal synthesis methods are described below.

Guyan Reduction

In the MSC Guyan reduction process, the omitted relative accelerations, $\ddot{u}_o^o$, in **Eq. 3-14** are approximated by **Eq. 3-18** and the solution system is

$$[M'_{aa}]\{\ddot{u}_a\} + [K'_{aa}]\{u_a\} = \{P'_a\}$$ Eq. 3-22

The system described by **Eq. 3-18** has several desirable properties. The overall mass and center of gravity properties are preserved in the mass matrix. Also note that the static stiffness is exact. If accelerations occur, the errors may be estimated by solving for u_o^o after u_a is obtained. The omitted points, u_o^o, could be recovered by solving the lower part of **Eq. 3-14**.

However, in most applications, the stiffness terms of **Eq. 3-14** dominate and the normal modes of the omitted degrees-of-freedom are of higher frequency than the solution set. Therefore, we may ignore the left-hand mass and solve for u_o directly from **Eq. 3-2** by the equation

$$[u_o] = [G_o]\{u_a\}$$ Eq. 3-23

The errors in **Eq. 3-23** are proportional to the vector $\{u_o^o\}$, which becomes small when the individual masses and applied loads in the omit set are small. Because of the same assumption, the errors of the upper half of **Eq. 3-14** are also small. (In MSC.Nastran, u_o^o is neglected in the dynamic data recovery process.)

General Dynamic Reduction

In most applications, GDR is used directly to find the modes of the u_f set and no u_a points are retained. The method then becomes a straightforward Rayleigh-Ritz/Lanczos procedure. However, it is a recommended practice in MSC.Nastran to extend the u_a set to include any large masses to avoid numerical roundoff problems and provide more accurate results.

Approximate Mode Shapes. If u_a grid point displacements are retained in the GDR process, the u_o^o set is approximated by a set of generalized coordinates, u_q, where

$$\{u_o^o\} \cong [\phi_{oq}]\{u_q\}$$ Eq. 3-24

where ϕ_{oq} are a set of approximate eigenvectors or natural shapes. In its simple form[1], with u_t replacing u_a, the GDR transformation corresponding to **Eq. 3-9** is

---

[1]In these solution sequences u_a includes u_q and the previous equations for the u_a set are

$$\left\{\begin{matrix} u_t \\ \hline u_o \end{matrix}\right\} = \left[\begin{matrix} I & 0 \\ \hline G_o & \phi_{oq} \end{matrix}\right] \left\{\begin{matrix} u_t \\ \hline u_q \end{matrix}\right\} \qquad \text{Eq. 3-25}$$

The transformed matrix system is then

$$\left[\begin{matrix} M'_{tt} & M_{tq} \\ \hline M_{qt} & M_{qq} \end{matrix}\right] \left\{\begin{matrix} \ddot{u}_t \\ \hline \ddot{u}_q \end{matrix}\right\} + \left[\begin{matrix} K'_{tt} & 0 \\ \hline 0 & K_{qq} \end{matrix}\right] \left\{\begin{matrix} u_t \\ \hline u_q \end{matrix}\right\} = \left\{\begin{matrix} P'_t \\ \hline P_q \end{matrix}\right\} \qquad \text{Eq. 3-26}$$

where M'_{tt} is defined by **Eq. 3-15** with u_t replacing u_a, as follows:

$$[M_{tq}] = [M_{ot}^T][\phi_{oq}] + [G_o^T M_{oo}][\phi_{oq}] \qquad \text{Eq. 3-27}$$

$$[M_{qq}] = [\phi_{oq}^t M_{oo} \phi_{oq}] \qquad \text{Eq. 3-28}$$

$$[K'_{tt}] = [K_{tt}] + [K_{to}][G_o] \qquad \text{Eq. 3-29}$$

$$[K_{qq}] = [\phi_{oq}^T K_{oo} \phi_{oq}] \qquad \text{Eq. 3-30}$$

$$\{P'_t\} = \{P_t\} + [G_o^T]\{P_o\} \qquad \text{Eq. 3-31}$$

$$\{P_q\} = [\phi_{oq}^T]\{P_o\} \qquad \text{Eq. 3-32}$$

Error Analysis. Note that, as in Guyan Reduction, the exact static stiffness is retained. If accelerations exist, errors will occur when the modal displacements do not match the exact solution for u_o^o. Assume that the displacement error, ε_o, is:

$$\{\varepsilon_o\} = [\phi_q]\{u_q\} - \{u_o^o\} \qquad \text{Eq. 3-33}$$

The modal force error is

$$\{\delta_q\} = [\phi_{oq}^T K_{oo}]\{\varepsilon_o\} = [K_{qq}]\{u_q\} - [\phi_{oq}^T K_{oo}]\{u_o^o\} \qquad \text{Eq. 3-34}$$

However, from **Eq. 3-14**, we obtain

$$[K_{oo}]\{u_o^o\} = \{P_o\} - [M_{oo}]\{\ddot{u}_o^o\} - [M'_{ot}]\{\ddot{u}_t\} \qquad \text{Eq. 3-35}$$

and from the lower half of **Eq. 3-26** and **Eq. 3-30** through **Eq. 3-32**, we obtain

$$[K_{qq}]\{u_q\} = [\phi_a^T]\{P_o\} - [\phi_a^T M_{oo} \phi_o]\{\ddot{u}_q\} - [\phi_o^T M'_{ot}]\{\ddot{u}_b\} \qquad \text{Eq. 3-36}$$

Substituting **Eq. 3-35** and **Eq. 3-36** into **Eq. 3-34**, we obtain

$$\{\delta_q\} = [\phi_{oq}^T M_{oo}]\left\{\ddot{u}_o^o - [\phi_{oq}]\{\ddot{u}_q\}\right\} \qquad \text{Eq. 3-37}$$

Therefore, we observe that the loading errors for GDR will be proportional to the size of the omitted masses, M_{oo}, and with the quality of the approximation

$$\ddot{u}_o \cong [\phi_q]\{\ddot{u}_q\} \qquad\qquad \text{Eq. 3-38}$$

Relative to **Eq. 3-37**, the equivalent load error for Guyan reduction was

$$\{\delta_o\} = [M_{oo}]\{\ddot{u}_o^o\} \qquad\qquad \text{Eq. 3-39}$$

Even when the mode shapes are only approximate, as in GDR, we conclude that the results (for the same u_o set) will be improved from the Guyan results. However, note that when a u_t set is not used, the modes of the u_o^o system have the same lower frequencies as the system modes and the approximation might not improve. In other words, the use of physical u_t points in the GDR process combines the best parts of both Guyan and Rayleight-Ritz reductions.

Component Mode Synthesis

In MSC.Nastran, the Component Mode Synthesis procedure is identical to the GDR process except that:

1. The approximate eigenvectors are replaced with results from the module which calculates modes of the superelement.
2. Boundary set points (u_t, u_c, or u_r) will be retained for connection to other superelements.
3. Special operations are performed for free-body motions.

Note that in Guyan Reduction the relative displacements, u_o^o, for the omitted point are only approximated in dynamics. In the GDR and modal synthesis methods, interior results are obtained by solving for its eigenvector displacements and added directly into the matrix solution system.

A special case, known as the inertia relief effect, occurs when the structural component is excited at low frequencies (below the first modal frequency). The effect is defined by **Eq. 3-20** when $\ddot{u}_a$ is a low frequency excitation, having little effect on the vibration modes, resulting in a relative quasi-static displacement, u_o^o, where

$$\{u_o^o\} = -[K_{oo}]^{-1}[M'_{oa}]\{\ddot{u}_a\} \qquad\qquad \text{Eq. 3-40}$$

The displacement vector is called the inertial relief shape when $\ddot{u}_a$ is a rigid body acceleration vector. It may cause a significant redistribution of the internal forces in the structure.

In the solution of a single structural component, the inertia relief effects may be obtained after the solution, u_a, is obtained. However, for multiple superelements connected at the u_t boundary points, the load distributions on the boundary will be affected by these internal loads. Note that the errors defined in **Eq. 3-23** and **Eq. 3-34** will be affected since the eigenvectors may only approximate the vectors defined in **Eq. 3-37**.

The solution used in MSC.Nastran provides for inertia relief modes by adding six vectors to the approximation set ϕ_o. These vectors are obtained from **Eq. 3-40** and use the equation:

$$[\phi_o^{ir}] = [K_{oo}]^{-1}[M'_{oa}][D_a] \qquad \text{Eq. 3-41}$$

where D_a is a matrix of six rigid body motions defined by the grid point geometry. Each column of the matrix ϕ_o^{ir} is scaled to a reasonable value and added to the ϕ_o matrix, and a corresponding u_q displacement is also included.

3.3   Dynamics of Rotating Structures

The following sections provide a description of the dynamic loads on a rotating structure defined in the rotating coordinate system. While the stiffness and damping terms measured in a rotating system are the same as those measured in a stationary system, the terms due to inertial resistance are dependent upon the rotation of the structure. These inertial dependent terms need to be determined and added to the total impedance of the structure before static and dynamic analyses in a rotating system can be performed.

Technical Approach

A rotating structure is usually modeled under the assumption that the coordinate system used in the description of the structure will rotate at a constant rate about a fixed axis. Displacements of the structure and forces applied to the structure are measured in this rotating system. Because the rotating system is accelerating relative to a stationary inertial system, the inertial or mass dependent impedance cannot be directly calculated in the rotating system. The inertial impedance in the rotating system must first be determined in the stationary reference frame, and then transformed to the rotating system.

The impedance due to stiffness and damping is unaffected by the choice of reference frames. The stiffness and damping impedances in a rotating reference system are identical to those in a stationary reference system.

To determine the inertial impedance in a rotating system requires the development of general transformation techniques between stationary and rotating systems. The following section describe the general transformation of a vector between stationary and rotating system coordinates. The second section discusses inertial forces defined in a rotating coordinate system. The third section applies these results to develop the impedance of a rotating structure. The fourth section describes the DMAP procedure to add the gyroscopic terms to the structural matrices for analysis in the rotating system.

Vector Transformation from Stationary to Rotating Coordinates

It is important to keep in mind that the essential features of a vector are magnitude and direction, but not location. A vector defined in one coordinate system can just as easily be defined in a different coordinate system through the use of a coordinate transformation matrix. Also keep in mind that vectors may be time dependent in both their magnitude and direction and that coordinate systems may rotate with respect to each other resulting in a time-dependent transformation matrix.

The remainder of this discussion concerns transforming a vector defined in stationary system coordinates to rotating system coordinates. The choice of which system is rotating and which system is stationary is completely arbitrary at this point. No physical significance (such as position, velocity, etc.) is assigned to the vector; the only important qualities are its magnitude and direction.

The general transformation of a time-dependent vector from a stationary coordinate system to a rotating coordinate system at the same origin may be written as

$$\{v(t)_r\} = [A(t)]\{v(t)_s\} \qquad \text{Eq. 3-42}$$

where:

$\{v(t)_r\}$ = rotating coordinate system definition of time-dependent vector.

$[A(t)]$ = time-dependent transformation matrix from rotating to stationary system.

$\{v(t)_s\}$ = stationary coordinate system definition of time-dependent vector.

The above transformation is valid for any vector, real or complex.

The fundamentals of this transformation are demonstrated for the two systems shown below.
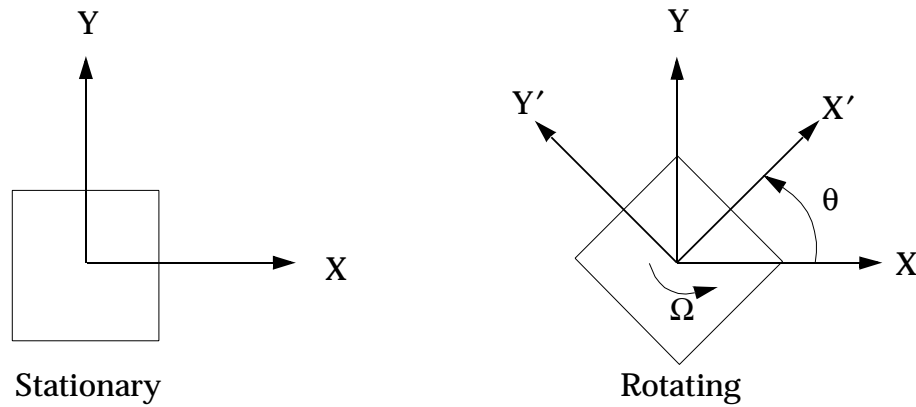
Figure 3-1 Stationary and Rotating Coordinate Systems

Assume the rotating system spins about the z-axis at a constant rate, Ω, relative to the stationary system. $x(t)_s$, $y(t)_s$, and $z(t)_s$ are the time-dependent components of the vector in the stationary system. $x(t)_r$, $y(t)_r$, and $z(t)_r$ are the time-dependent components of the vector in the rotating system.

For this example the transformation of the coordinates from the stationary to rotating system is

$$\begin{Bmatrix} x(t)_r \\ y(t)_r \\ z(t)_r \end{Bmatrix} = \begin{bmatrix} \cos\theta & \sin\theta & 0 \\ -\sin\theta & \cos\theta & 0 \\ 0 & 0 & 1 \end{bmatrix} \begin{Bmatrix} x(t)_s \\ y(t)_s \\ z(t)_s \end{Bmatrix} \qquad \text{Eq. 3-43}$$

where $\theta = \Omega t$. Equation **Eq. 3-43** is simply an expanded form of **Eq. 3-42**.

Using complex identities for $\cos\theta$ and $\sin\theta$,

$$\cos\theta = \frac{1}{2}(e^{i\theta} + e^{-i\theta}) \qquad \text{Eq. 3-44}$$

$$\sin\theta = -\frac{i}{2}(e^{i\theta} - e^{i\theta}) \qquad \text{Eq. 3-45}$$

Equation **Eq. 3-43** is written as

$$
\begin{Bmatrix} x(t)_r \\ y(t)_r \\ z(t)_r \end{Bmatrix} = \left(\frac{e^{i\theta}}{2} \begin{bmatrix} 1 & -i & 0 \\ i & 1 & 0 \\ 0 & 0 & 0 \end{bmatrix} + \frac{e^{-i\theta}}{2} \begin{bmatrix} 1 & i & 0 \\ -i & 1 & 0 \\ 0 & 0 & 0 \end{bmatrix} + \begin{bmatrix} 0 & 0 & 0 \\ 0 & 0 & 0 \\ 0 & 0 & 1 \end{bmatrix} \right) \begin{Bmatrix} x(t)_s \\ y(t)_s \\ z(t)_s \end{Bmatrix}
$$

Eq. 3-46

or

$$
\begin{Bmatrix} x(t)_r \\ y(t)_r \\ z(t)_r \end{Bmatrix} = (e^{i\theta}[T_1] + e^{-i\theta}[T_1]^* + [T_0]) \begin{Bmatrix} x(t)_s \\ y(t)_s \\ z(t)_s \end{Bmatrix}
$$

Eq. 3-47

where:

$$
[T_1] = \frac{1}{2} \begin{bmatrix} 1 & -i & 0 \\ i & 1 & 0 \\ 0 & 0 & 0 \end{bmatrix}
$$

Eq. 3-48

and the conjugate matrix is

$$
[T_1]^* = \frac{1}{2} \begin{bmatrix} 1 & i & 0 \\ -i & 1 & 0 \\ 0 & 0 & 0 \end{bmatrix}
$$

Eq. 3-49

$$
[T_0] = \begin{bmatrix} 0 & 0 & 0 \\ 0 & 0 & 0 \\ 0 & 0 & 1 \end{bmatrix}
$$

Eq. 3-50

Additionally, we can write the vectors in terms of complex components

$$
\begin{Bmatrix} x(t) \\ y(t) \\ z(t) \end{Bmatrix} = \begin{Bmatrix} \bar{x}(t)e^{i\psi_x(t)} \\ \bar{y}(t)e^{i\psi_y(t)} \\ \bar{z}(t)e^{i\psi_z(t)} \end{Bmatrix}
$$

Eq. 3-51

where:

$x(t)$, $y(t)$, and $z(t)$ are time-dependent magnitudes and

$\psi_x(t)$, $\psi_y(t)$, and $\psi_z(t)$ are time-dependent phase functions.

Substituting the above definition into **Eq. 3-47** produces the complex transformation

$$
\begin{Bmatrix} x(t)_r \\ y(t)_r \\ z(t)_r \end{Bmatrix} = [T_1] \begin{Bmatrix} \bar{x}(t)_s e^{i\psi_x(t) + \Omega t} \\ \bar{y}(t)_s e^{i\psi_y(t) + \Omega t} \\ \bar{z}(t)_s e^{i\psi_z(t) + \Omega t} \end{Bmatrix} + [T_1]^* \begin{Bmatrix} \bar{x}(t)_s e^{i\psi_x(t) - \Omega t} \\ \bar{y}(t)_s e^{i\psi_y(t) - \Omega t} \\ \bar{z}(t)_s e^{i\psi_z(t) - \Omega t} \end{Bmatrix}
$$

$$
+ [T_0] \begin{Bmatrix} \bar{x}(t)_s e^{i\psi_x(t)} \\ \bar{y}(t)_s e^{i\psi_y(t)} \\ \bar{z}(t)_s e^{i\psi_z(t)} \end{Bmatrix}
$$

Eq. 3-52

Inspection of the above equation shows that a vector defined in stationary system coordinates can be defined as three vectors in rotating system coordinates. One vector will have the phasing of its motion advanced by Ωt with respect to the stationary system definition, the second will have its phasing delayed by Ωt, and the third will have its phase unaffected.

Progressive and Regressive Vectors.

$$
\begin{Bmatrix} x(t)_r \\ y(t)_r \\ z(t)_r \end{Bmatrix} = \begin{Bmatrix} x(t)_r \\ y(t)_r \\ z(t)_r \end{Bmatrix}_+ + \begin{Bmatrix} x(t)_r \\ y(t)_r \\ z(t)_r \end{Bmatrix}_- + \begin{Bmatrix} x(t)_r \\ y(t)_r \\ z(t)_r \end{Bmatrix}_0
$$

Eq. 3-53

where

$$
\begin{Bmatrix} x(t)_r \\ y(t)_r \\ z(t)_r \end{Bmatrix}_+ = e^{i\Omega t} [T_1] \begin{Bmatrix} x(t)_s \\ y(t)_s \\ z(t)_s \end{Bmatrix}
$$

Eq. 3-54

$$
\begin{Bmatrix} x(t)_r \\ y(t)_r \\ z(t)_r \end{Bmatrix}_- = e^{-i\Omega t} [T_1]^* \begin{Bmatrix} x(t)_s \\ y(t)_s \\ z(t)_s \end{Bmatrix}
$$

Eq. 3-55

$$
\begin{Bmatrix} x(t)_r \\ y(t)_r \\ z(t)_r \end{Bmatrix}_0 = [T_0] \begin{Bmatrix} x(t)_s \\ y(t)_s \\ z(t)_s \end{Bmatrix}
$$

Eq. 3-56

It is convenient to specify the vector defined by **Eq. 3-54** as the progressive vector in rotating system coordinates, the vector defined by **Eq. 3-55** as the regressive vector in rotating system coordinates, and the vector defined by **Eq. 3-56** as the collective vector in rotating system coordinates. Care must be taken when discussing progressive and regressive vectors to establish whether the definition is in terms of the rotating or

nonrotating system. By reformulating **Eq. 3-43** as a transformation from rotating to nonrotating coordinates, one can define progressive and regressive vectors in terms of the nonrotating system.

$$
\begin{Bmatrix} x(t)_s \\ y(t)_s \\ z(t)_s \end{Bmatrix} = (e^{i\theta}[T_1]^* + e^{-i\theta}[T_1] + [T_0]) \begin{Bmatrix} x(t)_r \\ y(t)_r \\ z(t)_r \end{Bmatrix}
\qquad \text{Eq. 3-57}
$$

In this discussion, progressive and regressive are defined relative to the rotating system.

Inertial Forces in a Rotating Coordinate System

The calculation of inertial forces in a rotating coordinate system requires the introduction of an inertial reference system. An inertial reference system is defined as a coordinate system in which the motion of a particle with respect to these coordinates adhere to Newton's laws of motion. Implied in these laws is that acceleration of a particle is measured in a nonaccelerating and nonrotating coordinate system. In the above discussions the stationary coordinate system can be considered an inertial coordinate system.

Inertial force is defined as the resistance of a particle to a change in its state of rest or straight-line motion. It is expressed as Newton's well-known equation

$$
F = ma \qquad\qquad \text{Eq. 3-58}
$$

or

$$
F - ma = 0 \qquad\qquad \text{Eq. 3-59}
$$

where:

F = applied force

m = mass of the particle

a = acceleration of the particle

The term $-ma$ is referred to as the inertial force. Inertial force represents the resistance of a particle to a change in its velocity vector. It is equal in magnitude to the applied force but acts in the opposite direction.

To determine the inertial forces in a rotating coordinate system, it is necessary to transform the vector representing the acceleration of a particle in the inertial coordinate system to the rotating coordinate system. This requires: 1) determining the acceleration vector in the inertial coordinate system, then 2) transforming the acceleration vector from the inertial system coordinates to the rotating system coordinates. This results in the inertial coordinate system acceleration vector being defined in terms of rotating system vectors.

Eq. 3-57 defines a vector transformation from rotating system coordinates to stationary system coordinates. Let a vector ρ_s be defined as the position vector for a particle in the stationary system coordinates, and ρ_r be defined as the position vector in the rotating system coordinates.

$$\{\rho(t)_s\} = (e^{i\theta}[T_1]^* + e^{-i\theta}[T_1] + [T_0])\{\rho(t)_r\} \qquad \text{Eq. 3-60}$$

Taking the second derivative with respect to time produces

$$\frac{d^2\{\rho(t)_s\}}{dt^2} = (e^{i\theta}[T_1]^* + e^{-i\theta}[T_1] + [T_0])\frac{d^2\{\rho(t)_r\}}{dt^2} \qquad \text{Eq. 3-61}$$

$$+ i2\Omega(e^{i\theta}[T_1]^* - e^{i\theta}[T_1])\frac{d\{\rho(t)_r\}}{dt}$$

$$- \Omega^2(e^{i\theta}[T_1]^* + e^{-i\theta}[T_1])\{\rho(t)_r\}$$

The equation above defines the acceleration vector in the stationary or inertial coordinate system.

Eq. 3-47 represents the vector transformation from stationary system coordinates to rotating system coordinates. Applying this transformation to the stationary system acceleration vector given by **Eq. 3-61** results in the inertial system acceleration defined in rotating system coordinates, as follows:

$$\left(\frac{d^2\{\rho(t)_s\}}{dt^2}\right)_r =$$

$$(e^{i\theta}[T_1] + e^{-i\theta}[T_1]^* + [T_0])(e^{i\theta}[T_1]^* + e^{-i\theta}[T_1] + [T_0])\frac{d^2\{\rho(t)_r\}}{dt^2}$$

$$+ i2\Omega(e^{i\theta}[T_1] + e^{-i\theta}[T_1]^* + [T_0])(e^{i\theta}[T_1]^* - e^{-i\theta}[T_1])\frac{d\{\rho(t)_r\}}{dt} \qquad \text{Eq. 3-62}$$

$$- \Omega^2(e^{i\theta}[T_1] + e^{-i\theta}[T_1]^* + [T_0])(e^{i\theta}[T_1]^* + e^{-i\theta}[T_1])\{\rho(t)_r\}$$

Using the identities

$$[T_1][T_1]^* = [T_1]^*[T_1] = [0] \qquad \text{Eq. 3-63}$$

$$[T_1][T_0] = [T_1]^*[T_0] = 0 \qquad \text{Eq. 3-64}$$

$$[T_1][T_1] = [T_1] \qquad \text{Eq. 3-65}$$

$$[T_1]^*[T_1]^* = [T_1]^* \qquad \text{Eq. 3-66}$$

$$[T_0][T_0] = [T_0] \qquad \text{Eq. 3-67}$$

$$[T_1]^* + [T_1] = 2\operatorname{Re}([T_1])$$
<div align="right">Eq. 3-68</div>

$$[T_1]^* - [T_1] = -i2\operatorname{Im}([T_1]) = i2\operatorname{Re}(i[T_1])$$
<div align="right">Eq. 3-69</div>

Eq. 3-62 reduces to

$$\left(\frac{d^2\{\rho(t)_s\}}{dt^2}\right)_r = \frac{d^2\{\rho(t)_r\}}{dt^2} - 4\Omega\operatorname{Re}(i[T_1])\frac{d\{\rho(t)_r\}}{dt} - 2\Omega^2\operatorname{Re}([T_1])\{\rho(t)_r\}$$
<div align="right">Eq. 3-70</div>

The term $4\Omega\operatorname{Re}(i[T_1])$ is commonly referred to as the Coriolis acceleration and the term $-2\Omega^2\operatorname{Re}(i[T_1])$ is referred to as the centripetal acceleration. This equation provides a means of representing inertial or stationary system acceleration in terms of rotating system coordinates.

Using **Eq. 3-70**, the inertial force on a particle whose position is measured relative to a rotating coordinate system is written as

$$\begin{aligned}
\{F(t)_{inertial}\}_r &= -[M]\left(\frac{d^2\{\rho(t)_s\}}{dt^2}\right)_r \\
&= -[M]\left(\frac{d^2\{\rho(t)_r\}}{dt^2} - 4\Omega\operatorname{Re}(i[T_1])\frac{d\{\rho(t)_r\}}{dt} - \Omega^2 2\operatorname{Re}([T_1])\{\rho(t)_r\}\right)
\end{aligned}$$
<div align="right">Eq. 3-71</div>

This equation can be written as

$$\{F(t)_{inertial}\}_r = -\left([M]\left(\frac{d^2\{\rho(t)_r\}}{dt^2}\right) - \Omega[B^c]\left(\frac{d\{\rho(t)_r\}}{dt}\right) - \Omega^2[K^c]\{\rho(t)_r\}\right)$$
<div align="right">Eq. 3-72</div>

where (for rotation about the z-axis)

$$[M] = \begin{bmatrix} m & 0 & 0 \\ 0 & m & 0 \\ 0 & 0 & m \end{bmatrix}$$
<div align="right">Eq. 3-73</div>

$$[B^c] = \begin{bmatrix} 0 & 2m & 0 \\ -2m & 0 & 0 \\ 0 & 0 & 0 \end{bmatrix}$$
<div align="right">Eq. 3-74</div>

$$[K^c] = \begin{bmatrix} m & 0 & 0 \\ 0 & m & 0 \\ 0 & 0 & 0 \end{bmatrix}$$
<div align="right">Eq. 3-75</div>

Structural Impedance of a Rotating Structure

In Eq. 3-72, the inertial forces are dependent on the time-varying position of a mass particle. This position vector can be written in terms of an initial component and a time-varying component.

$$\{\rho(t)\}_r = \{\rho_r\} + \{u(t)_r\}$$

Eq. 3-76

Eq. 3-72 can be rewritten using the above equation as

$$\{F(t)_{inertial}\}_r = -\left([M]\left(\frac{d^2\{u(t)_r\}}{dt^2}\right)\right.$$
$$\left. - \Omega[B^c]\left(\frac{d\{u(t)_r\}}{dt}\right) - \Omega^2[K^c](\{\rho_r\} + \{u(t)_r\})\right)$$

Eq. 3-77

Inertial forces due to the mass are resisted by structural stiffness and damping.

$$[B]\left(\frac{d\{u(t)_r\}}{dt}\right) + [K]\{u(t)_r\} = \{F(t)_{inertial}\}_r$$

Eq. 3-78

Substituting Eq. 3-77 in the above equation and collecting all time-dependent terms on the left-hand side results in

$$[M]\left(\frac{d^2\{u(t)_r\}}{dt^2}\right) + ([B] - \Omega[B^c])\left(\frac{d\{u(t)_r\}}{dt}\right) + ([K] - \Omega^2[K^c])\{u(t)_r\}$$
$$= \Omega^2[K^c]\{\rho_r\}$$

Eq. 3-79

The above equation is the equation of motion for a particle in a rotating elastic structure with no externally applied forces. The loading on the right-hand side of Eq. 3-79 is often called the centripetal force. The centripetal force is always present on a rotating structure and produces an additional stiffness-like term. This additional term can be determined from consideration of the standard static equilibrium equation for a single element.

$$Ku = P$$

Eq. 3-80

where:

K is the element stiffness in global coordinates (coordinates used to define motion).

u is the displacement in global coordinates.

P is the load in global coordinates.

The deformation, u, produces element reaction forces, F, which balance the applied load, P. The stiffness, K, can be viewed as the change in the element reaction forces with respect to a change in displacement.

$$K = \frac{dF}{du} = \frac{d(TF_e)}{du} \qquad\qquad \text{Eq. 3-81}$$

$$K = T\left(\frac{dF_e}{du}\right) + F_e\left(\frac{dT}{du}\right) \qquad\qquad \text{Eq. 3-82}$$

$$K = T\left(\frac{du_e}{du}\right)\left(\frac{dF_e}{du_e}\right) + F_e\left(\frac{dT}{du}\right) \qquad\qquad \text{Eq. 3-83}$$

where:

F is the internal element force in global coordinates.

T is a transformation from element to global coordinates.

F_e is the internal element force in element coordinates.

u_e is a displacement in element coordinates.

For a linear material and a loading which is not dependent on displacement, the term dF_e/du_e is constant, the element forces are linearly related to the element displacements. The terms T and du_e/du are dependent only on the orientation of the element coordinate system with respect to the global coordinate system. For small displacement problems, T and du_e/du are assumed constant and are calculated from the undeformed geometry. The three terms (T, du_e/du, and dF_e/du_e) are used to calculated the linear element stiffness matrix in global coordinates. The element stiffness matrices are assembled to create the complete linear stiffness matrix for the structure.

The second part of the stiffness calculation, $F_e(dT/du)$, is usually ignored in standard linear analysis. It arises from small changes in the element orientation with respect to the applied load. For example, consider a bar under axial and transverse loading.
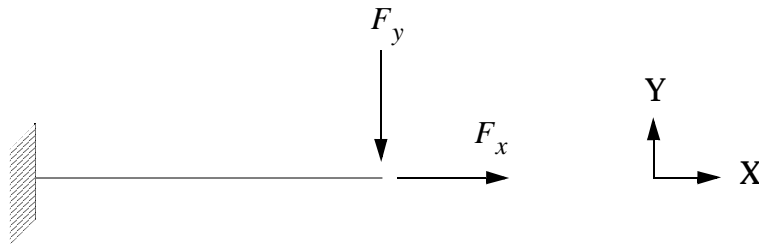
Figure 3-2 Cantilevered Bar With Axial and Transverse Loading

In a standard linear analysis, the y-directed load is reacted by the bar bending and shear forces. The x-directed load is reacted by the bar axial forces. The calculated y displacement is independent of the x-directed load. Likewise, the calculated x displacement is independent of the y-directed load. On closer inspection, one would find that as the free end of the bar rotates with respect to the applied loads, a component of the bar axial force reacts against the y-directed load. Likewise, a component of the bar bending and shear react to the x-directed load.
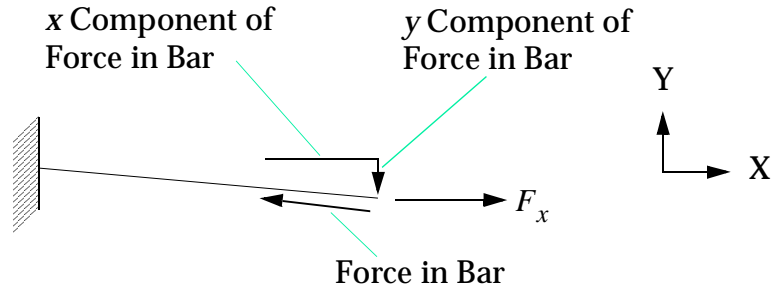
Figure 3-3 Bar Forces Due to Axial Loading

This results in a stiffness coupling which is not taken into account by standard linear analysis. This effect is due to the $F_e(dT/du)$ term in **Eq. 3-83** and is referred to as the *differential* stiffness term. Its calculation requires knowledge of the element force F_e and the transformation matrix T. The total stiffness matrix, often referred to as the tangent stiffness matrix, is the sum of the linear and differential stiffnesses.

Eq. 3-79 shows that a centripetal load is always present in a rotating structure. This constant loading results in a differential stiffness term which must be included for accurate analysis of rotating structures. The differential stiffness is added to the stiffness terms on the left-hand side of **Eq. 3-79**. The complete equation of motion for a rotating structure, neglecting the centripetal loading is

$$[M]\left(\frac{d^2\{\Delta\rho(t)_r\}}{dt^2}\right) + ([B] - \Omega[B^c])\left(\frac{d\{\Delta\rho(t)_r\}}{dt}\right)$$ Eq. 3-84

$$+ ([K] + \Omega^2[K^d] - \Omega^2[K^c])\{\Delta\rho(t)_r\} = 0$$

The above equation can be used to determine the motion of a rotating structure about the deformation due to the centripetal loading.

DMAP Procedure to Add Rotation-Dependent Terms to MSC.Nastran Dynamic Analyses

These alters may be used for the following problems:

- To determine critical speeds of rotating machinery, such as shafts and turbines.

- To predict effects of unbalanced forces at selected rotational speeds.

- To simulate transient behavior relative to the steady-state rotation.

Note: In rotor dynamics shafts are often modeled with BEAM elements and the axisymmetric disks as rigid bodies (CONM2s). Due to the polar movement of inertia of these disks, there is a gyroscopic effect on the critical speeds. Unfortunately, the DMAP alters discussed below do not allow for this gyroscopic effect.

The procedure to add rotation-dependent terms to an MSC.Nastran analysis is done in two steps: 1) Calculate the rotation-dependent terms and add them to the structural damping

The first step is performed in SOL 101 (linear static analysis) or SOL 114 (cyclic linear static analysis). A centripetal load is specified (RFORCE entry in the bulk data) as the only loading (one subcase only). A DMAP alter uses this information to calculate all rotation-dependent terms, adds them to the structural damping and stiffness matrices, and stores the modified matrices on the database.

The second step is performed as a restart in any structured linear solution sequence. The modified matrices are reduced and the analysis is performed. The user may change the SPCs, MPCs, and loading, but not the actual structure.

Three alters are available in the SSSALTER library; they are:

segyroa.vxx Adds gyroscopic and differential stiffness terms to noncyclic symmetry superelement models. The alter is added to SOL 101. Restarts to any structured superelement solution sequence are allowed.

cygroa.vxx Adds gyroscopic and differential stiffness terms to cyclic symmetric superelement models. The alter is added to SOL 114. Restarts to any structured cyclic symmetry solution sequence is allowed.

nlgyroa.vxx Adds gyroscopic terms to the normal modes calculation in SOL 106 (nonlinear statics). No restart is required, normal modes are calculated in SOL 106 if PARAM,NMLOOP is included in the input file.

A readme file (readme.gyro) and example problems are also included in the SSSALTER library.

3.4   Overview of Aeroelastic Analysis

MSC.Nastran provides efficient solutions to the problems of aeroelasticity, which is a branch of applied mechanics that deals with the interaction of aerodynamic, inertial, and structural forces. It is important in the design of airplanes, helicopters, missiles, suspension bridges, and even tall chimneys and power lines. Aeroservoelasticity is a variation in which the interaction of automatic controls requires additional consideration.

The primary concerns of aeroelasticity include flying qualities (stability and control), flutter, and structural loads arising from maneuvers and atmospheric turbulence. Methods of aeroelastic analysis differ according to the time dependence of the inertial and aerodynamic forces that are involved. For the analysis of flying qualities and maneuvering loads wherein the aerodynamic loads vary relatively slowly, quasi-static methods are applicable. The remaining problems are dynamic, and methods of analysis differ according to whether the time dependence is arbitrary (transient or random) or simply oscillatory in the steady state.

MSC.Nastran considers three classes of problems in aeroelasticity:

- Static Aeroelastic Response
- Aerodynamic Flutter
- Dynamic Aeroelastic Response

Each is described in the text that follows. In addition, information is provided on the ability to include aeroelastic responses within the MSC.Nastran optimization capability, the aerodynamic methods available, and on special features that make the MSC.Nastran aeroelastic capability unique.

Static Aeroelastic Response

For the analyses of flying qualities and maneuvering loads, the assumption of quasi-steady motion is valid, i.e., the dynamics of the flexible structure are neglected and quasi-static methods are applicable. By assuming linear behavior of the aerodynamic, inertial and structural forces during the motion, the equations of equilibrium in quasi-steady flight are solved in closed algebraic (matrix) form. Linear and/or surface splines may be used to connect the aerodynamic and structural grid points.

The static aeroelastic analysis solves for the trim condition in a prescribed maneuver. The formulation of the equilibrium equations provides the aerodynamic stability and control derivatives as an integral part of the trim process. The external flight loads and the corresponding internal loads and stresses on the finite elements, are available as postprocessing operations on the trim solution.

Static aeroelastic divergence is a non-oscillatory instability condition that can occur when the aerodynamic forces overpower the stiffness of the structure. For free-flying vehicles, this phenomenon is typically not of concern, but it can be critical in the structural design of restrained wind tunnel models. Static aeroelastic divergence analysis can be performed as an option within the overall static aeroelastic capability.

Aerodynamic Flutter

Flutter is the oscillatory aeroelastic instability that occurs at some airspeed at which energy extracted from the airstream during a period of oscillation is exactly dissipated by the hysteretic damping of the structure. The motion is divergent in a range of speeds above the flutter speed. Flutter analysis utilizes complex eigenvalue analysis to determine the combination of airspeed and frequency for which the neutrally damped motion is sustained.

Three methods of flutter analysis are provided: the American flutter method (called the K-method in MSC.Nastran), an efficient K-method (called the KE-method) for rapid flutter evaluations, and the British flutter method (called the PK-method) for more realistic representation of the unsteady aerodynamic loads as frequency dependent stiffness and damping terms. The complex eigenvalue analysis is specified by the user with the K-method, and the QR-transformation method is used with the KE- and PK-methods. Again, linear and/or surface splines may be used to connect the aerodynamic and structural grid points.

Dynamic Aeroelastic Response

The dynamic aeroelastic response problem is one of determining the response of the aircraft to time-varying excitations. Atmospheric turbulence is the primary example of this type of excitation, but store ejection loads and landing gear impact can also have an aeroelastic component. Methods of generalized harmonic (Fourier) analysis are applied to the linear system to obtain the response to the excitation. The turbulence model may be regarded either as a stationary random loading or as a discrete gust.

The gust analysis capability computes response to random atmospheric turbulence and discrete one-dimensional gust fields. The random response parameters calculated are the power spectral density, root mean square response, and mean frequency of zero-crossings. The response to the discrete gust is calculated by direct and inverse Fourier transform methods since the oscillatory aerodynamics are only known in the frequency domain. Time histories of response quantities are the output in the discrete case.

Aeroelastic Optimization

The integration of the aeroelastic analysis capability contained in MSC.Nastran with a design sensitivity and optimization capability provides a new (Version 68) design tool for the aeroelastician. Sensitivity analysis entails the determination of the effects that changes in structural properties have on response quantities, such as displacements or stresses. Optimization utilizes information on the response values and their sensitivities to automatically determine a design that meets a design objective, such as limits on stresses, deformations, or flutter characteristics. The static aeroelastic and flutter analyses are available within the MSC.Nastran optimization capability and can be used in multidisciplinary fashion along with standard static analysis, normal modes analysis, and dynamic response analysis. Dynamic aeroelastic response is not available for

optimization. Aeroelastic responses available for the sensitivity and optimization include stability derivatives and trim settings from the static aeroelastic analysis and flutter damping level from the flutter analysis.

Aerodynamic Methods

Five oscillatory aerodynamic theories are available for flutter analysis. There is one subsonic method, the Doublet-Lattice Method with body interference, and three supersonic methods: the Mach Box Method, Piston Theory, and a new (Aero II option) multiple interfering surface method called ZONA51. The fifth method is rudimentary Strip Theory, which can be applied at any Mach number. The static and dynamic aeroelastic response solutions use both the subsonic Doublet-Lattice and supersonic ZONA51 aerodynamic methods.

Special Features

Aeroelastic analysis in MSC.Nastran provides several advances in the state of-the art. The fundamental problem of interconnecting the aerodynamic and structural grids in the finite element models is solved by a closed form solution to an infinite plate over multiple supports. This two-dimensional interpolation was developed in addition to a generalization of the one-dimensional spline for a bending, twisting beam (elastic axis) on multiple collinear supports.

The implementation of the lined-up British flutter method, called the PK-method in MSC.Nastran, was the first attempt to popularize the British approach to flutter analysis in the United States. This, along with the transfer function capability for control systems, makes analysis of aeroservoelastic problems a routine matter. The transfer function representation is for second order systems: a single output from multiple inputs.

The analysis of response to a discrete gust requires Fourier transform methods, because the aerodynamics assume harmonic motion. First, a direct transform of the discrete gust profile is necessary to place the forcing function in the frequency domain. Second, an inverse Fourier transform of the forced frequency response is necessary to obtain the transient response of vehicles to the gust. Both the direct and inverse Fourier transform calculations have been implemented in MSC.Nastran.

The quasi-steady equations of motion of a free-flying vehicle require consideration of the inertial relief effects. For the unrestrained vehicle, the inertial effects are contained in the basic stability and control derivatives. However, derivatives that are independent of weight distribution are desirable for use in flight simulators, and are obtained by assuming the aircraft to be restrained in some reference support configuration. The equations of motion using restrained aeroelastic derivatives require not only additional inertial derivatives, but also the rotations of the mean axes relative to the support for each aerodynamic variable (e.g., angle of attack, elevator rotation, pitch rate). These additional aeroelastic coefficients permit the support to be unloaded and angular momentum to be conserved. MSC.Nastran provides both restrained and unrestrained aeroelastic derivatives, and in the restrained case, the inertial derivatives and mean axis rotations.

Control systems can also be included in dynamic response analysis using MSC.Nastran transfer functions. With this feature, the aeroservoelastic interactions of ride comfort and load alleviation systems can be investigated.

The MSC.Nastran procedure has general capabilities that are beyond those listed here, and their application to aeroelastic design is limited only by the analyst's ingenuity. For example, aerothermoelasticity considers the effects of thermal stresses on structural stiffness and the subsequent aeroelastic interactions. MSC.Nastran provides a capability for nonlinear static analysis that includes temperature loadings. Aerothermoelastic problems of high speed flight can therefore be addressed by restarting any of the three aeroelastic analyses from a database created by the nonlinear analysis that has generated the stiffness of the heated structure.

Boundary Conditions and Coupling to Other Disciplines

- Overview

- Enforced Motion with Loads

- Lagrange Multiplier Technique

- Axisymmetric Fluids in Tanks

- Virtual Fluid Mass

- Coupled Acoustic Analysis

4.1　Overview

This chapter extends the discussion of basic dynamic loads and boundary conditions given in the *MSC.Nastran Basic Dynamic Analysis User's Guide*. This chapter describes some of the more advanced methods available in MSC.Nastran for dealing with these problems.

Although applying dynamic loads to a structure is a relatively straightforward task when using the finite element method, the process of specifying a moving boundary requires more work. Examples of enforced motions of a structural boundary include earthquakes on a building, automobile suspensions, and any vibration affecting a light, flexible structure connected to a massive, moving body. This chapter describes approximate and exact solution techniques for this type of problem.

Another type of boundary condition is a fluid or gas coupled with the surface of a structure. If these fluids are assumed to have small motions, they generate linear matrices and allow the use of conventional solution methods. This chapter describes three approaches to the coupled fluid-boundary problem, each with a unique set of capabilities.

4.2 Enforced Motion with Loads

Three distinct methods are used in MSC.Nastran for dynamic enforced motions: the Large Mass/Spring approach, the Inertial Loads method, and the Lagrange Multiplier (LMT) method (described in "**Lagrange Multiplier Technique**" on page 92). The first two are covered in this section.

Large Mass/Spring Method

The Large Mass/Spring approach is actually a modeling technique in which the user places an element with a large mass or stiffness at the points of known acceleration or displacement. In effect, this large element acts as a constraint on the connected point. The user then supplies a corresponding large force via RLOADi or TLOADi inputs to produce the desired motion. If the added element is sufficiently stiff or heavy, the reaction forces from the actual structure will not affect the input motions. The actual input data and controls are described in "**Enforced Motion**" on page 197 of the *MSC.Nastran Basic Dynamic Analysis User's Guide*. Refer to them for modeling details. More advanced applications of both large mass and large spring techniques are discussed below.

Using a large mass to enforce boundary motions is a standard practice in MSC.Nastran. It works well on a simply supported structure when a single grid point is excited by a well defined acceleration input. A typical example is the earthquake analysis of a tall building where a single base input is assumed. However the method may be abused when other types of boundary conditions are attempted.

Some additional considerations for the advanced analyst are listed below:

1. If enforced motion is applied to a redundant set of boundary points, a danger exists that the large masses (or springs) may create fictitious forces and stresses in the structure. This occurs when the enforced displacements inputs are not precisely synchronized. Also, in a modal formulation, the extra masses will cause fictitious low frequency modes to occur. The recommended procedure is to connect the redundant points with RBE (rigid) elements to prevent their independent motions. The Lagrange Multiplier method is much better, but will not correct for errors in the loading functions. (See next note.)

2. Small errors in the loading history may cause large errors in the structural response. When using enforced accelerations in a transient solution, a small bias in the inputs (from instrumentation or processing) may cause a large spurious drift where the structure displaces a large amount as a rigid body. Solutions to remove the drift are as follows:

   • Supply a corrective load function, obtained from an initial run, to cancel the measured drift;

   • Add dampers and springs in parallel with mass and tuned to filter the input signal; or

   • Use the modal method and drop the zero-frequency modes. (See item 4 below.)

An example of a mechanical filter is shown in the sketch below. A large mass, M_0, is attached to the base of a structure to allow enforced accelerations. For control of the spurious displacements and velocities, attach a scalar spring, K, and damper element, B, between the mass and ground for each direction. If the first modal frequency is f_1 then set $K = 0.4\, M f_1^2$ for a filter frequency approximately one tenth of the first vibration mode frequency, f_1. Set the damping coefficient to a value near critical to eliminate spurious oscillations.
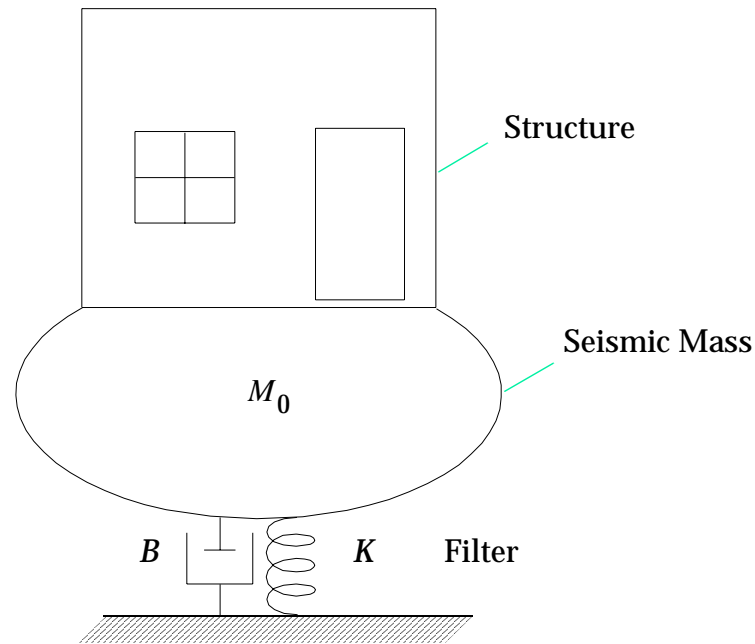
3. In the nonlinear transient solutions, large springs can affect the error tests and convergence logic. The internally calculated error ratios are dimensionless numbers obtained by dividing the errors by an average force or total energy. The forces and energy created by the large mass/spring approach will dominate these values, resulting in underestimates of the errors and false convergence. The solution is to decrease the error allowables on the TSTEPNL Bulk Data inputs.

4. Using these methods in a modal formulation requires some attention. For output of total displacements, the user should retain the zero or low frequency modes that the large masses produce (i.e., set the parameter *LFREQ* = − .01). Note that if the low frequency modes are dropped from the dynamic solution, the output will be the correct relative motion.

   Large springs for enforced displacements are not recommended for the modal formulations. They should generate high frequency modes that are usually missing from the system. The resulting dynamic solution is not valid since the large springs are not included in the modal stiffness matrix.

5. Numerical conditioning of the matrix solution may be affected by the method used to connect the large mass or spring. Numerical roundoff of the results may occur. MPCs, RBEi's, and ASET operations all use a matrix elimination procedure that may couple many degrees-of-freedom. If a large mass or spring is not retained in the solution set, its matrix coefficient will be distributed to other solution points. Then, matrix conditioning for decomposition operations

becomes worse, when the large terms dominate the significant finite element coupling terms). On the other hand, if the degrees-of-freedom with the large terms remain in the solution set, they remain on the diagonal of the matrix and the matrix decomposition is unaffected.

In summary, the large mass method is recommended for cases with known accelerations at a single point. It works well with the modal formulation, providing good stress and forces near the mass, and is easy to understand and use. In many cases, the structure is actually excited by the motions of a large, massive, base (for instance, the geological strata) which can actually be used as a value for the mass.

The large spring method is recommended for cases in which displacements are known at one point and a direct formulation is used. The primary advantage is its simplicity. However, the inertial loads approach or Lagrange Multiplier technique, described below, are more general and have better reliability.

The Inertial Loads Approach

By changing to a moving coordinate system, the reference accelerations may be converted to inertial loads. If the dynamic problem involves a free body connected to a single rigid base, the GRAV and dynamic load inputs may be used to supply forces proportional to the base acceleration. The solution will be defined by the displacements measured relative to the fixed base.

Approach

The basic approach is shown in the sketch below:
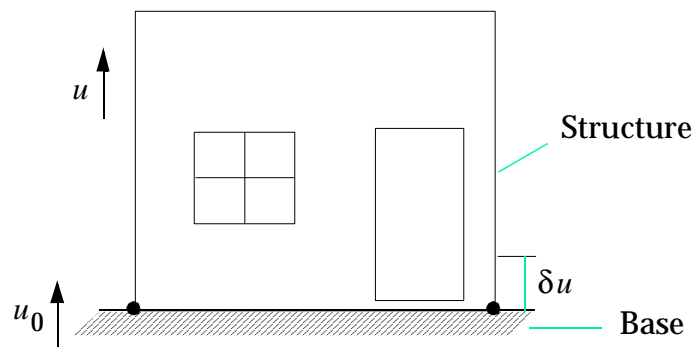
We assume that the motions of the rigid base are known and the structure is fixed only to the base. Define the displacement vector, u, as a sum of the known base motion, u_0 and the relative displacements, δu by the equation

$$\{u\} = \{\delta u\} + [D]\{u_0\}$$

Eq. 4-1

where $[D]$ is the rigid body transformation matrix that includes the effects of coordinate systems, offsets, and multiple directions. If the structure is a free body and aerodynamic effects are neglected, the base motions should not cause any static or viscous forces and

$$[K][D] = 0$$

Eq. 4-2

$$[\quad][\quad]$$

where $[K]$ is the stiffness matrix and $[B]$ is the damping matrix. These properties allow us to remove the reference motions from the solution as shown below.

The equilibrium equation for the whole system is

$$[M]\{\ddot{u}\} + [B]\{\dot{u}\} + [K]\{u\} \;=\; \{P\} \qquad\qquad \text{Eq. 4-3}$$

Substituting Eq. 4-1 and Eq. 4-2 into Eq. 4-3, we obtain

$$[M]\{\delta\ddot{u}\} + [B]\{\delta\dot{u}\} + [K]\{\delta u\} \;=\; \{P\} - [M][D]\{\ddot{u}_0\} \qquad\qquad \text{Eq. 4-4}$$

The solution matrices have not changed, but the solution, δu, must be zero at the base attachment points. The right-hand term in Eq. 4-4 may be calculated in MSC.Nastran using one of several options. One option is the response spectra analysis described in "Shock and Response Spectrum Analysis" on page 221. Another is a recent MSC.Nastran implementation that now allows time-dependent gravity loads. By definition, the GRAV input generates load vectors of the form

$$\{P^g\} \;=\; [M][D]\{g\} \qquad\qquad \text{Eq. 4-5}$$

where g is the gravity vector. Then if g were time dependent, it could be used to replace u_0 in Eq. 4-4 if

$$\{g(t)\} \;=\; -[\ddot{u}_0(t)] \qquad\qquad \text{Eq. 4-6}$$

Input Data

The inertial loads method is available for all dynamic response solutions. Refer to the *MSC.Nastran Basic Dynamic Analysis User's Guide* for the complete input procedure for using static loads in a dynamic response analysis. The method is valid for both direct and modal formulations and is automatic in nonlinear and superelement models. Briefly, the necessary input data is as follows:

1. LOADSET = N – a Case Control request for processing a LSEQ (load sequence) set.
2. LSEQ – Bulk Data that connects the forces resulting from the GRAV data to a dynamic DAREA set. Several load vectors may be included in the same LSEQ set.
3. GRAV– Bulk Data defining an acceleration vector. Several may be included to define different functions of time for the different directions.
4. SPC – remember to fix the base attachments.
5. TLOADi or RLOADi Bulk Data for the dynamic load definition. Refers to the DAREA set defined in the LSEQ data.

Other necessary inputs are the conventional DLOAD and TABLEDi data to help define the time functions. DAREA Bulk Data is not necessary.

Recommendations

The following comments describe the benefits and drawbacks to the method:

1. The solution will avoid the problem of rigid body drift that occurs in the other methods when small errors are present in the input accelerations.

2. By eliminating large constant terms, the stress and force calculations may be numerically more precise.

3. The method is compatible with superelement and nonlinear solution sequences.

4. No special sets or SUPORT data is necessary.

5. The main drawback is that the output accelerations are also relative and will not correlate to measured accelerations.

For a method that solves for total response directly, see "**Lagrange Multiplier Technique**" on page 92.

4.3   Lagrange Multiplier Technique

The Lagrange Multiplier Technique (LMT) is a special option for processing constraints in matrix solutions. It can be used for all constraints and reduction methods such as SPC, MPC, and rigid elements. LMT can also be used for enforced motion analysis in dynamic analysis. Unlike the approximate large mass approach, the LMT is an exact method. The LMT requires adding extra degrees-of-freedom to the matrix solution that are used as force variables for the constraint functions. Coefficients are added to the matrices for the equations that couple the constrained displacement variables to the points at which enforced motion are applied.

The LMT produces indefinite system matrices that require special resequencing of variables for numerical stability by either the user or by a special solver. The sparse matrix solver first introduced in Version 67 includes an automatic row and column interchange capability that allows reliable and efficient solution of indefinite matrices without the need for the user to sequence variables for numerical stability. This solver is installed in several more modules in the current version of MSC.Nastran such as the transient and frequency response solver modules. The alter package takes advantage of their capability.

The DMAP alter introduces the LMT variables automatically without the need for special user input. The user interface is basically unchanged. The only new inputs are the INCLUDE entry to bring in the alter package, some optional new PARAM entries for special operations, and a new enforced motion specification that is less complex than that of the large mass method for enforced motion while providing better accuracy and numerical stability. A few capabilities are blocked in this implementation as described at the end of the user interface description. Details of the user interface are given below.

In summary, the DMAP implementation of the LMT method may be considered for any linear analysis. It brings the largest advantages when the number of boundary constraint equations is large or when superelement models are involved.

A Comparison of Condensation and Augmentation Solution Methods

A small model is used here to contrast the conventional method of constraint elimination and the LMT method of constraint augmentation. Consider the statics model shown below.
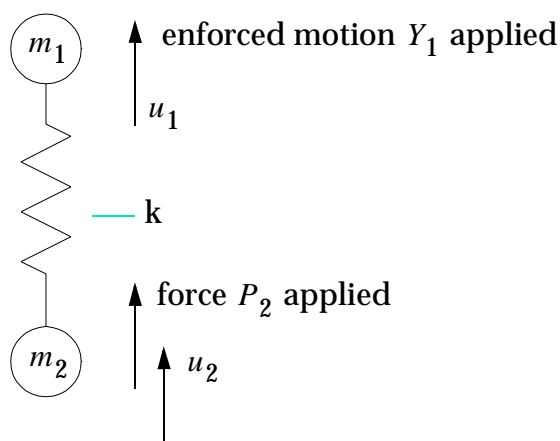
Given this model, static equations of motion are as follows:

$$[K]\{u\} = \{P\} + \{q\}$$

<div align="right">Eq. 4-7</div>

$$u_1 = Y_1$$

<div align="right">Eq. 4-8</div>

$\{q\}$ contains the unknown constraint forces required to cause the enforced motion and react to the applied force. Y_1 is the known enforced displacement, and P_2 is the known applied force.

In the LMT method, the constraint equations are included in the system equations. The displacement constraint can be written in matrix form after q_1 is moved to the left side,

$$\begin{bmatrix} 0 & 1 & 0 \end{bmatrix} \begin{bmatrix} -q_1 \\ u_1 \\ u_2 \end{bmatrix} = Y_1$$

<div align="right">Eq. 4-9</div>

This row and a corresponding column are added to the system matrix to produce

$$[K] = \begin{bmatrix} 0 & 1 & 0 \\ 1 & k & -k \\ 0 & -k & k \end{bmatrix}, \quad \{P\} = \begin{Bmatrix} Y_1 \\ 0 \\ P_2 \end{Bmatrix}, \quad \{u\} = \begin{Bmatrix} -q_1 \\ u_1 \\ u_2 \end{Bmatrix}$$

<div align="right">Eq. 4-10</div>

In the equation $[K]\{u\} = \{P\}$, the known vector quantities are now all on the right side, and the unknown vector quantities on the left side. This equation can be solved directly without the need for partitioning or constraint elimination. In dynamic analysis, enforced motion can be input on velocity and acceleration variables directly by similar techniques. The system has a unique solution even though there are null terms on the diagonal of $[K]$. These null terms are an indication of an indefinite matrix.

For a conventional modal solution, the unconstrained equation for eigensolution is

$$\begin{bmatrix} k - \lambda m_1 & -k \\ -k & k - \lambda m_2 \end{bmatrix} \begin{Bmatrix} u_1 \\ u_2 \end{Bmatrix} = \{0\}$$

<div align="right">Eq. 4-11</div>

When the constraint reduction process is used, the first row and column are eliminated. The resulting equation for the eigenvalue λ is then

$$\lambda = k/m_2$$

<div align="right">Eq. 4-12</div>

Alternatively, using the LMT process, the system is augmented with the constraint variables, with the resulting determinant

$$
\begin{bmatrix} 0 & 1 & 0 \\ 1 & k - \lambda m_1 & -k \\ 0 & -k & k - \lambda m_2 \end{bmatrix} = 0 \qquad \text{Eq. 4-13}
$$

When this determinant is evaluated, the only non-null product results from the $(12)(21)(33)$ terms, resulting in the same expression, $\lambda = k / m_2$.

Three counter-intuitive consequences are as follows:

1. m_1 does not enter into the determinant at all, even though it is present in the matrix. In a constraint reduction process, by contrast, any mass term that appears in the matrix used for eigensolution affects the eigenvalues.

2. Although the matrix has three rows and columns and two mass terms on its diagonal, only one value of λ is defined. One might expect that this system would have two or three values for λ, but it does not. Other values of λ beyond this single value are neither zero nor infinity nor any other value. They are simply undefined.

3. The results from a condensation solution and an augmentation solution are identical. This is a general rule.

The resulting eigenvector is

$$
\{\phi\} = \begin{Bmatrix} -r \\ \phi_{c1} \\ \phi_{c2} \end{Bmatrix} = \begin{Bmatrix} k \\ 0 \\ 1.0 \end{Bmatrix} \qquad \text{Eq. 4-14}
$$

Where ϕ_c is the constrained eigenvector for the displacements and r is the reaction force. Note the scale factor of the whole eigenvector may be affected by r if the normalization method is MAX. For a dynamic solution using a modal formulation, the matrices are transformed using the modes above. In the stiffness, mass, and damping matrices, the constraint coefficients have no effect. However, if Y_1 is an enforced displacement, the generalized modal forces are

$$
P_\xi = \phi c^T P_g - r^T Y_1 = P_{2-k} Y_1 \qquad \text{Eq. 4-15}
$$

The result of applying an enforced displacement on the LMT coordinates, Y_1, will be a modal force in the opposite of the direction of motion. The results of a modal solution will be relative to Y_1. See below for a solution that provides total displacements.

Matrix Theory for Dynamic Response

Notation

The notation of the conventional solutions is described in "**Constraint and Set Notation**" on page 255 of the *MSC.Nastran Reference Manual*. It is maintained with the following changes. The Lagrange Multiplier Technique requires the definition of enforced motion

variables. Their DOFs are placed in the u_1, u_2, and u_3 sets. These sets are members of the USET table but are not used in the conventional solution method. They are defined on USETi Bulk Data entries. They are regarded as members of the b-set in the alter package, and have the following meanings:

New Unique Sets for Enforced Motion

u_1 Enforced displacement set

u_2 Enforced velocity set

u_3 Enforced acceleration set

The Unique Sets

Almost all of the letters of the alphabet are already in use to describe sets in the conventional solutions. Therefore, sets with integers for names are added to the present set names which use letters of the alphabet instead.

Direct Solutions in the Frequency and Time Domains

The statement of the frequency response problem is

$$[A_{dd}(\omega)]\{u_d\} \;=\; \{P_d(\omega)\} \qquad\qquad \text{Eq. 4-16}$$

where:

$$[A_{dd}(\omega)] \;=\; [K + i\omega B - \omega^2 M]_{dd} \qquad\qquad \text{Eq. 4-17}$$

$[K]$, $[B]$, and $[M]$ are the stiffness, damping, and mass matrices, respectively, and ω is the excitation frequency. If static or dynamic reduction are not used, most of the constraints are placed in the stiffness matrix. The advantage of this placement is that the constraints are not multiplied by ω. This allows the solution of the equations at an excitation frequency near to zero. The remaining constraints are associated with enforced motion variables. These constraints are placed in the stiffness, damping, or mass matrix depending on whether the enforced motion is the displacement, velocity, or acceleration type, respectively. If static or dynamic reduction is performed, all m- and s-set constraints are eliminated along with the o-set. The u_3-set is then the only constraint set in the d-set.

The DOFs listed on USET entries are input points for enforced motion. Data conventionally used to define dynamic loads applied to these points is interpreted to be time- or frequency-varying enforced motions. The value of the SETNAME entry on the USET entries determines the type of input. A value of u_1 indicates an enforced displacement type. A value of u_2 indicates an enforced velocity type, and a value of u_3 indicates an enforced acceleration type. These dynamic quasi-loads are transferred to the enforced motion variables by the transformation matrix $[T_{4\underline{p}}]$ as follows:

$$[P_4(\omega)] \;=\; [T_{4\underline{p}}][P_{\underline{p}}(\omega)] \qquad\qquad \text{Eq. 4-18}$$

$[P_{\underline{p}}]$ is the load vector output by the FRLG module. In this context it may contain both applied forces and enforced motions. $[T_{4\underline{p}}]$ has a unit term in each row at the column corresponding to the u_i-set point where enforced motion is applied. The enforced motions are removed from the displacement variables by the transformation matrix $[T_{\underline{pp}}^x]$,

$$[P_{\underline{p}}(\omega)] = [T_{\underline{pp}}^x][P_{\underline{p}}(\omega)] \qquad \text{Eq. 4-19}$$

where $[T_{\underline{pp}}^x]$ is an identity matrix except for the rows associated with enforced motion terms, where it has a zero row. The $\underline{p}$-set and u_4-set components are merged to form $[P_p(\omega)]$.

The stiffness and constraint components are separated into $[K_{aa}^g]$ and $[R_{aa}]$, respectively, where $[K_{aad}] = [K_{aa}^g] + [R_{aa}]$. This is done in the GMA subDMAP to ensure that the constraints are not multiplied by the damping factor iG.

The equations for transient response analysis are similar to those for frequency response analysis. The subDMAPs for the two types of analysis closely parallel each other.

A new set of partitions not actually used in the DMAP implementation is introduced here. This set aids in understanding the effects of the enforced motion variables. Let

$$\{u_d\} = \begin{Bmatrix} q_3 \\ u_3 \\ u_c \end{Bmatrix} \qquad \text{Eq. 4-20}$$

and

$$\{P_d\} = \begin{Bmatrix} Y_3 \\ P_3 \\ P_c \end{Bmatrix} \qquad \text{Eq. 4-21}$$

The 3-set contains the constraint force and displacement variables associated with enforced motion. $\{q_3\}$ is the vector of constraint forces and $\{u_3\}$ the vector of constraint displacements. Both are partitions of the $\{u_d\}$ vector and $\{u_c\}$ is their complement. $\{Y_3\}$ is the vector of enforced displacements, $\{P_3\}$ additional forces placed on the enforced motion points, and $\{P_c\}$ their complement. The enforced motions of any LMT variables contained in $\{P_c\}$ are zero by definition. $\{u_c\}$ contains both displacement and constraint force unknown variables, while $\{P_c\}$ contains both known input displacements and applied forces.

Consider the case of enforced displacement. $[K]$ then has the partitions

$$[K] = \begin{bmatrix} 0 & R_{33} & R_{3c} \\ & K_{33} & K_{3c} \\ \text{Sym.} & & K_{cc} \end{bmatrix} \qquad \text{Eq. 4-22}$$

$[R_{33}]$ is a subset of the constraint matrix $[R_{4_g}]$. By inspection, $[R_{33}] = [I_{33}]$, an identity matrix, and $[R_{3_c}]$ is null. The form of the equation of motion is then

$$[M_{dd}]\{\ddot{u}_d\} + [B_{dd}]\{\dot{u}_d\} + \begin{bmatrix} 0 & I_{33} & 0 \\ I_{33} & K_{33} & K_{3c} \\ 0 & K_{c3} & K_{cc} \end{bmatrix} \begin{Bmatrix} q_3 \\ u_3 \\ u_c \end{Bmatrix} = \begin{Bmatrix} Y_3 \\ P_3 \\ P_c \end{Bmatrix} \qquad \text{Eq. 4-23}$$

For this case $[M_{dd}]$ and $[B_{dd}]$ have no terms for the u_3-set variables. Their partitions are not shown. Evaluating the first row of this equation, we obtain

$$\{u_3\} = \{Y_3\} \qquad \text{Eq. 4-24}$$

Note that q_3 is the force of constraint with a sign change.

Enforced Accelerations. Now consider the case of enforced acceleration. The equation of motion is then

$$\begin{bmatrix} 0 & I_{33} & 0 \\ I_{33} & M_{33} & M_{3c} \\ 0 & M_{c3} & M_{cc} \end{bmatrix} \begin{Bmatrix} \ddot{q}_3 \\ \ddot{u}_3 \\ \ddot{u}_c \end{Bmatrix} + [B_{11}]\{\dot{u}_d\} + \{K_{dd}\}\{u_d\} = \begin{Bmatrix} \ddot{Y}_3 \\ P_3 \\ P_c \end{Bmatrix} \qquad \text{Eq. 4-25}$$

Again, from the first row,

$$\{\ddot{u}_3\} = \{\ddot{Y}_3\} \qquad \text{Eq. 4-26}$$

The input quantity $\{\ddot{Y}_3\}$ is an acceleration vector because the first partition of $\{P_d\}$ is equated to an acceleration vector. That is, the type of the matrix where the constraint equations are placed determines the type of motion of $\{Y_3\}$. In this DMAP alter package enforced motion variables may be placed in any or all of the matrices. Mixed types of enforced motion are therefore supported.

Note that in this case, $\ddot{q}_3$ is the force of constraint.

Modal Equations in the Frequency and Time Domains

All constraint equations are initially placed in the stiffness matrix to allow the solution of the eigenvalue problem when rigid body modes are present. The system eigensolution is obtained from the equation

$$[K_{aa} - \omega^2 M_{aa}^2]\{\phi_{az}\} = 0 \qquad \text{Eq. 4-27}$$

where ω is a natural frequency, $\{\phi_{az}\}$ is the corresponding eigenvector, and z is the number of eigenvectors calculated. After the equations are reduced to modal variables, the constraints for enforced motion are moved to the damping or mass matrix for enforced velocity or enforced acceleration, respectively, using the same user interface as the direct solutions.

Each static constraint mode is computed by fixing all constraint DOFs except one and applying a unit motion to it. The motion of the physical variables is the superposition of the motion of the flexible modes and the constraint modes.

Let $\{u_d\} = [T_{dh}]\{u_h\}$, where $\{u_d\}$ is defined in **Eq. 4-20**. $[T_{dh}]$ is the transformation between the modal and physical dynamic variables. $\{u_h\}$, the unknown variable vector for modal analysis, has the components

$$\begin{Bmatrix} u_z \\ q_3 \\ u_3 \end{Bmatrix} = \{u_h\}$$

Eq. 4-28

$\{u_z\}$ is the vector of generalized displacements for the flexible modes. $\{q_3\}$ and $\{u_3\}$ are the unknown constraint force variables and displacement variables for the constraint modes. The corresponding known variables are

$$\{P_h\} = \begin{Bmatrix} P_z \\ Y_3 \\ \underline{P}_3 \end{Bmatrix}$$

Eq. 4-29

$\{P_z\}$ is the modal force vector and $\{Y_3\}$ and $\{\underline{P}_3\}$ the known enforced motion variables and applied forces of the enforced motion points.

$\{P_h\}$ is obtained from the equation

$$\{P_h\} = [T_{dh}]^T\{P_d\}$$

Eq. 4-30

where $\{P_d\}$ is defined in **Eq. 4-21**.

The equation relating $\{u_d\}$ and $\{u_h\}$ is used to replace $\{u_d\}$ in **Eq. 4-16**. The resulting equation is pre-multiplied by $[T_{dh}^T]$ to form the reduced basis equations of motion as follows:

$$[T_{dh}]^T[Z_{dd}(\omega)][T_{dh}]\{u_h\} = [T_{dh}]^T\{P_d\} = \{P_h\}$$

Eq. 4-31

When the multiplication of **Eq. 4-31** is carried out, the components of the modal force vector expressed in the partitions of **Eq. 4-29** become:

$$\{P_z\} = [q_{3z}]^T\{Y_3\} + [\phi_{3z}]^T\{P_3\} + [\phi_{cz}]^T\{P_c\}$$

Eq. 4-32

$$\{\underline{u}_3\} = \{u_3\} = \{Y_3\}$$

Eq. 4-33

$$\{\underline{P}_3\} = [q_{33}]^T\{Y_3\} + \{P_3\} + [u_{c3}]^T\{P_c\}$$

Eq. 4-34

The modal forces $\{P_z\}$ have components from all three partitions of $\{P_d\}$. $\{\underline{u}_3\}$ is identically $\{u_3\}$. $\{\bar{P}_3\}$ includes loads applied directly to 3-set points $\{P_3\}$, as well as the constraint forces needed to maintain the motion of the unknown input point variables $\{u_3\}$ at the prescribed input motion $\{Y_3\}$. (In this implementation the $\{P_3\}$ forces are moved to $\{Y_3\}$.)

If there are enforced motion terms, the rows and columns of the constraint terms, $\{u_3\}$ and $\{q_3\}$, are moved to the corresponding stiffness, damping or mass matrices. The load vector $\{P_d\}$ has enforced motion inputs transferred to the LMT variables by the same technique used in the direct solutions. Note that the presence of enforced motion variables results in nondiagonal h-set matrices, requires the use of the coupled solution algorithms for frequency response and transient analysis. The matrices are sparse, however, with off-diagonal terms occurring only in the columns associated with enforced motion so that the effect on solution cost is small.

User Interfaces

A description of the user interface for the current DMAP implementation of the LMT method is given below, followed in turn by a description of the nomenclature and theory used in the implementation. Please refer to the SSSALTER Library delivered with MSC.Nastran for the most current filenames and descriptions. (These are also provided on the MSC Web page at http://www.mscsoftware.com.)

User Interface for the DMAP Alter Implementation

The alter package names and contents are listed in "**SSSALTER Library For MSC.Nastran**" on page 269. The files are:

File Name	Applies to Solution Sequence
Imt01	101, Static Analysis
Imt03	103, Real Eigensolution Analysis
Imt07	107, Direct Complex Eigensolution Analysis
Imt08	108, Direct Frequency Response Analysis
Imt09	109, Direct Transient Analysis
Imt10	110, Modal Complex Eigensolution Analysis
Imt11	111, Modal Frequency Response Analysis
Imt12	112, Modal Transient Analysis

Most input is conventional. The exceptions are described here.

Executive Input File

Add INCLUDE '[filename].vxx' before the CEND statement (where xx is the current version number for MSC.Nastran).

Case Control Input File

The input here is conventional. In dynamic analysis the reaction forces required to produce enforced motion can be printed or plotted with SPCFORCE requests.

Bulk Data Input File

The Bulk Data entries for static and dynamic analysis are conventional. A new option is available for enforced motion analysis. There are new parameters for other new options described below. Some input types are also not allowed, as described below.

Place all DOFs at which enforced motion is to be applied on USET Bulk Data entries. The SETNAME field of the USET entry specifies the type of input as shown in the example below. For example, if one grid point is to be given three different types of input, the Bulk Data entries for it would be:

```
$USET    SETNAME    GID   CID
USET     U1         12    2       $ U1 SELECTS ENFORCED DISPLACEMENT
USET     U2         12    3       $ U2 SELECTS ENFORCED VELOCITY
USET     U3         12    4       $ U3 SELECTS ENFORCED ACCELERATION
```

Input Details. All DOFs listed on USETi entries must be in the b-set of the model. If there are no OMITi, ASETi, BSETi or CSETi entries present in the Bulk Data file all free DOFs are in the b-set by default. No other input is necessary. If there are ASETi entries, the DOFs listed on USETi entries should also be listed on ASETi entries. All of these DOFS are then in both the b-set and the a-set. If there are BSETi or CSETi entries, all DOFS listed on USETi entries should also be listed on BSETi entries. An error exit is taken if any ui DOFs are not in the b-set. All rigid body modes of the model must be constrained by combinations of SUPORT entries, SPC entries, and USETi entries. The r-set retains its traditional meaning. It is fixed in static analysis and free in dynamic analysis. The u_1, u_2, and u_3 sets comprise a superset which is fixed in all types of analysis.

The TLOAD1 and TLOAD2 Bulk Data entries offer a provision for a "TYPE" input for use with the large mass approach for enforced motion. (See field 5 on the "TLOAD1" on page 1395 of the *MSC.Nastran Quick Reference Guide.*) When TYPE is set to the values 1 or 2, the input function or table is differentiated to convert a velocity or displacement signal into an acceleration signal. This is the only type of signal that the large mass approach can handle directly. The LMT approach, by contrast, allows any of these signals to be used directly. For this reason, it is recommended that the TYPE field be set to zero (or blank, which is equivalent). Use the SETNAME values on the USET entry as illustrated above instead. They offer the necessary and sufficient input.

Put the enforced motion time history or frequency variation on the Bulk Data entries normally used for dynamic load inputs. (This technique is illustrated in the example problem descriptions below.) This data is treated as enforced motion values rather than as applied forces when the DOFs referenced are also listed on USET entries. You should

ensure that these points are not inadvertently loaded by other applied loads such as pressure loads on elements or inertial loads. This condition can be checked by inspecting the motion at the input points to ensure that the only signal present is that of the enforced motion desired. The large mass approach can also be affected by this user error, but it is less serious in that context because the large scale factor used on the enforced motion tends to be much larger in magnitude than these unintended enforced motions. The enforced motion time history or frequency variation appears in the displacement, velocity, and acceleration output and should be checked when loads and enforced motions are applied simultaneously to ensure that only the motion intended is applied to these points.

Option for Component Mode Synthesis of the Residual Structure

The Lanczos method of eigensolution is preferred for the LMT formulation. When this option is selected, eigenvectors are computed for the v-set of the residual structure. The v-set requires that an o-set be present. It also includes c-set and r-set DOFs when they exist. These vectors are used to reduce the v-set in a manner analogous to GDR, except that exact eigenvectors are used in contrast to the approximate eigenvectors of the GDR method. The following additional entries must be present:

- The residual structure must contain QSETi entries and SPOINT or GRID entries for them.
- A METHOD(FLUID) entry must present in Case Control.
- An EIGR or EIGRL Bulk Data entry must be present.

This option is not available for fluid-structure analysis, where the METHOD(FLUID) command is used to select a solution method for the fluid elements. The large mass method may be used with this alter for those with a desire to continue with this method. In this event, the user interface is the same as without the alter package.

Optional Parameters and Blocked Capabilities

Some capabilities are blocked or not implemented because they require module changes or because the DMAP alters for their implementation with the LMT approach are excessive in scope. These conditions are detected by DMAP operations and cause a DMAP User Fatal Message (UFM) which describes the symptoms of the error and a corrective action.

- Generalized Dynamic Reduction. Use the Lanczos option called by the METHOD(FLUID) command instead. GDR input causes a fatal error message (UFM).
- Complex eigensolutions when the model contains enforced motion variables are not possible, and cause a UFM. The HESS method with static or modal condensation is the most reliable method to use with this implementation.
- Skipped output steps in transient analysis are not supported. The skip factor (field 5 on the TSTEP Bulk Data entry) must be set to 1. A UFM results when the skip factor is larger than 1.
- Initial conditions in transient dynamic analysis (requested by an IC Case Control

- Mode acceleration in modal analysis results in a UFM. This is the feature selected by PARAM,MODACC.

- Virtual mass causes a UFM.

- Inertia relief shapes for dynamic analysis.

Computation Time

The ratio of computation time between a conventional and an LMT solution is problem dependent. The LMT solution should be appreciably faster when the matrix is sparse and of large dimension, and when there are many multipoint constraints. These constraints tend to increase the connectivity of the reduced matrix used in conventional analysis. The cost of the matrix multiplication used to remove the dependent degrees-of-freedom grows rapidly with the percentage of dependent DOFs. A series of test problems were used to test cost ratios. These problems are known as the BSTAT series and are often used by MSC in benchmark studies. They are square plate models constrained along opposite edges by single-point constraints.

Use of the Superelement Capability

Superelements may also be used to alleviate numerical conditioning problems. For example, if there are a few very stiff elements in a model made primarily of softer elements, the stiff elements may be placed in superelements. Placing the stiff elements in the o-set has a similar effect. Unlike the previous alter package, all superelement reductions are done with the LMT approach.

Scaled Response Spectra

The user interface is similar to that for the standard solution sequences with the large mass approach except that the LMT interface for enforced motion is used. The input file changes which need to be made when converting a large mass approach input file to the LMT approach are given below:

- OFREQ Case Control Command (Optional) – This entry is used to select the mode shapes to be used for the calculations. When converting a model set up for the large mass method for which the OFREQ command is present, delete the frequencies from the selected set that are related to the very low frequency modes. If it is desired to delete the effects of any constraint mode from the calculations, set its input spectrum to a zero value at zero frequency. A nonzero value for PARAM,LFREQ will remove all constraint modes.

- SUPORT Entry – Replace any SUPORT Bulk Data entries used for enforced motion with USET entries with a SETNAME value of U3.

- Large Masses – Delete large masses used at enforced motion DOFs from the input file. They are not needed.

The remainder of the input file needs no changes. The alter directory delivered with MSC.Nastran contains two annotated input files that show the conversion process between the two approaches. (See the files RFLAG4.DAT and RFLAG5.DAT, which are based on problems D0312D and D0312R documented in the *MSC.Nastran Demonstration Problem Manual*.)

Example Problem Descriptions

A series of verification and demonstration problems are available on the RFA library where the alter packages are stored. These problems are related to the first model described here. Problems RFLAG1 through RFLAG6 have been converted to Version 68 with annotations.

Verification Test Model RFLAG1, Direct Frequency Response

A spring of unit value has a unit mass placed at node 2 and is given a unit sinusoidal displacement input at node 1. A uniform structural damping rate of 0.1 is applied to the model. A sketch of this model and the input file for this model are given below:
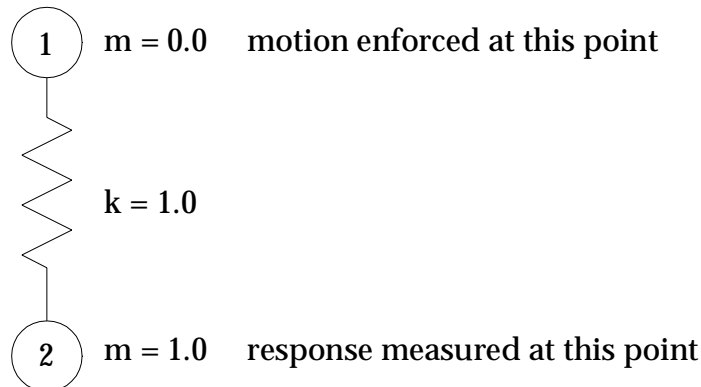

```
$ FILE RFLAG1. DAT   VERIFICATION PROBLEM. VERSION xx
INIT MASTER(S) $ DISCARD DATA BASE AT END OF RUN
TIME 5
SOL 108 $ DIRECT FREQUENCY RESPONSE
INCLUDE 'rflag. vxx' $ Assumes a copy of the alter is in the current
$ directory
CEND $
TITLE = FREQ. RESP. OF SINGLE DOF OSCILLATOR          RFLAG1
SUBTITLE = ENFORCED DISPLACEMENT, PARAM G DAMPING
DLOAD = 2 $ SELECT THE ENFORCED MOTION INPUTS
FREQ = 3  $ SELECT THE EXCITATION FREQUENCIES
DISP = ALL$ PRINT THE INPUT AND OUTPUT
SPCF = ALL$ PRINT THE FORCE REQUIRED AT THE INPUT
BEGIN BULK
SPOINT, 1      2 $ SCALAR POINTS DEFINING X1, X2
CELAS2, 12,    1.0     1,      ,       2 $ SPRING BETWEEN X1, X2
CMASS2, 2,     1.0,    2 $ UNIT MASS ON X2
USET,   U1,    1,      0 $ SPECIFY ENFORCED DISPLACEMENT INPUT
DAREA,  100,   1,      0,     1.0 $ UNIT SCALE FACTOR ON INPUT
RLOAD2, 2,     100,    , , 200 $ APPLY FUNCTION 200 ON DAREA 100
TABLED1,200
,      0.0,    1.0,    100.,   1.0,   ENDT $ APPLY UNIT
$ FUNCTION OVER ALL FREQUENCIES
FREQ,   3,     0.0,    0.159155, 15.9155 $ EXCITATION FREQUENCIES OF
$ 0.0; 1/(2*PI), THE NATURAL FREQUENCY WN; AND 100 TIMES WN,
$ CYCLES/UNIT TIME
PARAM,  G,     0.1 $ DAMPING CONSTANT TO MULTIPLY TIMES K
```

The solution sequences supported for this capability may all use the same DMAP alters that are stored in rflag.vxx. The Case Control input file is conventional for dynamic analysis except that the SPCFORCE command requests the printing of the applied force required to cause the prescribed enforced motion, as well as conventional SPC force output. The method used to generate DOFs for constraint variables is described in the Theory section. The scalar point variables have only one component, while the DAREA entry lists the same GID and C value as the USET entry. The RLOAD2 entry correlates the DAREA and TABLED1 entries. PARAM,G is used to apply structural damping over all elements in the model.

```
SUBCASE 1 $ SUPERELEMENT 1 SUBCASE
SUPER = 1 $
METHOD = 3 $ FOR CMS MODES OF S.E. 1
```

The SUPER entry names the SEID of the superelement being described. The METHOD entry selects an EIGRL entry which determines the number of eigenvectors of the component to be computed. Bulk Data entries are added to define variables for generalized coordinates (SPOINT). Other entries attach the variables to the superelement and place them in the generalized coordinate set (SEQSET1).

Concluding Remarks

The current MSC.Nastran implementation of the rflag.vxx alter should be considered for use in the following conditions:

- When it is desired to reduce the amount of storage space and computation time. This is especially true when many MPC entries and rigid elements are used.

- When an alternate method to the large mass method is desired for enforced motion in dynamic analysis.

4.4   Axisymmetric Fluids in Tanks

MSC.Nastran's axisymmetric hydroelastic capability allows the user to solve a variety of fluid problems with small motion, compressibility, and gravity effects. A complete derivation of the MSC.Nastran model and an explanation of the assumptions are given in *The NASTRAN Theoretical Manual,* Section 16.1. The input data and the solution logic have many similarities to those for a structural model. The standard normal modes analysis, transient analysis, complex eigenvalue analysis, and frequency response solutions are available with minor restrictions. The differences between a fluid model and an ordinary structural model are due to the physical properties of a fluid. The characteristics of an axisymmetric fluid model are summarized as follows:

1. The independent degrees-of-freedom for a fluid are the Fourier coefficients of the pressure function (i.e., harmonic pressure) at fluid points in a cylindrical or spherical coordinate system. The locations of these points are on the r-z plane.

2. Much like the structural model, the fluid data will produce "stiffness" and "mass" matrices. Because they now relate pressures and flow instead of displacement and force, their physical meaning is quite different. The user may not apply loads, constraints, sequencing, or omitted coordinates directly on the fluid points involved. Instead, the user supplies information related to the boundaries and MSC.Nastran internally generates the correct constraints, sequencing, and matrix terms. Indirect methods, however, are available to the user for utilizing the internally generated points as normal grid or scalar points. See "**Hydroelastic Data Processing**" on page 111 for the identification code.

3. When a physical structure is to be connected to the fluid, the user supplies a list of fluid points on a plane and a related list of special structural grid points on the circles corresponding to the fluid parts. Unsymmetric matrix terms define the actual physical relations. A special provision is included in MSC.Nastran in the event that the structure has planes of symmetry. The user may, if so desired, define only a section of the boundary and solve the problem with symmetric or antisymmetric constraints. The fluid-structure interface will take the missing sections of structural boundary into account.

4. Because of the special nature of fluid problems, some user convenience options are absent. The fluid elements and harmonic pressures are not available in the structural plots. Plotting the harmonic pressures versus frequency or time may not be directly requested. Because mass matrix terms are automatically generated if compressibility or free surface effects are present, the weight and C.G. calculations with fluid elements present may not be correct and should be avoided. Also, the inertia relief rigid format uses the mass matrix to produce internal loads, and if fluids are included, these special fluid terms in the mass matrix may produce erroneous results.

5. The general acoustic capability in MSC.Nastran, described in "**Coupled Acoustic Analysis**" on page 124, shares the same small-motion pressure formulation and also produces unsymmetric matrices. For more generality, the acoustic fluid model is defined by three-dimensional HEXA and PENTA elements and the structural boundary is defined with conventional GRID points. Although it lacks an option for gravity waves on the free surface, it can replace the axisymmetric hydroelastic modeling for most problems.

In spite of the numerous differences between a structural model and a fluid model, the similarities allow the user to formulate a problem with a minimum of data preparation and obtain efficient solutions to large-order problems. The similarities of the fluid model to the structural model are as follows:

1. The fluid is described by points in space and finite element connections. The locations of the axisymmetric fluid points are described by rings (RINGFL) about a polar axis and defined by their r-z coordinates. The rings are connected by elements (CFLUIDi) which have the properties of density and bulk modulus of compressibility. Each fluid ring produces, internally, a series of scalar points p^n and p^{n^*} (i.e., harmonic pressures), describing the pressure function, $P(\phi)$, in the equation

$$P(\phi) \;=\; P^0 + \sum_{n=1}^{N} p^n \cos n\phi + \sum_{n=1}^{N} p^{n^*} \sin n\phi \;\; 0 < N < 100$$

where the set of harmonics 0, n and n^* are selected by the user. If the user desires the output of pressure at specific points on the circular ring, he may specify them as pressure points (PRESPT) by giving a point number and an angle on a specified fluid ring. The output data will have the values of pressure at the angle ϕ given in the above equation. The output of free surface displacements normal to the surface (FREEPT) are also available at specified angles, ϕ. The Case Control command AXISYM = FLUID is necessary when any harmonic fluid degrees-of-freedom are included. This command may not be used when F = NONE on the AXIF Bulk Data entry (no harmonics specified).

2. The input file may include all existing options except the axisymmetric structural element data. All existing Case Control options may be included with some additional fluid Case Control requests. All structural element and constraint data may be used but not connected to RINGFL, PRESPT, or FREEPT fluid points. The structure-fluid boundary is defined with the aid of special grid points (GRIDB) that may be used for any purpose that a structural grid point is currently used.

3. The output data options for the structural part of a hydroelastic model are unchanged from the existing options. The output values of the fluid will be produced in the same form as the displacement vectors but with format modifications for the harmonic data.

- Pressures and free surface displacements, and their velocities and accelerations, may be printed with the same request (the Case Control command PRESSURE = SET is equivalent to DlSP = SET) as structural displacements, velocities, and accelerations.

- Structural plots are restricted to GRID and GRIDB points and any elements connected to them.

- X-Y plot and Random Analysis capabilities are available for FREEPT and PRESPT points if they are treated as scalar points.

- The RINGFL point identification numbers may not be used in any plot request; instead, the special internally generated points used for harmonics may be requested in the X-Y plots and random analysis. (See "**Hydroelastic Data Processing**" on page 111 for the identification number code.)

- No element stress or force data is produced for the fluid elements.

- As in the case of the axisymmetric conical shell problem, the Case Control command HARMONlCS = N is used to select output data up to the Nth harmonic.

Input Data

Several special Bulk Data entries are required for fluid analysis problems. These entries are compatible with structural entries. A brief description of the uses for each Bulk Data entry follows:

AXIF

AXIF controls the formulation of the axisymmetric fluid problem. It is a required entry if any of the subsequent fluid-related entries are present. The data references a fluid-related coordinate system to define the axis of symmetry. The gravity parameter is included on this entry rather than on the GRAV entry because the direction of gravity must be parallel to the axis of symmetry. The values of density and elastic bulk modulus are conveniences in the event that these properties are constant throughout the fluid. A list of harmonics and the request for the nonsymmetric (sine) coefficients are included on this entry to allow the user to select any of the harmonics without producing extra matrix terms for the missing harmonics. A change in this list, however, will require a RESTART at the beginning of the problem.

RINGFL

The geometry of the fluid model about the axis of symmetry is defined with RINGFL entries. The RINGFL data entries serve somewhat the same function for the fluid as the GRID entries serve in the structural model. In fact, each RINGFL entry will produce, internally, a special grid point for each of the various harmonics selected on the AXIF data entry. They may not, however, be connected directly to structural elements (see the GRIDB and BDYLlST entries). No constraints may be applied directly to RINGFL fluid points.

CFLUIDi

CFLUIDi defines a volume of fluid bounded by the referenced RlNGFL points. The volume is called an element and logically serves the same purpose as a structural finite element. The physical properties (density and bulk modulus) of the fluid element may be defined on this entry if they are variables with respect to the geometry. If a property is not defined, the default value on the AXlF entry is assumed. Two connected circles (RINGFL) must be used to define fluid elements adjacent to the axis of symmetry. A choice of three or four points is available in the remainder of the fluid.

GRIDB

GRIDB provides the same functions as the GRID entry for the definition of structural grid points. It will be attached to a particular RINGFL fluid point. The particular purpose for this entry is to force the user to place structural boundary points in exactly the same locations as the fluid points on the boundary. The format of GRIDB is identical to the format of GRID except that one additional field is used to identify the RINGFL point. The GRDSET entry, however, is not used for GRIDB data, and no superelement partitioning is allowed.

GRIDB entries may be used without a fluid model. This is convenient in case the user wishes to solve the structural problem first and to add the fluid effects later without converting GRID entries to GRIDB entries. The referenced RINGFL point must still be included in a boundary list (BDYLIST; see below), and the AXIF entry must always be present when GRIDB entries are used. (The fluid effects are eliminated by specifying no harmonics.)

FREEPT, PRESPT

FREEPT and PRESPT are used to define points on a free surface for displacement output and points in the fluid for pressure output. No constraints may be applied to these points. Scalar elements and direct matrix input data may be connected to these points, but the physical meaning of the elements will be different from in the structural sense.

FSLIST, BDYLIST

FSLIST and BDYLIST define the boundaries of the fluid with a complete freedom of choice. The FSLIST entry defines a list of fluid points which lie on a free surface. The BDYLIST data make up a list of fluid points to which structural GRIDB points are connected. Points on the boundary of the fluid for which BDYLlST or FSLIST data are not defined are assumed to be rigidly restrained from motion in a direction normal to the surface.

With both of these lists, the sequence of the listed points determines the nature of the boundary. The following directions will aid the user in producing a list:

1. Draw the z-axis upward and the r-axis to the right. Plot the locations of the fluid points on the right-hand side of z.

2. If one imagines himself traveling along the free surface or boundary with the fluid on his right side, the sequence of points encountered is used for the list. If the surface or boundary touches the axis, the word AXIS is placed in the list. AXIS may be used only for the first and/or last point in the list.

3. The free surface must be consistent with static equilibrium. With no gravity field, any free surface consistent with axial symmetry is allowed. With gravity, the free surface must be a plane perpendicular to the z-axis of the fluid coordinate system.

4. Multiple free surface lists and boundary lists are allowed. A fluid point may be included in any number of lists.

Figure 4-1 illustrates a typical application of the free surface and structural boundary lists.

FSLIST: 36, 37, 38, 39, 40
BDYLIST #1: AXIS, 22, 23, 29, 36
BDYLIST #2: 40, 35, 28, 21, 14, 7, 6, 5, 4, 3, 2, 1, AXIS
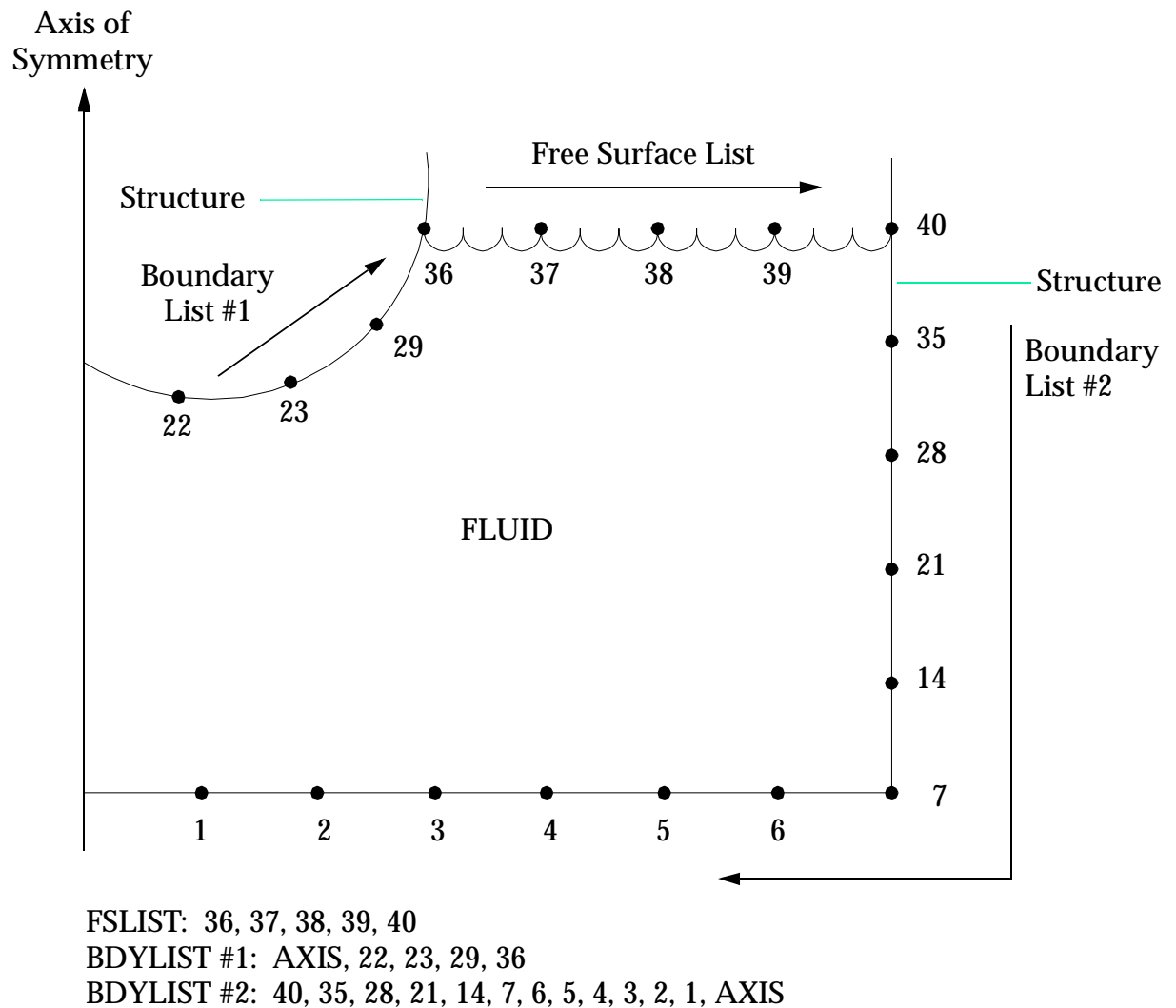
Figure 4-1 Examples of Boundary Lists

FLSYM

FLSYM allows the user an option to model a portion of the structure with planes of symmetry containing the polar axis of the fluid. The first plane of symmetry is assumed at $\phi = 0.0$ and the second plane of symmetry is assumed at $\phi = 360°/M$ where M is an integer specified on the entry. Also specified are the types of symmetry for each plane, symmetric (S) or antisymmetric (A). The user must also supply the relevant constraint data for the

structure. The solution is performed correctly only for those harmonic coefficients that are compatible with the symmetry conditions, as illustrated in the following example for quarter symmetry, M = 4.

Series	Plane 1	Plane 2	
		S	A
Cosine	S	0,2,4,...	1,3,5,...
	A	none	none
Sine (*)	S	none	none
	A	1,3,5,...	2,4,6,...

DMIAX

DMIAX is used for special purposes such as the specification of surface friction effects. DMIAX is equivalent to DMIG except harmonic numbers are specified for the degrees-of-freedom. A matrix may be defined with either DMIG or DMlAX entries, but not with both.

Solution Sequences

Restrictions. The characteristics of the fluid analysis problems which cause restrictions on the type of solution are as follows:

1. The fluid-structure interface is mathematically described by a set of unsymmetric matrices. Since most solution sequences are restricted to the use of symmetric matrices, the fluid-structure boundary is ignored. Thus, for any of these solution sequences, MSC.Nastran solves the problem for a fluid in a rigid container with an optional free surface and an uncoupled elastic structure with no fluid present.

2. No means are provided for the direct input of applied loads on the fluid. The only direct means of exciting the fluid is through the structure-fluid boundary. The fluid problem may be formulated in any solution sequence. However, only some will provide nontrivial solutions.

The suggested solution sequences for the axisymmetric fluid and the restrictions on each are described as follows:

SOL 103 or 200 – Normal Modes Analysis

The modes of a fluid in a rigid container may be extracted with a conventional solution request. Free surface effects with or without gravity may be accounted for. Any structure data in the section will be treated as a disjoint problem. (The structure may also produce normal modes.) Normalization of the eigenvectors using the POINT option will cause a fatal error.

SOL 107 (with RF28D78) – Direct Complex Eigenvalue Analysis

If no damping or direct input matrices are added, the resulting complex roots will be purely imaginary numbers whose values are the natural frequencies of the system. The mode shape of the combination may be normalized to the maximum quantity (harmonic pressure or structural displacement) or to a specified structural point displacement.

SOL 108 or 200 (with RF26D78) – Direct Frequency and Random Response

This solution may be used directly if the loads are applied only to the structural points. The use of overall structural damping (parameter g) is not recommended since the fluid matrices will be affected incorrectly.

SOL 109 (with RF27D78) – Direct Transient Response

Transient analysis may be performed directly on the fluid-structure system if the following rules apply:

1. Applied loads and initial conditions are given only to the structural points.

2. All quantities are measured relative to static equilibrium. The initial values of the pressures are assumed to be in equilibrium.

3. Overall structural damping (parameters ω_3 and g) must not be used.

SOLs 110, 111, 112, and 200 – Modal Formulation

Although these solution sequences may be used in a fluid dynamics problem, their practicality is limited. The modal coordinates used to formulate the dynamic matrices will be the normal modes of both the fluid and the structure solved as uncoupled systems. Even though the range of natural frequencies would be typically very different for the fluid than for the structure, the program will select both sets of modes from a given fixed frequency range. The safest method with the present system is the extraction of all modes for both systems with the Tridiagonalization Method. This procedure, however, results in a dynamic system with large full matrices. The Direct Formulation is more efficient in such cases. At present, the capability for fluid-structure boundary coupling is not provided with the modal formulation. However, the capability may be provided by means of an alter using the same logic as in the direct formulations.

Hydroelastic Data Processing

The fluid-related Bulk Data entries are converted by the program into equivalent grid point, scalar point, element connection, and constraint data entry images. Each specified harmonic, N, of the Fourier series solution produces a complete set of special grid point and connection entry images. In order to retain unique identification numbers, the user identification numbers are encoded by the algorithm below:

RINGFL Points

Grid point ID $=$ User ring ID $+ 1,000,000 \times I_N$

where:

$I_N = N + 1$ cosine series

$I_N = N + 1 / 2$ sine series

CFLUIDi Connection Entries

Element ID $=$ User ring ID $+ 1,000 \times I_N$

where I_N is defined above for each harmonic N.

For example, if the user requested all harmonics from zero to two, including the sine series, each RINGFL entry will produce five special grid entries internally. If the user's identification number (in Field 2 of the RINGFL data entry) were 37, the internally generated grid points would have the following identification numbers:

Harmonic	ID
0	1,000,037
1*	1,500,037
1	2,000,037
2*	2,500,037
2	3,000,037

These equivalent grid points are resequenced automatically by MSC.Nastran to be adjacent to the original RlNGFL identification number. A RINGFL point may not be resequenced by the user.

The output from matrix printout, table printout, and error messages will have the fluid point labeled in this form. If the user wishes, he may use these numbers as scalar points for Random Analysis, X-Y plotting, or for any other purpose.

In addition to the multiple sets of points and connection entries, the program may also generate constraint sets. For example, if a free surface (FSLIST) is specified in a zero-gravity field, the pressures are constrained to zero. For this case, the internally generated set of single-point constraints are internally combined with any user-defined structural constraints and will always be automatically selected.

If pressures at points in the fluid (PRESPT) or gravity-dependent normal displacements on the free surface (FREEPT) are requested, the program will convert them to scalar points and create a set of multipoint constraints with the scalar points as dependent variables. The constraint set will be internally combined with any user-defined sets and will be selected automatically.

The PRESPT and FREEPT scalar points may be used as normal scalar points for purposes such as plotting versus frequency or time. Although the FREEPT values are displacements, scalar elements connected to them will have a different meaning than in the structural sense.

Sample Hydroelastic Model

Table 4-1 contains a list of the input data for a sample hydroelastic problem. Figure 4-1 describes the problem and lists the parameters. The relatively small number of grid points were chosen for purposes of simplicity and not accuracy. The symbols for the fields in the hydroelastic data entries are placed above each group. Structural data entries are included in their standard forms. The explanations for the data are given in the following notes:

1. The AXISYM = FLUID entry is necessary to control the constraint set selections and the output formats for a fluid problem. It must appear above the subcase level.

2. DISPLACEMENT and PRESSURE Case Control commands are pseudonyms. DISP = ALL produces all structure displacements, all free surface displacements, and all fluid pressure values in the output. The HARMONICS control is a limit on the harmonic data and has the same function as in an axisymmetrical conical shell problem.

3. The AXIF entry defines the existence of a hydroelastic problem. It is used to define overall parameters and control the harmonic degrees-of-freedom.

4. The RINGFL entries included define the five points on the fluid cross section.

5. The CFLUIDi entries are used to define the volume of the fluid as finite elements connected by the RINGFL points. Since parameters p and B are missing, the default values on the AXIF entry are used.

6. The FSLIST entry is used to define the free surface at z = 10.0. The density factor ρ is placed on the entry in this case. If blank, the default value on the AXIF entry is used.

7. The fluid-structure boundary is defined on the BDYLIST entry. The AXIF default density is used.

8. The GRIDB entries define the structure points on the fluid boundary. Points 3 through 6 are connected to fluid number 2 ring. The rotation in the r direction ("4" in field 8) is constrained.

9. The fact that one-quarter symmetry was used for the structure requires the use of the FLSYM entry. Symmetric-antisymmetric boundaries indicate that only the cosine terms for the odd harmonics interact with the structure. If symmetric-symmetric boundary conditions were chosen on FLSYM, only the even harmonics of the cosine series would interact with the structure.

10. The PRESPT entries define locations of pressure points in the fluid for pressure output.

11. The FREEPT entries define locations on the free surface for displacement output.

Table 4-1 Sample Hydroelastic Problem

```
        $ FLUID MASS DEMO - D107D2 DEMO PROBLEM
        SOL 107
        TIME 2
        CEND

1.      TITLE = SAMPLE HYDROELASTlC PROBLEM
        SUBTITLE = EIGENVALUE ANALYSIS WITH FLEXIBLE BOUNDARY
        AXISYM = FLUID
        SPC = 3
        CMETHOD = 1
        OUTPUT
            PRESS = ALL
2.          HARMONICS = ALL
            ELFORCE = ALL
        BEGIN BULK

                                BULK DATA FIELD

3.      $AXIF,CID,G,DRHO,DB,NOSYM
        AXIF,2,32.2,0.03,,NO
        $,N1,N2
        1,3

        CORD2C,2,,0.,0.,0.,0.,0.,1.0
        1.0,0.,0.

4.      $RINGFL,IDF,Xl,X2,X3,IDF,X1,X2,X3
        RINGFL,1,4.0,,10.0,2,8.0,,10.0
        RINGFL,7,4.0,,5.0,8,8.0,,5.0
        RINGFL,13,4.0,,0.0

5.      $CFLUID,EID,IDF1,IDF2,IDF3,IDF4,RHO,B
        CFLUID2,101,1,7
        CLFUID2,102,7,13
        CFLUID3,103,7,8,13
        CFLUID4,104,1,2,7,8

6.      $FSLIST,RHO,IDF1,IDF2,IDF3
        FSLIST,0.03,AXIS,1,2

7.      $BDYLIST,RHO,IDF1,IDF2,IDF3
        BDYLIST,,2,8,13
```

Table 4-1 Sample Hydroelastic Problem (continued)

```
8.      $GRIDB,ID,,,PHI,,CD,PS,IDF
        GRIDB,3,,,0.0,,2,4,2
        GRIDB,4,,,30.0,,2,4,2
        GRIDB,5,,,60.0,,2,4,2
        GRIDB,6,,,90.0,,2,4,2
        GRIDB,9,,,0.0,,2,,8
        GRIDB,10,,,30.0,,2,,8
        GRIDB,11,,,60.0,,2,,8
        GRIDB,12,,,90.0,,2,,8
        GRIDB,14,,,0.0,,2,,13
        GRIDB,15,,,30.0,,2,,13
        GRIDB,16,,,60.0,,2,,13
        GRIDB,17,,,90.0,,2,,13

        CQUAD4,10,11,3,9,10,4
        CQUAD4,11,11,4,10,11,5
        CQUAD4,12,11,5,11,12,6
        CQUAD4,13,11,9,14,15,10
        CQUAD4,14,11,10,15,16,11
        CQUAD4,15,11,11,16,17,12
        PSHELL,11,12,0.5
        MAT1,12,10.6+6,,0.3,0.05
        SPC1,3,246,3,9,14
        SPC1,3,135,6,12,17
        SPC1,3,135,14,15,16

9.      $FLSYM,M,S1,S2
        FLSYM,4,S,A

10.     $PRESPT,IDF,,IDP,PHI,IDP,PHI,IDP,PHI
        PRESPT,7,,27,30.,28,60.
        PRESPT,8,,30,30.,31,60.
        PRESPT,13,,33,30.,34,60.

11.     $FREEPT,IDF,,IDP,PHI,IDP,PHI,IDP,PHI
        FREEPT,1,,40,15.,41,30.,42,45.
        FREEPT,1,,43,60.,44,75.
        FREEPT,2,,45,15.,46,30.,47,45.
        FREEPT,2,,48,60.,49,75.

        EIGC,1,INV,MAX
        0.,0.,0.,5.,3.,2,2
        ENDDATA
```
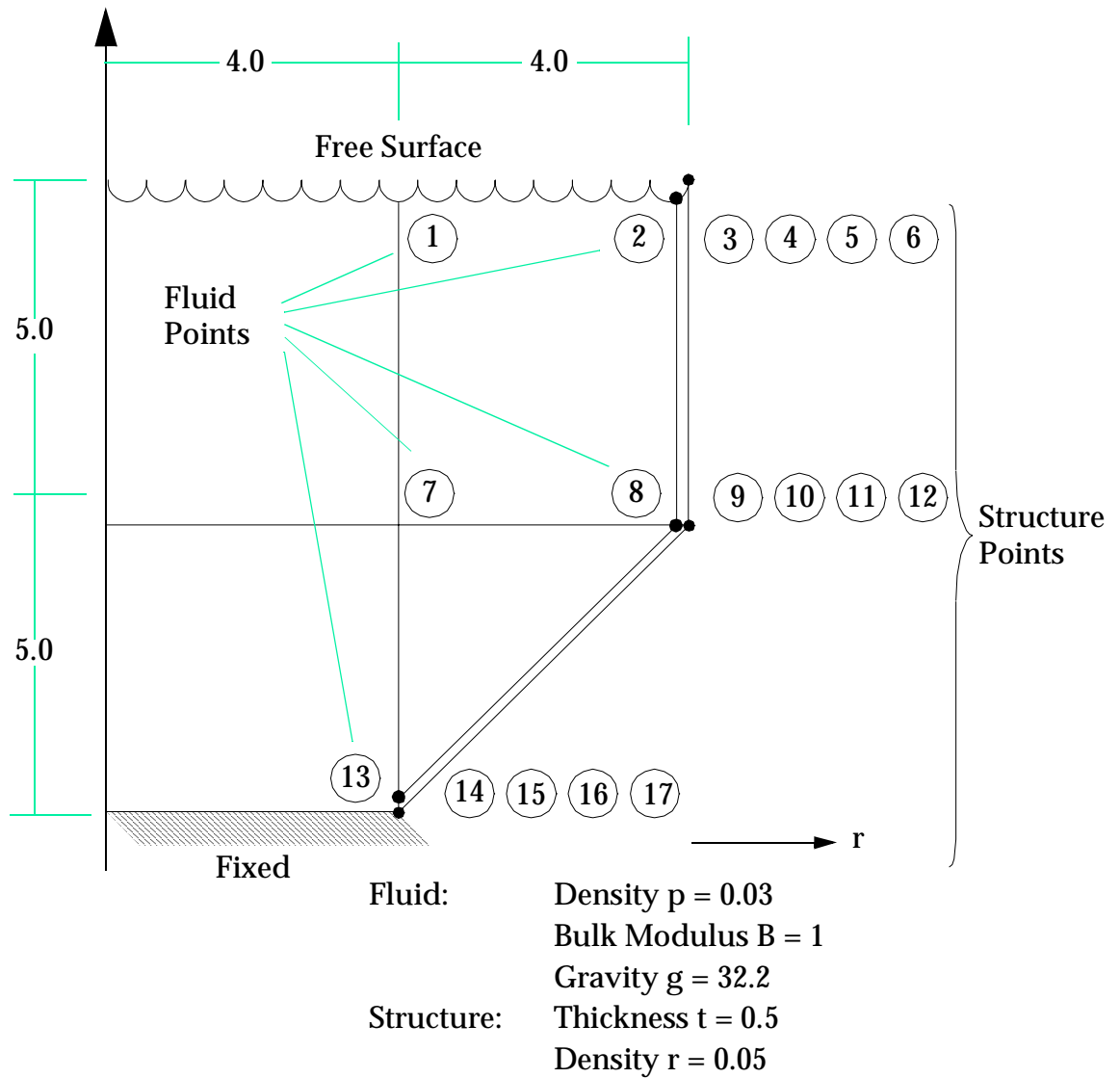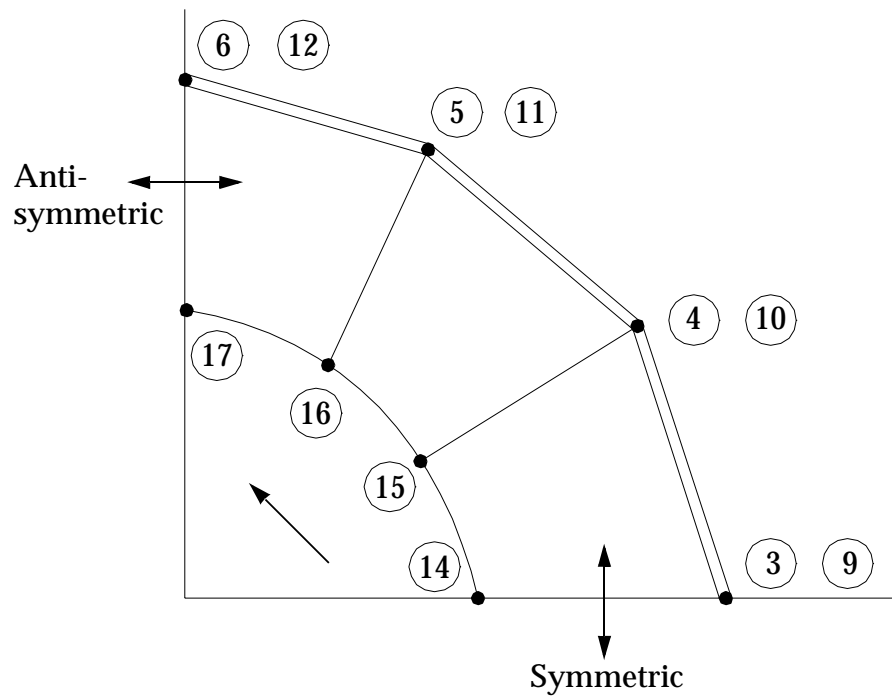
Figure 4-2 Sample Hydroelastic Problem

4.5   Virtual Fluid Mass

A virtual fluid volume produces a mass matrix which represents the fluid coupled to a boundary consisting of structural elements and other effects, such as free surfaces, planes of symmetry, and infinite fluids. The incompressible fluid produces a mass matrix defined with full coupling between accelerations and pressures on the flexible structural interfaces. For each requested volume, the boundaries may be combinations of the following:

1. Structural finite element faces, with one or two wetted sides.

2. Free surfaces with zero pressure, but no sloshing effects.

3. Planes of symmetry with symmetric or antisymmetric motion.

4. Infinite boundaries, by default, on nonclosed volumes.

The virtual mass method is well suited for the following problem types:

1. An infinite fluid surrounding part of a structure.

2. A fluid with a free surface contained within a flexible structure.

3. Multiple fluid volumes with combinations of the options above such as a half of a ship floating in water with several internal tanks, each with free surfaces and symmetric boundaries.

Note that compressibility and surface gravity effects are neglected. It is assumed that the important frequency range for the structural modes is above the gravity sloshing frequencies and below the compressible acoustic frequencies. It is further assumed that the density within a volume is constant and no viscous (rotational flow) or aerodynamic (high velocity) effects are present. In other words, a ship traveling at a high rate through a thick oil patch would require some extra modeling effort.

User Interface

The user interface for a virtual fluid mass analysis is simple and straightforward. The sketch below illustrates some of the features.
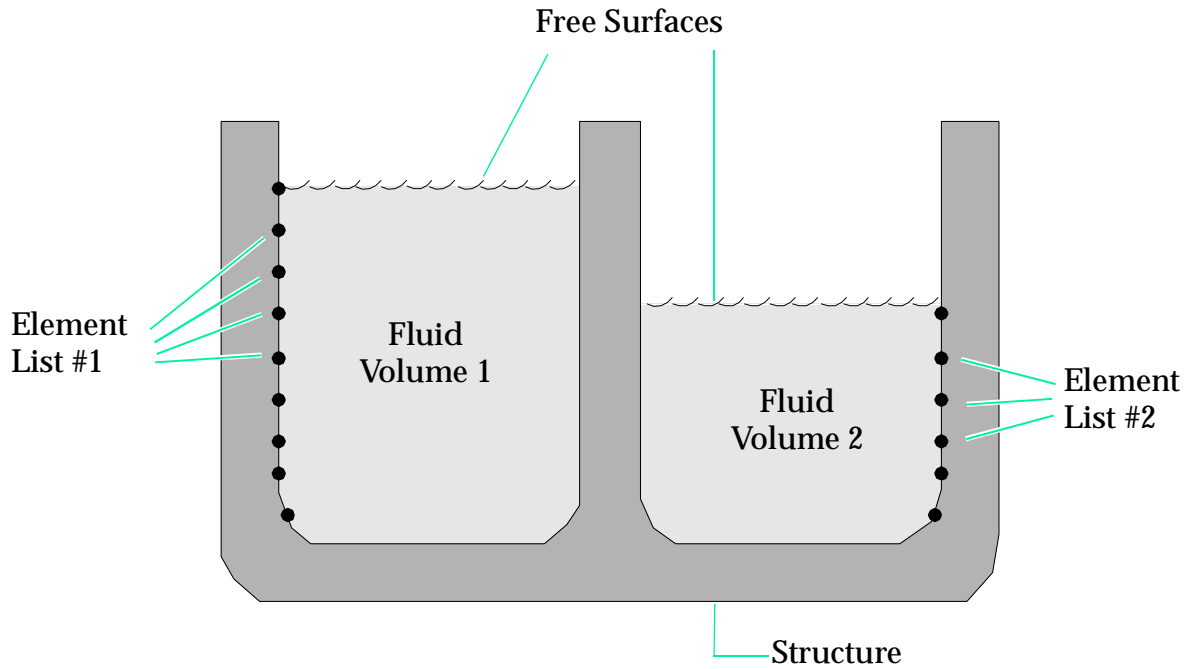
Figure 4-3 Virtual Mass Terminology

1. The fluid/structure interface is defined with ELIST Bulk Data, which specify a set of wetted TRIA3 and QUAD4 elements that define the structural portion of the fluid boundary.

2. Each fluid volume is defined on an MFLUID Bulk Data input, which defines the fluid density, the ELISTs, and other boundaries.

3. A set of MFLUID volumes are requested in the case control request MFLUID = SID.

4. If pressure outputs are desired they will be printed if the case control request MPRES = is used to define a set of elements. The elements must also be active in an ELIST/MFLUID volume.

An example set of input data for a small problem is shown below:

Case Control

```
MFLUID = 25
MPRES= ALL
etc.
```

Bulk Data

```
1       ,2        ,3        ,4        ,5        ,6        ,7        ,8        ,9        ,10
$MFLUID, SID   , CID   , ZFS   , RHO   , ELIST1, ELIST2, PLANE1, PLANE2
MFLUID , 25 , 0 , 115.4, .0246, 255 , , S
$ELIST , ELID  ,E1       , E2    , E3     , etc.
ELIST , 255 , 1 , THRU , 25
ETC...
```

In the input above we have defined a fluid volume with a free surface normal to the basic z direction. The xz plane (PLANE1) is a plane of symmetry and the density is 0.0246. ELIST set 255 defines the positive faces of elements in the range 1 through 25 (missing numbers are allowed) as the structural/fluid boundary.

The connected elements may be wetted on one or both sides by the same volume. For instance a baffle plate extends partially into a tank and have two sides in the same fluid volume. If a plate completely separates the two parts of the tank, it is recommended that a separate volume be used for each side. Each side of an element should be listed on a separate ELIST.

Special terms are calculated if enclosed fluid volumes do not have a free surface or a plane of anti-symmetry. Otherwise, the incompressible fluid would produce a spurious low frequency mode with a mode shape corresponding to the volume change. This mode will not affect the structural response, but it is eliminated. Because the free surface allows the fluid volume to expand, it does not have these problems.

A free surface is defined as an x-y plane in any local rectangular coordinate system. The user simply specifies a value of z as the upper limit of the fluid volume. Different fluid volumes may have different levels and orientation. It is not required that the surface coincide with the element properties since partially wetted elements are allowed.

The virtual mass fluid option may be used in all MSC.Nastran dynamics solutions, including the following special approaches:

- Superelements – (Residual Only)

- Nonlinear Analysis – (SOL's 99 and 129)

- Optimization – (does not create sensitivity matrices.)

Theoretical Summary

The following is a brief overview of the virtual mass approach. For more information, refer to the standard references on boundary elements.

The Helmholtz method used by MSC.Nastran solves Laplace's Equation by distributing a set of sources over the outer boundary, each producing a simple solution to the differential equation. By matching the assumed known boundary motions to the effective motion caused by the sources, we can solve a linear matrix equation for the magnitude of the sources. The values of the sources determine the effective pressures and, thereby, the forces on the grid points. Combining all of these steps into a matrix equation results in a virtual mass matrix as derived below.

If σ_j is the value of a point source of fluid (units are volume flow rate per area) located at location r_j, and is assumed acting over an area A_j, the vector velocity $\dot{u}_i$ at any other point r_i is

$$\dot{u}_i = \sum_j \int_{A_j} \frac{\sigma_j e_{ij}}{|r_i - r_j|^2} dA_j \qquad \text{Eq. 4-35}$$

where e_{ij} is the unit vector in the direction from point j to point i. Note that the gradient of the vector $\dot{u}_i$ is the potential function which satisfies Laplace's Equation on a term by term basis.

The other set of necessary equations are the pressures, p_i, at any point, i, in terms of the density, ρ, sources and geometry, namely

$$p_i = \sum_j \int_{A_j} \frac{\rho \dot{\sigma}_j e_{ij}}{|r_i - r_j|} dA_j \qquad \text{Eq. 4-36}$$

The results of integrating **Eq. 4-35** and **Eq. 4-36** over the finite element surfaces are collected respectively in two matrices, $[\chi]$ and $[\Lambda]$ where

$$\{\dot{u}\} = [\chi][\sigma] \qquad \text{Eq. 4-37}$$

and

$$\{F\} = [\Lambda]\{\dot{\sigma}\} \qquad \text{Eq. 4-38}$$

where F are the forces at the grid points. The matrix $[\Lambda]$ is obtained by integrating **Eq. 4-36**. An additional area integration is necessary to convert the pressures to forces. A mass matrix may now be defined using **Eq. 4-37** and **Eq. 4-38** as

$$\{F\} = [M^f]\{\ddot{u}\} \qquad \text{Eq. 4-39}$$

where the virtual fluid mass matrix, $[M^f]$ is

$$[M^f] = [\Lambda][\chi]^{-1} \qquad \text{Eq. 4-40}$$

Singularities for Enclosed Volumes

Note that if $[\chi]$ is singular or nearly singular, the mass matrix will cause problems with the coupled solution. The singularity is active when a set of nonzero sources can produce zero velocities on the structural surfaces. This occurs when the fluid is completely enclosed by the structure and with planes of only symmetric motion. Large pressures could occur within the fluid volume from an infinitesimal volume change on the incompressible fluid.

An alternate calculation is performed when the $[\chi]$ matrix is potentially singular. See Remark 8 on the MFUID Bulk Data description for the specific instances. An additional source, s_2, is added near the center of each MFLUID volume. The expanded versions of **Eq. 4-37** and **Eq. 4-38** are

$$\{\dot{u}\} = [\chi]\{\sigma\} + \{\chi_2\}s_2 \qquad \text{Eq. 4-41}$$

$$\{F\} = [\Lambda]\{\dot{\sigma}\} + \{\Lambda_2\}s_2 \qquad \text{Eq. 4-42}$$

An additional equation provides that the sum of the squares of the ordinary sources in the vector, $\{\sigma_1\}$ is minimized and a set of Lagrange multipliers, λ are used to enforce **Eq. 4-41**

$$U = \frac{1}{2}[\sigma]^T\{\sigma\} + [\lambda]^T\{\{\dot{u}\} - [\chi]\{\sigma\} - \{\chi_2\}s_2\} \qquad \text{Eq. 4-43}$$

Taking the derivatives of U with respect to λ, σ_1, and s_2, we obtain three sets of equations. Combining them, we obtain the following matrix equation:

$$\begin{bmatrix} 0 & \chi & \chi_2 \\ \chi^T & -I & 0 \\ \chi_2^T & 0 & 0 \end{bmatrix} \begin{Bmatrix} \lambda \\ \sigma \\ s_2 \end{Bmatrix} = \begin{Bmatrix} \dot{u} \\ 0 \\ 0 \end{Bmatrix} \qquad \text{Eq. 4-44}$$

The vector $\{\sigma\}$ may be eliminated by solving the second row partition and substituting into the first row partition of the matrix, with the result:

$$\begin{bmatrix} \chi\chi^T & \chi_2 \\ \chi_2^T & 0 \end{bmatrix} \begin{Bmatrix} \lambda \\ s_2 \end{Bmatrix} = \begin{Bmatrix} \dot{u} \\ 0 \end{Bmatrix} \qquad \text{Eq. 4-45}$$

Eq. 4-45 may be solved for $\{\lambda\}$ and s_2, which are then used to obtain pressure. To obtain the pressure, we substitute for $\{\sigma\}$ in **Eq. 4-42** to obtain the matrix equation

$$\{p\} = \begin{bmatrix} \Lambda\chi^T & \Lambda_2 \end{bmatrix} \begin{Bmatrix} \dot{\lambda} \\ \dot{s}_2 \end{Bmatrix} \qquad \text{Eq. 4-46}$$

Eq. 4-45 and **Eq. 4-46** may then be combined into a single matrix defining the fluid, namely

$$\{F\} = [M_f]\{\ddot{u}\} \qquad \text{Eq. 4-47}$$

where:

$$[M_f] = \begin{bmatrix} \Lambda\chi^T & \Lambda_2 \end{bmatrix} \begin{bmatrix} \chi\chi^T & \chi_2 \\ \chi_2^T & 0 \end{bmatrix}^{-1} \begin{bmatrix} I \\ 0 \end{bmatrix} \qquad \text{Eq. 4-48}$$

Note that the size of the matrix equation is only one term larger than the nonconstrained case. Although it will be well behaved for the enclosed volume case, the overall incompressible constraint is lost.

Other methods to avoid the singular matrix are as follows:

1. Put one or more small holes in the boundary by removing an element ID in an unimportant area from the ELIST. The fluid will then leak out to an infinite domain of fluid.

2. Define a free surface near the top of the container and modify the ELIST to remove elements above the surface.

3. Constrain the structure to eliminate any net change to the enclosed volume. In other words generate an MPC equation such that

$$\sum_i A_i \bar{n}_i \cdot \bar{u}_i = 0 \qquad\qquad \text{Eq. 4-49}$$

where i is a boundary grid point and A_i and u_i are the effective area and normal vector, respectively. (This is not an easy task.)

Fortunately, there are no problems in which free surfaces or planes of symmetry with antisymmetric motion are present since the pressure must be zero on these boundaries.

Using Phantom Structural Boundaries

In many cases an ELIST boundary is desired where no CQUAD4 or CTRIA3 elements exist. Examples occur:

- When grid points connected by other element types, such as CHEXA, CSHEAR, CBEAMs, form the boundary.

- When only a small hole connects two separate fluid volumes (since poor numerical conditioning (less roundoff) is expected with a single MFLUID).

- If the fluid contains two free surfaces due to entrapped air at a different pressure.

- If the fluid volume is a complex labyrinth, such as a boiler made with many tubes.

The phantom boundary may be constructed from CTRIA3 and CQUAD4 elements which have zero or nearly zero stiffness in the normal direction. The PSHELL bending thickness is used for this purpose. The membrane stiffness is optional. If no other structural elements are present, a small stiffness is desired for both directions to avoid automatic constraints.

Note that this method will couple only the fluid displacements in the normal direction. Edge/corner effects and tangential motions will be approximate.

Gravity Effects

The free surfaces produced by the Virtual Fluid Mass option are simple planes of antisymmetric motion with a null pressure assumed at the location of the free surface plane. Effects such as fluid sloshing due to gravity waves are assumed to be uncoupled from the higher frequency structural modes.

An approximation to the gravity effects for fluids with finite boundaries may be modeled using a phantom boundary instead of a free surface. Spread grid points and plate elements over the surface and constrain the in-plane motions and rotations to zero. Give the plates a small membrane thickness and no bending material property. Add scalar springs (CELASi) in the direction normal to the plane with stiffnesses, K_i, calculated from

$$K_i = A_i \cdot \rho g \qquad\qquad \text{Eq. 4-50}$$

where A_i is the area under the point, ρ is the density, and g is the gravitational constant. Note that these springs will affect the rigid body motion of the whole system and this method should be used with caution. Another drawback is that the extra gravity boundary may result in a completely enclosed fluid volume.

Examples

The legal and illegal types of fluid boundaries are illustrated in **Figure 4-4**. The categories are GOOD = legal configuration, BAD = illegal boundary, and MAYBE = conditionally legal, which could be permitted if a phantom boundary is used.
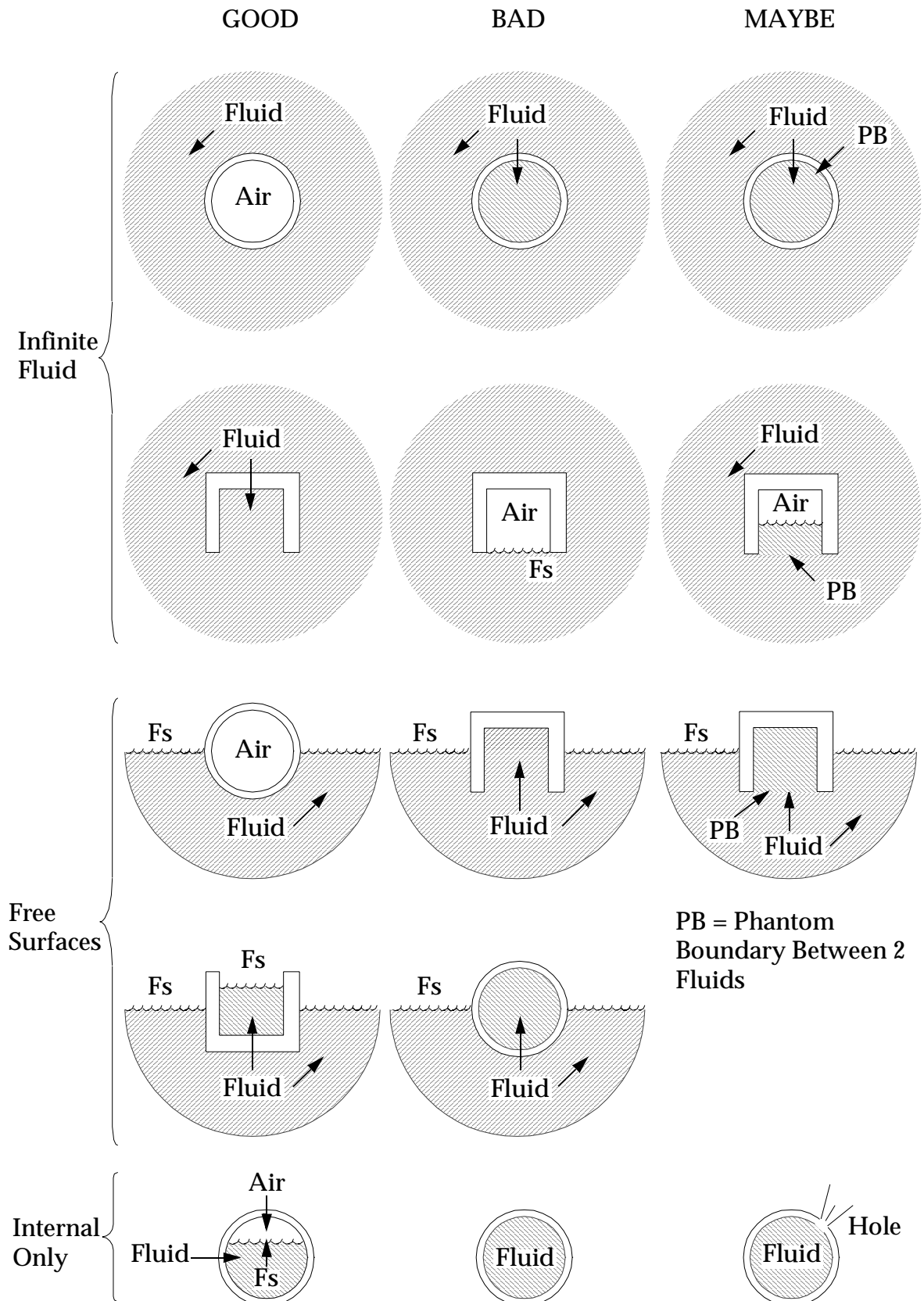

Figure 4-4 Fluid Combinations

4.6   Coupled Acoustic Analysis

Acoustic analysis in MSC.Nastran is used to determine vibrations in structural cavities filled with fluid or air. The boundaries of the cavities may be defined as rigid, open, damped, or flexible as defined by constraints and finite elements. Typical applications are automobile or aircraft interiors, musical instruments, loudspeaker boxes, and solid rocket motors. Any type of problem that involves small, linear motions of the fluid and structure may be a candidate. The analyst may obtain natural frequencies and damping factors along with mode shapes for both the structure and the coupled fluid. Other solution sequences may be used to obtain results for forced response in the frequency or time domain.

The analyst starts with the geometry of the the acoustic cavity boundary. The interior fluid volume is modeled in three dimensions with conventional MSC.Nastran solid finite elements connected to a special set of GRID points. Boundary motions are included if the structure lies on the boundary, or fixed if no structural elements are connected (by default). The structural interface simply requires that finite elements lay on the exterior fluid boundaries. Note that coupled interactions between the fluid and structural model are generated internally using the geometry definitions of the elements of the two models and require very little user intervention.

Other types of boundaries that are available are free surfaces, acoustic barriers, and acoustic absorbers. The free boundary is modeled by simply constraining the fluid pressure degrees-of-freedom to zero. The barrier and absorber elements provide a spring/mass/damper system between the fluid and the structure.

Limitations. Very few limitations are placed on the analyst. Small motion theory prohibits the use of the models in high velocity flows (more than Mach 0.5) such as mufflers and jet engines. Exterior fluids may be modeled with extra effort by extending the fluid model out to a large distance and by providing a damped and/or constrained exterior. Surface sloshing effects caused by gravity such as those in fuel tanks can be modeled with additional effort by simulating the gravity effects on the free surface with scalar springs.

A formal theoretical discussion is provided in "**Additional Topics**" on page 439 of the *MSC.Nastran Reference Manual.*

Building the Models

The following steps are recommended for avoiding difficulties later.

1. Define the geometry and select the mesh sizes.

    The first step in the modeling process is to estimate the overall FE mesh size and the level of detail needed in the geometric approximations. A set of three-dimensional elements and special fluid GRID points (with CD = –1) are used to define the fluid while normal structural elements and points define the container. A rule of thumb for fluids is that six-elements-per-wave are acceptable for the highest frequencies exciting the fluid. For acoustics this usually translates

into a corresponding coarse mesh. For incompressible fluids, the only waves occur due to gravity effects on the free surface. For heavy liquids, the mass effects are usually more important than with air, and the fluid FE mesh should be modeled to match the structural mesh.

It is generally easier to build the three-dimensional fluid mesh first and then use the outer faces to model the structure (which is usually modeled with plates). Unfortunately, most engineers start with the structure that has been used for another analysis and encounter difficulties when they attempt to construct a three-dimensional FE model within the enclosure. In most cases, the fluid model will have a different number of points on opposite faces and the engineer cannot construct a simple, matching mesh without having leftover points and lines. In this case, he should proceed with a simple fluid model and let MSC.Nastran control the mismatched connections.

Although MSC.Nastran is more efficient when the structural GRID points coincide with the fluid boundaries, it will process misaligned meshes when the fluid faces are larger than the adjacent structural elements. The basic model interface definitions are defined on the ACMODL Bulk Data entry. The user may define the sets of points on the interface and a tolerance to define the distance allowed between a fluid surface element and a connected structural point. This tolerance will be important when several points are close together and only one is wetted by the fluid.

2. Building the Fluid Finite Element Model

Each GRID point that defines the fluid mesh will have one degree-of-freedom defining the pressure at a point at a fixed location. The fluid itself is modeled with existing three-dimensional connection data (CHEXA, CPENTA, and CTETRA Bulk Data). The existence of a fluid is defined on the property data (Field **8** of the PSOLID Bulk Data) which also references the ID of the fluid material properties (on a MAT10 Bulk Data entry).

User-input fluid coefficients are density, bulk modulus, and/or compressible wave speed. Incompressible fluids are approximated by using a large bulk modulus or wave speed. (A typical value for incompressible fluid would be a wave length of 10 times the size of the structure.) The integration options on the PSOLID data should be full Gaussian Integration with no shear reduction scheme.

The higher-order elements (with midside nodes) will generally give better results than the basic linear elements. The CHEXA, CPENTA and CTETRA elements can be connected together without the problems that occur in structural elements. However, mixing high-order and low-order elements is not recommended.

At this stage in the modeling process, it is advisable to set up the loading and desired output points on the fluid. Acoustic sources such as a small loudspeaker may be specified directly by scalar loading functions (ACSRCE, SLOAD, DAREA, and/or RLOAD Bulk Data) without the need to model the structural details. The output displacement printout will actually be the scalar pressure values.

Guidelines on building the models are different for the fluid elements than for normal MSC structural elements. The lack of shear locking allows larger aspect ratios and more distorted shapes for individual elements. Unlike structures, the fluid CHEXA elements have no particular accuracy advantages over the CTETRA and CPENTA elements. However, in theory, fluid finite element accuracies will be more sensitive to sharp corners and abrupt openings. In these cases, a model should be refined using smaller elements around the discontinuity.

3. Automatic Boundaries

Fluid boundaries may be fixed, flexible, or free. With no applied loads, the outer surfaces of the fluid elements define a fixed, rigid boundary condition, approximating a normal pressure gradient of zero. However, if structural finite elements are attached, they will generate flow into the fluid and affect the pressures. The pressure degrees-of-freedom may be treated exactly like displacement DOFs, i.e., constraints may be necessary to fix the pressure of an open boundary to zero. Also, they may be constrained with SPC or MPC Bulk Data for various other reasons, such as symmetry.

If no structure is connected and the problem involves only fluid, then the effects of the boundary flexibility may be ignored and the problem is greatly simplified. A stand-alone fluid model may be analyzed by any of the standard MSC.Nastran solution sequences. For instance, the natural frequencies or resonances may be obtained from SOL 103 using symmetric real methods at greatly reduced costs.

The user controls the structural interfaces with the ACMODL Bulk Data and the locations of the boundary GRID points. The input defaults are recommended that automatically prompt MSC.Nastran to search all elements for potential interfaces. If only a set of fluid or structural points are desired to be connected, the searching process can be restricted to user-selected points defined on a SET1 Bulk Data entry. When identical meshes are used, an MSC.Nastran branch is also provided to generate area factors more efficiently and accurately.

Problems may occur when plate elements are wetted on both sides by the fluid and a single structural point must be connected to both sides. The recommended method for this case is to use separate fluid points for each side of the panel with no physical separation. (The thickness is ignored.) No provision is made for other special cases such as flow through holes in the plates. No surface friction, surface tension, gravity, or other indirect boundary effects are calculated for the simple fluid-structure interface. Damping effects due to acoustic surface materials are described in the next section.

4. Absorbers, Barriers, and Panels

The acoustic absorber and barrier are used for advanced analysis when special boundary effects are needed to model soundproofing materials on the structural surface or baffles within the fluid.

The absorber elements (CHACAB and PACABS Bulk Data) are used to attenuate the reflections of the acoustic waves when they encounter the structural boundary. They are connected between the structure and an additional set of displacement GRID points which serve as the actual fluid interface. They provide a simple tuned circuit with a mass on the point, and a spring and damper in parallel connected to the structure.

The recommended procedure to implement the CHACAB elements is to move all of the fluid boundary points a small distance away from the surface to avoid the automatic connections. An additional set of GRID points corresponding 1:1 with the structural points are placed on the new fluid boundary to replace the structural points. These absorber points are constrained to allow only normal displacements and connected to the structure with CHACAB elements. Note that the damping factors are important in complex eigenvalue and frequency response analysis but will be ignored in real eigenvalue analysis.

The barrier elements CHACBR are similar except that they provide masses on both sets of points and have no damping matrix. They may be used without structural elements to simulate heavy acoustic baffling panels that have little stiffness in the frequency of interest. Either side may be connected to fluid boundaries or one side may be constrained.

The PANEL Bulk Data entry is a convenient method for combining sets of structural elements for output purposes.

Setting Up MSC.Nastran

A number of solution control parameters and commands may be used to guide the acoustic solutions. These are as follows:

- Executive and Case Control

  The solution sequences that currently support the 3-D acoustic boundaries are the Structured Dynamic Sequences, SOLs 107 through 112. These include both modal and direct formulations for transient and frequency response, as well as complex eigenvalue analysis. Superelement controls and restarts are automatic in these solutions and no special data is needed for the acoustics.

  The Case Control data should be set up as a normal dynamics solution. A CMETHOD = request is necessary to obtain coupled eigenvalues. DLOAD and FREQ requests are necessary to analyze forced response in the frequency domain. DLOAD, IC, and TSTEP requests are necessary for transient analysis. The main concern here is to avoid costly runs caused by an excessive number of time steps or frequencies. Be aware that the unsymmetric dynamic solution matrices with complex terms used in this system may run several times longer per solution point than a corresponding structural model.

- Estimating Job Costs

  Although the fluid GRID points will only add one degree-of-freedom per point to the model a three-dimensional mesh in the fluid can be several times the size of the basic structural matrix. Furthermore the boundary coupling terms are unsymmetric and probably damped causing more numerical processing. As a rough estimate, each matrix solve step will be 4X to 10X the cost of a structural static solution. In direct frequency analysis each frequency requires a matrix decomposition. The complex eigenvalues will require approximately 2 to 5 solves. The transient solutions are dominated by vector operations which are several times faster per time step. However, most transient problems require many time steps for adequate accuracy.

- Run Strategies

  For large models, the superelement (SE) reduction methods are recommended to reduce the size of the solution matrices. The interior points of the fluid and the non-boundary structure grid points may each be defined as a separate Tip SEs, which are reduced to a smaller solution size, while the boundary points remain in the residual SE. The residual SE may also contain generalized modal displacements in place of the interior of both fluid and structural points by using the modal synthesis method.

  For moderately large problems, the ASET/OMIT method of reduction is available for both the fluid and structural degrees-of-freedom. However, the accuracy is highly dependent on the analyst's choice of retained degrees-of-freedom. For instance, if all interior fluid points were omitted, the internal acoustic waves would not be sinusoidal and the waves would instantly travel from end to end. The most effective application would be a highly refined structural model connected to a coarser 3-D fluid model. Removing most of the extraneous structural DOF (i.e., rotations, tangential motion, and nonwetted points) could reduce the costs significantly.

The recommended first analysis for the coupled problem is the Direct Complex Eigenvalue Solution Sequence (SOL 107). This solution will indicate the overall dynamic behavior dominated by the lowest frequency natural modes and resonant frequencies. The following are recommendations:

1. The EIGC input to control complex eigensolutions is substantially different from the real mode EIGR data. Read and understand the input definitions. Avoid the default values.

2. The frequency range definitions are specified in units of Radians per Second. Multiply the frequencies of cycle per second by 2π.

3. Do not use damping on the initial runs. The results will be easier to debug and the job will run faster.

4. Beware that an additional mode with zero frequency occurs in closed containers. This mode causes problems with both INVP and LANC methods. Avoid it by specifying a lower frequency range nearly as large as the lowest nonzero mode. An alternative is to add a CELAS spring connected between a fluid point and ground.

- The HESS method should be used only with some form of matrix reduction for typical problems. See the comments above regarding the use of ASET/OMIT an Superelement partitioning.

Running the Jobs

Several diagnostics will be generated automatically by MSC.Nastran. Examples are shown in the following pages.

The following special output is produced by the program when acoustic boundaries are encountered. The first shows the automatic connections found by matching GRID locations:

```
        ***********************************************************
        *                                                         *
        *                MATCHING GRID TABLE                      *
        *                                                         *
        ***********************************************************
        *                 USER GRID IDS.                          *
        *      ACOUSTIC GRIDS    *      STRUCTURAL GRIDS           *
        *                        *                                *
        ***********************************************************
        *                        *                                *
        *            1           *             1001               *
        *                        *                                *
        *            2           *             1002               *
        *                        *                                *
        *            3           *             1003               *
        *                        *                                *
        *            4           *             1004               *
        *                        *                                *
        *            5           *             1005               *
        *                        *                                *
        *           11           *             1011               *
        *                        *                                *
     ETC
        ***********************************************************
```

The following message is a sample of a case when the boundaries do not match:

```
*** USER WARNING MESSAGE 6151, ACOUSTIC COUPLING
    MATRIX WILL NOT BE CREATED FOR FACE =      42     82     83     43
    OF ELEMENT ID =      42 ,BECAUSE ITS FLUID GRID POINTS DO NOT HAVE CORRESPONDING
    STRUCTURAL GRID POINTS.
    USER ACTION: IF COUPLING IS DESIRED, THEN CHECK GRID POINT DATA.
    *
    *
    *
    *
    ETC....ETC.
```

and:

```
 ^^^ DMAP INFORMATION MESSAGE 9055 (SEMG) -  THE FL./STR. INTERFACE CHECK IS FORCES AND MOMENTS
RESULTING FROM A UNIT INCREASE IN PRESSURE, OR CHANGES IN THE FLUID PRESSURE RESULTING FROM RIGID BODY
MOTIONS OF THE STRUCTURE. THESE VALUES ARE DIRECTLY PROPORTIONAL TO THE OPEN SURFACE OF THE FLUID.
```

The following message indicates the error factors in area for free body motions. Nonzero numbers indicate a hole in the model as indicated by the T2 value.

```
                            FL./STR. INTERFACE CHECK
          T1              T2              T3              R1              R2              R3
  1   2.3554080E-18  -8.4260993E-02  -1.4653091E-28   6.0271138E-10   2.6100844E-19   1.8405548E-10
```

- Restarts

   The only major reasons to restart a fluid/structure interaction job are to use superelement processing and/or to change the output requests. In typical jobs the cost in the solution phase is more than 50% of the run, and a restart for a model or load change is not worth the cost of saving a large database.

If the uncoupled structural model is large compared to the size of the actual coupled surface, it may be defined as one or more Tip superelements and run as a separate initial job. The interior points in the fluid may also be treated in this manner. Many acoustic analysis runs can then be restarted each from a copy of the initial database without recalculating the large matrices.

Print and plot output requests may need many changes after the initial runs are made. An output-only restart can be very cost efficient on a large job. Note that most graphical displays do not display complex numbers on model views (i.e., contour plots or deformed shapes). Printed output of selected grid point or element sets may be necessary and is recommended.

Diagnosing Problems

Most of the problems in starting to use acoustics are expected to occur in the definition of the area factors which define the fluid/structure boundary. Some restrictions are necessary to control errors in the case of overlapping fluid and structural FE meshes, and in most cases the user will be warned of discrepancies. Some recommended techniques are as follows:

- Carefully check the special diagnostic outputs shown above. Holes in the boundaries will cause nonzero resultant area factors.

- Run tests without the boundary coupling to estimate the frequencies.

- Temporarily switch to an alternate eigenvalue method and/or a smaller range to ensure modes are correct.

- If a model is large, try subdividing it into smaller sections that can be checked more conveniently.

- Try changing the fluid density to a large number (e.g., water) and run with free structural boundaries. The fluid should not restrain the free-body motions and these modal frequencies should remain at zero.

Advanced Methods

Many of the other MSC.Nastran features should be available for acoustic analysis. Some potential advanced modeling and solution features that will be useful are as follows:

- Modal formulation with superelements: The use of Component Mode Synthesis is recommended for reducing the size of the matrices and the solution costs. The degrees-of-freedom of the interior fluid points will be replaced by the modes of the fluid with rigid container boundaries. The uncoupled structural points may be replaced by modal coordinates defined by a structure in a vacuum.

- Virtual Fluids: The MFLUID Bulk Data input may be used to represent incompressible fluids attached to the structure. This may be used to approximate the low frequency effects of an infinite exterior fluid.

- Decoupled Response Solutions: In most acoustic problems with a load-carrying structure, the structural modes are not affected by the small mass of the air. In turn, the high stiffness of the structure is effectively rigid for the purposes of computing acoustic modes in the air. Forced vibration problems may then be analyzed as two decoupled symmetric solutions:

  - Constrain the entire structural model and perform a forced response analysis on the air (use SLOAD inputs to define the volume inputs from a known source) and save the resulting boundary pressures.

  - Restart the job with the fluid points constrained and a DMAP alter to add the pressure forces to the frequency- or time-dependent load vectors. The resulting structural model will respond to the pressures from the first run.

- Random and Response Spectrum Methods: The MSC.Nastran random analysis options will also be useful for acoustic analysis. This capability requires a set of unit forced responses in the frequency domain (SOLs 108 and 111) and spectral densities of the forcing functions (RANDPS inputs). It will calculate the combination spectral densities and autocorrelations of selected output quantities. In acoustic problems, it could be used for problems having several correlated sources such as an automobile interior.
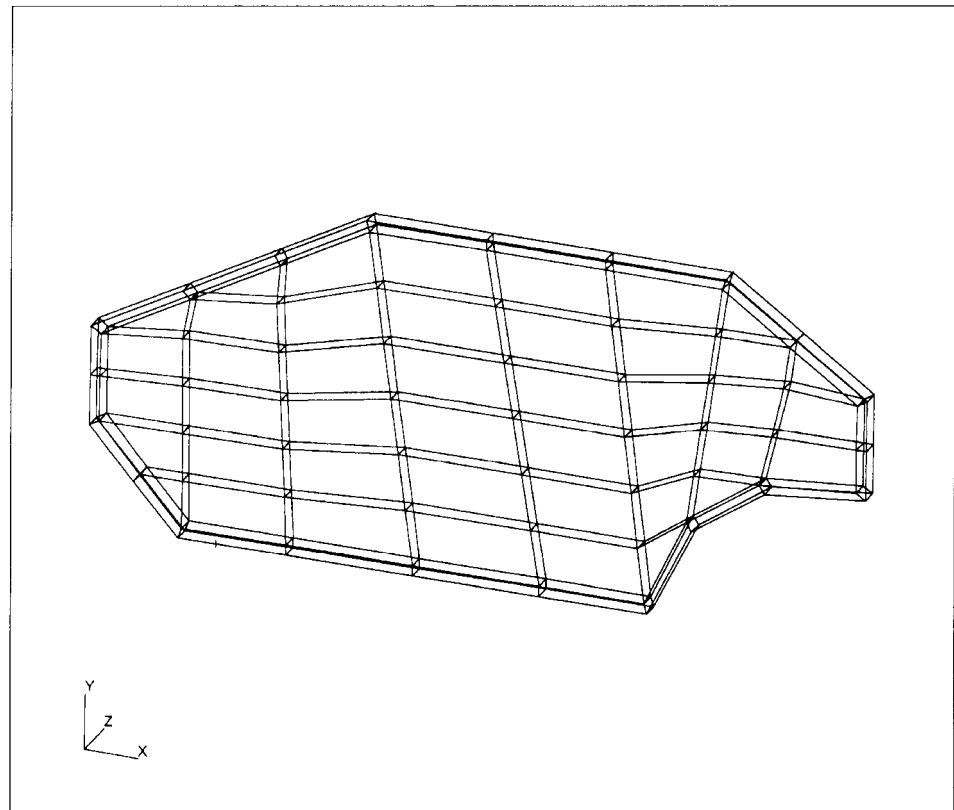
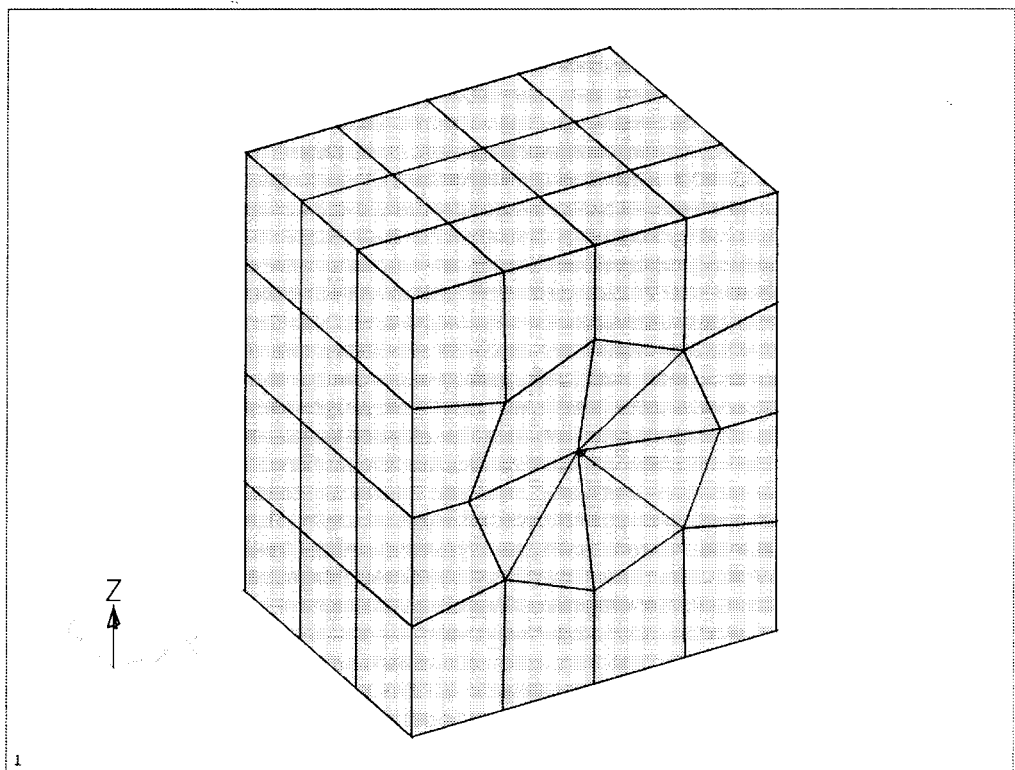**Figure 4-5 Example of Two-Dimensional Automotive Model With Absorbers**

Figure 4-6 Acoustic Suspension Loudspeaker

Test Problem Description

A simple test problem illustrates the fundamentals of acoustic analysis for enclosed containers with flexible walls. The physical problem represents an initial attempt at design and analysis of an enclosure for an acoustic suspension loudspeaker system. The objective was to calculate the resonant frequencies and responses of the system without the mass and impedance of the speaker coil and magnet components.

Physical Description

The structure consists of a simple rectangular box with wood walls as shown by the plate model in **Figure 4-6**. A single cutout is provided for the speaker and a thin polyethylene cone was modeled with triangular shells. The physical properties of the model are listed below. Note the use of the MKS system of units, which illustrates the flexibility of MSC.Nastran.

Width:	0.5 M	Depth:	0.4 M
Height:	0.6 M	Hole Diam.	0.345 M
Box E Modulus:	11.61E9	Box Density:	562 Kg/M**3
Wall thickness:	0.015 M		
Air Wave speed:	344 M/Sec	Air Density:	1.11KG/M**3
Cone E Modulus:	3.4E9	Cone Density:	450.0
Cone thickness:	0.1E-3 M	Cone Depth:	0.04 M

Executive and Case Control

The Executive and Case Control inputs are used for selecting the type of solution, loads, boundaries, and outputs. Several different runs using the same model were made to check results and investigate the effects of structural coupling. The configuration shown below was a Direct Complex Modal solution using the Lanczos method to extract eigenvalues. An SPC request was used to constrain the structure and an output set was defined to limit the printed displacements. All other data was normal, recommended control and label input.

Bulk Data

The key data of note in the Bulk Data section are as follows:

1. The ACMODL input uses the minimum form which connects fluid and structural points at identical locations.

2. PARAM,NEWSEQ,-1. Turns the resequencer off.

3. Several eigenvalue methods were used. It is recommended that complex roots always be checked by another method.

4. The speaker cone consisted of a light, thin plastic material. The virtual mass of the exterior air was estimated and added as nonstructural mass on the PSHELL input.

Results from MSC.Nastran

Three runs (out of many) are described below. They illustrate a recommended sequence for the analysis process.

Run 1: Real Eigenvalue Analysis

Before the coupled structure is analyzed, it is important to understand the behavior of the structural and fluid models separately. Fortunately they can be included in the same data file and the Real Eigenvalue Solution Sequence (SOL 103) may by used. The results for the uncoupled speaker box and the acoustic modes are shown below. Note that the natural frequencies for both systems occur in the same range, which indicates that the enclosure modes will interact with the acoustic cavity resonances. Results for the acoustics were checked by one-dimensional wave solutions. Results for the box were checked against calculated natural frequencies of simply-supported plates.

Mode No.	Frequency, Hz	Type
1	0.0	Air- Constant Pressure (fictitious)
2	292	Air- 1st z (up/down)
3	297	Box- u(y) Back panel
4	351	Air- 1st x (Left/Right)
5	359	Box- u(x) Sides in-Phase
6	379	Box- u(x) Sides out-of-phase
7	450	Box- u(z) Top/bottom
8	453	Air- 1st y (Fore/Aft)

-etc.-

Run 2: Complex Eigenvalue Analysis, Coupled Modes.

The coupled natural frequencies must be obtained from an unsymmetrical matrix equation which requires a Complex Eigenvalue method even in the undamped case. The CLAN method is recommended for most large-order non-superelement jobs. The only changes from the Real Modes job was the addition of an ACMODL input and the changes in eigenvalue method.

Mode No.	Frequency	Type of Dominant Motion
1	0.0	Air- Constant Pressure
2	291	Air- u(z)
3	295	Coupled- u(y)- back panel
4	336	Coupled- u(x)- sides
5	371	Coupled- u(y)- cone

Mode No.	Frequency	Type of Dominant Motion
6	373	Coupled- u(x)- sides
7	445	Coupled- u(z)- top/bottom
8	453	Coupled- u(y)- cone

Results above are interpreted by examining the frequency shifts from the uncoupled system. The modes with u(y) fore-aft motion are most likely to be excited by the speaker. Modes 1, 2, 3, 4, 6, and 7 are close to their uncoupled equivalent. Modes 5 and 8 are new combinations of higher modes. The results were confirmed by several methods:

1. The job was rerun using the INV method on the EIGC Bulk Data and produced nearly identical results.

2. A printout of the interface area matrix was obtained by using a DMAP alter and verified by hand calculations.

3. The natural symmetry of the geometry produced symmetric and antisymmetric results relative to the natural structural planes of symmetry (except for roots with close frequencies).

Run 3: Complex Eigenvalue Analysis, Modal Formulation

A more efficient method for solving a coupled matrix problem is to reduce the size of the matrices by using modal coordinates. In this case, both the structural displacements and fluid pressures are replaced in the matrix solution by generalized coordinates representing the uncoupled real modes. For the modal cases below the real modes (25 total) below 800 Hz. were used. In the coupled cases 13 modes were obtained below 500 Hz. All results compared to within 1%.

On a Sun SPARCstation 1+ the CPU time comparisons are:

Type Solution	Solution Size	CPU Time (Seconds)
Uncoupled Modes	538	110.2
Direct, No Modes	538	586.3
Struct. Modes Only	114	143.2
All Modes	25	106.9

The conclusion is that the modal method (SOL 110) will reduce the costs with very little effect on accuracy. The user is cautioned to use a liberal number of real modes (twice the number of coupled modes) to represent the system.

```
ACOUSTIC TEST PROBLEM DATA FILES
ID SPEAK39F,DNH
SOL 107
DIAG 8,12 $ PRINTS MATRIX TRAILERS AND ROOT-TRACKING MESSAGES.
CEND
TITLE=SPEAKER BOX -WITH CONE, SIMPLE CORNER SUPPORTS
SUBTITLE = COUPLED BOUNDARY, NON-MATCHING ELEMENTS
ECHO= UNSORT
SEALL=ALL
SPC=20
$ USES MKS SYSTEM
CMETHOD = 7  $LANCZOS
SET 20= 3,13,23,43,82,83,84,91,93,95,103,113,123,
     131,135,153,163,171,173,175,183,
     1013,1023,1043,1082,1083,1084,1091,1095,1113,
     1131,1135,1163,1173,1183,1193
DISP= 20  $ FOR MINIMUM PRINTOUT
$ DISP(PLOT)=ALL  $ FOR MSC/XL CONTOUR PLOTS
$
BEGIN BULK
$
$ DEFINE FLUID/STRUCTURE INTERFACE: COINCIDENT POINTS
ACMODL,IDENT
$
PARAM,POST,0
PARAM,COUPMASS,1
$ SUPPRESS SEQUENCER
PARAM,NEWSEQ,-1
$
$ BOX PROPERTIES - WOOD
MAT1,11,11.61+9,,0.3,562.0
PSHELL,1000,11,.015,11,,11
$
$ SPEAKER CONE
MAT1,3,3.4+9,,0.3,450.0
PSHELL,10,3,0.1-3,3,,,0.223
$
$ PROPERTIES OF AIR
MAT10,100,131.94+3,1.115
PSOLID,100,100,,2,,1,PFLUID
$
$ EIGEN METHODS
EIGR,20,MGIV,1.0,600.0
EIGC,7, CLAN,,,,,,,+CLAN
+CLAN,0.0,10.0,0.0,1600.0,100.0,,20
$ USE INVERSE POWER TO CHECK LOW ROOTS
EIGC,107,INV,MAX,,,,,,+EC1
+EC1,0.0,100.0,0.0,1800.0,100.0,12,9
$
$ FIX BOX AT BOTTOM CORNERS
SPC1,20,123,1001,1005,1031,1035
$ COORDINATE SYSTEM AT CENTER OF HOLE
CORD1C,83,283,113,85
$
$
$FLUID GRID POINTS
$ NOTE VALUE OF -1 IN FIELD 7 INDICATES 1 DOF.
GRID,1,, -.25, -.2, -.3,-1
GRID,2,,-.125, -.2, -.3,-1
GRID,3,,  0.0, -.2, -.3,-1
GRID,4,, .125, -.2, -.3,-1
```

```
GRID,5,,   .25, -.2, -.3,-1
GRID,11,, -.25, -.0667, -.3,-1
GRID,12,,-.125, -.0667, -.3,-1
GRID,13,,  0.0, -.0667, -.3,-1
GRID,14,, .125, -.0667, -.3,-1
GRID,15,,  .25, -.0667, -.3,-1
GRID,21,, -.25, 0.0667, -.3,-1
GRID,22,,-.125, 0.0667, -.3,-1
GRID,23,,  0.0, 0.0667, -.3,-1
GRID,24,, .125, 0.0667, -.3,-1
.25, -.2, 0.,-1
-
ETC
-
$ STRUCTURE GRIDS
GRID,1001,, -.25, -.2, -.3
GRID,1002,,-.125, -.2, -.3
GRID,1003,,  0.0, -.2, -.3
GRID,1004,, .125, -.2, -.3
GRID,1005,,  .25, -.2, -.3
GRID,1011,, -.25, -.0667, -.3
GRID,1012,,-.125, -.0667, -.3,,6
GRID,1013,,  0.0, -.0667, -.3,,6
-
ETC.
-
$ OPTIONAL ASET DATA TO USE WITH HESS METHOD
$ASET1,1,1,THRU,195
$ASET1,123,1003,1012,1014,1022,1024,1033
$ASET1,123,1163,1172,1174,1182,1184,1193
$ASET1,123,1042,1043,1044,1081,1082,1083,1084
$ASET1,123,1065,1122,1123,1124
$ASET1,123,1072,1074,1112,1113,1114,1152,1154
$ASET1,123,1051,1061,1131,1141
$ASET1,123,1055,1065,1135,1145
$
$
$SOLID ELEMENTS FOR AIR
CHEXA   1       100     1       2       12      11      41      42      +001
+001    52      51
CHEXA   2       100     2       3       13      12      42      43      +011
+011    53      52
CHEXA   3       100     3       4       14      13      43      44      +021
+021    54      53
CHEXA   4       100     4       5       15      14      44      45      +031
+031    55      54
CHEXA   11      100     11      12      22      21      51      52      +041
+041    62      61
CHEXA   12      100     12      13      23      22      52      53      +051
+051    63      62
CHEXA   13      100     13      14      24      23      53      54      +061
+061    64      63
CHEXA   14      100     14      15      25      24      54      55      +071
+071    65      64
CHEXA   21      100     21      22      32      31      61      62

+081
+081    72      71
-
ETC
-
```

```
$STRUCTURAL ELEMENTS
CQUAD4  1001    1000    1001    1002    1012    1011
CQUAD4  1002    1000    1002    1003    1013    1012
CQUAD4  1003    1000    1003    1004    1014    1013
CQUAD4  1004    1000    1004    1005    1015    1014
CQUAD4  1011    1000    1011    1012    1022    1021
CQUAD4  1012    1000    1012    1013    1023    1022
CQUAD4  1013    1000    1013    1014    1024    1023
CQUAD4  1014    1000    1014    1015    1025    1024
-
ETC
-
$
$SIMPLE CONE
$
CTRIA3, 5042,10,1042,1043,1083
CTRIA3, 5043,10,1043,1044,1083
CTRIA3, 5044,10,1044,1084,1083
CTRIA3, 5084,10,1084,1124,1083
CTRIA3, 5124,10,1124,1123,1083
CTRIA3, 5123,10,1123,1122,1083
CTRIA3, 5122,10,1122,1082,1083
CTRIA3, 5082,10,1082,1042,1083
ENDDATA
```

CHAPTER
5

Dynamic Solution Techniques

- ■ Overview

- ■ Review of Dynamic Excitations

- ■ Complex Eigensolutions

- ■ Nonlinear Transient Response Analysis

- ■ Fourier Transform

- ■ Viscoelastic Material Properties

- ■ Free Body Techniques

- ■ Aeroelastic Solutions

- ■ Dynamic Optimization and Design Sensitivity

5.1　Overview

While planning the modeling process and making provisions for the reduction steps and boundary conditions, the dynamics engineer should also consider the various options in the actual solution. In addition to the basic linear transient and frequency response processes, which are described fully in the *MSC.Nastran Basic Dynamic Analysis User's Guide*, other solution options and variations for dynamic analysis are available.

Complex eigenvalue analysis is used for determining stability and assessing the overall dynamic response of a system. Complex eigenvalue analysis must be used for eigenvalue analysis when unsymmetric matrix terms or large damping effects are present.

Nonlinear transient analysis accounts for nonlinear element effects caused by nonlinear materials, variable surface contact, and large displacements. The procedures for the data input and controls are significantly different than those for the basic linear transient solutions.

An option for using Fourier transform methods is available for the solution of special problems that involve repeating loads in time.

Viscoelastic parameters, which can be applied in the solution of problems involving rubber-like materials, are available as a special process in the direct frequency response solutions.

The solution methods for free bodies are both necessary analysis procedures for unconstrained models and diagnostic tools for constrained bodies. For instance, an airplane or missile in flight (without proper supports) will have a singular stiffness matrix and (will) produce large displacements in the results.

Finally, aeroelastic solutions such as flutter analysis, gust response, and static aeroelasticity are also discussed in this chapter because of their unique algorithms and solution procedures.

5.2   Review of Dynamic Excitations

The methods used for generating dynamic loads in MSC.Nastran are very different from those used for static loads. Dynamic loads generally vary with time or frequency. They may also be applied with different phases or time lags to different portions of the structure. The most general case would be a structure having a different load history for each direction on each point on the model, which could require thousands of tabular inputs.

Fortunately, most applications require only a simple pattern of load variations with time and geometry. The engineer usually encounters a single time function applied to a portion of the structure or a general time function applied to a few structural points. An example of the first case would be wind gust loads on an aircraft. An example of the second case would be an automobile traveling over a rough road. MSC.Nastran requires only a minimum input for either case.

Because of the many possible types of dynamic loading conditions, the input options are also numerous. Most of the basic options are described in "**Modal Versus Direct Frequency Response**" on page 114 and "**Modal Versus Direct Transient Response**" on page 164 of the *MSC.Nastran Basic Dynamic Analysis User's Guide*. Some of the advanced methods are described below.

Subcases in Dynamic Analysis

The Case Control options in dynamic analysis are less flexible than statics and nonlinear analysis. Some of the statics options that are *not* available in dynamic response analysis and complex eigenvalue analysis include:

- Changes in boundary conditions between subcases.
- SUBSEQ and SUBCOM solution combinations.
- Grid point forces and element strain energy outputs.

Otherwise, each type of solution uses the Case Control subcase for a different purpose. Some uses for subcases in dynamics analysis are given below.

1. Subcases are essential for most dynamic optimization problems (SOL 200). Each subcase may define a different type of analysis or a different load.

2. In a superelement analysis, the subcases may be used to specify different upstream LOADSET data and output processing for different SE components.

3. Subcases are recommended in nonlinear transient analysis (SOL 129) for applying loads in a sequence or changing the time step method. A single load may be applied in steps or a second load may be added with new subcases. Changing time step size or the solution method may be necessary to overcome a troublesome divergence region. Subcases also define the allowable solutions that may be used in restarts. Use them liberally.

4. Multiple subcases are available for frequency response analysis (SOLs 108, 111 and 118) for the purpose of solving multiple loading conditions more efficiently. (Each frequency requires a matrix decomposition and each additional load vector may be processed at this time with small cost.) Another use is in random analysis where several loads need to be combined, each with a different spectral density distribution.

5. Subcases are used in complex eigenvalue analysis (SOLs 107 and 110) for processing multiple direct input matrices. Typical applications are multiple control system parameters or externally generated aerodynamic matrices representing a variety of flight conditions.

6. Cyclic symmetry analysis (SOLs 114 through 118) requires subcases to distribute the loads over different petals (i.e., sections of the structure). The methods are identical to cyclic static analysis.

7. Multiple subcases are not recommended for linear transient analysis.

Loading Methods

An overview of the dynamic load algorithm is shown in **Figure 5-1**. The input data follow two major paths: the DAREA method versus the LSEQ method. The details of the data inputs are given in the appendices and in the *MSC.Nastran Basic Dynamic Analysis User's Guide.*
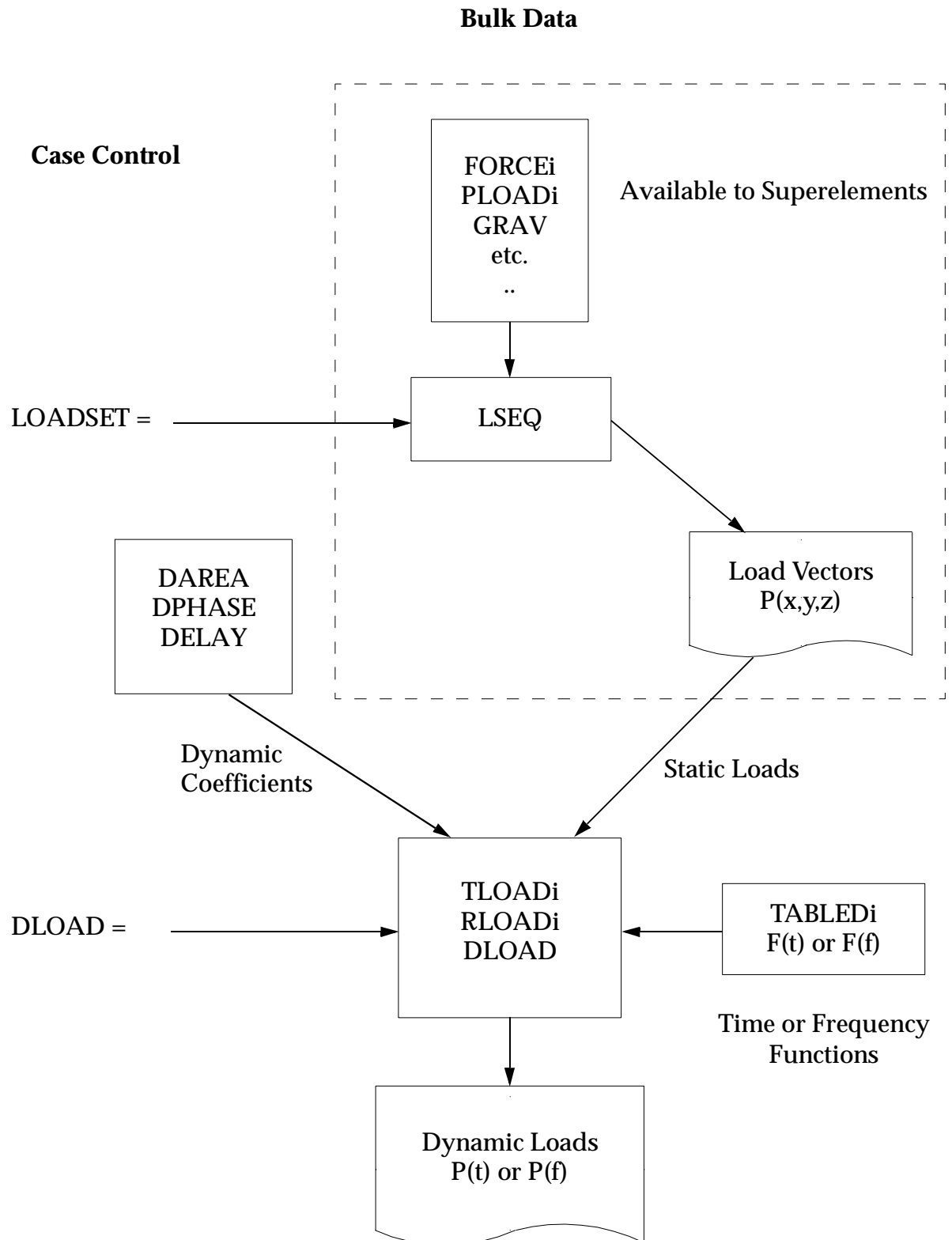
Bulk Data

Figure 5-1 Input Data Relationships for Dynamic Loads

- The LSEQ Bulk Data act much like a set of Case Control commands to generate static loads and assign them to a specific static load vector. These vectors are assembled, reduced, and combined for all superelements. A different load vector may be required for each unique function of time or frequency.

- The DAREA, DPHASE, and DELAY Bulk Data provide a direct method of distributing the dynamic loads over the grid points. The DAREA factors correspond to a specific load factor for a specific degree-of-freedom, much like an area under a pressure load. The DPHASE and DELAY data are used when the same load versus time function is applied to different points at different times. An example of a DPHASE application is the frequency response of an automobile traveling over a highway with a sinusoidal undulation. As the speed increases the input frequency changes, but the phase difference between the axles is constant.

The TLOADi Bulk Data inputs each define a function of time with coefficients or TABLEDi references. The RLOADi Bulk Data inputs each define a function of load versus frequency with complex TABLEDi inputs. The DLOAD entry is used to combine the different load functions, either time or frequency dependent. These functions may be associated with LSEQ-type vectors or DAREA coefficients, or both.

Recommendations

The following guidelines should be observed when applying dynamic loads.

TABLEDi

1. Remember that the tables are extrapolated at each end from the first or last two points. If the load actually goes to zero, add two points with values of y = 0.

2. Linear interpolation is used between tabular points. This may lead to accumulated roundoff and drift errors over a long-period transient analysis. Fix this problem by adding a correcting load function to the same points on subsequent runs.

3. If a jump occurs (two points with equal values of X), the value of Y at the jump is the average of the two points.

Static Preloads

1. An initial linear static preload that is released suddenly for a transient analysis may be performed in two stages in one run. In stage 1, apply the static loads and use large time steps to suppress the higher frequency motions. In stage 2, remove the loads and use small time steps to capture the dynamic action. Alternatively, a nonlinear analysis may be restarted from a nonlinear static analysis, making the process nearly automatic.

2. Simple static loads may be included through the dynamic load methods. Define a TLOAD2 or an RLOADi with a constant function and add it via the DLOAD Bulk Data input.

3. Thermal loads may be applied via the LSEQ method, but note that the dynamic stress recovery method will not account for the additional strain or stress.

Matching Initial Conditions

1. In linear transient analysis, the load at time, $t = 0.0$ is always ignored. If the load is actually a preload, the initial conditions (TIC data) should correspond to this condition. Otherwise, if the load is being suddenly applied, the loading functions will start at $t = \Delta t$.

2. If a free body is being accelerated by an applied load, the calculated response will also be delayed by a fraction of a time step.

Setup for Random Analysis

An MSC.Nastran random analysis requires a preliminary frequency response analysis to generate the proper transfer functions that define the output/input ratios. The squared magnitudes of the results are then multiplied by the spectral density functions of the actual loads. Normally, the inputs are unit loads (e.g., one g constant magnitude base excitation or a unit pressure on a surface).

Fluids and Acoustic Loads

Normally, fluid and acoustic elements are not loaded directly, but are excited by the connected structures. However, loads on these special grid points may be used to represent sources of fluid motion such as a small loudspeaker. The actual units of these loads are the second derivative of volume flow with respect to time. See "**Axisymmetric Fluids in Tanks**" on page 105 for details.

5.3   Complex Eigensolutions

Complex eigenvalue analysis is necessary when the matrices contain unsymmetric terms, damping effects, or complex numbers where real modes analysis cannot be used. It is used for the analysis of aeroelastic flutter, acoustics, rotating bodies, and many other physical effects.

The unforced motion of a system of equations can be expressed as the sum of the motion of its eigenvectors, oscillating and decaying or expanding with terms of the form

$$u(t) \; = \; Real\left(\sum \{\phi_i\} e^{(\alpha_i + i\omega_i)t} \right) \qquad\qquad \text{Eq. 5-1}$$

The value of α_i gives a measure of the rate of decay or divergence of the i-th natural dynamic mode. If the value of ω_i is nonzero, it gives a measure of the rate of oscillation of the solution. For the most general case, ϕ_i, which represents the shape of the mode, contains complex numbers. The relative size of these numbers indicates which parts of the structure are most active in this mode of motion. The imaginary parts of $\{u\}$ signify phase differences or lag times between the degrees-of-freedom.

The results of complex eigenvalue analysis are used for tasks such as measuring the effect of damping materials on system performance and determining the stability of a system when it contains sources of energy such as rotating components. The complex eigensolution is an end product in MSC.Nastran. There are no provisions for using these shapes for modal solutions of frequency response analysis or transient response analysis, as is done for the real eigensolution capability.

The Two Forms of Eigensolution

There are many special classes of eigenvalue problems. MSC.Nastran breaks all of them into two major categories. The *real eigenvalue problem* is expressed by the two matrix equation

$$[K - \lambda_i M]\{\phi_i\} \; = \; 0 \qquad\qquad \text{Eq. 5-2}$$

where K and M are real and symmetric, and M is positive semi-definite. This type of eigenvalue problem is discussed in the *MSC.Nastran Basic Dynamic Analysis User's Guide*. All damping effects are ignored. It can be shown that the eigenvalues λ_i and eigenvectors ϕ_i of this problem must be real, not complex, and that the eigenvectors can be made orthonormal with respect to the mass matrix and orthogonal to the stiffness matrix; that is,

$$\phi^t M \phi \; = \; I \qquad\qquad \text{Eq. 5-3}$$

where I is the identity matrix, and

$$\phi^t K \phi \; = \; \Lambda \qquad\qquad \text{Eq. 5-4}$$

where Λ has the eigenvalues stored along its diagonal. This property is used to separate eigenvectors for repeated eigenvalues into linearly independent sets.

Any problem whose input matrices do not meet these restrictions is called a *complex eigenvalue problem* in MSC.Nastran. In general, the solution may include real or complex numbers, and the orthogonality properties of this more general case are less powerful.

The matrix equation used for the complex eigenvalue problem is

$$[K + pB + p^2M]\{\phi\} \ = \ 0$$

Eq. 5-5

and

$$p \ = \ \alpha + i\omega$$

where any of the matrices may contain real or complex numbers, and may also be symmetric or unsymmetric. If all matrices are symmetric, there is a transformation similar to **Eq. 5-3** and **Eq. 5-4** that can transform all three matrices to a diagonal form. If any of the matrices is complex or unsymmetric, only a weaker orthogonality condition applies. If all of the eigenvalues are distinct (that is, there are no repeated roots), each matrix can be reduced to diagonal form by also computing the left hand eigenvectors ϕ_L, that is, the eigenvectors of **Eq. 5-5** when all of its matrices are transposed. One orthogonality condition for any two roots of the system happens to be

$$\lfloor \phi_{Li} \rfloor^T [(p_i + p_j)M + B]\{\phi_{Rj}\} \ = \ 0 \text{ if } p_i \neq p_j$$

Eq. 5-6

where ϕ_R are the right-hand eigenvectors of **Eq. 5-5**. Some of the eigensolution methods use these orthogonality conditions to improve the linear independence of the eigenvectors, while others do not. None of the MSC.Nastran complex eigensolution methods has a special provision for repeated roots. They may return the same eigenvector for each of the repeated roots.

A special form of **Eq. 5-5**, called the shifted form, is used by some methods to provide faster convergence in the iterations. If we introduce a shift point, p_0, the relative distance of the root is

$$\Delta \ = \ p - p_0$$

Eq. 5-7

and **Eq. 5-5** becomes

$$[K + p_0B + p_0^2M]\{\phi\} \ = \ -\Delta[p_0B + 2p_0M + M\Delta]\{\phi\}$$

Eq. 5-8

One may iterate **Eq. 5-8** by solving for trial vectors on the left side using previous estimates on the right side to produce vectors corresponding to the smallest values of Δ. This procedure is used in the Lanczos method to obtain sets of approximate vectors and in Inverse Power to obtain actual vectors.

The Complex Eigensolution Methods

There are three basic methods available at present. They are all based on iteration in some form or other, with the result that their computation costs are somewhat unpredictable. They are discussed in the order of their general utility, the most widely used first. Details

The Complex Hessenberg Method

The basic algorithm solves the single matrix eigenvalue problem

$$[A - \lambda_i I]\{u_i\} = 0 \qquad\qquad \text{Eq. 5-9}$$

A is transformed to an upper Hessenberg form. In this form all terms below the subdiagonal are null. All of the roots of this transformed problem are computed by the double QR algorithm of Francis. The eigenvectors are then found by inverse iteration. Convergence is usually within one or two iterations because the roots are known at this point. There are similarities in this solution process with the tridiagonal methods of real eigenvalue analysis.

The three-matrix form is transformed to the single matrix form by premultiplying by the inverse of the mass matrix,

$$[M^{-1}K + pM^{-1}B + p^2I]\{u\} = 0 \qquad\qquad \text{Eq. 5-10}$$

If B is null then $A = M^{-1}K$ and $\lambda_i = -p^2$. If B is not null the velocity vector v is defined from u,

$$v = pu \qquad\qquad \text{Eq. 5-11}$$

Eq. 5-10 and **Eq. 5-11** are combined to form

$$\left[\begin{bmatrix} M^{-1}B & M^{-1}K \\ -I & 0 \end{bmatrix} + p \begin{bmatrix} I & 0 \\ 0 & I \end{bmatrix} \right] \begin{Bmatrix} v \\ u \end{Bmatrix} = \{0\} \qquad\qquad \text{Eq. 5-12}$$

If B is null **Eq. 5-10** is used to produce n eigenvalues (only roots with $\omega \geq 0$ are calculated), while if B exists **Eq. 5-12** will produce 2n eigenvalues. The user can control the number of eigenvectors computed in the Inverse and Lanczos methods.

The fact that M must have an inverse means that M may not contain null rows or columns, or other sources of singularity. The rows and columns for these singular DOFs may be removed by omitting them with OMITi entries, or, what is often less labor for large models, by retaining important DOFs with independent mass with ASETi entries. All other unconstrained DOFs are then placed in the omitted set. In general, translation DOFs with attached masses are safe candidates for the a-set. Care should be taken with rotational DOFs. An example of a DOF with nonnull mass but which is not independent is a rotation DOF to which a CONM2 element is attached, and the CONM2 element has a point mass and an offset, but zero moments of inertia. The rotation DOF will be singular when the matrix is inverted.

No special logic is used for repeated roots, which return the same eigenvector. There is a system cell which requests that a newer method with spill capability be used. The default value for this system cell uses an algorithm with no spill capability. System cells can be set on the NASTRAN command. Refer to the "**EIGC**" on page 874 of the *MSC.Nastran Quick Reference Guide* for details.

This method does not take advantage of matrix sparsity or banding. Solution costs are proportional to n^4.

The Complex Lanczos Method

Ritz vectors (that is, trial eigenvectors) are computed from **Eq. 5-8** by inverse iteration, after inserting a trial eigenvalue called a shift. Shift points are selected by the user. These vectors are used to reduce the problem to tridiagonal form using the Lanczos reduction method. The roots are computed by the QL algorithm in this reduced basis, and the eigenvectors are computed by inverse iteration. The eigenvectors are then back-transformed to the original basis. Both left- and right-hand eigenvectors are computed to improve the convergence of the method. The left-hand eigenvectors are an optional output of the eigensolution module.

The roots are computed near the shifts specified by the user. The method attempts to compute all roots near a shift before going on to the next shift, but it can not be guaranteed that all roots near the shift will be found. If more roots are calculated than were requested, all are output.

This method takes advantage of the bandedness and sparsity of the input matrices.

Solution costs are proportional to $(r/10)nb^2$ where b is the semi-bandwidth and r the number of eigenvectors computed. Many roots can be computed from each shift.

The Complex Inverse Power Method

The basic equation is solved by inverse iteration from the shifted equation similar to the initial stage used for the Lanczos method. Each eigenvector and its eigenvalue are determined simultaneously until a solution has converged to a user-specified tolerance. The user inputs subregions in the complex plane for root searches. The same qualifications that all roots in a region may not be found applies here, too. Costs are proportional to $3rnb^2$ because several shifts are usually required for each root found. This method is useful for finding a few roots in a small region where poorly conditioned matrices cause problems with the other methods.

The Modal Hessenberg Method

For many problems this method combines the best features of the real eigensolution methods and the Complex Hessenberg method. The real eigensolutions from the structural stiffness and mass matrices are found first. The Lanczos and SINV real eigenvalue methods use a Sturm sequence technique that guarantees that all roots in a range have been found or identified as being missing. The tridiagonal real eigensolution methods also find all roots of the problem, so that none can be missing. Unfortunately, there is no similar technique for roots in the complex plane. Using a modal approach provides the following benefits:

1. The user can be assured that all the undamped roots of the system in a region specified by the user have been found with any of the real methods.

2. The complex eigenvalues are usually of the same order of magnitude as the real eigenvalues.

3. The real eigenvectors are then used to reduce the damping matrix and any other special dynamic effects that may be present to h-set size matrices.

4. The h-set mass matrix is guaranteed to be well conditioned for the inverse operation unless very strange effects are input with the M2PP matrix or the counterpoint terms of transfer functions, so there is no need to omit massless physical DOF, a task which can be laborious on a complicated model. (It is necessary, however, to ensure that any extra points that are used have nonnull mass terms.)

5. All eigensolutions are then found in this reduced basis. The user is assured that there are no solutions which have been skipped over.

6. The economic trends are also favorable because the real eigensolutions do take advantage of matrix sparsity and banding (the Real Lanczos Method is the best in this respect today), and they reduce the problem to a much smaller size before the Hessenberg solution is attempted.

However, if strong nonstructural effects are present, such as those caused by direct input matrices or transfer functions, a large number of real modes may be necessary to account for these forces. An example would be a servo control that acts as a large mass on the structure. This mass could reduce the frequency of some local high frequency modes and move them into the important range.

The Complex Lanczos and Inverse Power methods may also be used in the modal method, but the economic rewards are less, and they may also miss roots. They should be used as backup methods in this context, used to check the solution produced by the Hessenberg method when there is some question about its correctness.

User Interface

Various form of the eigenvalues are used as inputs and are provided as outputs. The real eigensolution outputs the eigenvalues in three forms. The complex eigenvalue, p, is formed from the real quantities α and ω where $p = \alpha + i\omega$. If $\alpha = 0.$, the radian frequency, ω of complex eigenvalue analysis is the same as that of real eigensolutions. The real part, α, is a measure of the decay rate of a damped structure, or if negative, the rate of divergence of an unstable system. The imaginary part, ω, is the modified frequency in radians/unit time. However, roots with negative values of ω should be treated as special terms. The output labeled f is the circular frequency in cycles per unit time. It is equal to $\omega/(2\pi)$.

The CMETHOD = [SID] Case Control command selects the EIGC Bulk Data entry, which has the form

1	2	3	4	5	6	7	8	9	10
EIGC	SID	METHOD	NORM	G	C	E	ND1		

	2	3	4	5	6	7	8	9	10
	ALPHAAJ	OMEGAAJ	ALPHABJ	OMEGABJ	LJ	NEJ	NDJ		

NORM, G, and C have to do with the specification of the method of normalization. The eigenvectors may be normalized either to a unit value at grid point G for coordinate C, or for the largest term to be of unit magnitude. E is used to specify the convergence criterion of the solution. Each method has a different default value for this criterion, and each is adequate for most problems. ND1 is the number of eigenvectors to be computed by the Hessenberg method. Data in this field is only allowed when there are no continuation entries, while the Hessenberg method ignores the data on the continuation entries.

The shift points for the Lanczos method are defined on the continuation entries. The recommended practice is to specify one point $\alpha_1 = 0.0$ and ω_1 at the lower bound of the expected range of eigenvalues, but not at 0.0 A second shift may be input at $\alpha_2 = 0.0$ and ω_2 at the upper bound of the expected range. All ALPHABj and OMEGABj must be blank. The number of Ritz vectors computed for the J-th shift is three times the number entered in NDJ. While each Ritz vector may be capable of defining an eigenvector, it is more likely that some of the Ritz vectors will be discarded because they are not orthogonal to lower-numbered Ritz vectors during the Lanczos reduction process. After the poor vectors are discarded, the remaining vectors are used to compute the eigensolutions.

The number of modes computed from all shifts up to the j-th shift may be more or less than NDJ. If there are less, the processing continues with the next shift; otherwise, the process ends and all eigensolutions are output. The ratio of discarded vectors to retained vectors is problem dependent. However, the recommended practice is to ask for all of the desired eigenvectors for ND1 on the first shift, but put in additional shifts. If it is possible to compute all solutions with one shift, this is the most economical option. If more shifts are needed, they will be used.

The subregions for searching for roots with the Inverse Power method are also specified on the continuation entries. (ALPHAAJ, OMEGAAJ) define one point in the complex plane, and (ALPHABJ, OMEGABJ) a second point. A line is drawn between these points, and a box of width LJ is placed around this line. NEJ is larger than the number of roots expected in the subregion, and NDJ the number desired. This defines the first subregion for searching for eigenvalues. More continuation entries may be used to define more subregions. Again, if more eigenvalues are computed than are requested, all are output.

The eigenvalue output for a sample problem is shown below:

```
C O M P L E X   E I G E N V A L U E   S U M M A R Y
ROOT      EXTRACTION           EIGENVALUE              FREQUENCY      DAMPING
NO.          ORDER          (REAL)        (IMAG)        (CYCLES)    COEFFICIENT
  1            9          -5.806441E+01 5.750383E+03   9.152019E+02  2.019497E-02
  2            8          -6.294888E+01 6.293917E+03   1.001708E+03  2.000309E-02
  3            7          -6.910709E+01 6.844852E+03   1.089392E+03  2.019243E-02
  4            1          -3.300980E+02 1.667092E+04   2.653260E+03  3.960164E-02
  5            5          -3.565692E+02 1.823559E+04   2.902285E+03  3.910694E-02
  . . .
```

The column labeled (REAL) contains α_1, and the column labeled (IMAG) contains ω_1. The column labeled (FREQUENCY) contains the circular frequency. The last column is the damping coefficient computed from the equation

$$(g) = -2\alpha / |\omega|$$

which is approximately twice the value of the conventional modal damping ratio. This form was more popular with the aeroelastic flutter specialists who were the primary users of this capability.

Note that if the magnitude of this term is computed to be less than 5.0×10^{-4}, it is reset to zero.

For small values, the damping coefficient is twice the fraction of critical damping for the mode. The eigenvalues are sorted on ω, with the negative values sorted first (there are none in this example), sorted on increasing magnitude, followed by the eigenvalues with positive ω, again sorted on magnitude. Roots with equal ω values are sorted next on α.

Modeling Techniques

All Methods

Repeated roots are usually due to planes of symmetry of a structure. For example, a pencil has a pair of repeated roots for each bending mode, with their eigenvectors being at 90 degrees to each other. In physical structures there is never absolute symmetry because of the effects of manufacturing tolerances, material inconsistencies, etc. The user may adopt this point of view when repeated roots cause problems by making small perturbations to the structure to destroy symmetry. For example, when doing an analysis for the damped modes of a pencil, a small mass term can be added in one direction. A small perturbation is usually adequate to separate the modes enough to eliminate numerical problems.

Hessenberg Method

1. If extra points or other DOFs are connected by only transfer functions or x2PP matrix terms, they may need to be differentiated to provide a mass term on these DOFs. For example, if the following equations are written for extra points e_1 and e_2, which are coupled to the structural DOFs u_{11} and u_{12},

$$c_1 \cdot e_1 = u_{11}$$

$$c_2 \cdot \dot{e}_1 = u_{12}$$

In these forms, c_1 would appear in the stiffness term of the transfer function, and c_2 in the damping term.

The first equation can be differentiated twice, and the second once, to provide

$$c_1 \cdot \ddot{e}_1 = \ddot{u}_{11}$$

$$c_2 \cdot \ddot{e}_1 = \dot{u}_{12}$$

The c_i terms are placed in mass terms slots in the transfer function, or in the M2PP matrix.

2. Avoid coupled mass. One apparent choice for obtaining mass terms on rotation DOFs is to request coupled mass by use of the PARAM entry that requests it (but this is usually a poor choice). The theories for coupled mass for some elements in MSC.Nastran do not provide rotational mass while other elements have theories that produce rotational mass in a manner that does not provide an independent mass term, leading to either failure in the inversion of $[M]$, or poor numerical conditioning. Null masses on rotational DOFs cause no problems in modal analysis.

    In direct analysis, if all unconstrained rotations are omitted, this potential singularity problem is avoided, with little or no loss in accuracy, and the cost of static reduction of the system is less than the savings of solving a smaller sized eigenproblem.

Example Problem: Complex Roots of a Friction Mechanism

This problem illustrates the modeling and solution of a model with unsymmetric matrix inputs. Complex eigenvalue analysis can predict the existence of unstable or undamped roots, which will be the cause of noise.

The model consists of three bodies illustrated in **Figure 5-2**, namely a rigid housing, a pad with an expendable friction surface, and a moving surface contacting the pad.
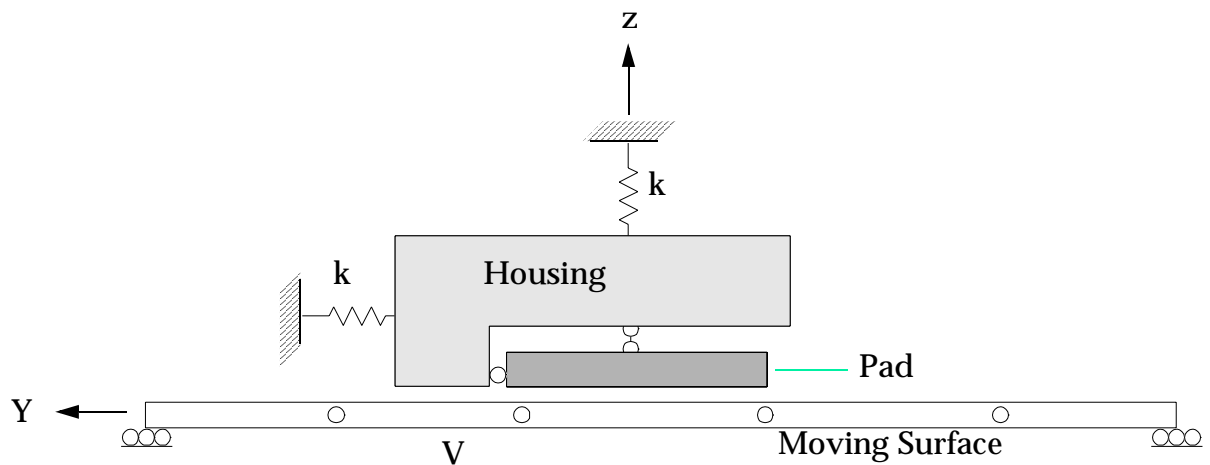

Figure 5-2 Sliding Friction Complex Eigenvalue Analysis

The objective of the analysis is to determine whether the friction effects can cause the onset of a divergent squeal mode. The following assumptions are made in the modeling:

1. The speed of the sliding surface is assumed to be much less than the speed of the traveling vibrational waves. Therefore, the elements representing the surface may be limited to small motions and the traveling wave effects are ignored.

2. Pure sliding friction is assumed. The magnitude of the pad vibration may be very small for the onset of the unstable mode. The analysis will be invalid when the vibrational velocities exceed the surface velocity.

3. A static preload is assumed to be large enough to maintain full contact on the pad surface. The frictional coefficient is assumed to be constant. (However, it could be varied over the contact region.)

Frictional forces on the pad and sliding surface are proportional to the normal contact forces, which in turn may vary with dynamic response. For small dynamic motions the relationship is

$$F_{py} = -F_{sy} = \mu N \qquad \text{Eq. 5-13}$$

where:

F_{py} is the tangential force on the pad.

F_{sy} is the tangential force on the sliding surface.

μ is the friction coefficient.

N is the normal compression force variable.

The value of N is only available indirectly from the element forces or by the use of Lagrange multipliers. The solution variables in a conventional model consist only of displacements, velocities, and accelerations.

An approximation to N may be generated from a penalty function method using large springs to represent the contact constraint. If a large spring, K (CELAS2 data), is connected to the two normal displacements at a point, the normal force is a function of the displacements

$$N = -K(u_{pz} - u_{sz}) \qquad \text{Eq. 5-14}$$

where u_{pz}, u_{sz} are the displacements in the normal direction.

Combining **Eq. 5-13** and **Eq. 5-14**, we obtain the following matrix relationship:

$$\left\{ \begin{matrix} F_{py} \\ F_{sy} \end{matrix} \right\} = \mu K \begin{bmatrix} -1 & 1 \\ 1 & -1 \end{bmatrix} \left\{ \begin{matrix} u_{pz} \\ u_{sz} \end{matrix} \right\} \quad \text{etc.} \qquad \text{Eq. 5-15}$$

Special Input

The matrix terms in **Eq. 5-15** may be input to the problem for each contact point directly as DMIG data. The resulting matrix will be unsymmetric. The Case Control command required for DMIG input is

$$K2PP = FRICTN$$

where FRICTN is the name of a DMIG Bulk Data entry, which starts with the header entry

$$DMIG, FRICTN, 0, 1, 1, 0 \ldots$$

where the inputs and their functions are as follows:

FRICTN	DMIG name
0	Required for all DMIG headers
1	Input format is single precision
0	Output format depends on the type of computer being used. The best format is chosen for each computer type.

A DMAP alter is used to allow multiplying this matrix by the user parameter FRIC.

Listing 5-1 shows the resulting MSC.Nastran input file. RBEi and CONM2 elements are used to simplify the model and eliminate spurious roots. The unique inputs are the DMIG data and the associated CELAS2 springs, (Ids = 311-314).

The Case Control for a complex LANCZOS method is shown here, with the provisions for the other methods preceded by a $ symbol. (Lines starting with $ are treated as comments, but are otherwise ignored.)

```
CMETHOD = 10   $CLAN
$CMETHOD = 11   $INVP
$CMETHOD = 12   $HESS
```

A METHOD command is required when using the modal method of SOL 110. This input is for the direct method of SOL 110. The CMETHOD command is required for complex eigensolution method selection. Eigenvector output is requested by the DISP command.

The Bulk Data entries selected by these commands are as follows:

```
EIGRL,1, , 4000.0, 12 $ real lanczos
EIGC, 10, CLAN, MAX, , , , , ,+ELAN1
+ELAN1, 0.0, 6000.0, , , , , 12,, +ELAN2
EIGC, 11, INV , MAX, , , , , ,+EINV
+EINV, 0.0, 10000.0,  0.0, 50000., 20000., 20, 12
EIGC, 12, HESS , MAX, , , , 12
```

Listing 5-1 Input Data for Complex Eigenvalue Stability Analysis

```
$ FILE CEADL693.DAT
INIT MASTER(S) $ DISCARD DATA BASE AT END OF RUN
DIAG 12 $ DIAGNOSTICS FOR LANCZOS
COMPILE GMA SOUIN=MSCSOU NOLIST NOREF
ALTER 'MTRXIN' $ USE STRING-BASED ALTERS FOR VERSION 68.2 AND SUBSEQUENT
ADD   K2PP, /K2PPX/V,Y,FRIC=(1.0,0.0) $
EQUIVX   K2PPX/K2PP/-1 $
ENDALTER
$SOL 103 $ USE FOR CHECK OF REAL MODES
SOL 107
$SOL 110 $ USE FOR MODAL HESSENBERG
DIAG 8 $ MATRIX TRAILERS
TIME  5
CEND
$
TITLE = SIMPLE COMPLEX EIGENVALUE ANALYSIS
SUBTITLE = UNSYMMETRIC, LANCZOS, FRICT=0.05
LABEL = 1% DAMPING
K2PP = FRICTN
$METHOD = 1 $ USE FOR MODAL HESSENBERG ANALYSIS
CMETHOD= 10  $CLAN
$CMETHOD= 11  $INVP
$CMETHOD= 12  $HESS
$SPC=10
MPC = 200
SVECT = ALL $ PRINT REAL EIGENVECTORS
SDISP = ALL $ PRINT REAL MODE COMPONENTS OF COMPLEX EIGENVECTORS
DISP = ALL $ PRINT COMPLEX EIGENVECTORS
SET 1 = 102, THRU, 202
BEGIN BULK
PARAM, GRDPNT, 0
PARAM, G, .02
PARAM, FRIC, 0.05
$
$ RIGID HOUSING MOUNTED ON SPRINGS, YZ MOTIONS ONLY
GRID,100,,0.0,0.0,35.0,,156
GRID,101,,0.0,0.0,15.0,,1456
GRID,102,,-50.0,30.0,7.5,,1456
GRID,103,,50.0,30.0,7.5,,1456
RBE2,101,100,23,101,102,103
$ LUMPED MASS AT CG
CONM2,100,100,,2.0 , , , , ,+CM1
+CM1,7200.0,,7200.0 , , ,7200.0
$ SPRINGS TO GROUND
CELAS2,102, 78.96+6, 100, 2
CELAS2,103, 78.96+6, 100, 3
CELAS2,104, 2.846+11,100,4
$
$ PAD IS A SINGLE HEXA WITH A POINT FOR THE HOUSING
CHEXA,200,200, 211, 212, 214, 213, 221, 222,+CHX1
+CHX1, 224, 223
RBE3,201,,201,123456,1.0,123,221,222,+RBE3
+RBE3,223,224
CONM2,202,201,,0.2
GRID, 201, ,0.0,0.0,15.0
GRID, 211, , -50., -30., 0.0,,1456
GRID, 212, ,  50., -30., 0.0,,1456
GRID, 213, , -50.,  30., 0.0,,1456
GRID, 214, ,  50.,  30., 0.0,,1456
GRID, 221, , -50., -30., 15.0,,1456
GRID, 222, ,  50., -30., 15.0,,1456
GRID, 223, , -50.,  30., 15.0,,1456
GRID, 224, ,  50.,  30., 15.0,,1456
```

Listing 5-1 Input Data for Complex Eigenvalue Stability Analysis (continued)

```
PSOLID, 200, 200, , THREE
MAT1,200,1.0+6,,0.3,1.111-6,,,0.02
$
$ RIGID LINKS FROM PAD FOR TANGENTIAL STOPS
MPC, 200, 213,2, 1.0,  223,2, 1.0, , +MPC21
+MPC21,,   102,2, -2.0
$MPC, 200, 213,3, 1.0,  223,3, 1.0, , +MPC22
$+MPC22,,   102,3, -2.0
MPC, 200, 214,2, 1.0,  224,2, 1.0, , +MPC31
+MPC31,,   103,2, -2.0
$MPC, 200, 214,3, 1.0,  224,3, 1.0, , +MPC32
$+MPC32,,   103,3, -2.0
$
$RBE3,202,,102, 234, 1.0, 123, 213 ,223,+RB31
$+RB31,UM ,213,23, 223,2
$RBE3,203,,103, 234, 1.0, 23 ,214, 224,+RB32
$+RB32,UM ,214,23, 224,2
$ SPRINGS CONNECTING HOUSING TO CENTER OF PAD
CELAS2,201, 15.791+6, 201,3 ,101,3
CELAS2,202, 15.791+6, 201,2 ,101,2
$
$ MOVING SURFACE SIMULATED WITH PLATES
$
CQUAD4,301,300,301,302,304,303
CQUAD4,302,300,303,304,312,311
CQUAD4,303,300,311,312,314,313
CQUAD4,304,300,313,314,322,321
CQUAD4,305,300,321,322,332,331
$
GRID, 301,,-50., -150.0, 0.0,, 12356
GRID, 302,, 50., -150.0, 0.0,, 12356
GRID, 303,,-50., -90.0, 0.0,, 1256
GRID, 304,, 50., -90.0, 0.0,, 1256
GRID, 311,,-50., -30.0, 0.0,, 1256
GRID, 312,, 50., -30.0, 0.0,, 1256
GRID, 313,,-50.,  30.0, 0.0,, 1256
GRID, 314,, 50.,  30.0, 0.0,, 1256
GRID, 321,,-50.,  90.0, 0.0,, 1256
GRID, 322,, 50.,  90.0, 0.0,, 1256
GRID, 331,,-50.,  150.0, 0.0,, 12356
GRID, 332,, 50.,  150.0, 0.0,, 12356
$
PSHELL, 300, 300, 15.0, 300,,300
MAT1, 300, 7.106+9, , 0.3, 4.444-6,,, 0.02
$
$ DUMMY SPRINGS TO MEASURE NORMAL FORCES
CELAS2, 311, 4.0+9, 311,3, 211,3
CELAS2, 312, 4.0+9, 312,3, 212,3
CELAS2, 313, 4.0+9, 313,3, 213,3
CELAS2, 314, 4.0+9, 314,3, 214,3
$
$ DMIG'S REPRESENT SLIDING FRICTION.
$ TANGENTIAL FORCES EQUAL NORMAL FORCES TIMES FRICTION COEFFICIENT
$ MU =1.0
DMIG,FRICTN, 0, 1, 1, 0
$
DMIG,FRICTN, 211,3,, 211,2, 4.0+9,,+C211
+C211, 311,2, -4.0+9
DMIG,FRICTN, 311,3,, 211,2, -4.0+9,,+C311
+C311, 311,2,  4.0+9
$
```

```
DMIG,FRICTN, 212,3,, 212,2, 4.0+9,,+C212
+C212, 312,2, -4.0+9
DMIG,FRICTN, 312,3,, 212,2, -4.0+9,,+C312
+C312, 312,2,  4.0+9
$
DMIG,FRICTN, 213,3,, 213,2, 4.0+9,,+C213
+C213, 313,2, -4.0+9
DMIG,FRICTN, 313,3,, 213,2, -4.0+9,,+C313
+C313, 313,2,  4.0+9
DMIG,FRICTN, 214,3,, 214,2, 4.0+9,,+C214
+C214, 314,2, -4.0+9
DMIG,FRICTN, 314,3,, 214,2, -4.0+9,,+C314
+C314, 314,2,  4.0+9
$
EIGRL,1, , , 20 $ USE FOR MODAL HESSENBERG
EIGC, 10, CLAN, MAX, , , , , ,+ELAN1
+ELAN1, 0.0, 6000.0, , , , , 12,, +ELAN2
EIGC, 11, INV , MAX, , , , , ,+EINV
+EINV, 0.0, 10000.0,  0.0, 50000., 20000., 20, 12
EIGC, 12, HESS , MAX, , , , 12
$ OMITS ARE NECESSARY WITH HESS TO REMOVE SINGULARITIES IN THE MASS MATRIX
$OMIT1, 4, 301, THRU, 332
ENDDATA
```

MSC.Nastran Results

This model was run with three different types of analysis. For the modal complex method, 20 real modes were requested to produce the reduced problem for complex eigensolution analysis. It was found that the twelfth mode was quite divergent, while all of the other modes were stable. The eigenvalues of this mode and the preceding and following modes by this method are given below:

```
                      C O M P L E X   E I G E N V A L U E   S U M M A R Y
0          ROOT    EXTRACTION            EIGENVALUE              FREQUENCY          DAMPING
           NO.      ORDER          (REAL)         (IMAG)          (CYCLES)        COEFFICIENT
. . .
           11        13        -5.377758E+03    5.013208E+04     7.978768E+03    2.145436E-01
           12        12         3.262632E+03    5.019004E+04     7.987992E+03   -1.300111E-01
           13         5        -1.215334E+03    5.960500E+04     9.486430E+03    4.077961E-02
. . .
```

When the same model is analyzed by the Lanczos method, without modal reduction, the roots in the same region are as follows:

```
           11        12        -5.339673E+03    5.010448E+04     7.974375E+03    2.131415E-01
           12        11         3.294983E+03    5.022236E+04     7.993137E+03   -1.312158E-01
           13        13        -1.200218E+03    5.960513E+04     9.486451E+03    4.027230E-02
```

Note that the results obtained by the two methods agree within a few percent, even though these special effects are rather strong. This agreement occurs because almost all of the real modes were found, including those at much higher frequencies than that of the twelfth complex mode. When the friction coefficient parameter was reduced from a value of 0.5 to 0.05, all roots became stable. The roots in the region of the twelfth mode are as follows:

```
11        11        -9.727523E+02      5.035683E+04       8.014539E+03       3.863437E-02
12        12        -1.070261E+03      5.304468E+04       8.442323E+03       4.035319E-02
13        13        -1.200928E+03      6.031671E+04       9.599703E+03       3.982073E-02
```

It would appear that there is a stability threshold somewhere between the friction coefficient values of 0.05 and 0.5. The precise threshold can be determined by resetting the value of this parameter and rerunning the model until the real value of this mode approaches zero. Hardware elements that affect this unstable mode can be identified by inspecting the eigenvector. The affect of hardware changes on the stability of this mode can be evaluated by changing the most active elements and rerunning the analysis.

This study shows that the prudent method for checking this answer is the Lanczos method, but the less expensive modal Hessenberg method can be used for the parameter variation studies to find the stability boundary, with a final check made by the Lanczos method.

The eigenvector computed for this mode from the Direct Lanczos results is shown below. This format contains two lines per grid point. The first line is the real value of displacement. The second line indicates the imaginary part. Magnitude and phase angles are an alternative choice.

```
COMPLEX EIGENVALUE =  3.294983E+03,  5.022236E+04
                        C O M P L E X   E I G E N V E C T O R   NO.      12
                                   (REAL/IMAGINARY)


POINT ID.   TYPE        T1              T2              T3              R1              R2              R3
   100      G        .0          -2.587344E-03   -1.831422E-04   -1.900947E-05      .0              .0
                     .0           1.218755E-02   -2.493365E-04    9.222361E-05      .0              .0
   101      G        .0          -2.967534E-03   -1.831422E-04      .0              .0              .0
                     .0           1.403202E-02   -2.493365E-04      .0              .0              .0
   102      G        .0          -3.110105E-03   -7.534264E-04      .0              .0              .0
                     .0           1.472369E-02    2.517372E-03      .0              .0              .0
   103      G        .0          -3.110105E-03   -7.534264E-04      .0              .0              .0
                     .0           1.472369E-02    2.517372E-03      .0              .0              .0
   201      G        .0           8.990854E-02    6.901190E-02   -1.932251E-03    2.106063E-17    4.727121E-17
                     .0          -1.349169E-01    6.873457E-02    1.091643E-02   -4.813858E-17   -1.377165E-16
   211      G        .0           6.394567E-01   -1.057253E-02      .0              .0              .0
                     .0           6.715296E-01   -2.787052E-02      .0              .0              .0
   212      G        .0           6.394567E-01   -1.057253E-02      .0              .0              .0
                     .0           6.715296E-01   -2.787052E-02      .0              .0              .0
   213      G        .0          -1.006220E+00   -1.589278E-02      .0              .0              .0
                     .0           2.944739E-02   -2.169513E-03      .0              .0              .0
   214      G        .0          -1.006220E+00   -1.589278E-02      .0              .0              .0
                     .0           2.944739E-02   -2.169513E-03      .0              .0              .0
   221      G        .0          -8.201829E-01    1.269795E-01      .0              .0              .0
                     .0          -2.698337E-01   -2.587584E-01      .0              .0              .0
   222      G        .0          -8.201829E-01    1.269795E-01      .0              .0              .0
                     .0          -2.698337E-01   -2.587584E-01      .0              .0              .0
   223      G        .0           1.000000E+00    1.104436E-02      .0              .0              .0
                     .0          -2.834362E-17    3.962275E-01      .0              .0              .0
   224      G        .0           1.000000E+00    1.104436E-02      .0              .0              .0
                     .0          -1.627032E-15    3.962275E-01      .0              .0              .0
   301      G        .0             .0              .0           -1.812334E-04      .0              .0
                     .0             .0              .0           -4.347274E-04      .0              .0
   302      G        .0             .0              .0           -1.812334E-04      .0              .0
                     .0             .0              .0           -4.347274E-04      .0              .0
   303      G        .0             .0           -9.851459E-03   -1.239709E-04      .0              .0
                     .0             .0           -2.265664E-02   -2.428152E-04      .0              .0
```

Note that two points have a value of 1.0, except for a very small imaginary part. These are the analysis set points with the largest value. (See points 223, 224.) Note that one point has a value which exceeds unity. (See point 214.) This point is the dependent point on a selected MPC entry. Only analysis set points are considered when performing the normalization. Dependent points for MPC equations and omitted points may be smaller or larger than unity.

The meaning of the imaginary parts of the displacement at the other points is a measure of the phase angle between motion at the normalizing point and the other points. A more meaningful result for the imaginary part can be obtained from the modal analysis by requesting SDISP output. This prints the modal contributions of the real modes which are used to synthesize the complex modes. The output for the twelfth mode, from a Modal Hessenberg analysis, is as follows:

```
        COMPLEX EIGENVALUE =  3.262632E+03,  5.019004E+04
                             C O M P L E X   E I G E N V E C T O R   N O .      12    (SOLUTION SET)
                                                        (REAL/IMAGINARY)


        POINT ID.    TYPE          T1              T2              T3              R1              R2              R3
0             1       M       2.723618E-02    2.382100E-04    5.274842E-04   -2.809022E-14   -2.894890E-02    5.665277E-02
                             1.177777E-02    6.993240E-04   -8.778612E-04   -3.353533E-16    3.104551E-02   -6.190442E-02
0             7       M      -9.730529E-15    2.098325E-14   -4.441694E-13   -4.738649E-02    1.000000E+00    1.575081E-01
                            -4.749197E-14   -2.213062E-14    3.112463E-13   -4.339022E-01    .0             -2.552028E-01
0            13       M       1.127128E-15   -1.005931E-01   -1.593949E-03    2.438817E-16   -6.407992E-05   -2.046400E-17
                            -3.111150E-14    3.855639E-02    3.900885E-04    1.721788E-15    4.127408E-05    6.070441E-16
0            19       M      -8.610454E-17    4.902618E-06
                            -1.722265E-16    1.007778E-06
```

Although the columns are labeled T1, T2, etc., they really represent the scalar modal variables printed six per row. For example, the largest value occurs for the eleventh real mode, printed in the row labeled "7 M" under R2. (M symbolizes modal variable in this context.) If the objective of the analysis is to find the parts of the structure that have the largest effect on stability, when changed, it is often easier to understand the physics from the real mode shapes rather than the displacement in a complex mode shape of physical variables.

The a-set values of the real mode shape can be printed by the SVECT Case Control command. The values of nonanalysis set DOFs, such as m-set or omitted points, appear as blank spaces. If the complete real mode shapes are needed for plotting, or if element strain energy is desired for the real modes, this input stream can be run in SOL 103, the real modes analysis, by changing only the SOL entry. Inputs not related to real eigenvalue analysis are ignored.

5.4　Nonlinear Transient Response Analysis

Nonlinear effects in structures occur mainly due to nonlinear materials, preloads, and large rotations. Contact problems exhibit nonlinear effects due to changes in boundary conditions. All of these effects may be represented by nonlinear elements.

The nonlinear element library of MSC.Nastran consists of:

- RODs, CONRODs, and TUBEs for unidirectional truss members.
- BEAMs for axially and laterally deforming line members.
- QUAD4s and TRIA3s for membrane, plate and shell modeling.
- HEXAs, PENTAs, and TETRAs for solid modeling.
- GAPs for contact and friction simulation.
- BCONPs for slideline contact.

Nonlinear elements may be combined with linear elements for computational efficiency if the nonlinear effects can be localized. Primary operations for nonlinear elements are the updating of element coordinates and applied loads for large displacements and the internal relaxation iteration for material nonlinearity. Refer to **Table 5-1** for a summary of the nonlinear element properties.

Table 5-1 Summary of Nonlinear Elements

Element	Connectivity
BCONP	Connection and type for slideline.
CBEAM	Connection for beam element.
CGAP	Connection for gap or frictional element.
CHEXA	Connection for six-sided solid element.
CONROD	Connection and properties for rod.
CPENTA	Connection for five-sided solid element.
CQUAD4	Connection for quadrilateral element with bending and membrane stiffness.
CQUADX	Properties for axisymmetric hyperelastic solid.
CROD	Connection for rod with axial and torsional stiffness.
CTETRA	Connection for four-sided solid element.
CTRIA3	Connection for triangular element with bending and membrane stiffness.
CTUBE	Connection for a tube.

Table 5-1 Summary of Nonlinear Elements (continued)

Element	Properties
PBCOMP	Properties for composite CBEAM.
PBEAM	Properties for CBEAM.
PCOMP	Properties for composite material laminate.
PGAP	Properties for CGAP.
PLSOLID	Hyperelastic properties for CHEXA, CPENTA, and CTETRA.
PROD	Properties for CROD.
PSHELL	Properties for CTRIA3 and CQUAD4.
PSOLID	Properties for CHEXA, CPENTA, and CTETRA.
PTUBE	Properties for CTUBE.

The geometric nonlinearity becomes discernible when the structure is subjected to large displacement and rotation. Geometric nonlinear effects are prominent in two different aspects: (1) geometric stiffening due to initial displacements and stresses, and (2) follower forces due to a change in loads as a function of displacements. These effects are included in the current release of MSC.Nastran, but the large deformation effect resulting in large strains is yet to be implemented.

Material nonlinearity is an inherent property of any engineering material. Material nonlinear effects may be classified into many categories. Included in the current release of MSC.Nastran are plasticity, nonlinear elasticity, creep, and viscoelasticity. Creep and viscoelasticity, implemented as a generalized nonlinear viscoelastic capability, may be coupled with plasticity. Many sophisticated options are available for yield criteria and hardening behavior in plasticity.

The primary solution operations are load and time steps, iterations with convergence tests for acceptable equilibrium error, and stiffness matrix updates. The iterative process is based on the modified-Newton's method combined with optional methods such as the quasi-Newton (BFGS) update and the line search. The tangent matrix updates are performed automatically to improve the computational efficiency, and may be overridden at the user's discretion.

For static analysis, a number of options such as arc-length methods is available for snapthrough or post-buckling analysis. For the transient response analysis, a number of options is available for implicit direct time integration, combined with adaptive and other iteration strategies similar to those implemented for static analysis.

The adaptive method is implemented using the two-point recurrence (or one-step) formula as its foundation. The optimum time step size, which is required for accuracy and efficiency, changes continuously in the transient dynamic environment. The primary concept of automatic time step adjustment is that the proper size of the time step can be predicted based on the dominant frequency in the incremental deformation pattern at the

prediction process. Furthermore, changes in nonlinearity cannot be predicted from the deformation pattern at the previous time step. This deficiency is overcome by the bisection process, which is activated when any difficulties arise in terms of convergence during the iteration.

User Interface

The input data required for SOL 129 is a combination of direct time integration control data, similar to SOL 109 (for direct linear transient with superelements), and nonlinear modeling data similar to SOL 106 (for nonlinear statics). The nonlinear properties and/or effects are defined by nonlinear material data (MATS1 and TABLES1), gap elements (GAP) for nonlinear interfaces, and PARAM,LGDISP for geometric nonlinearity. The transient effects are produced by time-dependent loading functions (TLOADi, DAREA, LSEQ, etc.), damping (parameters, elements and material data), and mass properties.

The unique data required for SOL 129 is supplied on the TSTEPNL Bulk Data entry. The TSTEPNL entry in itself is a combination of the TSTEP entry for direct time integration and the NLPARM entry for nonlinear iteration control. Restarts are controlled by parameters (LOOPID, STIME, SLOOPID and SDATA) which can be specified either in the Case Control Section or Bulk Data Section. Some optional parameters (TSTATIC, NDAMP) are provided for additional control or capabilities.

Case Control

Each subcase defines a time interval starting from the last time step of the previous subcase, subdivided into smaller time steps. The output time is labeled by the cumulative time, including all previous subcases. There are advantages in dividing the total duration of analysis into many subcases so that each subcase does not have excessive number of time steps. The data blocks containing solutions are generated at the end of each subcase for storage in the database for output processing and restarts. As such, converged solutions are apt to be saved at many intermediate steps in case of divergence and more flexible control becomes possible with multiple subcases.

The input loading functions may be changed for each subcase or continued by repeating the same DLOAD request. However, it is recommended that one use the same TLOAD Bulk Data for all the subcases in order to maintain the continuity between subcases, because TLOADi data defines the loading history as a function of cumulative time. Static loads (PLOADi, FORCEi, MOMENTi) may be associated with time-dependent functions by the Bulk Data LSEQ, which can be selected by a Case Control command LOADSET. However, no thermal loads or enforced displacements (SPCD) are allowed in the nonlinear transient analysis. Nonlinear forces as functions of displacements or velocities (NOLINi) may be selected and printed by the Case Control commands NONLINEAR and NLLOAD, respectively. Each subcase may have a different time step size, time interval, and iteration control selected by the TSTEPNL request. The Case Control requests that may not be changed after the first subcase are SPC, MPC, DMIG, and TF.

Output requests for each subcase are processed independently. Requested output quantities for all the subcases are appended after the computational process for actual output operation. Available outputs are DISPLACEMENT, VELOCITY, ACCELERATION, OLOAD, STRESS, FORCE, SDISPLACEMENT, SVELOCITY, SACCELERATION, NONLINEAR (NLLOAD), and SPCFORCE. However, element force output and GRID point stresses are not available for nonlinear elements.

Initial conditions (displacement or velocity) can be specified by the Bulk Data input, TIC, selectable by the Case Control command IC. If initial conditions are given, all of the nonlinear element forces and stresses must be computed to satisfy equilibrium with the prescribed initial displacements. On the other hand, initial conditions can be generated by applying static analysis for the preload using PARAM,TSTATIC in the first subcase. Then the transient analysis can be performed in the ensuing subcases. Associated with the adaptive time stepping method, the PARAM,NDAMP is used to control the stability in the ADAPT method. The parameter NDAMP represents the numerical damping (a recommended value for usual cases is 0.01), which is often required to improve the stability and convergence in contact problems.

All the superelement model generation options and matrix reduction options are allowed for the linear portion of the structure. The generalized dynamic reduction, component mode synthesis, and Guyan reduction may be performed for upstream superelements. The residual superelement may contain scalar degrees-of-freedom representing linear modal formulations.

Implicit Integration Control: TSTEPNL Data

The input fields of the TSTEPNL Bulk Data entry specify the time step size, the number of steps, and the output interval as well as the nonlinear iteration options. The TSTEPNL Bulk Data is selectable by the Case Control command TSTEPNL. Although the same TSTEPNL Bulk Data may be selected by more than one subcase, it is recommended to select a different TSTEPNL entry for each subcase in preparation for changes in the restarts.

The choice of time step size is determined primarily by the frequency content of the input load and the highest frequency mode of interest. A general guideline is that seven or more steps per cycle be provided for reasonable accuracy. Modes with shorter periods (higher frequency) will be attenuated by the numerical process. Highly nonlinear problems may require smaller step size. However, the adaptive time stepping capability will automatically adjust the time step size. Nevertheless, the initial time step size should be estimated by the user according to the aforementioned principles.

A caution is necessary in using the automatic time step adjustment if the forcing function is a short duration pulse. Since the automatic time step adjustment algorithm does not consider the loading history, short pulses could be skipped if the time step is automatically adjusted to a larger value than the pulse duration. It is advised that a drastic change in the time step size between subcases be avoided. A drastic change—e.g., ratio of the two time steps exceeding 1000—could cause a loss of accuracy upon subcase switch. In this case, an intermediate subcase should be provided for a transition period of short interval to reduce the ratio.

The parameters for controlling the accuracy and stability of the incremental and iterative process can be specified in the TSTEPNL Bulk Data entry. The controls are applicable to the automatic time step adjustment and bisection process in addition to stiffness matrix updates, BFGS updates, and line searches similar to those on the NLPARM Bulk Data entry. Since default values have been selected from numerous test runs, the analysis should be started with the default setting and changed if necessary. The TSTEPNL data format is shown below with default values:

Format:

	1	2	3	4	5	6	7	8	9	10
TSTEPNL	ID	NDT	DT	NO	METHOD	KSTEP	MAXITER	CONV	+TNL1	
+TNL1	EPSU	EPSP	EPSW	MAXDIV	MAXQN	MAXLS	FSTRESS		+TNL2	
+TNL2	MAXBIS	ADJUST	MSTEP	RB	MAXR	UTOL	RTOLB			

Example with Defaults (x is Required Input):

	1	2	3	4	5	6	7	8	9	10
TSTEPNL	x	x	x	1	ADAPT	2	10	PW	+TNL1	
+TNL1	1.E-2	1.E-3	1.E-6	2	10	2	0.2		+TNL2	
+TNL2	5	5	0	0.75	16.0	0.1	20.			

The TSTEPNL Bulk Data entry is selected using ID via the Case Control command TSTEPNL. Each subcase (residual superelement solutions only) requires a TSTEPNL entry. Multiple subcases are assumed to occur sequentially in time. Therefore, the initial conditions of each subcase are defined by the end conditions of the previous subcase.

The NDT field specifies the number of time steps with DT as the size of each time step. The total duration for the subcase can be assessed by multiplying NDT and DT (i.e., NDT*DT). The time increment (Δt) remains constant during the analysis in AUTO and TSTEP options, and is equal to DT. However, the time increment (Δt) changes during the analysis in the ADAPT option and the actual number of time steps will not be equal to NDT. In the ADAPT option, DT is used as an initial value for Δt.

The NO field specifies the time step interval for output; i.e., every NO-th step solution is saved for output. The data will be output at steps 0, NO, 2NO, ..., etc., and the last converged step for printing and plotting purposes. The Case Control command OTIME may also be used to control the output points.

The METHOD field selects an option for direct time integration and the stiffness matrix update strategies among ADAPT, AUTO and TSTEP. If the AUTO option is selected, MSC.Nastran automatically updates the stiffness matrix to improve convergence while the KSTEP value is ignored. If the TSTEP option is selected, MSC.Nastran updates the stiffness matrix every KSTEP-th increment of time. If the ADAPT option is selected, MSC.Nastran automatically adjusts the incremental time and uses the bisection algorithm in case of divergence. During the bisection process in the ADAPT option, stiffness is updated at

every KSTEP-th successful bisection. The ADAPT method allows linear transient analysis, but AUTO or TSTEP will abort the run if the model does not have any data representing nonlinearity. The stiffness matrix is always updated for a new subcase or restart, irrespective of the option selected.

The number of iterations for a time step is limited to MAXITER. If the solution does not converge in MAXITER iterations, the process is treated as a divergent process; i.e., either a bisection or stiffness matrix update takes place based on the value of MAXBIS. The sign of MAXITER provides a control over reiteration in case of failure in convergence or bisection. If MAXITER is negative, the analysis is terminated when the divergence condition is encountered twice during the same time step or the solution diverges for five consecutive time steps. If MAXITER is positive, MSC.Nastran computes the best attainable solution and continues the analysis.

The convergence test is controlled by convergence test flags (U for displacement error test, P for load equilibrium error test, W for work error test) and the error tolerances (EPSU, EPSP and EPSW) which define the convergence criteria. All requested criteria (a combination of U, P, and/or W) are satisfied upon convergence. It should be noted that at least two iterations are necessary to check the displacement convergence criterion.

The MAXDIV field provides control over diverging solutions. Depending on the rate of divergence, the number of diverging solutions (NDIV) is incremented by 1 or 2. The solution is assumed to be divergent when NDIV reaches MAXDIV during the iteration. If the bisection option is used with the ADAPT method, the time step is bisected upon divergence. Otherwise, the solution for the time step is repeated with a new stiffness based on the converged state at the beginning of the time step. If NDIV reaches MAXDIV twice within the same time step, the analysis is terminated with a fatal message.

In transient analysis, the BFGS quasi-Newton updates and the line search process work in the same way as in static analysis (except for the default settings). The MAXQN field defines the maximum number of quasi-Newton vectors to be saved on the database and the MAXLS defines the number of line searches allowed per iteration. Nonzero values of MAXQN and MAXLS activate the quasi-Newton update and the line search process, respectively.

The FSTRESS field defines a fraction of the effective stress ($\bar{\sigma}$) which is used to limit the subincrement size in the material routine. The number of subincrements in the material routines is determined such that the subincrement size is approximately $FSTRESS \cdot \bar{\sigma}$ (equivalent stress). FSTRESS is also used to establish a tolerance for error correction in the elasto-plastic material, i.e.,

$$Error \text{ in yield function} < FSTRESS \cdot \sigma$$

If the limit is exceeded at the converging state, MSC.Nastran will exit with a fatal error message. Otherwise, the stress state is adjusted to the current yield surface.

In the ADAPT method, MAXBIS is the maximum number of bisections allowed for each time step ($-9 \leq MAXBIS \leq 9$). The bisection process is activated when divergence occurs and MAXBIS $\neq 0$. The number of bisections for a time increment is limited to MAXBIS. If

solution is computed and the analysis is continued to the next time step. If MAXBIS is negative and the solution does not converge in MAXBIS bisections, the analysis is terminated.

The parameter ADJUST allows the user to control the automatic time stepping in the ADAPT option. A value of zero for ADJUST turns off the automatic adjustment completely. If ADJUST is positive, the time increment is continually adjusted for the first few steps until a good value of Δt is obtained. After this initial adjustment, the time increment is adjusted every ADJUST time steps only. A value of ADJUST an order greater than NDT will turn off adjustments after the initial adjustment. Since the automatic time step adjustment is based on the mode of response and not on the loading pattern, it may be necessary to limit the adjustable step size when the period of the forcing function is much shorter than the period of dominant response frequency of the structure. It is the user's responsibility to ensure that the loading history is properly traced with the ADJUST option. The ADJUST option should be suppressed for the duration of a short pulse loading. If unsure, the user should start with a value of DT that is much smaller than the pulse duration in order to properly represent the loading pattern.

MSTEP defines the desired number of time steps to obtain the dominant period response accurately ($10 \leq$ Integer ≤ 200). RB defines bounds for maintaining the same time step for the stepping function in the automatic time step adjustment method ($0.1 \leq$ Real ≤ 1.0). Parameters MSTEP and RB are used to adjust the time increment during the analysis in the ADAPT option. The adjustment is based on the number of time steps desired to capture the dominant frequency response accurately. The time increment is adjusted as

$$\Delta t_{n+1} = f(r)\Delta t_n \qquad \text{Eq. 5-16}$$

where:

$$r = \frac{1}{MSTEP}\left(\frac{2\pi}{\omega_n}\right)\left(\frac{1}{\Delta t_n}\right)$$

with:

$f = 0.25$ for $r < 0.5 \cdot RB$

$f = 0.5$ for $0.5 \cdot RB \leq r < 2$

$f = 1.0$ for $RB \leq r < 2$

$f = 2.0$ for $2. \leq r < 3./RB$

$f = 4.0$ for $r \leq 3./RB$

The recommended value of MSTEP for nearly linear problems is 20. A larger value (e.g., 40) is required for highly nonlinear problems. In the default options, MSC.Nastran automatically computes the value of MSTEP based on the changes in the stiffness.

The MAXR field defines the maximum ratio for the adjusted incremental time relative to DT allowed for time step adjustment ($1.0 \leq$ Real ≤ 32.0). MAXR is used to define the upper and lower bounds for adjusted time step size, i.e.,

$$MIN\left(\frac{DT}{2^{MAXBIS}}, \frac{DT}{MAXR}\right) \le \Delta t \le MAXR \cdot DT \qquad \text{Eq. 5-17}$$

The UTOL field defines the tolerance on displacement increment below which there is no time step adjustment ($0.001 < \text{Real} \le 1.0$). UTOL is used to filter undesirable time step adjustment; i.e., no time step adjustment is performed if

$$\frac{\left\|\dot{U}_n\right\|}{\left\|\dot{U}\right\|_{max}} < UTOL \qquad \text{Eq. 5-18}$$

The RTOLB field defines the maximum value of incremental rotation (in degrees) allowed per iteration to activate bisection ($\text{Real} > 2.0$). The bisection is activated if the incremental rotation for any degree-of-freedom ($\Delta\theta_x$, $\Delta\theta_y$, or $\Delta\theta_z$) exceeds the value specified for RTOLB. This bisection strategy based on the incremental rotation is controlled by the MAXBIS field.

Iteration Related Output Data

During the incremental and iterative computation, the process information consisting of iteration data is printed at the end of each iteration or time step. The data is printed under the following headings:

TIME	Cumulative time for the duration of the analysis
ITER	Iteration count for each time step
DISP	Relative error in terms of displacements
LOAD	Relative error in terms of load vectors
WORK	Relative error in terms of work
LAMBDA(I)	Rate of convergence in iteration
LAMBDA(T)	Ratio of the load error for two consecutive time steps
LAMBDA-BAR	Average of LAMBDA(T) over the last three steps, computed only for AUTO or TSTEP method
DLMAG	Absolute norm of the residual error vector, $\|R\|$. The absolute convergence is defined using DLMAG by $\|R\| < 10^{-12}$
FACTOR	Final value of the line search parameter
E-FIRST	Divergence rate error before line search
E-FINAL	Error at the end of line search
NQNV	Number of quasi-Newton vectors appended
NLS	Number of line searches performed during the iteration
ITR DIV	Number of occurrences of divergence detected during the adaptive iteration by the iteration module NLTRD2

MAT DIV	Number of occurrences of bisection conditions in the material routine (excessive stress increment) or in the rotation angle (excessive rotation) during the iteration using the ADAPT method
NO. BIS	Number of bisections executed for the current time interval
ADJUST	Ratio of time step adjustment relative to DT within a subcase

Three-Point Method (NLTRD Module)

The three-point method is chosen to be compatible with the MSC.Nastran linear transient integration method. The Newmark Beta method based on the three-step integration is combined with the modifications to Newton's method for nonlinear solutions. The additional iteration steps provide equilibrium solutions at each time step, thereby guaranteeing stability and accuracy for arbitrary time step size. This method can be used by selecting the AUTO or TSTEP method in the TSTEPNL Bulk Data entry.

Basic Equations

We may calculate the load equilibrium error vector, $\{R_n\}$ at time step n by the equation

$$\{R_n\} = \{P_n - M\ddot{u}_n - B\dot{u}_n - F_n\} \qquad \text{Eq. 5-19}$$

where:

$$\{P_n\} = \text{Average load over the time period } (t_{n-1} < t_n < t_{n+1}).$$

$$\{\ddot{u}_n\}, \{\dot{u}_n\} = \text{Corresponding acceleration and velocity vectors.}$$

$$\{F_n\} = \text{Average elasto-plastic element total force vector.}$$
$$(F = K\bar{u} \text{ for linear problems.})$$

The above equation is solved at the reduced (u_d) displacement vector size. The approximation errors due to dynamic reduction methods are not included in the error vector $\{R_n\}$. Applying Newmark's method over a finite time period, $t_{n-1} < t < t_{n+1}$, the average static forces are

$$\{F\} = \{\beta F(u_{n+1}) + (1 - 2\beta)F(u_n) + \beta F(u_{n-1})\} \qquad \text{Eq. 5-20}$$

where β is the Newmark Beta operator and $F(u_n)$ is the nonlinear force due to a generalized displacement vector $\{u_n\}$. An identical definition occurs for $\{P\}$ from the applied loads at each time step.

In summary, at each time step MSC.Nastran will iterate the displacements and forces until $\{R_n^i\}$ passes the convergence tests or the number of passes reaches an iteration limit. With a single step, i = i, calculating only R_0, the results will be identical to the existing NOLINi results in MSC.Nastran. For faster convergence the iterations may continue, the matrices may be updated, and/or the time step size may be reduced. For more details on this algorithm, refer to Chapter 9 of the *MSC.Nastran Nonlinear Handbook*.

Two-Point Method (NLTRD2 Module)

The multistep implicit integration method has difficulties when changing time step size. Therefore, to allow self-adapting time step sizes, the two-point integration method is introduced with module NLTRD2. This method can be selected by specifying the ADAPT method in the TSTEPNL Bulk Data entry.

Newmark Integration

For the adaptive scheme, Newmark's method is employed with the two-point recurrence formula for one-step integration, i.e.,

$$\{U_{n+1}\} = \{U_n\} + \Delta t\{\dot{U}_n\} + \frac{1}{2}\Delta t^2\{\ddot{U}_n\} + \beta\Delta t^2\{\ddot{U}_{n+1} - \ddot{U}_n\} \qquad \text{Eq. 5-21}$$

and

$$\{\dot{U}_{n+1}\} = \{\dot{U}_n\} + \Delta t\{\ddot{U}_n\} + \gamma\Delta t\{\ddot{U}_{n+1} - \ddot{U}_n\} \qquad \text{Eq. 5-22}$$

where $\{U\}$, $\{\dot{U}\}$, $\{\ddot{U}\}$ and Δt denote displacement, velocity, acceleration and the time step increment, respectively. The subscript n designates the time step and the parameters (β and γ) are to be selected for the best solution. An equilibrium equation to be satisfied at time step $(n+1)$ is

$$M\{\ddot{U}_{n+1}\} + C\{\dot{U}_{n+1}\} + \{F(U_{n+1})\} = \{P_{n+1}\} \qquad \text{Eq. 5-23}$$

where M and C denote mass and damping matrices, and $\{F\}$ and $\{P_{n+1}\}$ denote internal and external forces, respectively.

An alternative expression for the load vector can be derived for $\gamma = 0.5$ by introducing

$$M\{\ddot{U}_n\} + C\{\dot{U}_n\} = \{P_n - F_n\} \qquad \text{Eq. 5-24}$$

By virtue of **Eq. 5-24** the residual load error at each time step is effectively carried over to the next step and the error propagation is reduced, while the computation is significantly simplified.

$$\{R^i_{n+1}\} = \{P_{n+1} - F^i_{n+1}\} + \frac{4}{\Delta t}M\{\dot{U}_n\} + \{P_n - F_n\}$$
$$- \left[\frac{4}{\Delta t^2}M + \frac{2}{\Delta t}C\right]\{U^i_{n+1} - U_n\} \qquad \text{Eq. 5-25}$$

The iteration method calculates new values of R^i_{n+1} until it is sufficiently small. The results then become the starting point for the next time step.

Adaptive Time Stepping

It is desirable to have a fully automated method of time integration that renders effective and accurate solutions of nonlinear problems. The dynamic response characteristics of the structure may change due to the nonlinearity (geometric or material) or the mode of

excitation. When the type of nonlinear behavior changes, the time step size should be adjusted. The drawback is that in implicit methods, a change in the time step size requires a decomposition of the tangent matrix. After the solution is achieved for the original time step, the usual procedure will be resumed for the next time step.

In the present implementation of the automatic time stepping for nonlinear applications, the adjustment is designed to be adaptive to the severity of the nonlinearity in the problem by monitoring the changes in the stiffness. However, difficulties in the automatic time stepping have been discovered when plasticity or GAP elements are involved. In such cases an undesired time step adjustment can be caused by a drastic change in the stiffness, which may only be a temporary difficulty. A filtering scheme has been devised to suppress the effects of the spurious mass or stiffness in the automatic time step adjustments. In addition, the bisection method is chosen to be activated only at the time when divergence occurs. The bisection process is coordinated with the stiffness matrix update so that changes in nonlinearities are properly reflected while the bisection is in progress.

After the time step is completely converged, the integration proceeds to the next time step with the same increment (Atk). Further bisection may be required after achieving converged solution at the intermediate time steps.

If no further bisection is required and the solutions converge without any difficulty, some recovery process such as doubling time step may be activated. However, any adjustment to the time step would require additional matrix decomposition that offsets the advantages of adjusting time step size. Therefore, it has been determined to continue stepping through the specified time interval to completion. The normal process should be resumed when the user-specified time step at which bisection is activated is fully processed.

When the automatic time stepping is combined with the bisection method and if the bisection is activated, the automatic adjustment procedure will be deferred until the divergence is trapped and the solution process is stabilized. The solution process is considered stabilized when two successive solutions have converged without requiring further bisection. This is the time when the automatic time step adjustment is resumed.

The maximum number of bisections is limited by a user-specified parameter MAXBIS (defaulted to 5). The bisection process is activated on an as-needed basis. Users also have an option to suppress bisection by specifying MAXBIS = 0. If the bisection is required more than MAXBIS times, the solution process will continue without bisection by activating the reiteration procedure, by which the same iteration process is repeated to find the best attainable solution. The best attainable solution is a solution obtained from the iteration that yields the least average error. The average error is defined by averaging relative errors in displacements, loads and energy. If the i-th iteration yields the least average error, the reiteration procedure will end at the i-th iteration and the normal time stepping procedure will be resumed.

Quasi-Newton and Line Searches

The BFGS update and the line search processes are fully operational during the iteration. Quasi-Newton (QN) vectors are continuously accumulated up to MAXQN pairs (MAXQN is a user-specified parameter) until the new stiffness matrix is evaluated. Once the number

of QN vector pairs reaches MAXQN (defaulted to 10), the QN vectors will be updated selectively based on the condition number of the QN update matrix. As a requirement for the reiteration procedure, the QN vectors to be accumulated are stored on a temporary basis until a converged solution is obtained. All the accumulated QN vectors are purged if the stiffness matrix update or the decomposition (due to the change in Δt) is scheduled.

The iterative process for time step $(n + 1)$ can be summarized as follows:

1. Given at the beginning of the time step are Δt_n, ω_{ref}, $[M]$, $[C]$, $\{P_n\}$, $\{\Delta F_n\}$, $\{F_n\}$, $\{U_n\}$, $\{\dot{U}_n\}$, and the triangularized matrices (LDL^T) for $[A] = \left[\frac{4}{\Delta t^2} M + \frac{2}{\Delta t} C + \tilde{K} \right]$.

2. Adjust the time step size, if applicable.

3. Initialize $\{U_{n+1}^0\}$, $\{F_{n+1}^0\}$, and $\{P_{n+1}^0\}$.

4. Decompose, $[A] = LKL^T$, if $\Delta t_{n+1} \neq \Delta t_n$. Then, purge the QN vector file.

5. Compute $\{R_{n+1}^i\}$.

6. Solve for $\{\Delta U^{i+1}\}$ by forward and backward substitution, using the BFGS update if applicable.

7. Compute the line search error.

8. If divergence occurs, go to step 12.

9. Proceed to the next step if the line search error is less than the tolerance. Otherwise, perform the line search process and go back to step 7.

10. Compute the global error function and check convergence.

11. If the solution has converged, go to step 16. Otherwise, save the QN vector on a temporary basis (if applicable) and go to the next iteration in step 5.

12. If it is the first divergence or the divergence after the KSTEP-th converged bisection step, update the stiffness matrix, and go back to step 4. Otherwise, proceed to the next step.

13. Bisect Δt and go back to step 3. However, if the maximum number of bisections allowed for the time step is reached, proceed to the next step.

14. Go to step 5 to continue iteration. However, if the maximum number of iterations allowed for an increment is reached, proceed to the next step.

15. Perform the reiteration procedure to find the best attainable solution.

16. Accept the solution (U_{n+1} and F_{n+1}) and append temporary QN vectors to the permanent QN vector file.

17. Compute the velocity $\dot{U}_{n+1}$.

18. Advance to the next time step with $n = n + 1$.

Restarts

Since SOL 106 and SOL 129 share the same database storage formats for nonlinear tables and matrices, the restart system for transient analysis can use either a previous static or transient nonlinear analysis as its initial conditions.

Restarting From SOL 106 Into SOL 129

The options for a restart from SOL 106 into SOL 129 are static to static and static to dynamic analysis. For a restart from a previous static analysis, only the first subcase is affected. Simply provide a database created in SOL 106 and specify the parameter

> PARAM,SLOOPID,N

where N is the printed value of LOOPID for the desired static solution. The initial transient load should be identical to static loads at the restart state. Constraint sets, direct input matrices, mass, and damping may be changed.

Restarting Within SOL 129

Restarting within SOL 129 allows static to static, static to dynamic, and dynamic to dynamic analysis. Restarts from a previous nonlinear transient execution are available for a number of cases. If the same model is to be reexecuted, only the residual superelement needs to be reassembled. If the final results from the previous transient run are to be used as the initial conditions at t = 0, add dummy SUBCASE commands, corresponding to the previous run, to start the residual Case Control execution and set the parameter, STIME = 0.

The normal restart for a transient run is to be continued from the last step of a previous subcase with different loads and/or TSTEPNL data. For the normal restart provide the following parameters:

> LOOPID = N: Start from the N-th subcase
> STIME = t: Start from time t

Note that to avoid incompatible matrix sizes, constraint sets must not be changed. The values of LOOPID and STIME, which are printed with the iteration information for each subcase, can be directly read from the printout of the previous run. See the *MSC.Nastran Nonlinear Handbook* for more details and some examples.

$$t = \sum_{i=1}^{N} NDT_i \cdot DT_i \qquad \text{Eq. 5-26}$$

where NDT_i and DT_i are the number of time steps and the time increment of the i-th subcase, respectively.

If a SOL 129 run is terminated abnormally in the middle of a subcase, it may or may not be restartable depending upon the cause of the abnormal exit. If the job is stopped due to a diverging solution, it can be restarted either from the end of a previous subcase or from the last saved solution step. The restart procedure for the former is identical to that for the normal restart as described in the preceding paragraph. The latter case also requires parameters LOOPID and STIME; however, the input value for STIME differs depending on the value of METHOD specified on the TSTEPNL entry.

If METHOD = AUTO or TSTEP, STIME is the time corresponding to the last output step which may be calculated based on the output skip factor (i.e., the NO on the TSTEPNL entry). If METHOD = ADAPT, the last converged solution is always treated as an output step and is always saved for the restart so that STIME can be the time of the last converged step. The values of STIME and LOOPID can also be found in the printout, if the ADAPT method is used.

Once STIME and LOOPID are known, determine the number of remaining time steps in the subcase and create a new TSTEPNL entry for the remaining time. Insert a new subcase that references the new TSTEPNL entry prior to the remaining subcases in the Case Control Section.

A solution may be terminated in the middle of a subcase due to insufficient CPU time: (1) the CPU time specified in the Executive Control Section is insufficient so the run is forced to exit by MSC.Nastran, or (2) the CPU time exceeds the limit specified in the computer system which leads to a sudden job abortion by the system. In the first case, MSC.Nastran is able to detect the specified CPU time in the Executive Control Section and automatically activate the exit procedure before time expiration. When completed, the solution can be restarted from the termination point as in the solution diverging case. In the second case, the solution can only be restarted from the end of a subcase.

Restarts may also be performed solely for data recovery by providing the following parameters:

> SDATA = -1 : Recover data without running the solution module
> LOOPID = N : from the 1st through the N-th subcases

Note that solution sets DISP, VELO, ACCE, OLOAD, SPCF (printout and plotting) and NLLOAD (plotting only) are recoverable while STRESS, SDISP, SVELO and SACCE sets are not.

Expedient Iteration Strategies

The dynamic tangent matrix may change for the following reasons:

1. Stiffness (K) changes due to geometric, material, and/or kinematic nonlinearity.

2. Bisection or time-step adjustment causes changes in the effective stiffness.

While the second case only requires decomposition, the first case requires reformulation of the new stiffness matrix as well. The adaptive method is based on the following matrix update strategies:

1. Stiffness is updated at the previously converged position when the divergence is detected for the first time at a given time step.

2. Stiffness matrix update is allowed only once within the same time step.

3. If the bisection is in progress, additional K-updates are allowed within a given ΔT at every KSTEP-th converged bisection, where KSTEP is a user-specified parameter in the TSTEPNL entry.

4. Decomposition is performed within the module at every bisection or time step adjustment.

5. Whenever the decomposition is performed, the iteration starts from the previously converged position.

6. The stiffness matrix is updated at the beginning of each subcase.

5.5 Fourier Transform

The Fourier transform capability in MSC.Nastran allows a transient analysis to be performed using a frequency response solution. Time-dependent applied loads are transformed to the frequency domain and all frequency dependent matrix calculations are completed. The frequency response solution variables are then transformed back into the time domain.

Fourier transform methods have been implemented in MSC.Nastran to integrate the equations of motion in order to obtain the aeroelastic response of fixed wing aircraft. This capability is especially important for this type of analysis since the unsteady aerodynamic matrices are known only in the frequency domain. The Fourier transform method may also be used to solve for the transient response of conventional structural models (no aerodynamic effects) subjected to periodic loads.

This capability is available in SOLs 108 and 111 for frequency response output data. For transient type output, SOL 146 must be used. The transformation is performed when the requested load is the TLOADi form.

Theory

Two forms of the Fourier transform are available: the Fourier series and the Fourier integral. Both methods require necessary numerical compromises and hence produce numerical approximations. The inverse transform includes an infinite sum, for which only a finite number of terms are numerically evaluated. The inverse Fourier integral must be numerically integrated, which may result in integration errors. The number of frequencies at which the integrand is evaluated is limited by the cost of calculations.

In the Fourier series, the basic time interval is $0 < t < T$, with the function periodic. The circular frequencies are given by

$$\begin{cases} \omega_n = 2\pi n \Delta f \\ \Delta f = \dfrac{1}{T} \end{cases}$$

where T is a large time equal to the period of the lowest forcing frequency.

The load transformation for a load at point a is given by

$$\tilde{P}a(\omega_n) = \int_0^T P_a(t) e^{-i\omega_n t} dt \qquad \text{Eq. 5-27}$$

The response at point j is given by

$$\tilde{u}_j(\omega_n) = H_{ja}(\omega_n)\tilde{P}a(\omega_n) \qquad \text{Eq. 5-28}$$

where $H_{ja}(\omega_n)$ is the frequency response of any physical variable due to unit load. The response in the time domain is given by

$$u_j(t) = \frac{\Delta\omega}{\pi}\left[\left(\frac{1}{2}\right)\tilde{u}_j(0) + \sum_{n=1}^{\infty} Re(\tilde{u}_j(\omega_n)e^{i\omega_n t})\right] \qquad \text{Eq. 5-29}$$

In the Fourier Integral, the time interval is the limit as $T \to \infty$, $\Delta f \to 0$, and $2\pi n\Delta f \to \omega$ of the Fourier series. Here, ω is a continuous variable. **Eq. 5-27**, **Eq. 5-28**, and **Eq. 5-29** take the form

$$\tilde{P}_a(\omega) = \int_0^{\infty} P_a(t)e^{-i\omega t}dt \qquad \text{Eq. 5-30}$$

$$\tilde{u}_j(\omega) = H_{ja}(\omega)\tilde{P}_a(\omega) \qquad \text{Eq. 5-31}$$

$$u_j(t) = \left(\frac{1}{\pi}\right)\int_0^{\infty} Re(\tilde{u}_j(\omega)e^{i\omega t})d\omega \qquad \text{Eq. 5-32}$$

Transformation of Loads to the Frequency Domain

The transformation of the user-specified time dependent loads into the frequency domain is given in **Eq. 5-27**. With this transformation, the user must define a function that vanishes for $t > T$.

For piecewise linear tabular functions (TLOAD1), a table of pairs $(x_i, Y_i)(i = 1,N)$ prescribes $N-1$ time intervals. If an X1 shift and an X2 scale factor are included, the time-dependent load at point a is given by

$$P_a(t) = A_a Y_T\left(\frac{t - \tau_a - X1}{X2}\right) \qquad \text{Eq. 5-33}$$

where A_a is an amplitude factor and τ_a is a delay factor that may depend upon the loading point. Applying finite step-by-step integration to **Eq. 5-27**, the transformed load, $\tilde{P}_a(\omega)$, is obtained for each requested frequency.

Likewise, the general function (TLOAD2) is defined by

$$P_a(T) = \begin{array}{ll} A_a \tilde{t}^n e^{\alpha\tilde{t}}\cos(2\pi f\tilde{t} + \phi) & 0 < t < T_2 - T_1 \\ 0 & \text{Otherwise} \end{array} \qquad \text{Eq. 5-34}$$

where $t = t - T_1 - \tau_a$

The value of n must be an integer for transient analysis by the Fourier method. The transformation to the frequency domain is also obtained by numerical integration.

These loads, which appear in the form required for frequency response, are transformed to the modal coordinates exactly as in the modal frequency response method.

One other source of loads for aeroelastic problems is a one-dimensional gust. The same time dependencies are allowed as defined above; however, the amplitude (A_a) and delays (τ_a) for the aerodynamic elements are computed from areas, dihedrals, and coordinates in the flow direction.

Calculation of Frequency Response

Frequency responses are computed in the frequency domain by conventional MSC.Nastran methods for coupled equations.

Inverse Transformation of the Response to the Time Domain

The response in the time domain is found either from the Fourier integral approximation of **Eq. 5-32** or from the Fourier series result of **Eq. 5-29** (which can be thought of as a special form of the integral approximation.) Three approximation methods are available to evaluate the inverse transform which may be selected by the user via the parameter IFTM. In all cases, the quantity $\tilde{u}(\omega)$ is first calculated at a set of frequencies, ω_i, by the frequency response module where the ω_i's do not need to be equally spaced. For all methods, $\tilde{u}(\omega)$ is set equal to zero outside the range of ω's computed. These methods are:

Method 0   Approximate $\tilde{u}(\omega)e^{i\omega t}$ as a constant in each interval (the default method). For equal frequency intervals, this method reduces to the Fourier series approximation of Eq. 3.

Method 1   Fit $\tilde{u}(\omega)$ with a piecewise linear function, and do not approximate $e^{i\omega t}$.

Method 2   Fit $\tilde{u}(\omega)$ with a cubic spline function, and do not approximate $e^{i\omega t}$.

Consider Method 2. Solving the three-moment equations, the second derivatives $\tilde{u}(\omega)$, can be found for each ω for which a frequency response has been computed. Then, in any interval $\omega_i < \omega < \omega_{i+1}$,

$$\tilde{u}(\omega) = [\tilde{u}(\omega_i) \cdot s + \tilde{u}(\omega_{i+1}) \cdot r] - \left[\frac{(\omega_{i+1} - \omega_i)^2}{6}\right]$$
$$\cdot [\tilde{u}(\omega_i)s - s^3 + u(\omega_{i+1})(r - r^3)]$$

Eq. 5-35

where:

$$r = \frac{(\omega - \omega_i)}{(\omega_{i+1} - \omega_i)}$$

$$s = 1 - r$$

Integrate **Eq. 5-32** using **Eq. 5-35** for $\tilde{u}(\omega)$, and sum over the integrals. Then collect the terms for each ω_n with the result,

$$u(t) = \left(\frac{1}{\pi}\right) \sum_{n=1}^{N} \text{Re}\left\{[C_n(t)\tilde{u}(\omega_n) + D_n(t)\tilde{u}(\omega_n)]e^{i\omega_n t}\right\}$$

Eq. 5-36

$$C_n(t) = \frac{\omega_n - \omega_{n-1}}{2} E_2(-it(\omega_n - \omega_{n-1})) + \frac{\omega_{n+1} - \omega_n}{2} E_2(it(\omega_{n+1} - \omega_n)) \quad \text{Eq. 5-37}$$

$$D_n(t) = \frac{(\omega_n - \omega_{n-1})^3}{24} G(it(\omega_n - \omega_{n-1})) - \frac{(\omega_{n+1} - \omega_n)^3}{24} G(it(\omega_{n+1} - \omega_n)) \quad \text{Eq. 5-38}$$

For the first terms in **Eq. 5-36** ($n = 1$), use only the second terms on the right side of **Eq. 5-37** and **Eq. 5-38**. For the last term in **Eq. 5-36** ($n = N$), use only the first terms on the right side of **Eq. 5-37** and **Eq. 5-38**.

$$G(z) = 2E_2(z) - E_4(z) \quad \text{Eq. 5-39}$$

$$E_K(z) = \begin{array}{c} \dfrac{K!}{z^k} \\[8pt] e^z - \displaystyle\sum_{k=0}^{k=K} \dfrac{z^k}{k!} \\[8pt] 1 + \dfrac{z}{K+1} + \dfrac{z^2}{(K+1)(K+2)} + \dfrac{z^3}{(K+1)(K+2)(K+3)} \end{array} \quad \text{Eq. 5-40}$$

The above form of the inverse transform has two advantages. First, numerical problems for small values of $t\Delta\omega$ are efficiently evaluated by choosing the series form of **Eq. 5-40**. Also, the other two methods are easily derived as subcases. If u'' terms are removed from **Eq. 5-35**, a piecewise linear fit occurs. Thus, Method 1 results by deleting $\tilde{u}''$ from **Eq. 5-36**, i.e.,

$$u(t) = \left(\frac{1}{\pi}\right) \sum_{n=1}^{N} \text{Re}[C_n(t)u(\omega_n)e^{i\omega_n t}] \quad \text{Eq. 5-41}$$

with C_n defined by **Eq. 5-38**. Method 0 results if we replace E_2 by 1.0 in **Eq. 5-38**.

The above procedure for Method 0 always multiplies the first and last terms in the series by one-half. In order to force agreement with the Fourier series, which is the limiting case of equal frequency intervals, the first term in the series is multiplied by one-half only if the value of the first frequency is zero.

Some special considerations are given in the equal frequency interval case. When all Δf's are equal and the first frequency is an integer multiple of Δf, the time step δt is adjusted to make $\Delta f \cdot \Delta t = 1/\text{integer}$, reducing the number of distinct values of $\sin\omega_n t$ and $\cos\omega_n t$ used in **Eq. 5-41**. Also, $C_n(t)$ and $D_n(t)$ (**Eq. 5-37** and **Eq. 5-38**) become independent of n and do not need to be computed at every frequency.

Other important practical considerations must be observed to use these methods successfully. to illustrate one problem, consider the response of a simple damped oscillator to a pulse (**Figure 5-3**). The upper three curves show the pulse and the response of the system if it is very stable and slightly stable. Using the Fourier method, the pulse is replaced by a series of pulses, with period $1/\Delta f$.
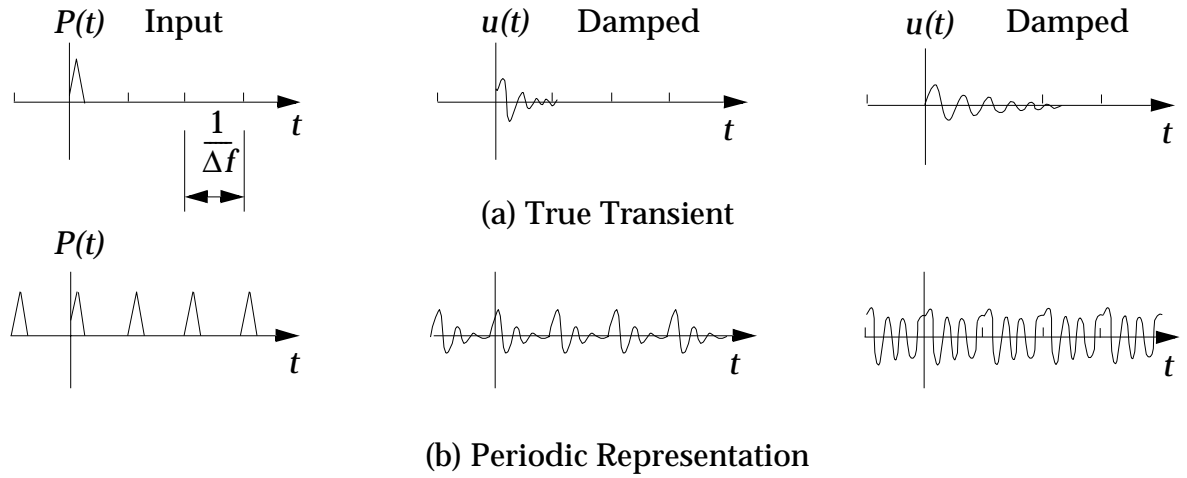
(a) True Transient

(b) Periodic Representation

Figure 5-3 Response of a Single Degree-of-Freedom for Three Types of Periodic Loads

Guidelines for Use. As can be seen, this method gives good results if the system is damped, but an incorrect impression if the system is lightly damped. Thus, in order for the results of the Fourier method to be valid:

1. The system should be reasonably well damped.

2. The forcing function should be zero for some time interval to allow decay.

3. The frequency interval $\Delta f \le 1/(T_{pulse} + T_{decay})$.

If the system has unstable modes, these will appear as a precursor before the pulse as a stable mode in the reverse time. In general, Methods 1 and 2 are more accurate than Method 0. However, these methods introduce positive artificial damping into the result that may lead to erroneous conclusions in stability studies. To see this, consider the function $C_n(t)$ in **Eq. 5-42**. If equal frequency intervals are chosen, then

$$C_n(t) = \begin{cases} \Delta\omega \cdot \dfrac{1 - \cos(t\Delta\omega)}{1/2(t\Delta\omega)^2} = \Delta\omega\left(1 - \dfrac{1}{6}(t\Delta\omega)^2 + ...\right) & \text{Method 0} \\ \Delta\omega & \text{Method 1} \end{cases}$$

Eq. 5-42

Thus, Method 1 (and also Method 2) produces a decaying envelope that the user may incorrectly interpret as additional damping.

The use of equal frequency intervals versus unequal intervals has been studied and results are shown in the *MSC.Nastran Aeroelastic Analysis User's Guide.*

5.6 Viscoelastic Material Properties

The mechanical behavior of many glasses, rubbers, and high polymers under stress is described in terms of a combination of elastic and viscous phenomena that may be approximated by linear viscoelastic theory. The dynamic behavior of such material is characterized by a strong dependence on frequency; and, under sinusoidal excitation, these materials exhibit a steady-state response in which the stress lags the associated strain. The general three-dimensional state of stress can then be described in terms of a complex frequency-dependent shear modulus and a real constant value for Poisson's ratio.

This method was developed for the analysis of rubber-like materials such as solid rocket propellants. In that case, the dominant strain energy terms were the shear strains.

MSC.Nastran provides the ability to represent a single complex frequency-dependent scalar material modulus of the form

$$G(f) \; = \; G'(f) + i G''(f) \qquad\qquad \text{Eq. 5-43}$$

where:

G' = Shear storage modulus

G'' = Shear loss modulus

The ratio

$$\frac{G''(f)}{G'(f)} \; = \; \tan \phi$$

is denoted as the shear loss tangent.

The above formulation of viscoelastic (frequency-dependent) material properties may be used in direct frequency analysis (SOL 108).

The stiffness and damping components of the dynamic matrices for direct frequency response analysis are documented in the *MSC.Nastran Basic Dynamic Analysis User's Guide* in the following form:

$$[K_{dd}] \; = \; (1 + ig)[K_{dd}^1] + [K_{dd}^2] + [K_{dd}^4] \qquad\qquad \text{Eq. 5-44}$$

$$[B_{dd}] \; = \; [B_{dd}^1] + [B_{dd}^2] \qquad\qquad \text{Eq. 5-45}$$

where:

g = overall structural damping specified through the PARAM,G Bulk Data entry

$[K_{dd}^1]$ = stiffness matrix for structural elements

$[K_{dd}^2]$ = stiffness terms generated through direct matrix input, e.g., DMIG Bulk Data entries

$[K_{dd}^4]$ = element damping matrix generated by the multiplication of individual element stiffness matrices by an element damping, g_e, entered on the MATi Bulk Data entry associated with the element or elements in question

$[B_{dd}^1]$ = damping matrix generated through CVISC and CDAMP1 Bulk Data entries

$[B_{dd}^2]$ = damping terms generated through direct matrix input, e.g., DMIG Bulk Data entries

Eq. 5-44 is of particular interest in the current discussion of viscoelastic material properties because the presence of these properties will be reflected in terms of this equation. For discussion purposes, frequency-dependent material properties will be denoted as viscoelastic materials and those material properties that are independent of frequency will be denoted as elastic materials. Thus, if the stiffness properties for the viscoelastic elements are initially computed on the basis of a representative reference modulus, G_{REF}, the stiffness matrix for the viscoelastic elements (denoted by the subscript V) may be written in the form

$$[K_{dd}(f)]_V = \left[\frac{G'(f) + iG''(f)}{G_{REF}}\right][K_{dd}^1]_V$$

Eq. 5-46

Input Description

To use the viscoelastic capability, the following conditions are necessary:

1. Assume the $[K_{dd}^1]$ matrix will be restricted only to the viscoelastic elements. This restriction implies that elastic elements will have a blank or zero entry for g_e on their associated MATi Bulk Data entries. Conversely, all viscoelastic materials must have representative reference values of g_e, and G_{REF} entered on their associated MATi Bulk Data entries. Then, by definition,

$$[K_{dd}^4]_V = g_{REF}[K_{dd}^1]_V$$

2. The TABLEDi tabular functions $TR(f)$ and $TI(f)$ are defined to represent the complex moduli of all viscoelastic materials.

These two conditions may be combined in Eq. 5-44 to provide the following expression:

$$[K_{dd}]_V = (1 + ig)[K_{dd}^1]_V + \{TR(f) + iTI(f)\}[K_{dd}^4]_V$$

$$= \{(1 + g_{REF}TR(f)) + i[g + g_{REF}TI(f)]\}[K_{dd}^1]_V$$

Eq. 5-47

A comparison of Eq. 5-46 and Eq. 5-47 yields the form of the tabular functions $TR(f)$ and $TI(f)$:

$$TR(f) = \frac{1}{g_{REF}}\left[\frac{G'(f)}{G_{REF}} - 1\right]$$

Eq. 5-48

$$TI(f) = \frac{1}{g_{REF}}\left[\frac{G''(f)}{G_{REF}} - g\right] \qquad \text{Eq. 5-49}$$

Note that the direct input matrix, $[K_{dd}^2]$, from **Eq. 5-44** is still available but not involved in the definition of viscoelasticity.

Direct frequency response analyses that involve viscoelastic materials require some special input data relative to analyses that involve only elastic materials. These special input requirements are given below:

1. Executive Control Section:

    None

2. Case Control Section:

    SDAMPING = n reference TABLEDi Bulk Data entry that defines the alternate tabular form of $TR(f)$

3. Bulk Data Section:

    a. MATi Bulk Data entry

       - $G = G_{REF}$, the reference modulus
       - $NU = $ Poisson's ratio for the viscoelastic material
       - $GE = g_{REF}$, the reference element damping
       - All other entries on the MATi Bulk Data entry are utilized in the standard manner.

    b. TABLEDi Bulk Data entries:

       - A TABLEDi Bulk Data entry with an $ID = n$ is used to define the function $TR(f)$ of **Eq. 5-48**.
       - A TABLEDi Bulk Data entry with an $ID = n + 1$ is used to define the function $TI(f)$ of **Eq. 5-49**.

All other input requirements to the MSC.Nastran Bulk Data entry are typical of direct frequency response analysis. Note that the overall structural damping, g, entered through the PARAM Bulk Data entry (PARAM,G,XX) applies to all elastic materials.

Compare With Theory. The functional form of **Eq. 5-48** and **Eq. 5-49** requires the user to perform some modest calculations that involve G_{REF} and g_{REF}. These two terms must also be input to MSC.Nastran through the MATi Bulk Data entry for the viscoelastic materials. In general, representative values of these parameters should be used. However, in those cases where the MSC.Nastran OMIT feature is not used, the calculation of $TR(f)$ and $TI(f)$ can be simplified. In this case, define

$$G_{REF} \ll G'$$

$$G_{REF} \ll \frac{G''}{g}$$

and select g so that

$$G_{REF} g_{REF} = 1$$

Then **Eq. 5-48** and **Eq. 5-49** reduce to the following form:

$$TR(f) = G'(f) \qquad\qquad \text{Eq. 5-50}$$

$$TI(f) = G''(f) \qquad\qquad \text{Eq. 5-51}$$

The above simplifications should not be used if OMIT calculations are involved in the analysis in order to avoid possible matrix ill-conditioning.

Note that stress and force data recovery calculations are performed with the reference moduli irrespective of frequency.

Example

To illustrate the representation of viscoelastic material properties in MSC.Nastran, consider the following structure that may undergo both axial extension along the z-axis and torsion about the z-axis:
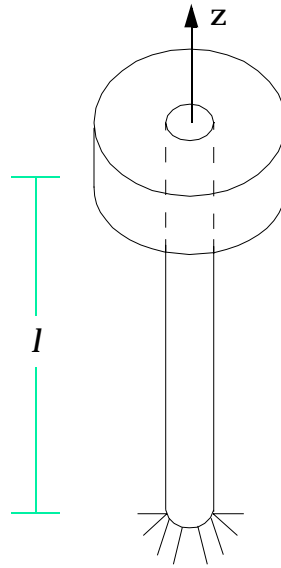
where:

flywheel mass, M_z = 2.0

flywheel inertia, I_z = 10.0

axial stiffness, K_z = $\dfrac{E(f)A}{l}$

torsional stiffness, K_{θ_z} = $\dfrac{G(f)J}{l}$

length, l = 2.0

area, A = .9

area moment, J = 2.0

The symbols $E(f)$ and $G(f)$ imply that the extensional and torsional moduli are functions of frequency, i.e., viscoelastic. For simplicity, it is assumed that $E(f) = G(f)$ and that these quantities have the following frequency-dependent characteristics:

f, hz	G'(f)	G''(f)
.8	1800.	180.
1.1	1850.	185.
1.4	1910.	191.
1.7	1970.	197.
2.0	2030.	203.
2.3	2070.	207.
2.6	2140.	214.
2.9	2210.	221.

A model for the system is shown in the following schematic:
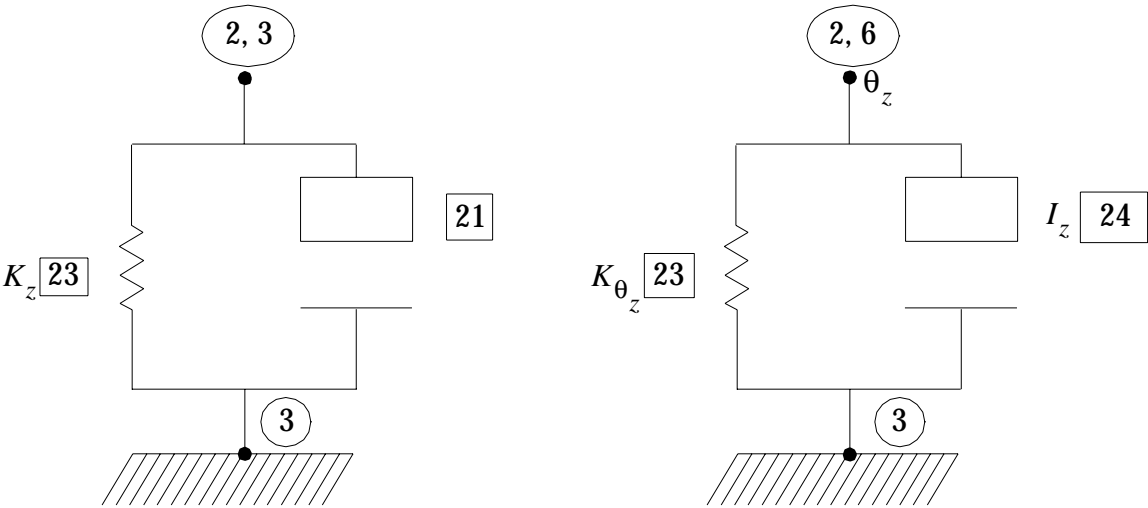
i = Grid Point ID

i,j = Grid Point ID and Component No.

k = Element ID

This model can be generated with the following MSC.Nastran Bulk Data entries:

1	2	3	4	5	6	7	8	9	10
GRID	ID	CP	X1	X2	X3	CD	PS		
GRID	2				2.		1245		
GRID	3						123456		

CMASS2	EID	M	G1	C1	G2	C2			
CMASS2	21	2.	2	3	3	3			
CMASS2	24	10.	2	6	3	6			

CROD	EID	PID	G1	G2					
CROD	23	1	2	3					

PROD	PID	MID	A	J					
PROD	1	1	.9	2.					

MAT1	MID	E	G	NU	RHO	A	TREF	GE	
MAT1	1	2000.	2000.					.09	

Note that the reference values of 2000. for both E and G are specified on the MAT1 Bulk Data entry. The reference value for structural damping, g_{REF}, is set to .09 under the GE field of the MAT1 Bulk Data entry. Once the reference values G_{REF} and g_{REF} have been assigned, one can evaluate **Eq. 5-48** and **Eq. 5-49** for the values to be assigned to $TR(f)$ and $TI(f)$. The values for these functions are entered on TABLEDi Bulk Data entries. As elastic portions of the structure may exist in addition to viscoelastic portions, assume that a value of overall structural damping, g, is to be utilized for these elastic portions of the model. The overall structural damping value of .06 is assigned through the following PARAM Bulk Data entry.

1	2	3	4	5	6	7	8	9	10
PARAM	N	V1	V2						
PARAM	G	.06							

This value of g must be considered in **Eq. 5-49**. The evaluation of **Eq. 5-48** and **Eq. 5-49** will result in the values shown in the following TABLED1 Bulk Data entries:

1	2	3	4	5	6	7	8	9	10
TABLED1	ID								
TABLED1	ID								TABR1

	X_1	Y_1	X_2	Y_2	X_3	Y_3	X_4	Y_4	
+ABR1	.0	.0	.8	−1.11111	1.1	−.833333	1.4	−.5	TABR2

	X_5	Y_5	X_6	Y_6	X_7	Y_7	X_8	Y_8	
+ABR2	1.7	−.166667	2.	.1666667	2.3	.3888889	2.6	.7777777	TABR3

	X_9	Y_9							
+ABR3	2.9	.5611111	ENDT						

TABLED1	ID								
TABLED1	11								TABI1

	X_1	Y_1	X_2	Y_2	X_3	Y_3	X_4	Y_4	
+ABI1	0.	0.	.8	.3333333	1.1	.3611111	1.4	.3944444	TABI2

	X_5	Y_5	X_6	Y_6	X_7	Y_7	X_8	Y_8	
+ABI2	1.7	.4277778	2.	.4611111	2.3	.4833333	2.6	.5222222	TABI3

	X_9	Y_9							
+ABI3	2.9	.5611111	ENDT						

To demonstrate that elastic as well as viscoelastic elements may be included in the same analysis, the following single degree-of-freedom is added to the Bulk Data Section:
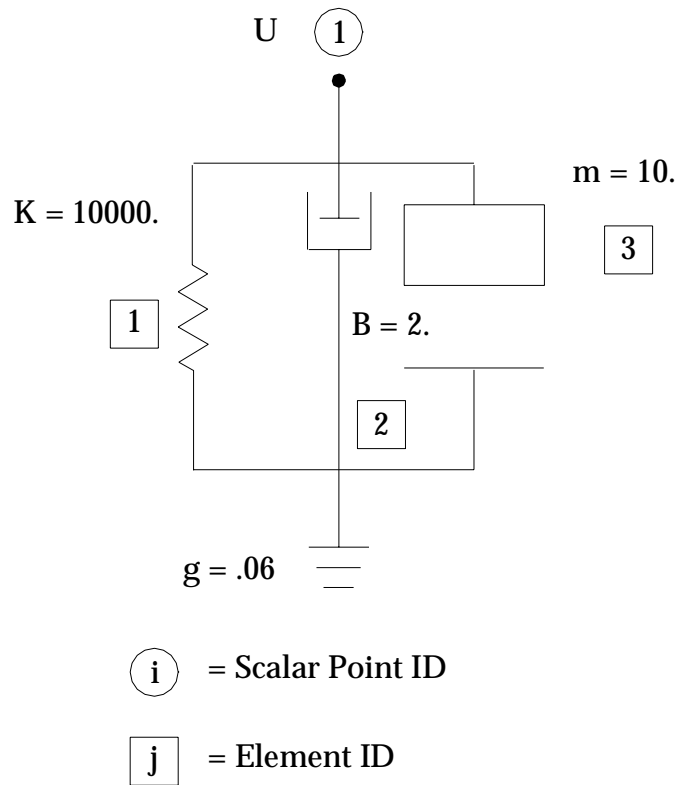
The following Bulk Data entries are required to represent the foregoing single degree-of-freedom oscillator:

1	2	3	4	5	6	7	8	9	10
CELAS2	EID	K	G1	C1	G2	C2	GE	S	
CELAS2	1	1000.	1						

CDAMP2	EID	B	G1	C1	G2	C2			
CDAMP2	2	2.	1						

CMASS2	EID	M	G1	C1	G2	C2			
CMASS2	3	10.	1						

The excitation for both disjoint models is a force (moment for the torsional system) with a magnitude of $\cos\omega t$. This function can be generated with the following Bulk Data entries:

1	2	3	4	5	6	7	8	9	10
RLOAD2	SID	L	M	N	TB	TP			
RLOAD2	1	1	0	0	1	0			

TABLED1	ID								
TABLED1	1								+ABC

	X_1	Y_1	X_2	Y_2	X_3	Y_3			
+ABC	0.	1.	1.	1.	100.	1.	ENDT		

DAREA	SID	P	C	A					
DAREA	1	2	3	1.					

DAREA	1	2	6	1.					
DAREA	1	1		1.					

To perform a frequency response analysis is necessary to provide a list of frequencies (Hz) at which solutions are desired. The following FREQ1 Bulk Data entry is used for this purpose.

FREQ1	SID	F1	DF	NDF					
FREQ1	1	.5	.3	10					

The complete MSC.Nastran data entry for the two disjoint problems is listed below:

```
ID TEST,DAMPING
SOL 26
CEND

TITLE=FREQUENCY RESPONSE
SUBTITLE=VISCOELASTIC AND ELASTIC MATERIALS
DLOAD=1
SDAMP=10
FREQ=1
SPC=1
SET 1=1,2
DISP=1
VELO=1
ACCE=1
SET 7=23
STRESS=7
BEGIN BULK

$ INCLUDE ALL BULK DATA ENTRIES FOR BOTH
$ DISJOINT MODELS DISCUSSED IN THE PRECEDING
$ REMARKS

ENDDATA
```

5.7 Free Body Techniques

Free body motion in a structure occurs when a structure may move freely without applied forces. Although the stiffness matrix will have one or more singularities, the combined dynamic system, with mass and damping, may not be singular. Examples are flying objects such as aircraft or rockets, and structures with kinematic mechanisms such as a gyroscope or a pendulum.

In most cases, the dynamic response solutions in MSC.Nastran do not require any special attention for free body motions. In general, MSC.Nastran will decompose matrix combinations that are not singular. For example, an unbalanced load applied to a free body has a unique dynamic solution, namely a constant acceleration. The only exception is that of a frequency response analysis at a frequency of zero. In this case it is recommended that a small frequency be used instead of zero for free bodies.

In some cases, it may be necessary to use the SUPORT Bulk Data to provide a method of defining the free body modes of a structure. The primary use for this process is in inertia relief option for static analysis. (See the *MSC.Nastran Linear Static Analysis User's Guide.*)

In other cases, the basic geometry is used for the definition of the rigid body displacements. The parameter GRDPNT specifies a grid point or a location for the six rigid body displacement vectors—three translations and three rotations. This method is used in the weight and CG calculations and is used for inertia relief with superelements.

The SUPORT Option

The SUPORT data defines a set of degrees-of-freedom that are used to restrain free motion of the structure *temporarily* for the purposes of calculating normal modes, providing a moving frame of reference, or measuring unbalanced loads. The basic theory and usage are given in "**Overview**" on page 88 of the *MSC.Nastran Basic Dynamic Analysis User's Guide*, and other MSC user's guides. Other bulk data variations that perform this function are CYSUP Bulk Data (cyclic symmetry) and SESUP Bulk Data (superelements).

In dynamic analysis, some specialized areas in which it is useful to apply free body SUPORTs include:

1. Calculation of pure zero-frequency eigenvalues and, if necessary, their eigenvectors. The result depends on the chosen eigenvalue extraction method. In the Inverse Power method, the zero frequency eigenvectors are obtained from the stiffness matrix. In the other real eigenvalue methods, the number of SUPORT degrees-of-freedom indicate the number of zero-frequency modes to be calculated.

2. Use of the large mass technique to enforce motion in a modal formulation. Here the SUPORTs are essential to obtain frequencies that are exactly zero. (See "**Enforced Motion with Loads**" on page 87.)

3. Response Spectra analysis with participation factors. Here the responses are calculated relative to a moving base, defined by SUPORTs (see "**Shock and Response Spectrum Analysis**" on page 221).

4. Verification of new FE models with a free body test will find several types of errors. It is useful to remove the constraints for a fixed structure to perform extra check runs. For instance, the calculations for SUPORT inputs will indicate if additional mechanism modes exist.

5. SUPORT data is required for mode acceleration data recovery of free bodies. In this calculation it is necessary to solve a quasi static equation using the stiffness matrix. The use of SUPORTs will eliminate singularities without over-constraining the structure.

6. SESUP data are used for modal analysis of individual superelements. This is used for Component Mode Synthesis when SECSET boundaries are used to obtain free body modes.

Each of these topics is described elsewhere in this guide. However, they all have the same limitations and requirements on the selection of the SUPORT set.

The SUPORT inputs define a set of degrees-of-freedom, u_r, which belong to the partitions

$$\{u_a\} = \begin{Bmatrix} q \\ u_l \\ u_r \end{Bmatrix}$$ Eq. 5-52

where q are the dynamic QSET or component modal coordinates, and u_l are the physical degrees-of-freedom for the restrained structure. The free body motions of the structure may be obtained by solving a problem with zero forces. The partitioned static matrix solution is

$$\begin{bmatrix} K_{ll} & K_{lr} \\ K_{rl} & K_{rr} \end{bmatrix} \begin{bmatrix} D_l \\ I \end{bmatrix} = \{P\} = \{0\}$$ Eq. 5-53

where $[D_l]$ is called the rigid body transformation matrix. It is obtained by solving the equation:

$$[K_{ll}][K_l] = -[K_{lr}]$$ Eq. 5-54

Depending on the type of solution, the $[D_l]$ matrix may be used for extracting zero-frequency mode shapes, for finding relative deformation vectors and for measuring resultants for load and force vectors. The number of columns of $[D_l]$ equals the number of user-selected SUPORT points. This number may be less than six if other constraints are applied, or may be greater than six if mechanisms are present. (Usually six degrees-of-freedom are chosen at a hard point near the center of gravity.)

The requirements for the u_r set are that they provide a nonredundant set of supports, namely that:

1. If the structure were to be constrained to zero displacement at the SUPORT DOF, no singularities will occur in the resulting stiffness matrix partition; i.e.,

$$[K_{ll}]^{-1} \text{ exists} \qquad\qquad \text{Eq. 5-55}$$

2. If the unloaded structure were to be given enforced displacements at each of the SUPORT DOF (with the others constrained), no stresses or forces should occur in the structure; i.e.,

$$[K_{rl}][D_{lr}] + [K_{rr}] = [0] \qquad\qquad \text{Eq. 5-56}$$

3. The SUPORT DOF are connected to structural elements which provide real supporting stiffness. (Points near the CG are preferred.)

4. In superelement analysis the final SUPORT set is restricted to the residual structure. (However, SESUP data may be used to define separate u_r sets for modal analysis of upstream superelements.)

If any of these criteria are violated, the table output with User Information Message 3035 will contain large values for the epsilon and strain energy. The equations defining these parameters are given in "**Overview**" on page 88 of the *MSC.Nastran Basic Dynamic Analysis User's Guide.*

Geometric Shape Methods

In these cases, the rigid body shapes are defined geometrically by the locations of the grid points and orientation of their displacement coordinate systems. The structure may or may not be a free body. Also, mechanisms that produce free body differences in displacements or rotations are not included.

The parameter GRDPNT is used normally to calculate the total weight, inertia, and CG properties of a structure. It is also used to generate geometric rigid body shapes. The matrix $[D_l]$ as defined in **Eq. 5-56** may be calculated directly from the geometry. The VECPLOT Module generates a 6×6 matrix, $[D_i]$, for every grid point, g, from basic kinematics. The definition is

$$\{u_{gi}\} = [D_i]\{u_o\} \qquad\qquad \text{Eq. 5-57}$$

where $\{u_{gi}\}$ is the vector of three displacements and three rotations in the local coordinate system. $\{u_o\}$ represents three displacements and three rotations at GRDPNT (or the origin) in basic coordinates. These 6×6 partitions are merged into a full-size matrix, $[D_{go}]$ with six rows for each grid point and six columns total. Note that the rows of $[D_{go}]$ are null for the scalar points and is a unit matrix for the six rows corresponding to the GRDPNT parameter.

If SUPORT data is present, the matrix is transformed to define motion relative to the supported degrees-of-freedom, $\{u_r\}$. The internal calculations are given below

Partition:

$$[D_{go}] \Rightarrow \begin{bmatrix} D_{\bar{g}o} \\ D_{ro} \end{bmatrix}$$

Eq. 5-58

Invert the support partition, and multiply:

$$[D_{\bar{g}r}] = [D_{\bar{g}o}][D_{ro}]^{-1}$$

Eq. 5-59

and merge:

$$[D_{gr}] \Leftarrow \begin{bmatrix} D_{\bar{g}r} \\ I \end{bmatrix}$$

Eq. 5-60

These matrices may be calculated at the superelement level as opposed to assembled residual SE level required by the SUPORT partition method.

The applications include:

1. Static inertia relief solutions for SOL 101. The requirement to combine and reduce mass matrices is eliminated with this method, saving nearly 50% of the execution cost. For inertia relief effects, these solutions also require the input PARAM,INREL,–1 and a set of six SUPORT degrees-of-freedom.

2. Component Mode Synthesis for superelements provides an option for inertia relief vectors. The advantage is improved accuracy in the final results with an equal or lesser number of component modes. These are deformation shapes that correspond to the six uniform acceleration loads on the constrained structure. The deformation shape vectors are appended to the mode shapes and are included as generalized degrees-of-freedom. The INRLM parameter controls this option.

Note that in addition to the limitation of six free body motions, the geometric method will not be correct for scalar points and fluid analysis methods.

5.8 Aeroelastic Solutions

The *MSC.Nastran Aeroelastic Analysis User's Guide* describes the theoretical aspects and the numerical techniques used to perform aeroelastic analyses with MSC.Nastran. As described in "Overview of Aeroelastic Analysis" on page 81, the system is used for flutter, frequency response, gust response, and static analysis of aerodynamically loaded structures. An outline of the capability is given here.

The aeroelastic analyses use the following features:

Structural Model. Any of the existing MSC.Nastran structural finite elements (except axisymmetric and p-elements) can be used to build the structural model. The structural stiffness, mass, and damping matrices required by the aeroelastic analyses are generated by MSC.Nastran from the user input of geometric, structural, inertial, and damping data, for subsequent use in the various aeroelastic analyses.

Fluid/Structure Connections. Matrices of aerodynamic influence coefficients are computed only from the data describing the geometry of the aerodynamic finite elements. The choice of aerodynamic grid points for the aerodynamic model is independent of the location of the structural grid points. An automated interpolation procedure is provided to relate the aerodynamic to the structural degrees-of-freedom. Splining techniques for both lines and surfaces are used to generate the transformation matrix from structural grid point deflections to aerodynamic grid point deflections where local streamwise slopes are also computed. The transpose of this matrix transfers the aerodynamic forces and moments at aerodynamic boxes to structural grid points.

Aerodynamic Theories. One subsonic and three supersonic lifting surface aerodynamic theories are available in MSC.Nastran, as well as Strip Theory. The subsonic theory is the Doublet-Lattice method, which can account for interference among multiple lifting surfaces and bodies. The supersonic theories are the Mach Box method, Piston Theory, and the ZONA51 method for multiple interfering lifting surfaces that was added to MSC.Nastran in Version 67.

Static Aeroelastic Analysis. The structural load distribution on an elastic vehicle in trimmed flight is determined by solving the equations for static equilibrium. The SOL 144 and SOL 200 processes will calculate aerodynamic stability derivatives (e.g., lift and moment curve slopes and lift and moment coefficients due to control surface rotation) and trim variables (e.g., angle of attack and control surface setting) as well as aerodynamic and structural loads, structural deflections, and element stresses.

Modal Formulation. Dynamic aero solutions provide for modal reduction of the system matrices. The number of degrees-of-freedom required for accurate solutions to dynamic aeroelastic problems is generally far less than the number of physical degrees-of-freedom used in the finite element structural model. The number of independent degrees-of-freedom can be greatly reduced by using the (complex) amplitudes of a series of vibration modes as generalized coordinates, e.g., by Galerkin's method. MSC.Nastran

can compute the vibration modes and frequencies and make the transformation to modal coordinates. The matrices of aerodynamic influence coefficients are also transformed to generalized aerodynamic forces by use of the vibration eigenvectors.

Flutter Analysis. The dynamic aeroelastic stability problem, flutter, is solved in SOL 145, by any of three methods. The traditional American flutter method developed by the Air Materiel Command (AMC) in 1942 is available in the first two methods. The first method is called the K-method and is a variation of the AMC method. The second method, called the KE-method, is more efficient from the point of view of tracking roots, but is limited in input (no viscous damping) and output (no eigenvectors). The third method, called the PK-method, is similar to the British flutter method, which was developed by the Royal Aircraft Establishment.

Frequency Response. The coupling with aerodynamic loads has also been added to the existing MSC.Nastran structural modal frequency response capability, SOL 146. Analyses of frequency response to arbitrarily specified forcing functions can be carried out using the oscillatory aerodynamic loads from any of the available aerodynamic theories. Frequency response to a harmonic gust field can be calculated at subsonic speeds using the Doublet-Lattice method for wing/body interference, and by the ZONA51 method for interfering lifting surfaces at supersonic speeds.

Transient Response. Because unsteady aerodynamic loads are obtained only for steady-state harmonic motion, they are known only in the frequency- and not the time-domain. In SOL 146, Inverse Fourier Transform techniques provide the appropriate methods by which transient response is obtained from the frequency response. Both forward and inverse Fourier transforms are provided so that the time-varying forcing function or the gust profile can be transformed into the frequency domain. Then, after convolution with the system frequency response, the inverse transform leads to the transient response of the system to the specified forcing function or gust profile.

Random Response. Stationary random response of the system, is available in SOL 146 from specified loadings and the power spectral densities of loads. Loads may be either specified force distributions or harmonic gust fields. The statistical quantities of interest in the response are $\bar{A}$, the ratio of standard deviations (rms values) of the response to that of the input loading, and N_o, the mean frequency of zero crossings (with a positive slope) of the response. The capability to compute these quantities was added to MSC.Nastran by modifying the existing random response module to include options to generate various atmospheric turbulence power spectra and to perform the calculation of N_o.

Design Sensitivities. The sensitivities of response parameters to changes in design variables are calculated by the perturbation techniques developed for structural optimization in MSC.Nastran and extended to include static aeroelasticity and flutter in SOL 200. The basic aeroelastic sensitivities that can be obtained include stability derivatives, trim variables, and flutter system dampings. The synthetic response technique of MSC.Nastran optimization also permits the calculation of sensitivities of user-specified functions of those standard response quantities.

Aeroelastic Optimization. Optimization of aeroelastic characteristics can be combined with the other optimization features of MSC.Nastran in SOL 200, and vehicles can now be designed optimally for aeroelastic loads, flying qualities, and flutter, as well as for strength, vibration frequencies, and buckling characteristics.

Introduction to Aeroelastic Analysis and Design

Aeroelastic analysis and design solution sequences extend the range of capabilities in MSC.Nastran beyond basic static and dynamic structural analysis.

Aeroelastic Modules. Options are available to:

- Generate aerodynamic grid points.
- Compute aerodynamic matrices.
- Provide connection (interpolation) between the structural and aerodynamic grid points.
- Solve the equations for static aeroelasticity.
- Solve the equations for flutter.
- Solve the equations for dynamic aeroelastic response.
- Calculate aeroelastic design sensitivities.
- Optimize aeroelastic and related structural characteristics.

Aeroelastic DMAP Sequences. Four solution sequences are available:

1. SOL 144 for static aeroelastic analyses.
2. SOL 145 for modal flutter analyses by the K-, KE-, or PK-methods.
3. SOL 146 for modal dynamic aeroelastic response analyses due to gusts or control surface deflections.
4. SOL 200 for design sensitivity and optimization including aeroelastic effects. Since this fourth sequence has applications to many areas other than aeroelasticity, the reader is referred to the *MSC.Nastran Design Sensitivity and Optimization User's Guide* for a more comprehensive treatment. Aeroelastic optimization is beyond the scope of this Guide and is not discussed further in this section.

Aerodynamic Theories

MSC.Nastran has implemented six aerodynamic theories:

1. Doublet-Lattice subsonic lifting surface theory (DLM)
2. ZONA51 supersonic lifting surface theory
3. Subsonic wing-body interference theory (DLM with slender bodies)
4. Mach Box method

    5. Strip Theory

    6. Piston Theory

Each of these methods is described in the *MSC.Nastran Aeroelastic Analysis User's Guide*. They all share a common matrix structure.

Three matrix equations summarize the relationships required to define a set of aerodynamic influence coefficients [see Rodden and Revell (1962)]. These are the basic relationships between the lifting pressure and the dimensionless vertical or normal velocity induced by the inclination of the surface to the airstream; i.e., the downwash (or normalwash),

$$\{w_j\} = [A_{jj}]\{f_j / q\} \qquad\qquad \text{Eq. 5-61}$$

the substantial differentiation matrix of the deflections to obtain downwash,

$$\{w_j\} = [D_{jk}^1 + ik\ D_{jk}^2]\{u_k\} + \{w_j^g\} \qquad\qquad \text{Eq. 5-62}$$

and the integration of the pressure to obtain forces and moments,

$$\{P_k\} = [S_{kj}]\{f_j\} \qquad\qquad \text{Eq. 5-63}$$

where:

w_j	=	downwash (dimensionless)
w_j^g	=	static aerodynamic downwash; it includes, primarily, the static incidence distribution that may arise from an initial angle of attack, camber, or twist
f_j	=	pressure on lifting element j
q	=	flight dynamic pressure
k	=	reduced frequency, $k = \omega b / V$ where ω is the angular frequency, b is a reference semichord, and V is the free-stream velocity
$A_{jj}(m,k)$	=	aerodynamic influence coefficient matrix, a function of Mach number (m), and reduced frequency (k)
u_k, P_k	=	displacements and forces at aerodynamic grid points
D_{jk}^1 , D_{jk}^2	=	real and imaginary parts of substantial differentiation matrix, respectively (dimensionless)
S_{kj}	=	integration matrix

The Aerodynamic Influence Coefficient Matrix. The three matrices of **Eq. 5-62** and **Eq. 5-63** can be combined to give an aerodynamic influence coefficient matrix:

$$[Q_{kk}] = [S_{kj}][A_{jj}]^{-1}[D_{jk}^1 + ik\ D_{jk}^2] \qquad\qquad \text{Eq. 5-64}$$

All aerodynamic methods compute the S, D^1 and D^2 matrices at user-supplied Mach numbers and reduced frequencies. The Doublet-Lattice and ZONA51 theories compute the A matrix. Then, matrix decomposition and forward and backward substitution are used in the computation of the Q matrix. The remaining methods compute A^{-1} directly and use matrix multiplications to form Q. Details of the various methods are described in the *MSC.Nastran Aeroelastic Analysis User's Guide.*

Generation of Aerodynamic Matrices

The aerodynamic equations described above form the basis of the aerodynamic computations required for static aeroelastic analysis with some special purpose modifications made for the MSC.Nastran implementation.

For static aeroelasticity, the downwash relation of **Eq. 5-62** becomes

$$\{w_j\} \;=\; [D_{jk}]\{u_k\} + [D_{jx}]\{u_x\} + \{w_j^g\} \qquad\qquad \text{Eq. 5-65}$$

where:

$\{w_j\}$ =   a vector of aerodynamic degrees-of-freedom (e.g., angles of attack)

$\{u_k\}$ =   a vector of aerodynamic displacements (deformations)

$\{u_x\}$ =   a vector of extra aerodynamic points used to describe, e.g., aerodynamic control surface deflections and overall rigid body motions

$\{w_j^g\}$ =   represents an initial static aerodynamic downwash. It includes, primarily, the static incidence distribution that may arise from an initial angle of attack, camber, or washout (twist)

$[D_{jk}]$ =   a substantial derivative matrix for the aerodynamic displacements. This is the D_{jk}^1 term of **Eq. 5-62**. The D_{jk}^2 term is not used for this quasi-steady analysis.

$[D_{jx}]$ =   a substantial derivative matrix for the extra aerodynamic points

Static Aeroelastic Equations of Motion

The aerodynamic forces are transferred to the structure reduced to the a-set to form an aerodynamic influence coefficient matrix, Q_{aa}, which provides the forces at the structural grid points due to structural deformations, i.e.,

$$\{F_a\} \;=\; [Q_{aa}]\{u_a\}$$

and a second matrix, Q_{ax}, which provides forces at the structural grid points due to unit deflections of the aerodynamic extra points, $\{u_x\}$:

$$\{F_x\} \;=\; [Q_{ax}]\{u_x\}$$

The complete equations of motion in the a-set degrees-of-freedom require

$[K_{aa}]$ Structural stiffness matrix

$[M_{aa}]$ Structural mass matrix

$\{P_a\}$ Vector of applied loads (e.g., mechanical, thermal, and gravity loads plus aerodynamic terms due to user input pressures and/or downwash velocities)

The a-set equations are then:

$$[K_{aa} - \bar{q}\, Q_{aa}]\{u_a\} + [M_{aa}]\{\ddot{U}_a\} \;=\; \bar{q}[Q_{ax}]\{u_x\} + \{P_a\} \qquad \text{Eq. 5-66}$$

This is the basic set of equations used for static aeroelastic analysis. In the general case, rigid body motions are included in the equations to represent the free-flying characteristic of an air vehicle. This is addressed in MSC.Nastran by a requirement that the user identify reference degrees-of-freedom equal in number to the number of rigid body motions using the SUPORT Bulk Data entry. **Eq. 5-66** is then partitioned into r-set (supported) and *l*-set (left over) degrees-of-freedom, yielding

$$\begin{bmatrix} K_{ll}^a & K_{lr}^a \\ K_{rl}^a & K_{rr}^a \end{bmatrix} \begin{Bmatrix} u_l \\ u_r \end{Bmatrix} + \begin{bmatrix} M_{ll} & M_{lr} \\ M_{rl} & M_{rr} \end{bmatrix} \begin{Bmatrix} \ddot{u}_l \\ \ddot{u}_r \end{Bmatrix} \;=\; -\begin{bmatrix} K_{lx}^a \\ K_{rx}^a \end{bmatrix} \{u_x\} + \begin{Bmatrix} P_l \\ P_r \end{Bmatrix} \qquad \text{Eq. 5-67}$$

where the notation

$$[K_{aa}^a] \;=\; [K_{aa} - \bar{q}\, Q_{aa}]$$

$$[K_{ax}^a] \;=\; -\bar{q}[Q_{ax}]$$

has been introduced.

At this point the MSC.Nastran implementation of aeroelastic analysis introduces a mathematical technique that is based on the MSC.Nastran inertia relief analysis without aeroelastic effects. The technique entails multiplying the first row of **Eq. 5-67** by D^T and adding the result to the second row. Assuming that a steady-state condition exists, the accelerations may be constrained and the system may be solved for steady-state loads or divergence. The stability derivatives and static control system coefficients may also be obtained.

Flutter Solution Techniques

Flutter is the dynamic aeroelastic stability problem. It can be solved in any speed regime simply by selecting the appropriate aerodynamic theory. In the linear case assumed throughout this guide, the solution involves a series of complex eigenvalue solutions; the eigenvalue problem to be solved depends on the way in which the aerodynamic loads are included in the equations of motion or whether certain damping terms are included.

The manner in which the aerodynamic loads are included depends on how the dimensionless oscillatory aerodynamic coefficients are defined. When Theodorsen (1935) first developed the American method (K-method) of flutter analysis, he introduced the aerodynamics into a vibration analysis as complex inertial terms and the flutter analysis became a vibration analysis requiring complex arithmetic. At the same time, he introduced an artificial complex structural damping, proportional to the stiffness, to sustain the assumed harmonic motion. Flutter analysis is then a double eigenvalue problem in frequency and velocity, and an iterative solution, using the reduced frequency of the assumed harmonic motion as the iteration parameter, leads to the neutrally stable conditions (flutter frequencies and velocities) at which no artificial damping is required. The artificial damping is therefore seen not to be physically meaningful, other than, perhaps, at speeds near flutter speeds.

Generalized Aerodynamic Matrices

Eq. 5-64 defines an aerodynamic influence coefficient matrix Q_{kk} that is computed based on the aerodynamic model. In order for this matrix to be useful in a flutter analysis, two transformations must take place:

1. The matrices must be applied to the structural model using the spline techniques.

2. A modal reduction must be applied to obtain the matrices in generalized form.

Mathematically, those transformations can be expressed as

$$[Q_{ii}] = [\phi_{ai}]^T [G_{ka}]^T [WTFACT][Q_{kk}][G_{ka}][\phi_{ai}] \qquad \text{Eq. 5-68}$$

where:

Q_{ii} = the generalized aerodynamic matrix

ϕ_{ai} = a matrix of i-set normal mode vectors in the physical a-set

G_{ka} = the spline matrix reduced to the a-set

$WTFACT$ = a weighting factor matrix W_{kk} defined by the user

A level of complexity is added if the flutter analysis includes the use of extra points. Extra points are used for the representation of control systems and are therefore required in aeroservoelastic analyses. The flutter analysis then uses a merged matrix

$$[Q_{hh}] = \begin{bmatrix} Q_{ii} & Q_{ie} \\ 0 & 0 \end{bmatrix} \qquad \text{Eq. 5-69}$$

in which the h-set is a combination of the i-set normal modes and the e-set extra points. It is seen that the lower e-set rows in the matrix are null. Physically, this indicates that the normal mode deflections do not produce aerodynamic forces on the extra points ($Q_{ei} = 0$) and that the extra point deflections do not produce aerodynamic loads on the extra points ($Q_{ee} = 0$).

The K-Method of Flutter Solution

The basic equation for modal flutter analysis by the K-method is

$$\left[-M_{hh}\omega^2 + iB_{hh}\omega + (1 + ig)K_{hh} - \left(\frac{1}{2}\rho V^2\right)Q_{hh}(m,k)\right]\{u_h\} = 0 \qquad \text{Eq. 5-70}$$

where:

M_{hh} = modal mass matrix, usually (but not necessarily) diagonal

B_{hh} = modal damping matrix

K_{hh} = modal stiffness matrix, usually (but not necessarily) diagonal; may be complex (with actual structural damping); will be singular if there are rigid body modes

m = Mach number

k = reduced frequency = $.\omega c/2V$

c = reference length

$Q_{hh}(m,k)$ = aerodynamic force matrix, which is a function of parameters m and k

ω = circular frequency = $2\pi f$

g = artificial structural damping

ρ = fluid density

V = overall forward velocity

u_h = modal amplitude vector, sometimes called modal participation factors

Note that k, V, and ω are not independent.

For the K-method of solution, the aerodynamic term is converted to an equivalent aerodynamic mass

$$\left[-\left[M_{hh} + \frac{\rho}{2}\left(\frac{c}{2k}\right)^2 Q_{hh}(m,k)\right]\frac{\omega^2}{1 + ig} + B_{hh}\frac{i\omega}{\sqrt{1 + ig}} + K_{hh}\right]\{u_h\} = 0 \qquad \text{Eq. 5-71}$$

The term involving B_{hh} in **Eq. 5-71** has been multiplied by $\sqrt{1 + ig}$ for mathematical convenience, and is valid only at flutter, i.e., when $g = 0$. **Eq. 5-71** is solved as an eigenvalue problem for a series of values for parameters m, k, and ρ. The complex eigenvalue is $\omega^2/(1 + ig)$, which can be interpreted as real values of ω and g. The velocity, V, is recovered from $V = \omega c/2k$. Flutter occurs for values of m, k, and ρ for which $g = 0$. The solutions are not valid except when $g = 0$, since the aerodynamic force terms are valid only for sinusoidal motion and g is not a physical damping.

The K-method of flutter analysis is a looping procedure. The values of V, g, and $f = \omega/2\pi$ are solved for various values of m, k, and ρ. Plots of V versus g can be used to determine the flutter speed(s) (where g goes through zero to positive values). The KE-method and

the PK-method are the other major flutter options. These are discussed in the *MSC.Nastran Aeroelastic Analysis User's Guide*. Typical flutter plots are shown in **Figure 5-4** and **Figure 5-5** for the output from the PK-method.
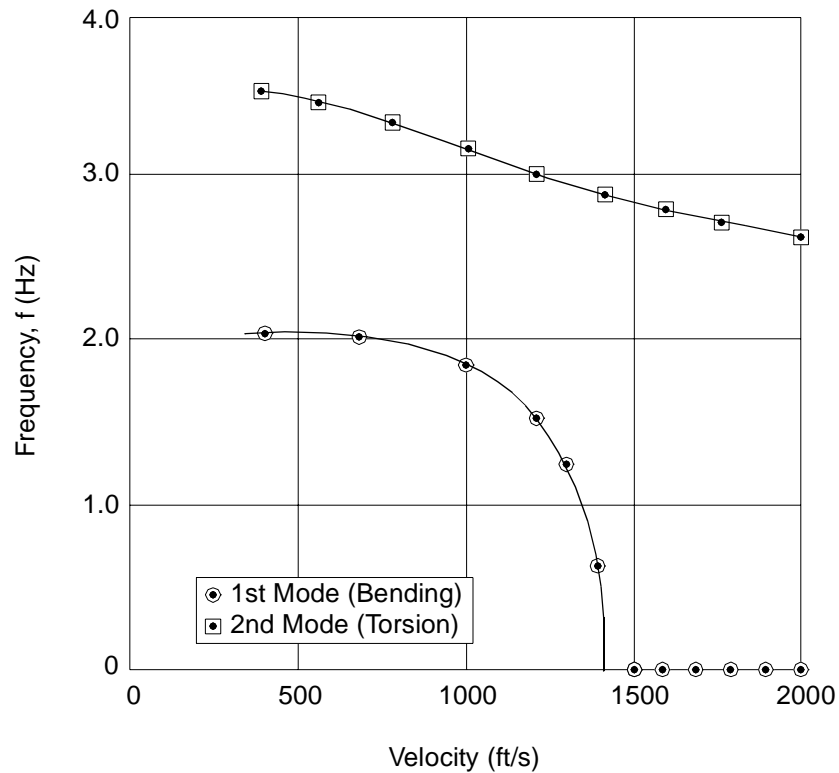
Figure 5-4 V-f Curve for BAH Wing
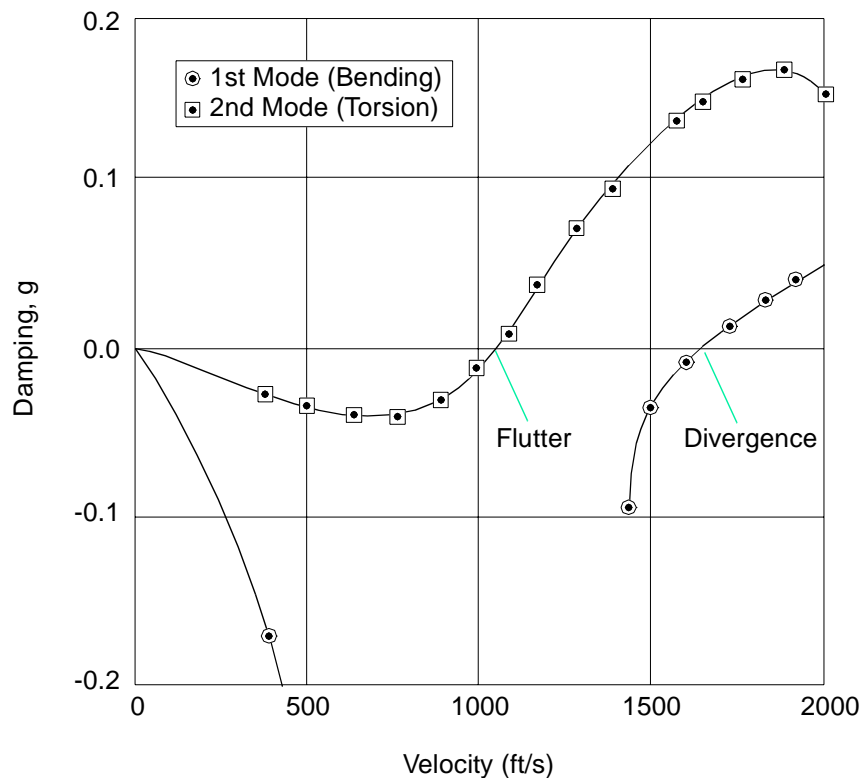
Figure 5-5 V-g Curve for BAH Wing

Note that the bending branch goes to zero frequency before the mode goes unstable.

Dynamic Aeroelastic Analysis

Dynamic aeroelasticity differs from the flutter analysis described in the previous section in that the right-hand side of **Eq. 5-70** is no longer zero. Instead, loading, which can be in either the frequency or the time domain, is applied. For both types of loading, MSC.Nastran performs the primary analyses in the frequency domain. If the user has supplied loadings in the time domain, Fourier Transform techniques are used to convert the loadings into the frequency domain, a frequency response analysis is performed, and the computed quantities are transformed back to the time domain using Inverse Fourier Transform techniques. This section first describes the frequency response analysis that is the basis of all MSC.Nastran dynamic aeroelastic analysis and then discusses the special topics of transient response analysis and random response analysis.

Aeroelastic frequency response analysis in MSC.Nastran is performed in modal coordinates and has a basic equation of the form

$$\left[-M_{hh}\omega^2 + iB_{hh}\omega + (1 + ig)K_{hh} - \frac{1}{2}\rho V^2 Q_{hh}(m,k) \right]\{u_h\} = \{P(\omega)\} \qquad \text{Eq. 5-72}$$

where all terms on the left-hand side are identical to those of **Eq. 5-70** and are defined with that equation. The right-hand side provides the loading in modal coordinates, which can be aerodynamic or nonaerodynamic in nature and is a function of the analysis frequency. Nonaerodynamic generalized loads, designated $\text{PHF}(\omega)$, are obtained in the standard fashion from the loadings applied to physical coordinates.

The solution of **Eq. 5-72** entails solving for the generalized displacements by decomposition/forward-backward substitution techniques applied to the coupled set of complex equations. Because modal reduction techniques have been applied, the solution costs are typically modest. Once the generalized displacements have been computed, standard data recovery techniques can be used to determine physical displacements, velocities, stress, etc.

Aeroelastic Transient Response Analysis

As discussed in the introduction to this section, Aeroelastic Transient Analysis relies on Fourier transform techniques. Transient analysis by a Fourier transformation is separated into three phases. First, the loads (defined as a function of time) are transformed into the frequency domain. Second, the responses are computed in the frequency domain using the algorithm of the preceding subsection. Third, these responses (in the frequency domain) are transformed back to the time domain.

Transformation of Loads

The user specifies loads in the same manner as given in "**Modal Versus Direct Transient Response**" on page 164 of the *MSC.Nastran Basic Dynamic Analysis User's Guide.* The two general forms are the tabular, piecewise linear function and the general purpose function.

These loads, which are in the form required for frequency response, are transformed to the modal coordinates exactly as in the modal frequency response method.

Inverse Transformation of the Response

The response is found from a numerical approximation to the inverse Fourier integral or from the Fourier series, the Fourier series result, which can be regarded as a special form of approximation to the integral. The quantity $\tilde{u}(\omega)$ is first calculated at a set of frequencies, ω_i, by the frequency response analysis. The ω_i do not need to be equally spaced and the integral is evaluated only over the frequency range for which the frequency response has been performed. This option is described in "**Fourier Transform**" on page 176.

Random Response Analysis

The major loads to which an aerospace vehicle is subjected can be predicted for the most part from its design mission and maneuvering requirements. However, the total environment cannot be predicted exactly and statistical methods based on the theory of random processes must be employed to complete the description. Examples of random processes in aeroelasticity include response to atmospheric gusts and to aerodynamic buffeting. The random process theory considered in MSC.Nastran is based on generalized harmonic analysis, i.e., frequency response techniques, and assumes that the system is linear and that both the excitation and response are stationary with respect to time. See "**Random Analysis with Coupled Excitations**" on page 238 for a description of the methods.

5.9   Dynamic Optimization and Design Sensitivity

Design optimization is a major area of innovation in the development of MSC.Nastran. The first version of the code, which was released in 1989, was the first to include a comprehensive structural optimization capability. Later versions provided the ability to automatically design a structure while considering limits on the structure's static, modal and buckling responses. This capability has been extended to superelement optimization, aeroelastic optimization, shape optimization, and dynamic optimization, the subject of this section. All of these capabilities can be made to couple with the same design task. A mixture of design variables (i.e., shape and sizing) can be used while constraining or minimizing responses from a number of analysis disciplines, such as statics, normal modes, flutter and modal frequency response.

The specific dynamic analyses that are supported are direct frequency response (i.e., the analysis takes place in physical coordinates), modal frequency response and modal transient response (i.e., the analysis model is reduced using modal approximations). The basis for performing the dynamic optimization is the dynamic sensitivity analysis described in the *MSC.Nastran Design Sensitivity and Optimization User's Guide*. One implementation consideration that is discussed in this reference, but that should be reiterated here, is that eigenvector sensitivities are not computed as part of the sensitivity analysis. Instead, the response sensitivities are computed directly from existing mode shapes. As a rule of thumb, it is recommended that sensitivity and optimization tasks retain at least twice as many modes as are felt to be adequate for the analysis.

User Interface

This section briefly discusses how the user invokes MSC.Nastran's design optimization capability, primarily to document the types of responses that are available for the dynamic process. Again, the reader is referred to the *MSC.Nastran Design Sensitivity and Optimization User's Guide* for complete details on the use of the capability.

Case Control Commands

- Subcases are used for multiple excitations and environments.
- The objective function is a constraint set selected by the user.
- The user selects the active design constraint set for a particular subcase.

Bulk Data Inputs

Example Response Definition. The DRESP1 Bulk Data entry defines a set of structural responses that is used in the design either as constraints or as an objective. As an example, the full Bulk Data description is included below.

Format:

1	2	3	4	5	6	7	8	9	10
DRESP1	ID	LABEL	RTYPE	PTYPE	REGION	ATTA	ATTB	ATT1	
	ATT2	-etc.-							

Example:

DRESP1	1	DX1	STRESS	PROD	2	3	15	102	
	103								

Field	Contents
ID	Unique entry identifier. (Integer > 0)
LABEL	User-defined label. (Character)
RTYPE	Response type. See table below. (Character)
PTYPE	Element flag (PTYPE = "ELEM") or property entry name. Used with element type responses (stress, strain, force, etc.) to identify the property type, since property entry IDs are not unique across property types. (Character: "ELEM", "PBAR", "PSHELL", etc.)
REGION	Region identifier for constraint screening. (Integer > 0)
ATTA, ATTB, ATTi	Response attributes. (Integer > 0 or Real or blank)

The DRESP1 entry shown above is used to identify the responses that are to be used in the design task. Responses are used for constraints on the design or as objective functions either directly or through the use of user-supplied equations. The RTYPE field on this entry selects the particular response type involved. There are ten optional RTYPE's available with dynamic analysis:

[FRDISP]   Displacement in a frequency response analysis.

[FRVELO]   Velocity in a frequency response analysis.

[FRACCL]   Acceleration in a frequency response analysis.

[FRSTRE]   Stress in a frequency response analysis.

[FRFORC]   Force in a frequency response analysis.

[TDISP]   Displacement in a transient response analysis.

[TVELO]   Velocity in a transient response analysis.

[TACCL]   Acceleration in a transient response analysis.

[TSTRE]   Stress in a transient response analysis.

[TFORC]   Force in a transient response analysis.

A response may be associated with a specific time step, frequency, or subcase—or it may be defined for all available solutions. In the latter case, an individual constraint is generated for every available time step, etc. The specification of location of the responses (e.g., grid ID or stress component) is performed using the ATTi fields on the entry. Note that no distinction is made between modal and direct frequency analysis. Instead, the user specifies the type of analysis by using Case Control requests.

The DRESP2, DEQATN, DCONSTR and DESOBJ Entries

Three additional Bulk Data entries are used for defining the design objective and constraints:

1. The DRESP2 entry, coupled with the DEQATN entry, can be used to synthesize a response based on DRESP1 responses and a user supplied equation. An example of the use of this feature is to specify a response that is the difference of two FRDISP responses. A synthesized response will be calculated for all time steps or frequencies defined on the DRESP1 data.

2. The DCONSTR entry is used to place lower and upper bounds on the DRESP1 and/or DRESP2 responses.

3. The DESOBJ entry identifies the objective function that is to be minimized by referring to a DRESP1 or DRESP2 entry. The objective must be a scalar quantity such as mass, error, or cost.

On the other hand, a single DRESPi entry may generate many responses at each frequency or time step the user specifies. Therefore, if the user invokes one of the dynamic response quantities as the objective, it is necessary to identify which of the frequencies or time steps is to be used for the objective.

Example: A Clamped-Free Plate

This example is a plate that is acted upon by a harmonically varying pressure loading (**Figure 5-6**). The structural model is the same as the one used in Reference 3 to validate the sensitivity analysis in the presence of dynamic loads. The plate is rectangular with a length of 20.0 inches and a width of 10.0 inches. It is clamped at three edges and free on the fourth. Since the pressure loading is uniform, only a one-half model with a symmetry boundary condition is required. The material has an elastic modulus of 1.0×10^7 psi and a density of 0.1 lbm/in^3. The uniform pressure load has a magnitude of 1.0 lbf/in^2 and is applied at 500 Hz.

Finite Element Model
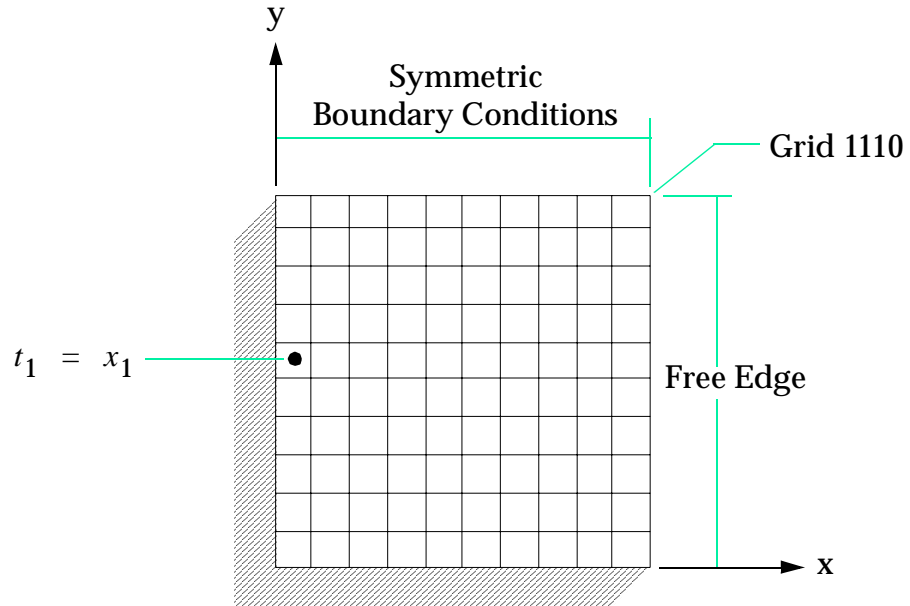
Figure 5-6 The Clamped-Free Plate
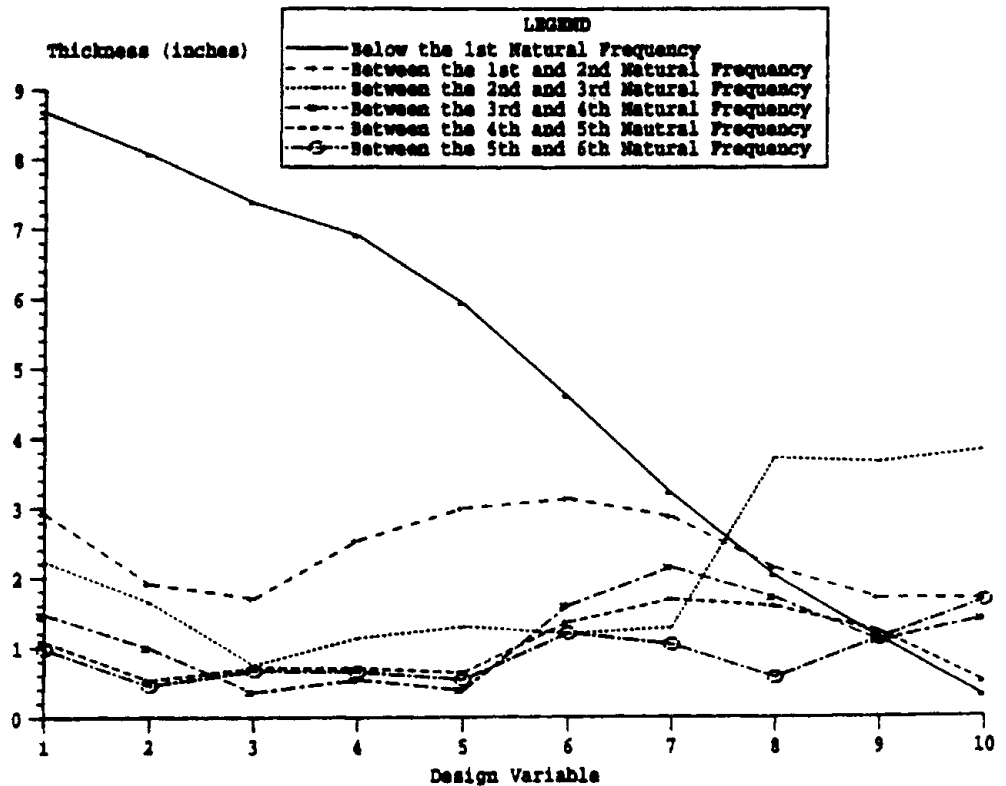
Figure 5-7 Final Thickness Distributions for the Clamped-Free Plate as a Function of the Imposed Frequency Constraints

The half model of the plate is modeled by a 10×10 array of four-noded plate elements. The elements are linked so that a single design variable controls a band of elements. That is, all 19 elements that are situated along the edge of the plate are controlled by the first design variable, the 17 elements that are one element in from the edge are controlled by the second

design variable and, finally, the single element at the center is controlled by the tenth design variable. The magnitude of the displacement at plate center is constrained to be less than 2.5 inches and the plate thickness is constrained to be greater than 0.01 inches.

Six different cases were run with the only difference being a constraint on the relation between the natural frequencies and the excitation frequencies. Each test case was a separate MSC.Nastran execution, which resulted in six different optimal designs. In the first case, the first natural frequency was constrained to be greater than the 500.0 Hz excitation frequency. For the remaining five cases:

$$\omega_i < 500.0 \text{ Hz} < \omega_{i+1} \quad i = 1, 5 \qquad \text{Eq. 5-73}$$

This frequency constraint was imposed to remove the disjoint design space phenomenon that occurs when a local minima exists near the original modal frequencies. In other words, we are forcing a major change in the modal frequency.

Results

Figure 5-7 shows the thickness distributions along either edge of the plate for the six cases. In this example, only in the first test, where the first natural frequency is greater than the excitation frequency, is the result intuitive. **Table 5-2** shows the final weights of the six designs. It can be seen that the weight is monotonically decreasing as the structure is made more flexible (i.e., more modes are below the fixed excitation frequency).

Table 5-2 Final Weights for the Clamped-Free Plate

Test	Constraint	Weight
1	$500.0 \text{ Hz.} < \omega_1$	5.163
2	$\omega_1 < 500.0 \text{ Hz.} < \omega_2$	1.963
3	$\omega_2 < 500.0 \text{ Hz.} < \omega_3$	1.831
4	$\omega_3 < 500.0 \text{ Hz.} < \omega_4$	1.310
5	$\omega_4 < 500.0 \text{ Hz.} < \omega_5$	0.740
6	$\omega_5 < 500.0 \text{ Hz.} < \omega_6$	0.613

Example: A Portal Frame with Transient Loading

The second example demonstrates the application of MSC.Nastran's optimization capabilities to transient analyses. The example is a simple portal frame acted upon by an enforced displacement at its base (**Figure 5-8**). This is a simple representation of a civil engineering structure subjected to seismic loading. The problem was obtained from

Reference 9, which demonstrated the possibility of disjoint design spaces when working in the time domain in an analogous fashion to the disjoint design space referred to earlier in the frequency domain. The portal has the following parameters:

Table 5-3 Parameters for the Portal Frame Example

PARAM	Meaning	Value
E	Young' Modulus	30.0×10^6 psi
ρ	Material density	0.28 lbm/in^3
I_{min}	Minimum allowable inertia	290.0 in^4
NSM	Nonstructural mass per unit length	10.0 lbm/in
ω_{min}	Minimum allowable fundamental frequency	60 rad/sec
δ_{max}	Maximum allowable displacement	± 3.0 in
σ_{max}	Maximum allowable stress	± 3.0 ksi
L	Height and width of the portal	180 in
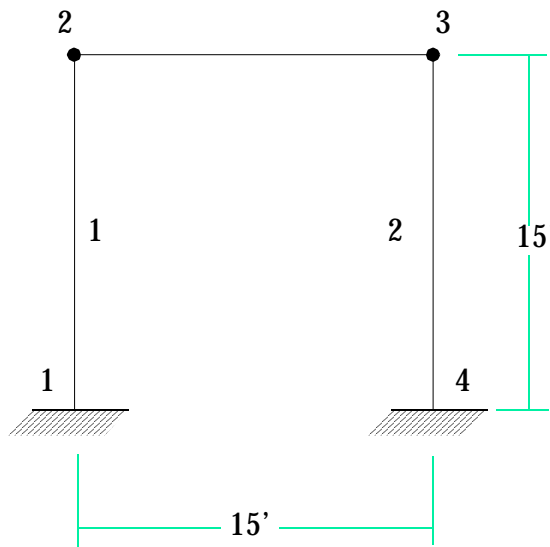
Figure 5-8 The Portal Frame

The frame is subjected to horizontal ground motion in the form of a half sine pulse:

$$u_g(t) \;=\; 1.0 \; \sin(30t), \quad t \leq \pi \, / \, 30.0 \qquad \text{Eq. 5-74}$$

The design task is to minimize the weight of the structure while imposing the limits on structural displacement, stress and natural frequency listed in **Table 5-3**.

Finite Element Model

The frame was modeled using three finite element bars (the symmetry of the problem could have been used to limit this to two elements). The stress is computed as the ratio of the bending moment in the beam divided by the section modulus.

The weight of the beam is simply its volume times the structural density. One design variable controls the bending moment of inertia of the vertical columns, while a second variable controls the inertia of the horizontal beam. Equations for the section modulus, S, and area, A, in terms of the moment of inertia of the beam, I, are taken from **Reference 9** in "**Selected Bibliography**" on page 299:

$$S \; = \; \sqrt{60.6I + 84000} - 290 \qquad\qquad \text{Eq. 5-75}$$

$$A \; = \; 0.465 \sqrt{I} \qquad\qquad \text{Eq. 5-76}$$

The transient response was performed over a period of 250 msecs at a time step of 1 msec. Responses were retained at every 5 msecs and the stress and displacement constraints were applied at each of the retained time steps. For the initial design, moment of inertia values of 600 in^4 were used for both design variables, making the initial objective value 1722.2 lbs (this ignores the weight of the nonstructural mass).

Results
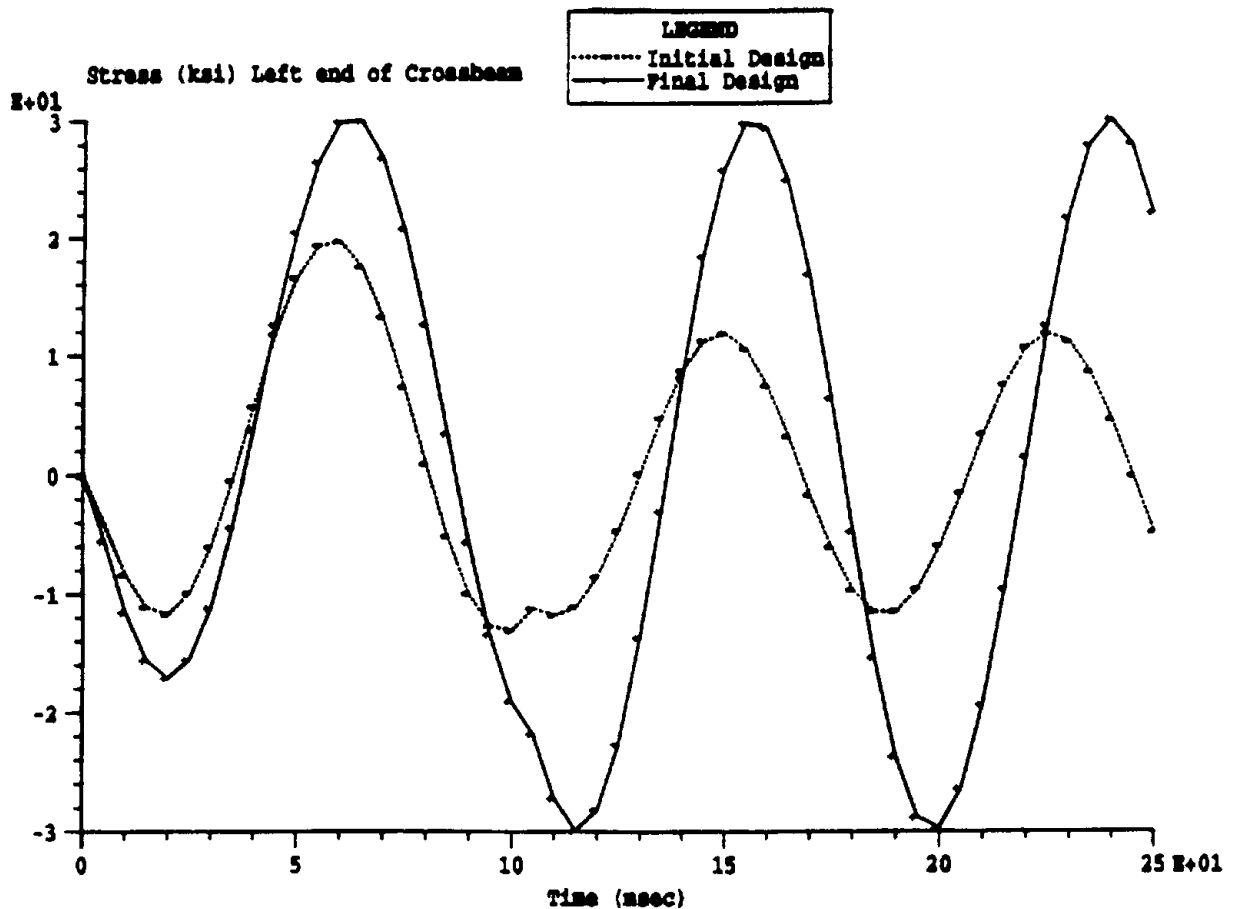
**Figure 5-9 Transient Stress Response for the Initial and Final Designs
of the Portal Frame**

Figure 5-9 shows the transient stress response of the end of the horizontal beam for the initial and final designs. It can be observed that the stresses for the initial design are well below the 30 ksi limits, while the response is right at this limit for the final design. Since there is no damping in the structural representation, the structure would continue to sway if a longer record were obtained, but the imposed limits should not be exceeded.

Table 5-4 compares the results from this analysis with those given in **Reference 9** in "**Selected Bibliography**" on page 299. Note that the MSC.Nastran results are somewhat higher than those given in the reference, which can be attributed to differences in the finite elements used in the two analyses.

Table 5-4 Comparison of Results for the Portal Frame

PARAM	MSC.Nastran	Reference
X1 (columns)	578.6 in^4	498.0 in^4
X2 (crossbeam)	301.7 in^4	330.0 in^4
Objective	1534. lbs	1463. lbs

Although the examples shown here are elementary, it should be apparent that the capabilities they demonstrate are quite powerful. MSC.Nastran's capabilities for dynamic response optimization can be coupled with design tasks that have requirements for static response, natural frequency, and buckling and aeroelastic responses. Note, too, that the models can include superelements. Furthermore, although all the examples here have properties for the design variables, the capability also interacts with MSC.Nastran's shape optimization capability.

One additional area in which dynamic response optimization can be applied is the system identification of structures to match modal test results. A modal test can be considered a forced excitation. Therefore, the capability described here could be used modify structural parameters in an MSC.Nastran analysis so that the responses obtained from an MSC.Nastran frequency analysis could match test results.

Data Recovery

- ■ Overview

- ■ Data Recovery for Modal Methods

- ■ Improving the Results

- ■ Shock and Response Spectrum Analysis

- ■ Random Analysis with Coupled Excitations

6.1   Overview

In dynamic analysis, the size of the calculated output data could become several orders of magnitude larger than the size of output for the equivalent statics analysis job. For instance, a typical transient run could produce thousands of solution vectors. If caution is not taken, the cost of processing the outputs for printing or plotting could exceed that of the entire solution process. Given these concerns, the dynamics engineer should use the SET logic in the Case Control Section of the MSC.Nastran input file to reduce the number of outputs. Wherever possible, he should also use a graphical postprocessor to visualize the results.

The choice of modal methods versus the direct method for dynamic solutions is discussed in the *MSC.Nastran Basic Dynamic Analysis User's Guide.* Each method uses a different technique to recover output answers. This chapter extends this discussion by describing several options available in the modal method to improve accuracy while reducing computation costs.

This chapter describes two methods for calculating physical results from a solution using modal degrees-of-freedom. The default method is the so-called matrix method, which is the most effective technique for the majority of dynamics problems. The alternative method uses the static approach to calculate results one vector at a time.

The mode acceleration method, also detailed in this chapter, is useful in some cases where accurate stress results are required for only a few peak time steps or frequencies. However, this option may be more expensive if many solution vectors exist.

In addition to the standard displacement, stress, and force outputs, dynamics engineers frequently use other types of output that combine the effects of random or spectral inputs. Shock and response spectral analysis provides a quick calculation of the probable peak values in a modal solution for base accelerations. Random analysis is a more formal method of determining power spectral densities, RMS averages, and other data for a structure in a random load environment. This chapter devotes a section to each of these topics.

6.2   Data Recovery for Modal Methods

Modal methods of analysis have the advantages of reducing the problem size, decoupling the equations, and providing an intuitive feeling for the results. However, they require additional calculation steps and may also result in a loss in accuracy. There are four different methods for calculating the detailed results in the data recovery stage of analysis using modal coordinates. Each of these options provide a unique tradeoff of efficiency vs. accuracy for a given size of problem, number of solutions, and number of output requests. Described below are the normal mode displacement method, the matrix method, the mode acceleration method, and the use of superelements for improved modal results.

Mode Displacement, Vector Method

This method is almost identical to the statics method of data recovery in MSC.Nastran. It is efficient when only a few time steps or frequencies are present in the solution and many outputs are requested (such as for contour plotting). Starting with the modal displacements, ξ, and the eigenvectors, $[\phi]$, we obtain a set of displacement vectors that are expanded as with statics or normal mode analysis. The steps are summarized below.

Analysis Set
$$\{u_a\} \;=\; [\phi_a]\{\xi\}$$
Eq. 6-1

Free Set
$$\{u_f\} \;=\; \begin{bmatrix} G_0 \\ I \end{bmatrix}\{u_a\}$$
Eq. 6-2

SPC Forces
$$\{Q_s\} \;=\; [K_{sf}]\{u_f\} - \{P_s\}$$
Eq. 6-3

Independents
$$\{u_n\} \;=\; \begin{Bmatrix} u_f \\ 0 \end{Bmatrix}$$
Eq. 6-4

Grid Set
$$\{u_g\} \;=\; \begin{bmatrix} G_m \\ I \end{bmatrix}\{u_n\}$$
Eq. 6-5

In the actual calculations, each vector at a particular frequency or time step becomes a column of the solution matrix $[u_g]$. Note that for all modal methods, no provisions are made for thermal loads or enforced displacements (which are only calculated in statics analysis.)

The element stresses and forces are calculated directly from the displacement vectors, one element and one vector at a time. Note that if a large number of solutions exist (for instance 10000 time steps), the size of the matrices defined above may be quite large and the calculation speed will be very slow.

Matrix Method for Modal Response

This method is very efficient when the number of solutions is much larger than the number of modes and when a limited number of output requests is made. The matrix method for modal response is the default for the modern modal solutions. In this method, the same operations as described above are performed on the eigenvectors and the results are saved. A matrix is calculated for every output request using the eigenvector matrix instead of a solution vector. The intermediate matrices are calculated from the output data recovery of the modal solution. These are summarized below.

Displacements
$$[u_g^m] = [\phi_g]$$
Eq. 6-6

SPC Forces
$$[Q_s^m] = [K_{sf}][\phi_f]$$
Eq. 6-7

Stresses
$$[S^m] = [\sigma(\phi)]$$
Eq. 6-8

Forces
$$[F^m] = [f(\phi)]$$
Eq. 6-9

Note that the number of rows of these matrices will correspond only to the requested output sets (DISP =, STRESS =, etc.). The number of columns is equal to the number of modes (which is usually smaller than the number of time steps of frequencies). For the final output printing or xy-plotting, the equations for calculating the transient solution outputs are as follows:

Displacements
$$[u_g^o(t)] = [u_g^m][\xi(t)]$$
Eq. 6-10

Forces of SPC
$$[Q_s(t)] = [Q_s^m][\xi(t)]$$
Eq. 6-11

Similar equations are used for SPC forces, stresses, and element forces, as well as for frequency response, by simply combining the modal responses with the modal factors as indicated above.

6.3 Improving the Results

Mode Acceleration Method

The mode acceleration method of data recovery is used to reduce the modal truncation errors that occur in the methods above. For good accuracy, a general recommendation is to use many more modes than in the frequency range of the excitation loads. For most applications this is adequate and the mode displacement method produces acceptable results. However, some cases that may not produce accurate results are the following:

1. Errors may occur in the deformations and stresses in the area of a concentrated load on a free point.

2. Concentrated damper elements or direct input matrices may change the characteristic response displacements to be much different from simple modal combinations.

3. Models with complex shapes may require an excessive number of modes to represent the stress distributions. Accuracy of the modes becomes an issue when more than a few hundred are necessary.

4. Massless points with external loads will have deformations and internal loads that cannot be represented by finite frequency modes.

Using the direct method may eliminate these errors but may excessively increase the run costs and file storage. The mode acceleration method is a useful compromise that eliminates the errors described above yet is cheaper to run than the direct method. However, it will cost more than the matrix method if a large number of solution vectors are to be processed. The derivation is given below.

For convenience, we will show the equations for a frequency response solution. However, the results are similar with a transient analysis. The ideal solution desired is that for the direct matrix solution at frequency ω, which is

$$[-\omega^2 M + j\omega B + K]\{u(\omega)\} = \{P(\omega)\} \qquad\text{Eq. 6-12}$$

where j is the imaginary unit value.

We may obtain an exact solution if we use all of the modes in the system; namely, if N is the order of the problem, then:

$$\{u\} = \sum_{i=1}^{N} \{\phi_i\}\xi_i \qquad\text{Eq. 6-13}$$

Note that this set of modes also includes modes with infinite frequencies. These are present with singular mass matrices. The modal identities are

$$\omega_i^2[M]\{\phi_i\} = [K]\{\phi_i\} \qquad\text{Eq. 6-14}$$

and for constant structural damping parameters, g and ω_3

$$[B]\{\phi_i\} = \left(\frac{g}{\omega_3}\right)[K]\{\phi_i\} \qquad \text{Eq. 6-15}$$

Eigenvalue of Modal and Direct Solutions. Substituting **Eq. 6-13**, **Eq. 6-14**, and **Eq. 6-15** into the terms defined in **Eq. 6-12**, we obtain the effect of each mode on the exact solution. These terms are

$$-\omega^2[M]\{u\} = \sum_{i=1}^{N} \left(\frac{\omega}{\omega_i}\right)^2 [K]\{\phi_i\}\xi_i \qquad \text{Eq. 6-16}$$

$$j\omega[B]\{u\} = \sum_{i=1}^{N} \left(\frac{jg\omega}{\omega_3}\right)[K]\{\phi_i\}\xi_i \qquad \text{Eq. 6-17}$$

and

$$[K]\{u\} = \sum_{i=1}^{N} [K]\{\phi_i\}\xi_i \qquad \text{Eq. 6-18}$$

If all modes were included, we know that the results would be identical to a direct solution. For the high frequency modes ($\omega_i > \omega_m$), it is apparent that their contribution will be much smaller for mass and damping effects than from their effect on the static solution of **Eq. 6-18**. Therefore, if we truncate the modes such that the primary error will be due to the forces generated by the missing modes in **Eq. 6-18**. In the frequency domain the approximations to **Eq. 6-16** through **Eq. 6-18** become

$$-\omega^2[M]\{u\} \approx -\sum_{i=1}^{M} \omega^2[M]\{\phi_i\}\xi_i \qquad \text{Eq. 6-19}$$

$$j\omega[B]\{u\} \approx \sum_{i=1}^{M} j\omega[B]\{\phi_i\}\xi_i \qquad \text{Eq. 6-20}$$

$$[K]\{u\} = \sum_{i=1}^{M} [K]\{\phi_i\}\xi_i + [K]\{\Delta u\} \qquad \text{Eq. 6-21}$$

The error can be expressed as a residual displacement vector $\{\Delta u(\omega)\}$.

Substituting **Eq. 6-19** and **Eq. 6-20** into **Eq. 6-15**, we obtain a corrected solution:

$$[K]\{u(\omega)\} = \{P(\omega)\} - \{R(\omega)\} \qquad \text{Eq. 6-22}$$

where:

$$\{R(\omega)\} = j\omega\sum_{i=1}^{M} \{\phi_i\}\xi_i - \omega^2\sum_{i=1}^{M} \{\phi_i\}\xi_i$$

An alternate method would be to solve the static part of **Eq. 6-15** using **Eq. 6-21**. Since the residual vector is orthogonal to the retained modes, then:

$$[\phi]^T[K]\{\Delta u\} \; = \; \{0\}$$

<div align="right">Eq. 6-23</div>

We can assume that $\{\Delta u\}$ contains static response, if $[K]$ is nonsingular, plus modal response in the form:

$$\{\Delta u\} \; = \; -[K]^{-1}\{P\} + [\phi]\{x\}$$

<div align="right">Eq. 6-24</div>

Premultiplying **Eq. 6-24** by $[Q^T K]$ and using **Eq. 6-23**, we obtain

$$x_i \; = \; -(m_i \omega_i^2)^{-1}[\phi_i]^T\{P\}$$

<div align="right">Eq. 6-25</div>

and, then from **Eq. 6-24** and **Eq. 6-25**, we obtain a decoupled residual solution

$$\{\Delta u(\omega)\} \; = \; [\Delta Z]\{P(\omega)\}$$

<div align="right">Eq. 6-26</div>

where:

$$[\Delta Z] \; = \; [K]^{-1} - [\phi]\begin{bmatrix} \cdot & & \\ & (m_i \omega_i^2) & \\ & & \cdot \end{bmatrix}[\phi]^T$$

The matrix, $[\Delta Z]$, is known as the residual flexibility matrix and has also been used for modal synthesis modeling. Here it could be used as a data recovery step.

In the MSC.Nastran design, **Eq. 6-22** has been chosen over **Eq. 6-26** for the calculation of the improved solution of large problems because the $[\Delta Z]$ matrix could be very dense and the singular free body case was easier to process.

Note that in the actual mode acceleration process other nonstructural effects, such as direct input matrices or transfer functions, are not included in the matrix, $[K]$, but are treated as terms on the right-hand side and added to $\{P\}$. For free bodies, the right hand loads are converted to equilibrium loads to permit a decomposition of the singular stiffness matrix, identically to the inertia relief solution. In fact, the entire process may be viewed as if all the dynamic modal solutions were converted into equivalent static loads, and linear static solutions were generated using the symmetric structural stiffness matrix.

Using Superelements for Data Recovery

If a structure has only a few points with dynamic loads or enforced boundary motion, a simple superelement (SE) operation will have an improvement in accuracy similar to the mode acceleration method. In transient analysis, the cost will be increased because the uncoupled modal solution step is changed to coupled solution with a few extra degrees-of-freedom. In frequency response analysis, the extra cost is very small. The basic procedure is as follows:

1. Subdivide the structure into two superelements corresponding to the external loads.

2. The residual (SE = 0) contains only the loaded structural points and scalar points for the modal coordinates.

3. The upstream (SE = N) contains all of the remaining points and all of the elements. It will also contain the residual SE points as boundary points.

4. Place a modal synthesis request for the upstream SE with a METHOD = request in the corresponding Case Control subcase.

5. By default, the mode shapes will be fixed at the residual points. Free boundary degrees-of-freedom may be specified on SECSET data.

6. The residual SE solution will contain both modal and grid point degrees-of-freedom. If the resulting size is small, a direct solution for the forced response is recommended.

7. The upstream solution will contain both modal response and static residuals (described above) due to motion of the residual grid points. Stresses and forces will be improved, especially on the interface elements.

In this method the static correction terms are assumed to be shapes corresponding to loads on the boundary points. The upstream displacements, $\{u_o\}$, are calculated from the equation

$$\{u_o\} = [G_{oa}]\{u_a\} + [[\phi_o] - [G_{oa}][\phi_a]]\{q\} \qquad \text{Eq. 6-27}$$

where:

$\{u_a\}$ = the residual SE displacements

$[G_{oa}]$ = the Guyan reduction matrix

$[\phi_o]$ = the u_o partition of the eigenvectors

$[\phi_a]$ = the u_a partition of the eigenvectors

$\{q\}$ = the modal degrees-of-freedom

The residual SE will obtain a dynamic solution for both u_a and $\{q\}$.

6.4　　Shock and Response Spectrum Analysis

Shock spectra analysis and response spectrum analysis are methods used by many engineers to estimate the maximum dynamic response of a structure. Most applications involve complicated time-dependent loads or accelerations that excite the base of a structure, such as an earthquake ground motion on a building or an explosive shock on a small component in a ship. (Note that the only difference between shock and response spectra is whether output displacements are measured in a fixed frame of reference or relative to the base motion.)

The advantage of these methods over a conventional transient analysis is economy and simplicity. The only major calculation step is obtaining a sufficient number of normal modes to represent the entire frequency range of the input excitation and resulting response. The disadvantage of the method is that the accuracy may be questionable and the requirement of special input data in the MSC.Nastran solution sequences. In many cases, a direct transient analysis with the actual excitation load will be more accurate, easier to use, and faster.

The procedure involves two stages. First the applied loads or base excitations are converted in a direct transient solution (SOL 109) into a spectrum table consisting of peak response magnitudes for a set of single degree-of-freedom oscillators. Each oscillator is a scalar spring/mass/damper having a different natural frequency and damping ratio. This stage is optional since the shock spectrum data is frequently given in the contractual design specifications or, in the case of earthquakes, is available through governmental agencies.

The second stage of the analysis consists of a modal analysis of the structure, data recovery, and the response calculation that combines the modal properties of the analysis model with the spectrum data of the applied loads. This stage is performed in a modal analysis solution sequence (SOL 103). If a database was saved from the first stage, a restart will provide the spectrum data automatically. Otherwise, the spectrum data must be supplied in a direct tabular input (response versus natural frequency for several damping ratios).

Theoretical Background

Starting with a modal transient analysis, the general approximation for a response quantity, u_k , is

$$u_k(t) \; = \; \sum_i \phi_{ik} \xi_i(t)$$

<div align="right">Eq. 6-28</div>

where ϕ and ξ are the modal outputs and generalized displacements. The actual modal equations are

$$\ddot{\xi}_i + g_i \omega_i \dot{\xi}_i + \omega_i^2 \xi_i \; = \; \lfloor \phi_i \rfloor^T \{P(t)\}$$

<div align="right">Eq. 6-29</div>

where P is the vector of loading functions. For loading due to base accelerations, the equivalent inertial loads are

$$\{P(t)\} \; = \; -[M_{aa}][D_{ar}]\{\ddot{u}_r(t)\}$$

<div align="right">Eq. 6-30</div>

where the columns of $[D_{ar}]$ represent vectors of rigid body motions of the whole structure and the accelerations correspond to the base motions. Substituting **Eq. 6-30** into **Eq. 6-29** and combining terms we can separate the modal quantities from the transient solutions. First we will develop the transient response functions. We begin by calculating the responses

$$\ddot{x}_r + g\omega\dot{x}_r + \omega^2 x_r = \ddot{u}_r(t) \qquad \text{Eq. 6-31}$$

where x_r is a response function in direction r, and is a function of the variables ω, g, and t. The peak values of x_r, obtained over a range of frequencies and damping factors is called the response spectrum for the excitation, $\ddot{u}_r$.

Next, from the normal mode analysis, we define the participation factors ψ_{ir}, for mode i and direction r, as

$$\psi_{ir} = -\lfloor \phi_i \rfloor^T [M_{aa}]\{D_{ar}\} \qquad \text{Eq. 6-32}$$

Then, from **Eq. 6-28**, the actual transient response at a physical point is

$$u_k(t) = \sum_i \sum_r \phi_{ik} \psi_{ir} x_r(\omega_i, g_i, t) \qquad \text{Eq. 6-33}$$

The peak magnitudes of u_k in **Eq. 6-33** are usually dominated by the peak values of $x(t)$ occurring at the natural frequencies. In spectrum analysis the peak values of u_k are approximated by combining functions of the peak values, $x_{ri}(\omega_i, g_i) = \max|x_{ri}(\omega_i, g_i, t)|$, in the approximation

$$\bar{u}_k(t) \cong \sum_i \sum_r |\phi_{ik}| |\psi_{ir} \bar{x}_{ri}(\omega_i, g_i)| \qquad \text{Eq. 6-34}$$

ABS Option. **Eq. 6-33** and **Eq. 6-34** define the ABS (Absolute Value) option. This method assumes the worst case scenario in which all of the modal peak values for every point on the structure are assumed to occur at the same time and in the same phase. Clearly in the case of a sudden impact, this is not very probable because only a few cycles of each mode will occur. However, in the case of a long term vibration, such as an earthquake when the peaks occur many times and the phase differences are arbitrary, this method is acceptable.

A second way of viewing the problem is to assume that the modal magnitudes and phases will combine in a probabalistic fashion. If the input loads are behaving randomly, the probable (RMS) peak values are

$$\bar{u}_k \cong \sqrt{\sum_i (\phi_{ik} \bar{\xi}_i)^2} \qquad \text{Eq. 6-35}$$

where the average peak modal magnitude, ξ_i is

$$\bar{\xi}_i = \sqrt{\sum_r \left(\psi_{ir} \bar{x}_r(\omega_i, g_{i_i})\right)^2} \qquad \text{Eq. 6-36}$$

SRSS Method. This approach is known as the SRSS (square root of sum-squared) method. Note that the results in each direction are summed in vector fashion for each mode first, followed by an SRSS calculation for all modes at each selected output quantity u_k. It is assumed that the modal responses are uncorrelated and the peak value for each mode will occur at a different time. These results are optimistic and represent a lower bound on the dynamic peak values.

The SRSS method may underestimate the actual peaks since the result is actually a probable peak value for the period of time used in the spectrum analysis. The method is normally augmented with a safety factor of 1.5 to 2.0 on the critical outputs.

NRL Method. As a compromise between the two methods above, the NRL (Naval Research Laboratories) method was developed. Here, the peak response is calculated from the equation

$$\bar{u}_k \cong \left| \phi_{jk} \bar{\xi}_j \right| + \sqrt{\sum_{i \neq j} (\phi_{ik} \bar{\xi}_i)^2} \qquad \text{Eq. 6-37}$$

where the j-th mode is the mode that produces the largest magnitude in the product $\phi_{jk} \bar{\xi}_j$. The peak modal magnitudes, $\left| \phi_{jk} \bar{\xi}_j \right|$, are calculated with **Eq. 6-36**.

The rationale for the method is that the peak response will be dominated by one mode and the SRSS average for the remaining modes could be added directly. The results will fall somewhere between the ABS and SRSS methods.

Modes that are close in frequency may have their peak response occur at about the same time (and with the same phase). For this reason, the SRSS and NRL methods contain a provision to sum modal responses via the ABS method for modes that have closely spaced natural frequencies. Close natural frequencies are defined by frequencies that meet the following inequality:

$$f_{i+1} < \text{CLOSE} \cdot f_i$$

The value for CLOSE is set by PARAM,CLOSE (the default is 1.0).

The modal summation option is set via PARAM,OPTION (the ABS method is the default). Both PARAM,OPTION and PARAM,CLOSE may be set in any subcase, allowing summation by several conventions in a single run.

Generating Response Spectra Curves

A response spectrum is generated as follows:

1. Assume that there is a series of small, single degree-of-freedom (SDOF) oscillators each attached to the same location at the connection to the base structure. (In the examples in the introduction to this section, the base structures are the building and the spacecraft). These oscillators each have a different resonant frequency, and all have the same modal damping ratio (2%, for example).

2. Apply a transient excitation to the base structure. Use the base structure's damping when computing the base structure's transient response at the location of the SDOF oscillators.

3. Use the base structure transient response as input to each SDOF oscillator. Compute the magnitude of peak response of each SDOF oscillator, and plot the peak response versus oscillator resonant frequency.

4. Change the modal damping ratio for the oscillators (to 5%, for example) and repeat Steps 2 and 3 for the range of expected damping.

The response spectrum, therefore, depicts the maximum response magnitude of an SDOF system as a function of resonant frequency and damping. **Figure 6-1** depicts the generation of a spectrum.
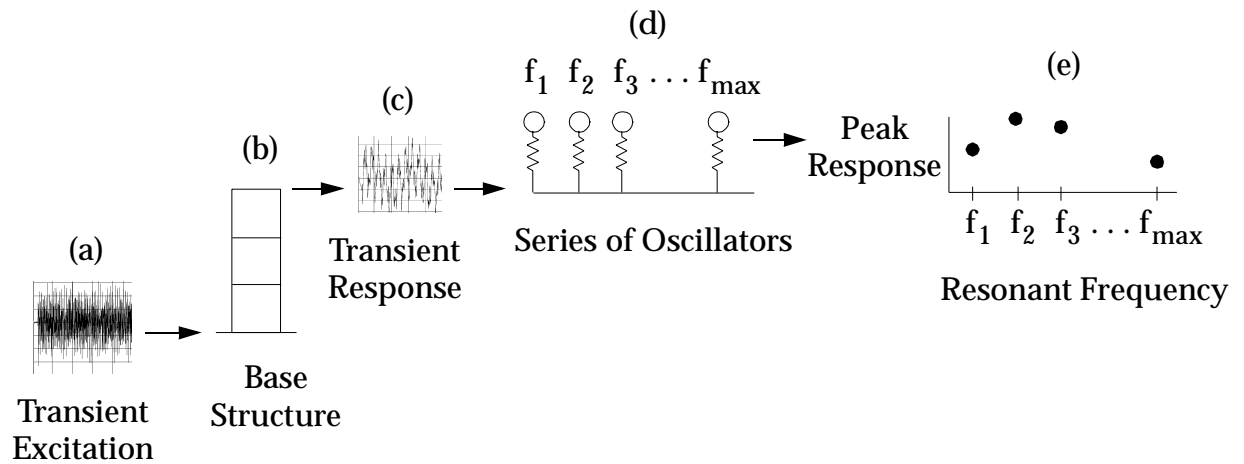
Transient excitation (a) is applied to a base structure (b), from which transient response (c) is computed for each floor. This response is applied to a series of oscillators (d), for which the peak response is plotted (e). Steps (d) and (e) are repeated for different damping values to form response spectra as shown below.
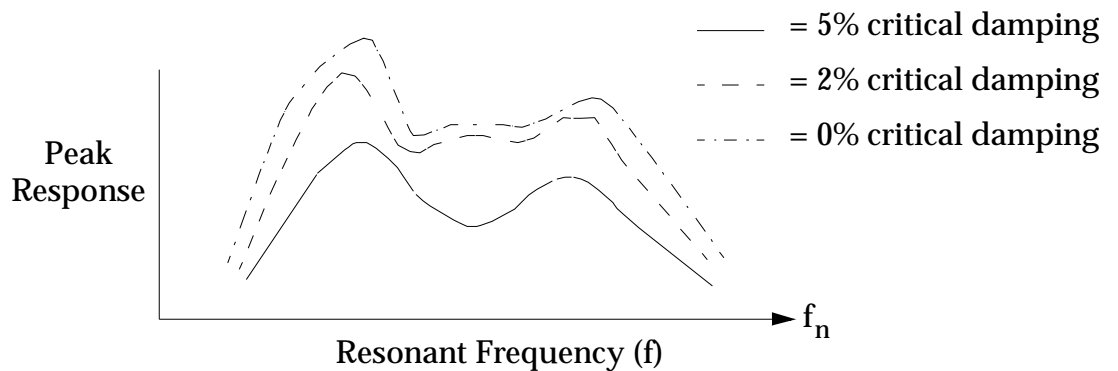
Figure 6-1 Response Spectrum Generation

Note that the peak response for one oscillator does not necessarily occur at the same time as the peak response for another oscillator. Note, too, that there is no phase information since only the magnitude of peak response is computed.

Several values of peak response are computed for the oscillators. These include the following response variable.

Relative velocity and absolute acceleration are approximately related to the relative displacement by

$$\dot{X}_r \approx \omega X_r$$

$$\ddot{X} \approx \omega^2 X_r$$

Eq. 6-38

Design spectra are most often defined in terms of x_r, $\dot{x}_r$, and $\ddot{x}$.

Note that for very low oscillator frequencies ($\omega \rightarrow 0$),

$$X \rightarrow 0$$

$$X_r \rightarrow U_b$$

Eq. 6-39

where U_b is the motion of the base of the oscillator.

Similarly, for very high oscillator frequencies ($\omega \rightarrow \infty$),

$$X \rightarrow U_b$$

$$X_r \rightarrow 0$$

Eq. 6-40

The approximate relationships between x_r, $\ddot{x}_r$, and $\ddot{x}$, shown in **Eq. 6-38**, are not valid at very low or very high oscillator frequencies or for large values of damping.

It is assumed in this process that the mass of each oscillator is very small relative to the base structure, so the oscillator's response does not influence the response of the base structure.

Dynamic Response Predictions. Once a spectrum is computed, it can be used for the dynamic response analysis of an MSC.Nastran model of the component. For example, the spectrum generated for a floor in a building that is subjected to an earthquake can then be applied to a complex model of a piece of equipment attached to that floor. The peak response of each mode of the equipment model is obtained from the spectrum, and these peak responses are combined to create the overall response.

Because response spectrum generation involves transient response, similar modeling and analysis considerations apply. In addition, the time step (field 4 on the TSTEP Bulk Data entry, DT) should not be changed during the run, because MSC.Nastran uses only the initial DT specification for the entire response spectrum generation run and therefore wrong answers could occur.

The time step, DT, and time duration, DT · N (where N is the number of time increments), must take into account the loading, the base structure, and the frequency range of the spectra generation. The time step must take into account the frequency content of the applied excitation, the frequencies of the base structure, and the highest frequency for which spectra are to be generated. There must be enough time steps per cycle of response for both the base structure and the highest frequency oscillator in order to accurately predict the peak response; 5 to 10 steps per cycle represents a typical value. In addition, the time duration of the loading, the frequencies of the base structure, and the lowest oscillator frequency must be considered when defining the time duration. There must be

a long enough time duration of response both for the base structure and the lowest frequency oscillator in order to accurately predict the peak response. For short duration loadings, the peak response often occurs well after the the load has peaked.

Initial conditions (specified via the TIC Bulk Data entry) are not used in response spectrum generation. Initial conditions are used in the calculation of the transient response of the base structure, but the calculation of the peak oscillator responses (i.e., the response spectrum calculation) ignores any initial conditions.

User Interface for Response Spectra Generation

Response spectra are generated in the transient response solution sequences (SOL 109 for direct and SOL 112 for modal). Transient response input is required to apply the transient excitation to the base structure. Additional input required to generate response spectra are described in **Table 6-1** and **Table 6-2**.

Table 6-1 Case Control Input for Response Spectrum Generation

Case Control Command	Description
XYPLOT SPECTRAL	Compute spectra.
XYPUNCH SPECTRAL	Punch spectra for subsequent use.

The XYPLOT and XYPUNCH commands are included in the OUTPUT(XYPLOT) section. Further details about the OUTPUT(XYPLOT) section are described in "**Structure Plotting**" on page 245 of the *MSC.Nastran Basic Dynamic Analysis User's Guide*.

Examples of these commands include:

```
$  Plot absolute acceleration spectra for grid point 85, T3 component
XYPLOT     ACCE     SPECTRAL     1     /85(T3RM)

$  Punch relative displacement spectra for grid point 3, T1 component
XYPUNCH    DISP     SPECTRAL     1     /3(T1IP)
```

Relative and absolute spectra are denoted by IP and RM, respectively, in the parentheses of the curve request.

Table 6-2 Bulk Data Input for Response Spectrum Generation

Bulk Data Entry	Description
PARAM,RSPECTRA,0	Requests calculation of spectra.
DTI, SPSEL, 0	Header for DTI.
DTI, SPSEL, 1	Selects oscillator frequencies, oscillator damping values, and grid points at which spectra will be computed.
FREQi	Specifies oscillator damping values.
FREQi	Specifies oscillator frequencies.

There are two FREQi entries: one to specify oscillator frequencies (i.e., frequencies for which spectra will be computed) and the other to specify oscillator damping. (Note that damping for the base structure is specified in another manner, such as with the TABDMP1 entry used for modal transient response analysis.)

Peak Response Calculation

Response spectra are applied to a structure for subsequent analysis. Note that the structure in this case is not the base structure for which the spectra were computed but, rather, a smaller structure such as a piece of equipment.

Response spectrum analysis approximates the peak structural response (typically stresses and displacements, though not limited to those quantities). Approximations are made by assuming:

1. Only the peak response is computed for the oscillators (see the preceding section).

2. There is no phase information or sign computed; only the magnitude of peak response is computed.

3. The oscillator mass is small relative to the base structure's mass.

4. The displacements, velocities, and accelerations are related by the approximate relationships in Eq. 6-38.

5. The peak modal responses are combined to form the overall response via various combination methods (see below).

The spectra themselves are often approximate. For example, design spectra have been developed for seismic analysis, and these have conservatisms built into them by the fact that safety factors are incorporated by either increasing the spectra values and/or by decreasing the damping values.

These approximations make response spectrum analysis a tool that is useful for design and efficiency. The effects of these approximations are further described in the remainder of this section.

Modeling and Analysis Considerations

Response spectrum application is a postprocessing function of normal modes analysis. It is run in the normal modes solution sequences, so the modeling and analysis considerations that apply for normal modes analysis also apply for response spectrum application. The additional considerations also need to be followed:

1. The structure is run as an unrestrained model in the direction(s) of the load spectrum application.

2. A large mass, on the order of 10^3 to 10^6 times the mass of the structure, must be used at the structure's base grid points where the input occurs. One way to do this is to use RBEs or MPCs to connect the base points to a separate grid point, and apply the large mass to that separate grid point. This separate grid point is where the spectrum is applied.

3. A SUPORT Bulk Data entry is required at the spectrum input location. See "**Free Body Techniques**" on page 190 for an explanation.

4. The modes must be mass normalized (which is the default).

The spectra that MSC.Nastran can apply are absolute acceleration, relative displacement, and relative velocity spectra. You specify A, D, or V for acceleration displacement or velocity, respectively, to specify the spectrum type.

Use all modes within the frequency range specified by the spectrum, but do not use modes outside of the spectrum range. Usually, spectra to apply are considered to have zero values outside of their range of definition; for example, an absolute acceleration spectrum defined from 0 to 30 Hz is assumed to be zero beyond 30 Hz. However, MSC.Nastran extrapolates spectral values for modes beyond the spectral range, which may lead to unexpected answers. You can limit the number of modes used in the spectrum application by limiting the number of computed modes (via the EIGRL or EIGR entry) or by using PARAM,HFREQ,r (where r is the highest frequency mode to use) or PARAM,LMODES,n (where n is the number of lowest modes to use).

Consider the entire response spectrum process—generation and application—as a two-step process. Step 1 is generation of the response spectra and Step 2 is the application of the response spectra. For a given input, transient applied to the base structure (Step 1), the same stresses occur (Step 2) regardless of whether acceleration or displacement spectra were computed in Step 1. However, displacements and accelerations are different, because answers computed by using the absolute acceleration spectrum contain the rigid body contribution, whereas answers computed by using the relative displacement spectrum do not contain the rigid body contribution. Displacement and acceleration responses can be made equal regardless of which spectra was used by using PARAM,LFREQ,0.01 (or some other small number) to remove the rigid body mode contribution from the answers.

Stresses and other element quantities are unaffected by the contribution of any rigid body modes. The same situation applies to relative velocity spectra as to relative displacement spectra. However, because the relationships in **Eq. 6-38** are approximate, all answers (including stresses) will be slightly different depending on whether displacement, velocity, or acceleration spectra were used.

User Interface for Spectrum Application

Response spectrum application is done in the normal modes solution sequences (SOL 103, for example). In addition to the input for computing normal modes, input is required for applying the spectra, as shown in **Table 6-3**.

Table 6-3 Input for Response Spectrum Application

Case Control Command	Description
METHOD	Selects eigenvalue extraction method.
SDAMP	Selects the TABDMP1 Bulk Data entry.
DLOAD	Selects the DLOAD Bulk Data entry.
Bulk Data Entry	**Description**
PARAM,SCRSPEC,0	Requests response spectrum application.
EIGR or EIGRL	Eigenvalue extraction method.
TABDMP1	Specifies damping for the structure.
DLOAD	Defines spectrum multipliers.
DTI,SPECSEL,0	Header for DTI.
DTI,SPECSEL,1	Specifies type of spectrum (A, V, or D) and selects damping.
	A = absolute acceleration spectrum. V = relative velocity spectrum. D = relative displacement spectrum.
TABLED1	Specifies input spectrum values.
SUPORT	Specifies input spectrum grid points.
CONM2,CMASS2, etc.	Defines large mass used for the input spectrum.
PARAM,OPTION,a	Specifies modal combination method (a = ABS [default], SRSS, or NRL).
PARAM,CLOSE,r	Specifies closeness parameter for modal combinations (the default is 1.0).

All input listed in the table is required with the exception of PARAM,OPTION and PARAM,CLOSE.

Response Spectrum Examples

This section provides an example of response spectra generation and an example of response spectrum application. The base structure for which response spectra are computed is a model of a five-story, shear-wall building, excited by an earthquake time history. The resulting spectra at a point on the fourth floor are applied to a bracket model

Response Spectrum Generation

Figure 6-2 depicts the five-story building model. The fifteen grid points at the base of the building are tied to a separate grid point (999) via RBE2 entries. Earthquake excitation is applied to this grid point, in the x direction (T1). The absolute acceleration response spectrum is computed for grid point 502. SOL 112, modal transient response, is used to compute the spectrum. Damping of 5% critical is used for the building and damping of 2% critical is used for the generated response spectrum. **Listing 6-1** shows a portion of the input file for this model.
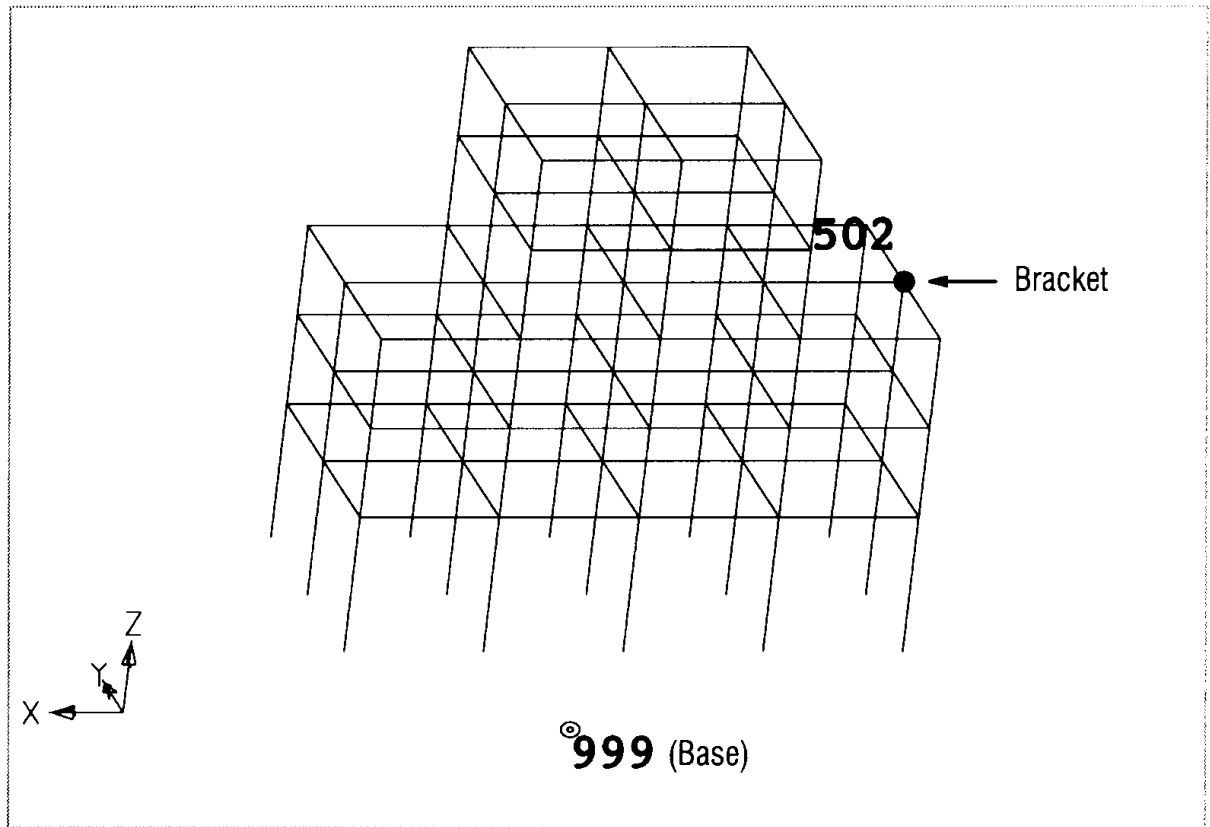
Figure 6-2 Five-Story Building Model

Listing 6-1 Abridged Input File for Response Spectrum Generation

```
$   RESPONSE SPECTRUM GENERATION
$
$   Compute spectrum for absolute acceleration
$    for grid point 502 for 2% oscillator damping
$
ID MSC, DUG
TIME 15
SOL 112    $ MODAL TRANS. RESP.
CEND
$
TITLE = FIVE-STORY BUILDING, SHEAR MODEL
SUBTITLE = RESPONSE SPECTRUM GENERATION, X DIRECTION
$
SET 777 = 999, 101, 201, 301, 401, 502, 602
$
DISPLACEMENT(PLOT) = 777    $ AT LEAST DISP AND VELO MUST BE REQUESTED
VELOCITY(PLOT) = 777        $ FOR SPECTRUM GENERATION POINT
```

```
$
METHOD = 999
DLOAD = 997
TSTEP = 995
SDAMPING = 991  $ DAMPING SPECIFICATION FOR THE BUILDING
$
OUTPUT(XYPLOT)
XGRID = YES
YGRID = YES
$
$   PLOT INPUT
XTITLE = TIME
YTITLE = ACCEL INPUT
XYPLOT ACCE /999(T1)
YTITLE = DISPL INPUT
XYPLOT DISP /999(T1)
$
$   RESPONSE SPECTRA GENERATION
XTITLE = FREQUENCY (HZ)
YTITLE = ABSOLUTE ACCELERATION
$
$   NOTE: IP -- IMAGINARY,PHASE -- IS RELATIVE
$   NOTE: RM -- REAL, MAGNITUDE -- IS ABSOLUTE
$
XYPLOT ACCE SPECTRAL 1 /502(T1RM)
XYPLOT ACCE SPECTRAL 1 /999(T1RM)
XYPUNCH ACCE SPECTRAL 1 /502(T1RM)
$
BEGIN BULK
$
$   REQUESTS CALCULATION OF SPECTRA
PARAM, RSPECTRA, 0
$
$   RESPONSE SPECTRUM GENERATION TABLE
$   DTI, SPSEL, RECNO, DAMPL, FREQL, Gi
$    RECNO = N, SELECTED BY XYPLOT
$    DAMPL = I, FREQi THAT SPECIFIES DAMPING VALUES
$    FREQL = FREQi THAT SPECIFIES FREQ. VALUES
$    Gi = K, L, ..., GRID POINTS FOR SPECTRA GENERATION
DTI, SPSEL, 0
DTI, SPSEL, 1, 885, 887, 101, 201, 301, 401,+DTI1
+DTI1, 502, 602
$
$   SPECIFY OSCILLATOR DAMPING VALUE (2%)
FREQ, 885, 0.02
$
$   SPECIFY FREQUENCIES FOR SPECTRA
FREQ1, 887, 0.01, 0.25, 121
$
$ -----------------------------------------------------
$
$   ... rest of model ...
$
ENDDATA
```

The XYPUNCH ACCE SPECTRAL command in the Case Control Section punches the response spectrum (which will be used later, in the response spectrum application). In the Bulk Data Section, PARAM,RSPECTRA,0 requests calculation of the spectrum. The DTI,SPSEL entry references the FREQ entries; one of the FREQ entries defines the oscillator damping and the other FREQ entry defines the frequency range over which to compute the spectra. The DTI,SPSEL entry also defines grid points at which to compute spectra; spectra are computed for grid points 101, 201, 301, 401, 502, and 602—one per floor—though only the one for grid point 502 is punched for subsequent use.

Note that a 2% damped spectrum was computed because that is the spectrum that will be applied to a component model (see below). In practice, however, spectra are often generated for multiple damping values (for example, 0%, 2%, and 5% damping).

The plotted absolute acceleration response spectra for grid points 999 and 502 are shown in **Figure 6-3**. Note that the response spectrum peaks in the region of about 1.5-7 Hz for grid point 999 and at about 2-3 Hz and again at about 7 Hz for grid point 502. The building has acted as both a filter (note the difference in frequency content) and magnifier (note the difference in spectral amplitudes). Floor response spectra computed closer to the base of the building will show less filtering and magnification.
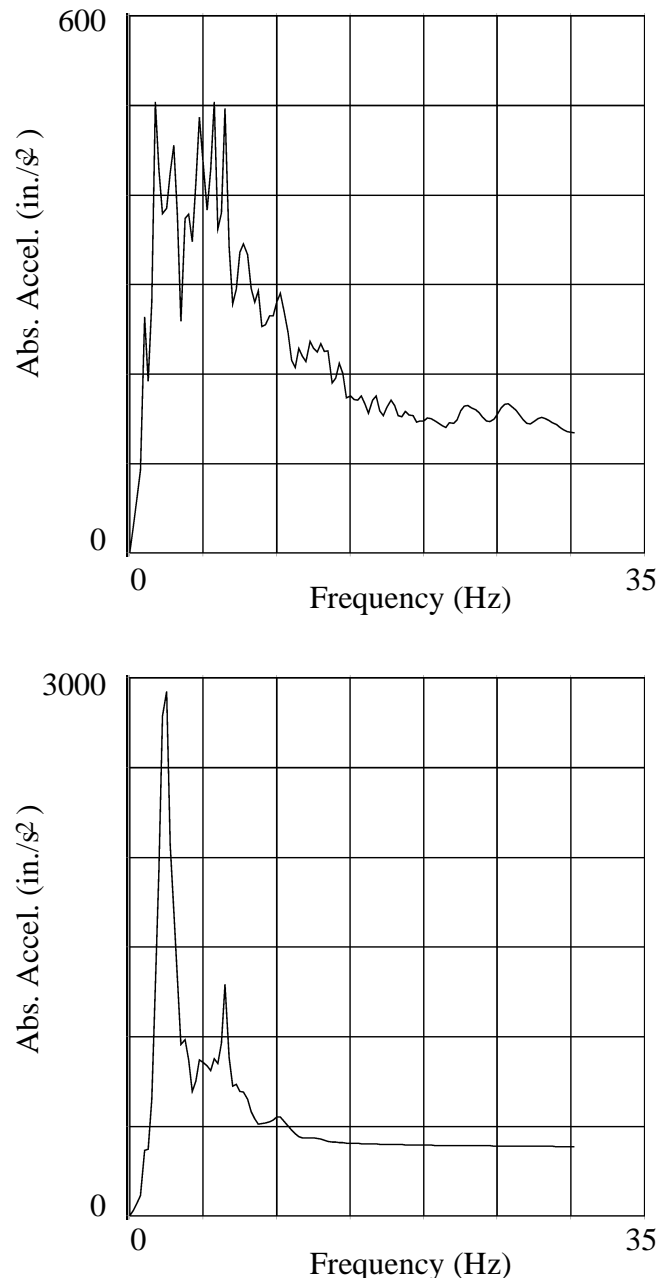
Figure 6-3 Absolute Acceleration Response Spectrum Plots for Grid Points 999 (top) and 502 (bottom)

A portion of the printed output file is shown in **Figure 6-4**. A portion of the absolute acceleration spectrum output for grid point 502 is shown. Spectra for the other grid points

spectra. The printed format for each spectrum is similar to that of frequency response analysis, with the absolute spectrum output in the real location and the relative spectrum output in the imaginary location. Because relative acceleration spectra are not calculated, those components are zero. The punched spectrum for grid point 502 is shown in Figure 6-5; this output is contained in the punch file.

```
    FRACTION OF CRITICAL DAMPING =  .02        ABSOLUTE IN REAL LOCATION,  RELATIVE IN IMAG. LOCATION
    POINT-ID =    502
                                    C O M P L E X   A C C E L E R A T I O N   V E C T O R
                                                  (REAL/IMAGINARY)
FREQUENCY  TYPE          T1               T2          T3            R1            R2            R3
1.000000E-02    G     8.300698E-02    5.819805E-06   0.0           0.0           0.0           0.0
                      0.0             0.0            0.0           0.0           0.0           0.0
2.600000E-01    G     3.203262E+01    2.812203E-04   0.0           0.0           0.0           0.0
                      0.0             0.0            0.0           0.0           0.0           0.0
5.100000E-01    G     7.052912E+01    1.082366E-03   0.0           0.0           0.0           0.0
                      0.0             0.0            0.0           0.0           0.0           0.0
2.951000E+01    G     2.725781E+02    3.764749E-02   0.0           0.0           0.0           0.0
                      0.0             0.0            0.0           0.0           0.0           0.0
2.976000E+01    G     2.703750E+02    3.731322E-02   0.0           0.0           0.0           0.0
                      0.0             0.0            0.0           0.0           0.0           0.0
3.001000E+01    G     2.681875E+02    3.697610E-02   0.0           0.0           0.0           0.0
                      0.0             0.0            0.0           0.0           0.0           0.0
3.026000E+01    G     2.659297E+02    3.663826E-02   0.0           0.0           0.0           0.0
                      0.0             0.0            0.0           0.0           0.0           0.0
```

Figure 6-4 Printed Output (Abridged)

```
$ACCE          3     502        3                                              1
$   2.000000E-02
TABLED1       2
       .01     .083007 .26       32.0326 .51       70.5291 .76       113.748
      1.01     365.142 1.26      371.666 1.51      648.599 1.76      1278.37
      2.01     1927.95 2.26      2781.64 2.51      2914.5  2.76      2063.92
      3.01     1700.21 3.26      1325.52 3.51      950.985 3.76      976.762
      4.01     865.546 4.26      688.777 4.51      743.792 4.76      863.43
      5.01     848.97  5.26      828.419 5.51      804.627 5.76      863.462
      6.01     835.807 6.26      949.985 6.51      1254.88 6.76      862.748
      7.01     707.527 7.26      715.255 7.51      680.692 7.76      679.488
      8.01     631.878 8.26      567.551 8.51      530.414 8.76      496.182
      9.01     499.051 9.26      501.652 9.51      506.18  9.76      514.3
     10.01     533.526 10.26     532.416 10.51     503.248 10.76     482.305
     11.01     459.648 11.26     440.015 11.51     423.567 11.76     414.748
     12.01     414.575 12.26     412.973 12.51     411.023 12.76     408.342
     13.01     403.66  13.26     396.885 13.51     389.822 13.76     386.508
     14.01     384.621 14.26     382.541 14.51     380.549 14.76     378.697
     15.01     376.879 15.26     375.092 15.51     373.363 15.76     371.656
     16.01     369.979 16.26     368.299 16.51     366.666 16.76     365.027
     17.01     363.346 17.26     361.717 17.51     360.109 17.76     358.52
     18.01     356.969 18.26     355.399 18.51     353.801 18.76     352.254
     19.01     350.629 19.26     348.945 19.51     347.336 19.76     345.734
     20.01     344.09  20.26     342.414 20.51     340.668 20.76     338.938
     21.01     337.25  21.26     335.535 21.51     333.848 21.76     332.16
     22.01     330.43  22.26     328.715 22.51     326.973 22.76     325.293
     23.01     323.609 23.26     321.914 23.51     320.195 23.76     318.484
     24.01     316.684 24.26     314.863 24.51     313.035 24.76     311.191
     25.01     309.398 25.26     307.578 25.51     305.594 25.76     303.672
     26.01     301.641 26.26     299.688 26.51     297.633 26.76     295.617
     27.01     293.648 27.26     291.57  27.51     289.516 27.76     287.5
     28.01     285.367 28.26     283.266 28.51     281.219 28.76     279.023
     29.01     276.953 29.26     274.742 29.51     272.578 29.76     270.375
     30.01     268.188 30.26     265.93  ENDT
```

-etc.-

Figure 6-5 Punched Response Spectrum

Response Spectrum Application

Figure 6-6 depicts a bracket model to which the spectrum will be applied. The twelve grid points shown in the figure are connected via an RBE2 element to a separate grid point (888); this grid point has a SUPORT applied in the y direction (T2) and a large mass attached to it. The twelve grid points are constrained in all but the T2 direction. This is the grid point to which the absolute acceleration spectrum generated in the previous run (see above) will be applied, in the y direction. Displacements, accelerations, and stresses are computed. A portion of the input file is shown in **Listing 6-2**.
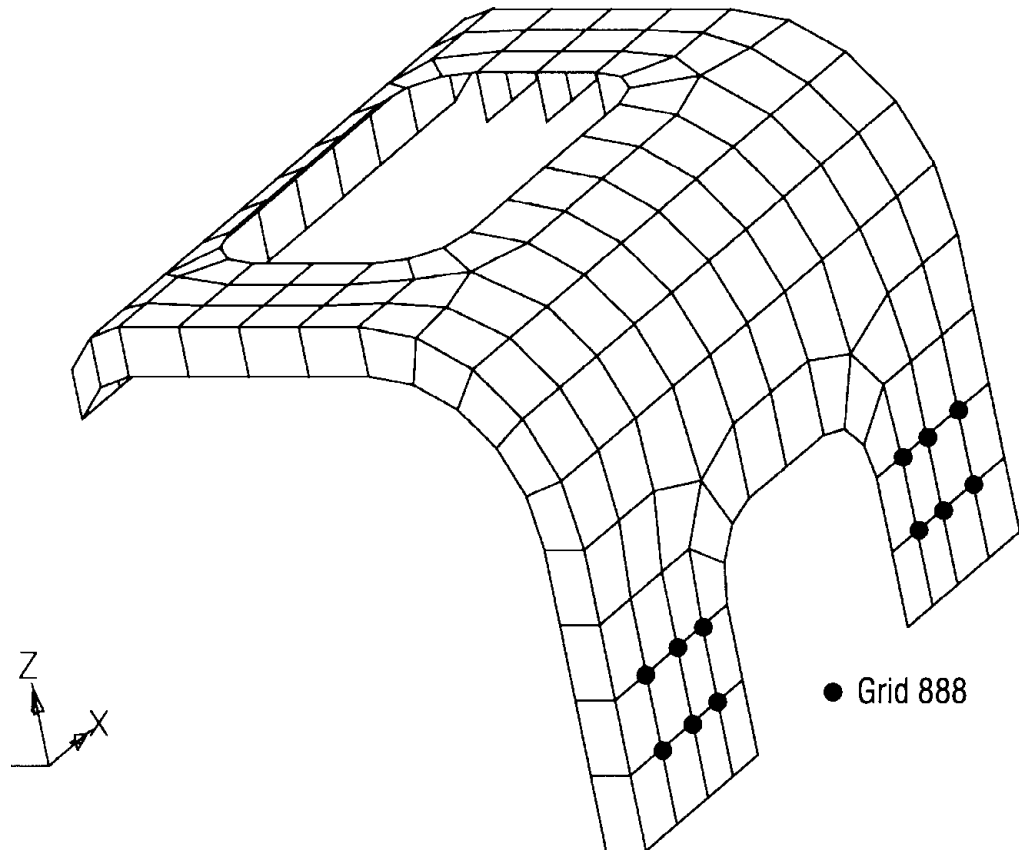
Figure 6-6 Bracket Model

Listing 6-2 Abridged Input File for Response Spectrum Application

```
$ RESPONSE SPECTRUM APPLICATION
TIME 60
SOL 103
CEND
TITLE =  BRACKET MODEL
SUBTITLE = APPLY ABS. ACCEL. SPECTRUM IN Y DIRECTION
SPC   = 1
$
METHOD = 777
SDAMP = 851   $ SELECTS TABDMP1 FOR MODAL DAMPING
DLOAD = 852   $ SELECTS DLOAD ENTRY
$
DISPLACEMENT = ALL
STRESS = ALL
ACCELERATION = ALL
$
$
```

```
PARAM,AUTOSPC,YES
$
$     SID  V1  V2  ND
EIGRL,777,    ,    ,3
$
$  PERFORM SHOCK SPECTRUM ANALYSIS
PARAM,SCRSPEC,0
$
$  2% CRITICAL DAMPING
TABDMP1, 851, CRIT, , , , , , ,+TB1
+TB1, 0.0, 0.02, 50.0, 0.02, ENDT
$
$  SPECIFY SPECTRUM
DLOAD, 852, 1.0, 1.0, 1
$
$  RELATES SPECTRA LINES TO DAMPING
DTI,SPECSEL,0
DTI,SPECSEL,1, ,A, 2, 0.02
$
$  SUPORT POINT FOR SPECTRA
GRID, 888, , 3.0, 0.0, 0.0
CONM2, 888, 888, , 1.0E6
SPC, 1, 888, 13456
SUPORT, 888, 2
RBE2, 888, 888, 2, 14, 15, 22, 23, 133,+RB4
+RB4, 134, 141, 142, 145, 146, 158, 159
$
$  PUNCHED SPECTRUM FROM GENERATION RUN
$ACCE          3     502        3                                               1
$   2.000000E-02
TABLED1        2
        .01     .083007 .26     32.0326 .51     70.5291 .76     113.748
        1.01    365.142 1.26    371.666 1.51    648.599 1.76    1278.37
        2.01    1927.95 2.26    2781.64 2.51    2914.5  2.76    2063.92
        3.01    1700.21 3.26    1325.52 3.51    950.985 3.76    976.762
        4.01    865.546 4.26    688.777 4.51    743.792 4.76    863.43
        5.01    848.97  5.26    828.419 5.51    804.627 5.76    863.462
        6.01    835.807 6.26    949.985 6.51    1254.88 6.76    862.748
        7.01    707.527 7.26    715.255 7.51    680.692 7.76    679.488
        8.01    631.878 8.26    567.551 8.51    530.414 8.76    496.182
        9.01    499.051 9.26    501.652 9.51    506.18  9.76    514.3
        10.01   533.526 10.26   532.416 10.51   503.248 10.76   482.305
        11.01   459.648 11.26   440.015 11.51   423.567 11.76   414.748
        12.01   414.575 12.26   412.973 12.51   411.023 12.76   408.342
        13.01   403.66  13.26   396.885 13.51   389.822 13.76   386.508
        14.01   384.621 14.26   382.541 14.51   380.549 14.76   378.697
        15.01   376.879 15.26   375.092 15.51   373.363 15.76   371.656
        16.01   369.979 16.26   368.299 16.51   366.666 16.76   365.027
        17.01   363.346 17.26   361.717 17.51   360.109 17.76   358.52
        18.01   356.969 18.26   355.399 18.51   353.801 18.76   352.254
        19.01   350.629 19.26   348.945 19.51   347.336 19.76   345.734
        20.01   344.09  20.26   342.414 20.51   340.668 20.76   338.938
        21.01   337.25  21.26   335.535 21.51   333.848 21.76   332.16
        22.01   330.43  22.26   328.715 22.51   326.973 22.76   325.293
        23.01   323.609 23.26   321.914 23.51   320.195 23.76   318.484
        24.01   316.684 24.26   314.863 24.51   313.035 24.76   311.191
        25.01   309.398 25.26   307.578 25.51   305.594 25.76   303.672
        26.01   301.641 26.26   299.688 26.51   297.633 26.76   295.617
        27.01   293.648 27.26   291.57  27.51   289.516 27.76   287.5
        28.01   285.367 28.26   283.266 28.51   281.219 28.76   279.023
        29.01   276.953 29.26   274.742 29.51   272.578 29.76   270.375
        30.01   268.188 30.26   265.93 ENDT
$
$-------------------------------------------------------
$
$  ...  rest of model  ...
$
ENDDATA
```

Response spectrum application is invoked via PARAM,SCRSPEC,0. The DTI,SPECSEL entry specifies that the input spectrum is acceleration (denoted by the A in field 5). The TABDMP1 entry defines the modal damping (every mode has 2% critical damping). The TABLED1 entry defines the input spectrum; this is the punch file that was generated from the spectrum generation run.

Discussion of Results. Figure 6-7 shows a portion of the resulting printed output. The eigenvalue summary shows the computed natural frequencies; note the rigid body mode, which occurred because the bracket was not constrained in the y direction (there was a SUPORT for that DOF). Matrix FN is the list of natural frequencies of the modes used for analysis with response spectrum input (two in this case—the rigid body mode is not included because our spectrum started at 0.01 Hz). Matrix PSIT lists the modal participation factors in transposed form, with one column for each mode (three in this case) and one row for each input point (one in this case). Note that the third mode (the second elastic mode) cannot be readily excited by base motion, since its response to the load is 10 orders of magnitude less than the second (first elastic) mode. Matrix UHVR occurs once for every analysis subcase with response spectrum input, and it lists the peak modal response. The first column is displacement, the second is velocity, and the third is acceleration. There is one row for each mode used in the response spectrum analysis (two in this case). A portion of the resulting maximum displacements, accelerations, and stresses—quantities selected for output via Case Control—are also shown. These quantities are computed using the ABS (default) method.

```
                                 R E A L   E I G E N V A L U E S
  MODE    EXTRACTION       EIGENVALUE          RADIANS             CYCLES          GENERALIZED        GENERALIZED
   NO.      ORDER                                                                    MASS             STIFFNESS
    1         1        0.0                 0.0                 0.0               1.000000E+00        0.0
    2         2        3.930305E+03        6.269214E+01        9.977764E+00      1.000000E+00        3.930305E+03
    3         3        2.878402E+04        1.696586E+02        2.700200E+01      1.000000E+00        2.878402E+04


^^^ DMAP INFORMATION MESSAGE 9047 (POSTREIG) - SCALED RESPONSE SPECTRA FOR RESIDUAL STRUCTURE ONLY


      MATRIX FN       (GINO NAME 101 ) IS A DB  PREC           1 COLUMN X          3 ROW RECTANG  MATRIX.
COLUMN     1     ROWS     2 THRU     3  --------------------------------------------------
ROW
    2)   9.977767703979D+00  2.700200654232D+01
THE NUMBER OF NON-ZERO TERMS IN THE DENSEST COLUMN =      2
THE DENSITY OF THIS MATRIX IS  66.66 PERCENT.
           PSIT
      POINT         VALUE    POINT          VALUE    P0INT          VALUE    POINT          VALUE    POINT          VALUE

COLUMN      1
      888 T2 -1.00000E+03
COLUMN      2
      888 T2  1.51209E-01
COLUMN      3
      888 T2  8.54947E-11
          U S E T   D E F I N I T I O N   T A B L E   ( I N T E R N A L   S E Q U E N C E ,   R O W   S O R T )
                                           R    DISPLACEMENT SET
            -1-          -2-          -3-          -4-          -5-          -6-          -7-          -8-          -9-          -10-

    1=      888-2
  SCALED SPECTRAL RESPONSE, ABS  OPTION, DLOAD =        852  CLOSE =        1.00
      MATRIX UHVR      (GINO NAME 101 ) IS A REAL                3 COLUMN X          3 ROW SQUARE   MATRIX.
COLUMN     1     ROWS     2 THRU     3  --------------------------------------------------
ROW
    2)   -2.0431E-02 -8.7238E-13
COLUMN     2     ROWS     2 THRU     3  --------------------------------------------------
ROW
    2)   -1.2808E+00 -1.4801E-10
COLUMN     3     ROWS     2 THRU     3  --------------------------------------------------
ROW
    2)   -8.0299E+01 -2.5111E-08
THE NUMBER OF NON-ZERO TERMS IN THE DENSEST COLUMN =      2
THE DENSITY OF THIS MATRIX IS  66.66 PERCENT.
    TIME =  0.000000E+00
                              D I S P L A C E M E N T   V E C T O R

    POINT ID.   TYPE        T1            T2            T3            R1            R2            R3
        5       G     1.982064E-05  5.079640E-04  1.304063E-05  4.452030E-04  0.0           3.272993E-04
        6       G     2.216715E-05  4.475303E-04  5.667240E-06  2.254874E-03  0.0           6.874480E-05
        7       G     5.777859E-05  3.471966E-03  3.236318E-05  1.011459E-02  0.0           1.185161E-02
        8       G     6.727507E-05  9.782481E-03  9.783542E-05  7.597393E-03  2.088506E-03  1.105588E-02
       13       G     4.799800E-06  2.431473E-04  1.162851E-05  2.776468E-03  0.0           1.267932E-03
       14       G     0.0           3.089312E-09  0.0           0.0           0.0           0.0
       15       G     0.0           3.089312E-09  0.0           0.0           0.0           0.0
      999       G     7.124796E-09  3.353467E-02  4.805730E-02  1.705154E-02  3.335225E-10  2.368395E-08
    TIME =  0.000000E+00
                              A C C E L E R A T I O N   V E C T O R

    POINT ID.   TYPE        T1            T2            T3            R1            R2            R3
        5       G     7.790122E-02  1.996455E+00  5.125370E-02  1.749785E+00  0.0           1.286387E+00
        6       G     8.712371E-02  1.758932E+00  2.227400E-02  8.862347E+00  0.0           2.701882E-01
        7       G     2.270876E-01  1.364589E+01  1.271973E-01  3.975345E+01  0.0           4.658046E+01
        8       G     2.644117E-01  3.844816E+01  3.845233E-01  2.986009E+01  8.208470E+00  4.345302E+01
       13       G     1.886469E-02  9.556437E-01  4.570363E-02  1.091238E+01  0.0           4.983363E+00
       14       G     0.0           1.214195E-05  0.0           0.0           0.0           0.0
       15       G     0.0           1.214195E-05  0.0           0.0           0.0           0.0
      999       G     2.806829E-05  1.318016E+02  1.888800E+02  6.701779E+01  1.318517E-06  9.310856E-05
    TIME =  0.000000E+00
                  S T R E S S E S   I N   Q U A D R I L A T E R A L   E L E M E N T S   ( Q U A D 4 )
ELEMENT    FIBRE              STRESSES IN ELEMENT COORD SYSTEM               PRINCIPAL STRESSES (ZERO SHEAR)
  ID.     DISTANCE          NORMAL-X      NORMAL-Y      SHEAR-XY      ANGLE      MAJOR            MINOR        VON MISES
   4    -2.500000E-02     9.571945E+02  1.588326E+02  6.315743E+02  28.8527  1.305162E+03   -1.891354E+02  1.409281E+03
         2.500000E-02     8.720101E+02  4.871640E+02  7.984738E+02  38.2254  1.500919E+03   -1.417454E+02  1.576578E+03
   6    -2.500000E-02     1.215178E+04  9.352043E+03  5.037602E+03  37.2351  1.598040E+04    5.523426E+03  1.405755E+04
         2.500000E-02     1.361088E+04  8.486970E+03  3.161832E+03  25.4915  1.511842E+04    6.979430E+03  1.310577E+04
 235    -2.500000E-02     2.137487E+02  3.799783E+00  1.563414E+00   0.4266  2.137604E+02    3.788147E+00  2.118917E+02
         2.500000E-02     1.987584E+02  4.320534E+00  9.967642E-01   0.2937  1.987635E+02    4.315422E+00  1.966413E+02
```

Figure 6-7 Printed Output (Abridged)

6.5 Random Analysis with Coupled Excitations

In MSC.Nastran, random response analysis is treated as a data reduction procedure that is applied to the results of a frequency response analysis. First, the frequency response analysis is performed for sinusoidal loading conditions, $\{P_a\}$, each a separate subcase, at a sequence of frequencies ω_i. Normal data reduction procedures are then applied to the output of the frequency response analysis module, resulting in a set of output quantities $u_{ja}(\omega_i)$, corresponding to an output j and subcase a. The calculations of power spectral densities and autocorrelation functions for the output quantities are performed in the random analysis module.

Each loading condition subcase represents a unique random load source, which may be applied to many grid points. Typically, these loads are chosen to be unit loads such as unit "g" loads or unit pressures. The probabilistic magnitude of each load source is defined by spectral density functions on RANDPS input data. If the load subcases are correlated, the coupling spectral density is also defined on one or more RANDPS functions. An example of coupled spectral density would be the forces on four wheels of a vehicle traveling over a rough road.

Figure 6-8 is a simplified flow diagram for the random analysis module. The inputs to the module are the frequency responses, $H_{ja}(\omega_i)$, of quantities u_j to loading conditions $\{P_a\}$ at frequencies ω_i, and the auto- and cross-spectral densities of the loading conditions S_a and S_{ab}. The response quantities, S_j, may be displacements, velocities, accelerations, internal forces, or stresses. The power spectral densities of the response quantities are calculated by different procedures depending on whether the loading conditions are correlated or uncorrelated. The spectral densities due to all sources, considered independent, will be combined into one set of outputs.

Enter

Cross Spectral Density ?

Yes

No

$$S_j = \sum_a \sum_b H_{ja} H_{jb}^* S_{ab}$$

$$S_{ja} = |H_{ja}|^2 S_a$$

Combined Loading ?

Yes

No

$$S_j = \sum S_{ja}$$

Autocorrelation? Yes

Compute Autocorrelation Functions

No

Compute rms value

Exit
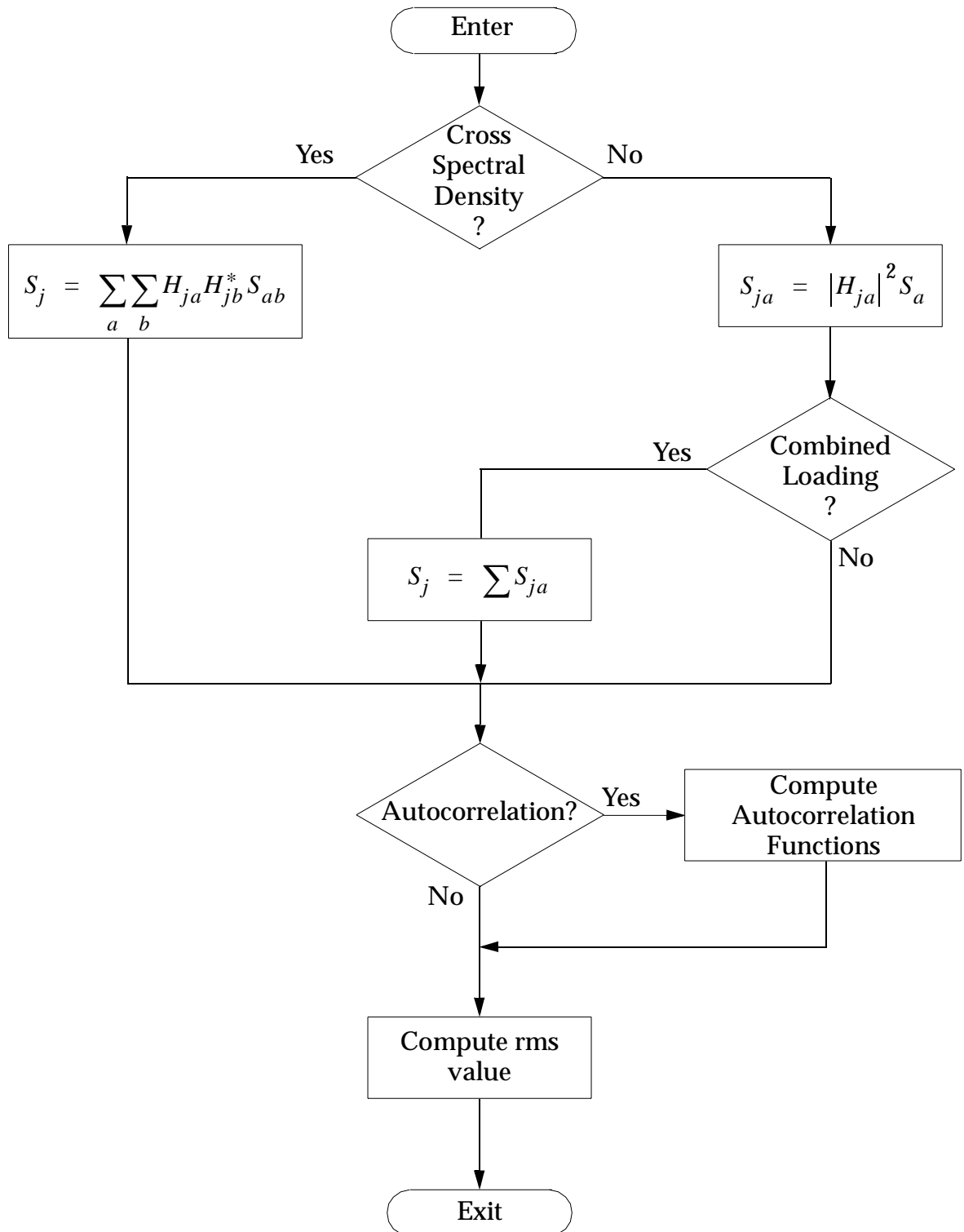
Figure 6-8 Flow Diagram for Random Analysis Module

Theory

The application of these frequency response techniques to the analysis of random processes requires that the system be linear and that the excitation be stationary with respect to time. The theory includes a few important theorems that will be reviewed.

An important quantity in random analysis theory is the autocorrelation function $R_j(\tau)$, of a physical variable, u_j, which is defined by

$$R_j(\tau) = T \overset{\lim}{\to} \infty \frac{1}{T} \int_0^T u_j(t) u_j(t-\tau) dt \qquad \text{Eq. 6-41}$$

Note that $R_j(0)$ is the time average value of u_j^2, which is an important quantity in the analysis of structural failure. The one-sided power spectral density $S_j(\omega)$ of u_j is defined by

$$S_j(\omega) = T \overset{\lim}{\to} \infty \frac{2}{T} \left| \int_0^T e^{-i\omega t} u_j(t) dt \right|^2 \qquad \text{Eq. 6-42}$$

It may be shown (using the theory of Fourier integrals) that the autocorrelation function and the power spectral density are Fourier transforms of each other. Thus, we define the autocorrelation function in terms of frequency response functions

$$R_j(\tau) = \frac{1}{2\pi} \int_0^\infty S_j(\omega) \cos(\omega\tau) d\omega \qquad \text{Eq. 6-43}$$

from the mean-square theorem, the rms (root mean squared) magnitude, u_j, is

$$\bar{u}_j^2 = R_j(0) = \frac{1}{2\pi} \int_0^\infty S_j(\omega) d\omega \qquad \text{Eq. 6-44}$$

The transfer function theorem states that, if $H_{ja}(\omega)$ is the frequency response of any physical variable, u_j, due to an excitation source, Q_a, which may be a point force, a loading condition or some other form of excitation, i.e., if

$$u_j(\omega) = H_{ja}(\omega) \cdot Q_a(\omega) \qquad \text{Eq. 6-45}$$

where $u_j(\omega)$ and $Q_a(\omega)$ are the Fourier transforms of u_j and Q_a, then the power spectral density of the response $S_j(\omega)$, is related to the power spectral density of the source, $S_a(\omega)$, by

$$S_j(\omega) = \left| (H_{ja}\omega) \right|^2 \cdot S_a(\omega) \qquad \text{Eq. 6-46}$$

Eq. 6-46 is an important result because it allows the statistical properties (e.g., the autocorrelation function) of the response of a system to random excitation to be evaluated via the techniques of frequency response. Another useful result is that, if sources Q_1, Q_2, Q_3, etc., are statistically independent, i.e., if the cross-correlation function between any pair of sources

$$R_{ab}(\tau) = T \overset{\lim}{\to} \infty \frac{1}{T} \int_0^T q_a(t) q_b(t-\tau) d\tau \qquad \text{Eq. 6-47}$$

is null, then the power spectral density of the total response is equal to the sum of the power spectral densities of the responses due to individual sources. Thus

$$S_j(\omega) = \sum_a S_{ja}(\omega) = \sum_a \left| H_{ja}(\omega) \right|^2 S_a(\omega) \qquad \text{Eq. 6-48}$$

If the sources are statistically correlated, the degree of correlation can be expressed by a cross-spectral density, S_{ab}, and the spectral density of the response may be evaluated from

$$S_j = \sum_a \sum_b H_{ja} H_{jb}^* S_{ab} \qquad \text{Eq. 6-49}$$

where H_{jb}^* is the complex conjugate of H_{jb}.

In applying the theory, it is not necessary to consider the sources to be forces at individual points. Rather, an ensemble of applied forces that are completely correlated (i.e., a loading condition) should be treated as a single source. For example, a plane pressure wave from a specified direction may be treated as a source. Furthermore, the response may be any physical variable including internal forces and stresses as well as displacements, velocities, and accelerations.

The power spectral densities, S_j, are plotted versus frequency using the XYOUT commands (XYPLOT, XYPRINT, XYPEAK, AND XYPUNCH). The autocorrelation functions, $R_j(\tau)$, are plotted versus selected time delays, τ, using XYOUT requests.

Because of the potential computational costs, cross-correlations and cross-spectral densities.

Example: Random Analysis of a Simple Structure

There are a number of physical phenomena that result in nondeterministic data where specific responses cannot be predicted in a deterministic sense. Examples are earthquake ground motion, the height and spacing of ocean waves, pressure gusts encountered by aircraft in flight, by bridges during storms, and acoustic excitation such as jet engine noise. The response of physical systems to such unpredictable values of excitation is an application of random analysis methods.

In MSC.Nastran, ergodic random analysis is treated as a data reduction process that expands the results of a frequency response analysis.

The inputs for these data recovery activities are output quantities from the frequency response analysis, and user-supplied spectral data for the loading conditions. The outputs are the power spectral density functions, the autocorrelation functions, the number of positive crossings of the line $y(t) = 0$ by the response record in a unit time, and the rms value of the response. These latter two items are of particular importance to the stress analyst. The number of positive crossings, N_0, is obtained from the joint probability density function and is a measure of the apparent frequency of the response. The rms value of the response is a measure of the dynamic magnitudes.

Simple output plots for the problem are shown in the following figures.

Model Description

The model illustrated here consists of three masses connected by springs and viscous dampers. The base mass, M_1, is considered to be the ground and is used to enforce a excitation. The base is excited by a noise excitation displacement $y(t)$ having a white noise

power spectral density $S_2(f)$inch^2/Hz. The middle mass is excited by a band-limited white noise excitation force $F(t)$ having a constant power spectral density $S_1(f)$lb^2/Hz. The two loadings are correlated through a cross-spectral density $S_{12}(f)$in-lb/Hz.
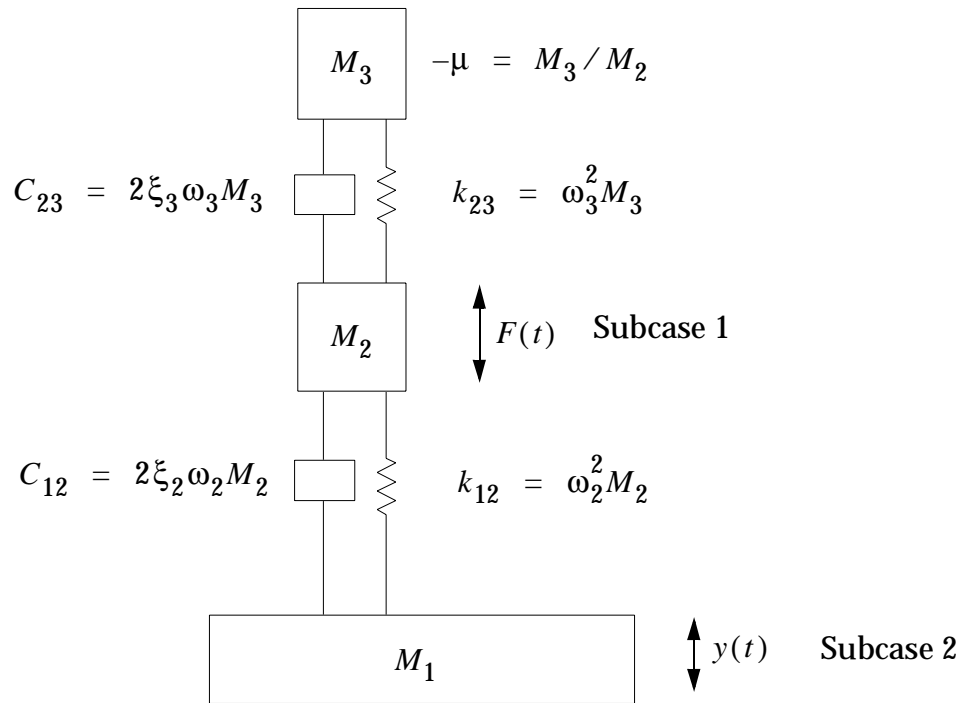
Figure 6-9 Example Model

In the figure, the following notation has been used:

M_i Mass of i-th grid point.

k_{ij} Stiffness between i-th and j-th grid points.

C_{ij} Viscous damping between i-th and j-th grid points.

$2\xi_j$ Nondimensional damping ratio = $C_{ij}/\sqrt{k_{ij}M_j}$.

ω_j Circular frequency = $\sqrt{k_{ij}/M_j}$.

Mass Properties		
EID	**G**	**M**
1	1	$1.0\,E9$ lb-sec^2 / in
2	2	$.1$ lb-sec^2 / in
3	3	$1.$ lb-sec^2 / in

Spring Properties	
EID	**K**
12	5.0E6 lb/in
23	10.0E6 lb/in

Damper Properties	
EID	**B**
120	14.14 lb-sec/in
230	63.25 lb-sec/in

Constraints	
Node	**Constraint**
1	13456
2	13456
3	13456

Frequencies (f)
200 Hz to 600 Hz by 10 Hz

	Loads	
Node	**Load**	**Subcase**
2	$F_y = 100.$	1
1	$F_y = (1.0\text{E}9)(2\pi f)^2$ lb	2

	Spectral Densities	
Excited Set (j)	**Applied Set (h)**	S_{jk}
1	1	$1 \times 10^5 \text{lb}^2 / \text{hz}$
2	2	$1 \times 10^4 \text{in}^2 / \text{hz}$
1	2	3 in-lb-hz

For a check on the MSC.Nastran results, the responses at 200 Hz, 280 Hz, and 500 Hz are tabulated. Results are given as magnitude/phase format.

Frequency	Response	Theoretical	MSC.Nastran
200 Hz	$100 \cdot H_{2f-d}$	3.3705×10^{-5} / $359.6029°$	3.3705×10^{-5} / $359.6029°$
	$100 \cdot H_{3f-d}$	4.0025×10^{-5} / $359.5175°$	4.0025×10^{-5} / $359.5175°$
	H_{2d-d}	1.6853 / $179.8065°$	1.6853 / $179.8065°$
	H_{3d-d}	2.0013 / $179.7211°$	2.0013 / $179.7211°$
280 Hz	$100 \cdot H_{2f-d}$	4.6806×10^{-4} / $347.2289°$	4.6806×10^{-4} / $347.2288°$
	$100 \cdot H_{3f-d}$	6.7782×10^{-4} / $346.9431°$	6.7782×10^{-4} / $346.9430°$
	H_{2d-d}	23.4031 / $167.5139°$	23.4031 / $167.5138°$
	H_{3d-d}	33.8912 / $167.2282°$	33.8911 / $167.2281°$
500 Hz	$100 \cdot H_{2f-d}$	2.4206×10^{-7} / $236.0504°$	2.4025×10^{-7} / $236.0506°$
	$100 \cdot H_{3f-d}$	1.0187×10^{-5} / $180.4626°$	1.0187×10^{-5} / $180.4626°$
	H_{2d-d}	1.2103×10^{-2} / $56.5594°$	1.2103×10^{-2} / $56.5600°$
	H_{3d-d}	$.50935$ / $.9717°$	0.50934 / $.9717°$

The auto-power spectral density of the j-th response is defined by the relationship

$$S_j(f) = \sum_a \sum_b H_a^*(f) S_{ab} H_b(f)$$ Eq. 6-50

The results for selected frequencies are tabulated below.

Frequency	PSD M_2	
	Theoretical	MSC.Nastran
200 Hz	5.6805×10^{-5}	5.6803×10^{-5}
280 Hz	1.0955×10^{-2}	1.0955×10^{-2}
500 Hz	2.9307×10^{-9}	2.9305×10^{-9}

As discussed in the problem description, the number of positive crossings N_0 is a measure of the apparent response frequency. This measure is compared below.

Frequency 1st Mode	N_0	
	Theoretical M_2	Displacement M_2
284.2 Hz	282.4 Hz	284.3 Hz10

Listing 6-3 Data File for Example from Figure 6-9

```
ID FREQRSPN,RANDOM
TIME 5
DIAG 8
SOL 111
CEND
TITLE=FREQ RSPN - RANDOM ANALYSIS DEMONSTRATION
ECHO=UNSORT
METHOD=1  $ Reduce to Modal Coordinates
FREQUENCY=1
RANDOM=1      $ Basic request
SVEC=ALL      $ Modal Coordinate output
SDISP(SORT2,PHASE)=ALL
DISP(SORT2,PHASE)=ALL
VELO(SORT2,PHASE,PLOT)=ALL
ACCEL(SORT2,PHASE,PLOT)=ALL
ELFORCE(SORT2,PHASE,PLOT)=ALL
ELSTRESS(SORT2,PHASE,PLOT)=ALL
SUBCASE 1
LABEL=FORCING FUNCTION ON MASS AT GRID POINT NUMBER 2
DLOAD=1
SUBCASE 2
LABEL=ENFORCED DISPLACEMENT ON GRID POINT NUMBER 1
DLOAD=2
$   *********************************************************
$   *** RANDOM ANALYSIS  ACE  ONTROL ***
```

```
OUTPUT (XYOUT)
XGRID=YES
YGRID=YES
XTITLE=FREQUENCY (HERTZ)
$$$$$$$$$$$$$$$$$$$$$$$$$$$$$$$$
XTITLE=FREQUENCY (HERTZ)
YTITLE=VELOCITY RESPONSE LOAD CASE 1
YLOG=YES
XYPLOT VELO RESPONSE 1 /2(T2RM),3(T2RM)
YLOG=NO
YTITLE=PHASE
XYPLOT VELO RESPONSE 1 /2(T2IP),3(T2IP)
$$$$$$$$$$$$$$$$$$$$$$$$$$$$$$$$
YLOG=YES
YTITLE=DISP P S D
XYPLOT DISP PSDF /2(T2)/3(T2)
YTITLE=ACCE P S
XYPLOT ACCE PSDF /2(T2)/3(T2)
YTITLE=FORCE P S D
XYPLOT ELFORCE PSDF /12(2)/23(2)
XTITLE=TIME (SEC)
YLOG=NO
YTITLE=VELOCITY AUTO CORROLATION
XYPLOT VELO AUTO /2(T2)/3(T2)
BEGIN BULK
$  *** STRUCTURE DEFINITION ***
GRID  1          0.   0.   0.         13456
GRID  2          0.   1.   0.         13456
GRID  3          0.   2.   0.         13456
CONM2 1     1          1.+9
CONM2 2     2           .1
CONM2 3     3          1.
CELAS212    5.+6 1     2    2    2              .5
CELAS223    10.+6 2    2    3    2              .5
CDAMP2120   14.14 1    2    2    2
CDAMP2230   63.25 2    2    3    2
SUPORT1     2
$  *** EIGENVALUE SETUP ***
EIGR  1     MGIV                3              EIGR1
+EIGR1MASS
$  *** FREQUENCY SELECTION ***
FREQ1 1     200.  10.   40
$  *** APPLIED DYNAMIC LOAD SUBCASE 1 ***
DAREA 10    2     2     1.+2
RLOAD11     10              10
TABLED110                                     TABD1
+TABD11.    1.    10000.1.    ENDT
$  *** ENFORCED DISPLACEMENT SUBCASE 2 ***
DAREA 20    1     2     1.+9
RLOAD12     20              110
TABLED4110 0.   1.    1.    10000.             TABD4
+TABD40.   0.    39.478ENDT
$  *** RANDOM ANALYSIS DATA ***
RANDPS1     1     1     1.+5        1000
RANDPS1     2     2     1.-4        1000
RANDPS1     1     2     3.          1000
TABRND11000                                   TABR1
+TABR10.   0.    199.990.    200.  1.    600.  1.    TABR2
+TABR2600.010.   10000.0.    ENDT
RANDT11     100   0.    .1
ENDDATA
```

The following is the key printed output:

```
 FREQ RSPN - RANDOM ANALYSIS DEMONSTRATION                          AUGUST  31, 1994  MSC.Nastran  8/17/94   PAGE    6



                                     R E A L   E I G E N V A L U E S
  MODE    EXTRACTION        EIGENVALUE            RADIANS             CYCLES           GENERALIZED          GENERALIZED
   NO.      ORDER                                                                         MASS              STIFFNESS
     1         1            .0                   .0                   .0              1.000000E+00           .0
     2         2          3.188542E+06         1.785649E+03         2.841949E+02     1.000000E+00         3.188542E+06
     3         3          1.568106E+08         1.252240E+04         1.993002E+03     1.000000E+00         1.568106E+08



 FREQ RSPN - RANDOM ANALYSIS DEMONSTRATION                          AUGUST  31, 1994  MSC.Nastran  8/17/94   PAGE   53



                      X Y - O U T P U T   S U M M A R Y   ( A U T O   O R   P S D F )
  PLOT   CURVE FRAME                 RMS        NO. POSITIVE  XMIN FOR   XMAX FOR   YMIN FOR    X FOR    YMAX FOR    X FOR*
  TYPE    TYPE   NO.    CURVE ID.    VALUE        CROSSINGS   ALL DATA   ALL DATA   ALL DATA    YMIN     ALL DATA    YMAX
  PSDF DISP       5     2(  4)    4.427970E-01  2.823553E+02 2.000E+02  6.000E+02  2.931E-09  5.000E+02  1.095E-02  2.800E+02
  PSDF DISP       6     3(  4)    6.487856E-01  2.843350E+02 2.000E+02  6.000E+02  2.025E-06  6.000E+02  2.297E-02  2.800E+02
  PSDF ACCE       7     2(  4)    1.400392E+06  2.856203E+02 2.000E+02  6.000E+02  2.855E+05  5.000E+02  1.049E+11  2.800E+02
  PSDF ACCE       8     3(  4)    2.091627E+06  2.934378E+02 2.000E+02  6.000E+02  1.997E+08  2.000E+02  2.201E+11  2.800E+02
  PSDF EL FOR     9    12(  2)    2.375014E+06  3.161015E+02 2.000E+02  6.000E+02  5.009E+08  2.200E+02  2.306E+11  2.800E+02
  PSDF EL FOR    10    23(  2)    2.091485E+06  2.934356E+02 2.000E+02  6.000E+02  1.997E+08  2.000E+02  2.201E+11  2.800E+02
  AUTO VELO      11     2(  4)    7.854708E+02  2.837833E+02 0.000E+00  1.000E-01 -5.550E+05  2.000E-03  6.170E+05  0.000E+00
  AUTO VELO      12     3(  4)    1.158947E+03  2.872666E+02 0.000E+00  1.000E-01 -1.179E+06  2.000E-03  1.343E+06  0.000E+00
 FREQ RSPN - RANDOM ANALYSIS DEMONSTRATION                          AUGUST  31, 1994  MSC.Nastran  8/17/94   PAGE   54
```
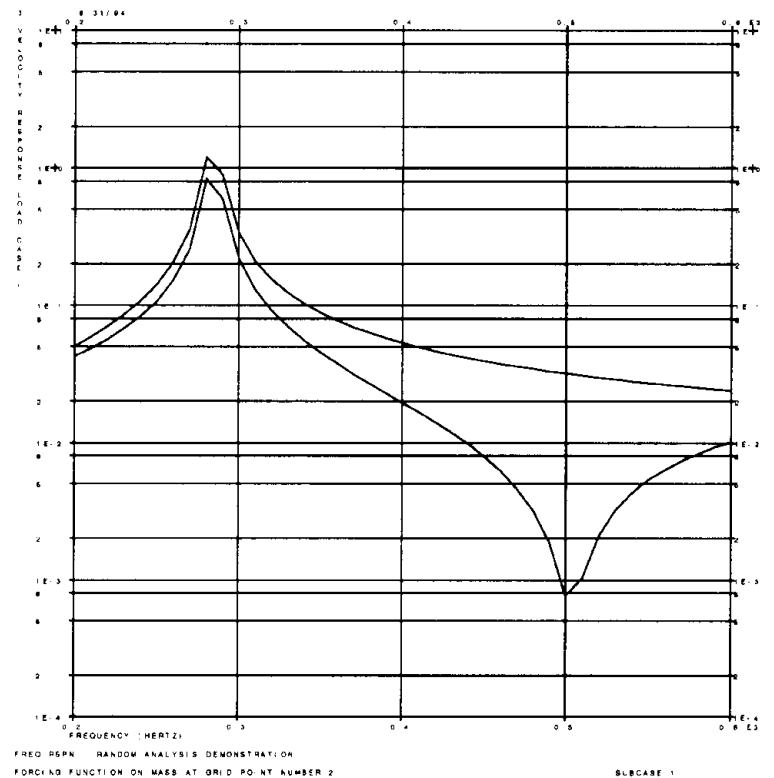

Figure 6-10 Velocity Response, Points 2 and 3 (Subcase 1)
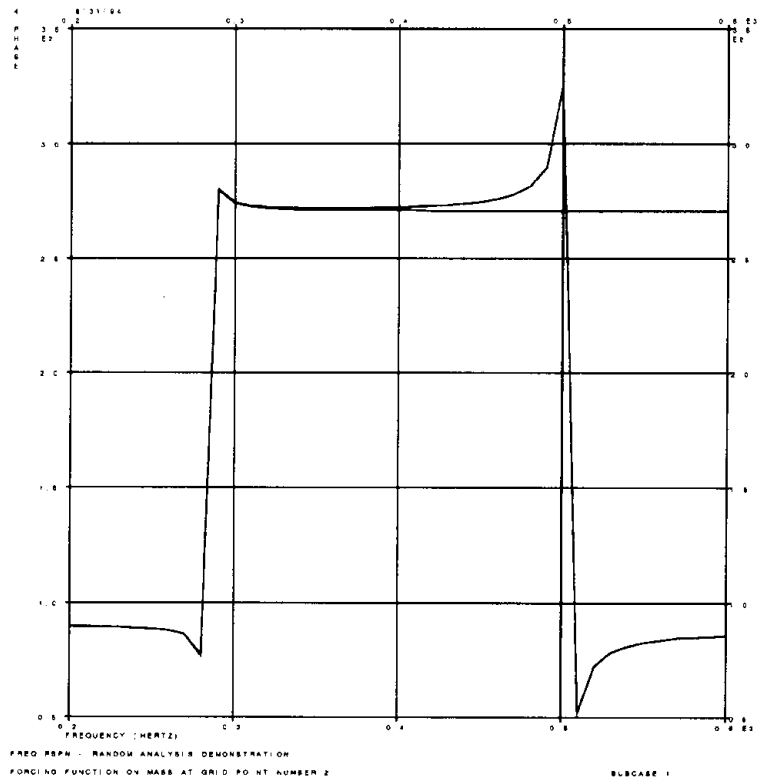
Figure 6-11 Velocity Phase Angle, Points 2 and 3 (Subcase 1)
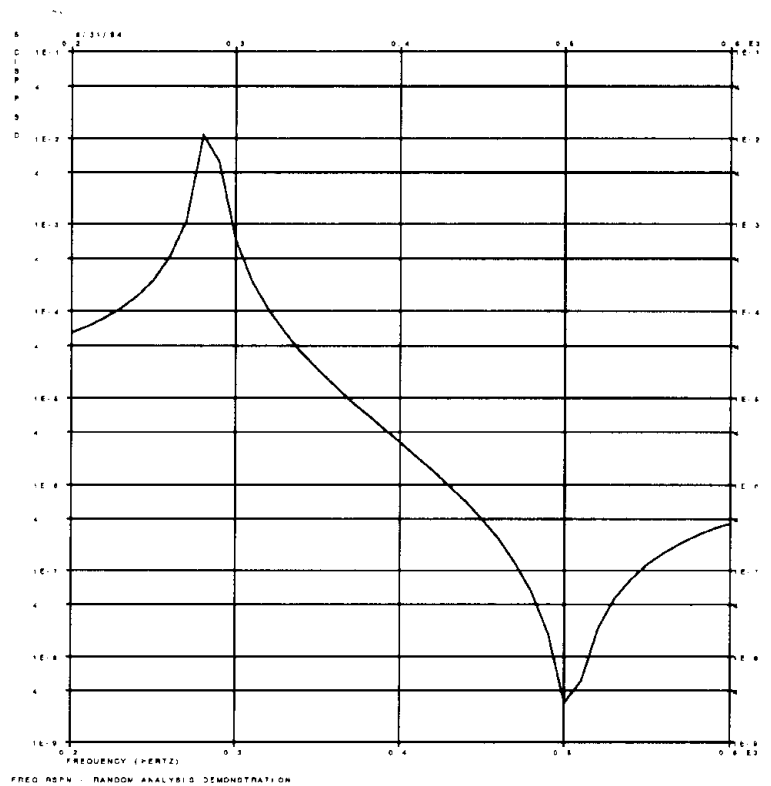
Figure 6-12 Power Spectral Density, Point 2 Displacement
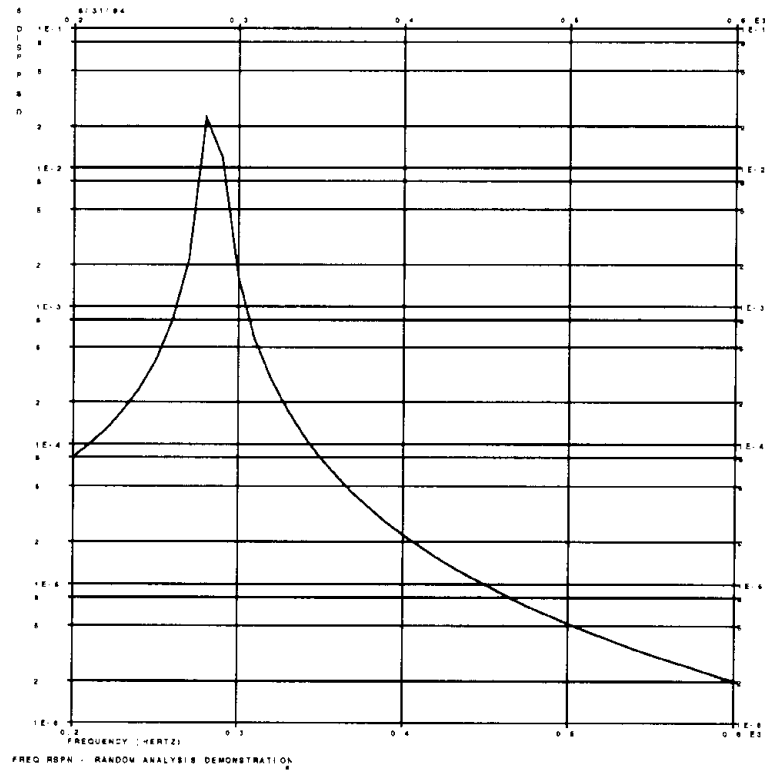
Figure 6-13 Power Spectral Density, Point 3 Displacement
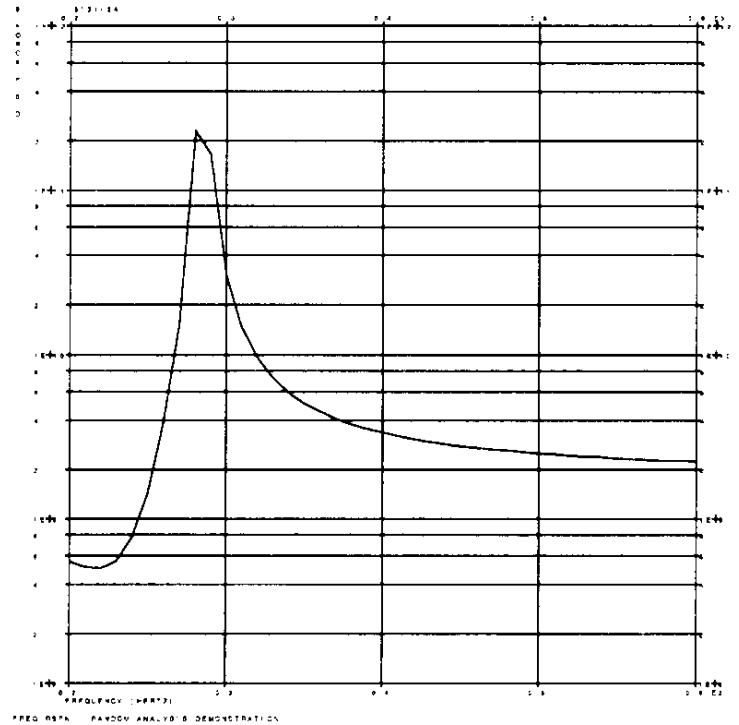
Figure 6-14 PSDF Forces in Element 12
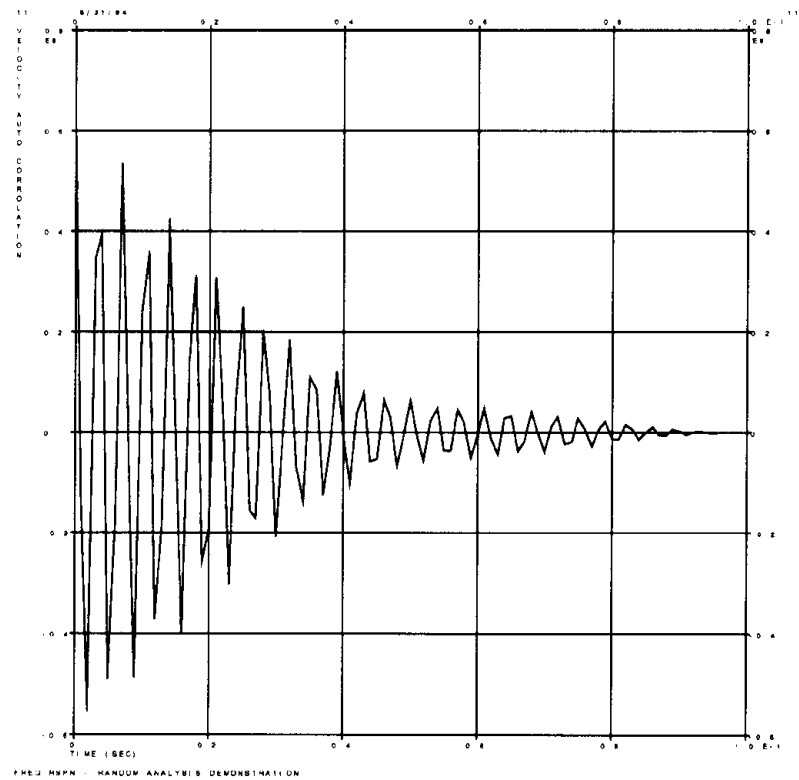
Figure 6-15 Autocorrelation, Velocity of Point 2

Theory of Eigenvalue Extraction Methods

- Sturm Sequence Theory

- Eigensolution Methods

A.1 Sturm Sequence Theory

Methods of Computation

A numerical technique which is very helpful in a modal extraction is Sturm Sequence. In this approach, a frequency is selected and computations are performed to determine the number of roots which exist below that frequency. In some cases this frequency is chosen manually by user input, other times it is selected automatically by MSC.Nastran. This choice depends upon which modal extraction technique is being used.

Starting with the basic characteristic equation

$$[K + \lambda_s M] = 0 \qquad \qquad \text{Eq. A-1}$$

a frequency, $\omega^2 = \lambda_s$ is substituted. This frequency is called the shift point. The determinant $K - \lambda_s M$ is evaluated for the frequency λ_s. The resulting matrix is factored into it $[L][D][L]^T$ components. The diagonal matrix, $[D]$, is known as the Factor Diagonal Matrix. The number of negative terms in the Factor Diagonal Matrix, known as the Sturm Number, are the number of frequencies that exist below the shift point frequency, λ_s.

Sturm Sequence logic is a very important part of the many of the modal extraction and dynamic reduction techniques. When it is utilized, the Sturm Sequence logic issues a number of messages which indicate the various shifts within the frequency range of interest. These messages help the various techniques to determine how many roots are in specific ranges and also if all modes have been found in the range.

A.2   Eigensolution Methods

Methods of Eigensolution

Seven methods of real eigenvalue extraction are provided in MSC.Nastran. These methods are numerical approaches to solving the equation of motion for its natural frequencies and modes shapes. The reason for seven different numerical techniques is related to the fact that no one method is the best for all problems. While most of the methods can be applied to all problems, the difference between the methods many times reduces to the efficiency of the solution process.

Most methods of algebraic eigenvalue extraction belong to one of two groups:

1. transformation methods, and
2. tracking methods.

In a transformation method, the eigenvalue equation is first transformed into a special form (such as tridiagonal) from which eigenvalues may easily be extracted. In a "tracking" method, the roots are extracted from the original dynamic matrix one at a time using an iterative procedure.

Four of the real eigenvalue extraction methods available in MSC.Nastran are transformation methods. These are:

1. Givens Methods
2. Householder Method
3. Modified Givens Method, and
4. Modified Householder Method.

These transformation methods use a "tridiagonal" solution method.

Two of the real eigenvalue extraction methods available in MSC.Nastran are classified as tracking methods. These are:

1. Inverse Power Method, and
2. Sturm Modified Inverse Power Method.

The final real eigenvalue extraction method available in MSC.Nastran is the Lanczos method. The Lanczos method combines the best characteristics of the tracking and transformation methods.

The Standard Tridiagonal Methods (GIV and HOU)

The Givens(GIV) and Householder (HOU) modal extraction methods require a positive definite mass matrix. There are no restrictions on the stiffness matrix other than that it must be symmetric. These matrices will always result in real (positive) roots. The tridiagonal methods are the most efficient methods for small problems and problems with dense matrices when a large portion of the eigenvectors are needed. These methods find all of the eigenvalues in the structure as a result of the transformation process. The user

methods do not take advantage of the sparse matrices, but they are efficient with the dense matrices sometimes created using dynamic reduction. The steps used in the tridiagonal methods are as follows:

1. Perform a Cholesky decomposition of the mass matrix:

$$[M] = [L][L]^T \qquad \text{Eq. A-2}$$

where $[L]$ is a lower triangular matrix.

2. The symmetric eigenvalue equation can be written as:

$$[J - \lambda I]\{w\} = 0 \qquad \text{Eq. A-3}$$

where $[J]$ is the symmetric matrix and $[I]$ is the identity matrix. To do this, premultiply **Eq. A-1** by $[L]^{-1}$ and substitute for $[M]$ from **Eq. A-2** to set the following:

$$[L]^{-1}[K]\{u\} - \lambda [L]^{-1}[L][L]^T\{u\} = 0 \qquad \text{Eq. A-4}$$

Then make the transformation:

$$\{w\} = [L]\{u\} \qquad \text{Eq. A-5}$$

which reduces **Eq. A-4** to **Eq. A-3** using the following:

$$[J] = [L]^{-1}[K][L]^{-1,T} \qquad \text{Eq. A-6}$$

3. The $[J]$ matrix is converted to a tridiagonal matrix by a transformation method according to the Givens or Householder method. (A tridiagonal matrix is a matrix where the only nonzero terms in the i-th column are the i – 1, i, i + 1 row.)

4. All the eigenvalues of the tridiagonal matrix are extracted using a modified QR algorithm.

5. The eigenvectors are computed over a given frequency range or, at user option, for a given number of eigenvalues using inverse iteration. Since the roots are known to high accuracy at this point, the vectors converge rapidly.

6. Physical eigenvectors are recovered by performing the inverse transformation to that made in Step 3 and then solving **Eq. A-5** as follows:

$$\{u\} = [L]^{T,-1}\{w\} \qquad \text{Eq. A-7}$$

7. If a SUPORT entry is used, the first N_r eigenvectors computed are discarded. The rigid body modes from the SUPORT computation are put in their place, and the corresponding eigenvalues are set to zero. The SUPORT operation does cause some redundant operations to be performed as the rigid body modes are computed by two methods and then one set is discarded. This is generally a minor issue.

8. The back-transformed vectors $[PHI]$ are given a final stage of orthogonalization with respect to the mass matrix. The modal mass matrix is calculated as follows:

$$[M_{modal}] = [\phi]^T [M][\phi]$$ Eq. A-8

then decomposed,

$$[M_{modal}] = [L]^T [L]$$ Eq. A-9

The refined eigenvectors, $[\bar{\phi}]^T$ are found by a forward pass on the equation:

$$[L][\bar{\phi}]^T = [\phi]^T$$ Eq. A-10

Note that the tridiagonal methods fail in Step 1 if the mass matrix is not positive definite. In order to minimize this eventuality, degrees-of-freedom with null columns are removed from (u) by the automatic application of static condensation. This is called AUTO-OMIT. (This procedure can be bypassed by using PARAM,ASING). The application of the AUTO-OMIT process is a precaution and may not remove all possible causes of mass matrix singularity such as, a point mass offset from a grid point, but it greatly improves the reliability and convenience of the standard tridiagonal methods.

The Modified Tridiagonal Methods (MGIV, MHOU, AGIV, AHOU)

The modified tridiagonal methods, Modified Givens (MGIV) and Modified Householder (MHOU), are similar to the standard tridiagonal methods (GIV, HOU) with the exception that the mass matrix can be singular.

The steps used in the modified methods are as follows:

1. Perform a Cholesky decomposition of the positive definite matrix

$$[K + \lambda_s M] = [L][L]^T$$ Eq. A-11

where λ_s is a positive number automatically selected by the program to optimize the reliability and accuracy of eigenvalue extraction. It is large enough to stabilize all rigid body modes but also be as small as possible to reduce the numerical contamination. The goal of the algorithm is to find a value near the first flexible frequency of the system. It uses the diagonal terms of the mass and stiffness matrices as follows:

$$\lambda_s = \frac{1}{N^{1/2} \sum_{i=1}^{N} \frac{M_{ii}}{K_{ii}}}$$ Eq. A-12

where N is the dimension of the matrices. If M_{ii} or $X_{ii} = 0$ (an under defined degree-of-freedom) or $M_{ii}/X_{ii} > 10^{**}8$ (a likely "very large" mass term used to approximate a rigid body mode), the corresponding term is omitted from the summation. If the value calculated by this approximate method does not result in a stable Cholesky decomposition, λ_s is increased by adding the arbitrary amount of 0.01. If this value also results in failure, the original value is increased by 0.02. If this value also fails, a fatal error is issued.

2. Write the eigen-equation standard form as:

$$[\bar{J} - \bar{\lambda}I]\{\bar{w}\} = 0 \qquad \text{Eq. A-13}$$

where:

$$\bar{\lambda} = \frac{1}{\lambda + \lambda_s} \qquad \text{Eq. A-14}$$

and:

$$[\bar{J}] = [L]^{-1}[M][L]^{-1,T} \qquad \text{Eq. A-15}$$

by rearranging the terms to read as follows:

$$[K + \lambda_s M - (\lambda + \lambda_s)M]\{u\} = 0 \qquad \text{Eq. A-16}$$

Then premultiply **Eq. A-16** by $-1/(\lambda + \lambda_s)$ and substitute for $[K + \lambda_s M]$ from **Eq. A-11** to obtain:

$$\left[M - \frac{LL^T}{\lambda + \lambda_s}\right]\{u\} = 0 \qquad \text{Eq. A-17}$$

Premultiply by $[L]^{-1}$ and then substitute:

$$\{\bar{w}\} = [L]^T\{u\} \qquad \text{Eq. A-18}$$

resulting in **Eq. A-13**, **Eq. A-14**, and **Eq. A-15**.

3. The remaining steps are identical to those for the unmodified methods where:

$$[J] = [\bar{J}] \text{ and } \{w\} = \{\bar{w}\} \qquad \text{Eq. A-19}$$

Although the mass matrix is not required to be nonsingular in the modified methods, a singular mass matrix can produce one or more zero eigenvalues, λ_s, which are equivalent to infinite eigenvalues, λ_i. Due to roundoff error, these will appear in the output as very large positive or negative eigenvalues. To reduce the incidence of such meaningless results, degrees-of-freedom with null masses are eliminated by the AUTO-OMIT static condensation as in the case of the unmodified methods. This step can be bypassed by using PARAM,ASING.

Many times the user is not conversant in the status of the mass matrix prior to the actual matrix assembly. To assist the user in choosing the appropriate method, two options,

automatic methods, AHOU and AGIV, initially use the standard methods. In the first step of the method, if the mass matrix is not well-conditioned for decomposition, the method shifts to the corresponding modified method. The modified methods are more expensive and introduce numerical "noise" due to the shift, but they resolve most of the numerical problems of the ill-conditioned mass matrix.

Operations involved in the computation of the natural frequencies and mode shapes is proportional to the number of degrees-of-freedom (N). The time-consuming operations for the tridiagonal methods are mass matrix decomposition and reduction to standard form ($5/2\ N^3$ for a full mass matrix, negligible for a diagonal matrix) tridiagonalization ($2/3\ N^3$ for HOU, $4/3\ N^3$ for GIV), QR root iteration ($9\ N^2$), inverse iteration for vectors (N^2 per vector), and inverse transformation of vectors (N^2 per vector for HOU, $2\ N^2$ for GIV). As N becomes large (greater than 100, perhaps), terms in N^3 dominate.

The Inverse Power Methods (INV, SINV)

The inverse power method with shifts is particularly effective when the mass and stiffness matrices are sparse and when only a few of the eigenvalues are required. In MSC.Nastran, the method is used as a stand-alone method to find all of the eigenvalues within a user-specified domain.

If we define the eigenvalue problem as:

$$[K - \lambda M]\{u\} = 0 \qquad\qquad \text{Eq. A-20}$$

Let:

$$\lambda = \lambda_o + \Lambda \qquad\qquad \text{Eq. A-21}$$

where λ_o is called the shift point.

The iteration algorithm is:

$$[K - \lambda_o M]\{w_n\} = [M]\{u_{n-1}\} \qquad\qquad \text{Eq. A-22}$$

$$\{u_n\} = \frac{1}{C_n}\{w_n\} \qquad\qquad \text{Eq. A-23}$$

where C_n is equal to the value of the element of $\{w_n\}$ with the largest absolute value. $\{u_n\}$ is then placed on the right side of **Eq. A-22** and iteration continues. It is easy to prove that $1/C_n$ converges to λ_1, the shifted eigenvalue nearest to the shift point, and that $\{u_n\}$ converges to the corresponding eigenvector of **Eq. A-20**. The following observations are pertinent.

1. A triangular decomposition of the matrix $[K - \lambda_o M]$ is required in order to evaluate $\{w_n\}$ from **Eq. A-22**. The effort required to perform the triangular decomposition is greatly reduced if $[K - \lambda_o M]$ is a narrow band matrix. Structural analysis is characterized by narrowly banded stiffness and mass matrices. From Sturm's theorem, the number of negative terms on the factor diagonal is exactly equal to the number of roots below λ_o. This number is printed out at every shift and is identified as the Sturm sequence number.

2. It is unnecessary for $[K]$ to be nonsingular, so that rigid body modes cause no special difficulty. Similarly, null rows in $[M]$ cause no problems. If they are removed by static condensation, they will increase the cost of the solution unnecessarily. This occurs primarily due to the increase in bandwidth inherent in static condensation

3. The shift point λ_o may be changed (at the cost of an additional triangular decomposition) in order to improve the rate of convergence toward a particular eigenvalue or to improve the accuracy and convergence rate after several roots have been extracted from a given shift point. The next shift point is computed from the residual terms remaining after computing the present root by a root estimation algorithm (See the *MSC.Nastran Numerical Methods User's Guide* for details.)

4. λ_o can be placed to obtain the eigenvalues within a desired frequency band and not just those that have the smallest absolute value.

5. The Sturm sequence data can be used to ensure that all eigenvalues within the requested frequency band have been found. This can be done manually with DIAG 16 for the INV method or automatically with the SINV method (see the *MSC.Nastran Numerical Methods User's Guide* for details). In the SINV method, the requested band is broken into subregions, and the Sturm number is determined at each boundary of the subregion. If the root estimation algorithm predicts that the next root is out of the subregion but the Sturm sequence data states that more roots remain in the subregion, a bisection method is used to iterate to the missing roots. All roots for a subregion must be found before the method is allowed to enter the next subregion. The INV method tends to compute shifts that wander more about the requested frequency band and computes more roots outside the band than the SINV method does.

In the practical application of the tracking methods, most of the numerical efficiency issues (trial eigenvectors, convergence criteria, etc.) are automatically handled by MSC.Nastran. The shift points must be selected so that the numerical algorithms can operate in an optimum manner. Generally, this is handled by MSC.Nastran, but the user can assist MSC.Nastran through a careful choice of frequency range.

If the SUPORT entry is used, the rigid body modes calculated are used directly as the first set of eigenvectors with their eigenvalues set to zero. Iteration then proceeds for the nonzero roots. Use of the SUPORT feature reduces costs of the INV and SINV methods considerably besides giving the aesthetic benefits of exact zero-frequency rigid body modes. The SUPORT entry is recommended for use with these methods.

The Shifted Block Lanczos Method

The Lanczos method (LAN) available in MSC.Nastran is an extremely reliable and accurate method for solving the large sparse eigenvalue problems typical of many structures.

A shifted block Lanczos algorithm is implemented in MSC.Nastran. A summary of that method is given here with special emphasis on the effect of user inputs.

For the standard eigenvalue problem written in the form:

$$[A]\{x\} = \lambda\{x\} \qquad \text{Eq. A-24}$$

the Lanczos method computes a sequence of vectors q called Lanczos vectors and scalars Q_j, A. The basic recurrence relation for the j-th step of the Lanczos algorithm can be written as follows:

$$\{r_{j+1}\} = [A]\{q_j\} - \alpha_j\{q_j\} - \beta_j\{q_{j-1}\} \qquad \text{Eq. A-25}$$

$$\alpha_j = \{q_i\}^T[A]\{q_j\} \qquad \text{Eq. A-26}$$

$$\beta_{j+1} = \|r_{j+1}\| \qquad \text{Eq. A-27}$$

$$\{q_{j+1}\} = \frac{\{r_{j+1}\}}{B_{j+1}} \qquad \text{Eq. A-28}$$

The first j-steps of the method can be combined and written in matrix form:

$$[A][Q_j] - [Q][T_j] = \beta_{j+1}\{q_{j+1}\}\{e_j\}^T \qquad \text{Eq. A-29}$$

where $\{e_j\}$ = unit vector with the j-th component equal to one and all other components equal to zero

$$\{Q_j\} = (\{q_1\}, \{q_2\}, ..., \{q_j\}) \text{ with } [Q_j^T][Q_j] = [I] \qquad \text{Eq. A-30}$$

$$[T_j] = \begin{bmatrix} \alpha_1 & \beta_2 & & & & \\ \beta_2 & \alpha_2 & \beta_2 & & & \\ & \beta_3 & \alpha_3 & \beta_4 & & \\ & & \ddots & \ddots & \ddots & \\ & & & \ddots & \ddots & \beta_j \\ & & & & \ddots & \ddots \\ & & & & & \beta_j & \alpha_j \end{bmatrix} \qquad \text{Eq. A-31}$$

The eigenvalues of the tridiagonal matrix $[T_j]$ are called Ritz values. Some of these Ritz values are good approximations to eigenvalues of $[A]$. The corresponding Ritz vectors (x_i) are computed from the eigenvectors of $[T_j]$ and the Lanczos vectors. An eigenpair is

defined as an eigenvalue (s_i) and its corresponding eigenvector $\{\theta_{ik}\}$. Let $(\{\theta_{ik}\}, s_i)$ be an eigenpair of the tridiagonal matrix $[T_j]$. Then an approximate eigenpair for the original problem is $(\lambda_i, \{x_i\})$ where:

$$\lambda_i = \theta_i \qquad\qquad \text{Eq. A-32}$$

$$\{x_i\} = \{Q_j\}\{s_i\} \qquad\qquad \text{Eq. A-33}$$

As implied by the formulation of the algorithm, the method computes a tridiagonal matrix and a set of Lanczos vectors that become larger with each iteration. The algorithm in exact arithmetic can be terminated when $B_{j+1} = 0$ or when sufficiently many eigenvalues of $[A]$ have been computed. Lanczos also handles the effects of roundoff.

The algorithm that has been incorporated in MSC.Nastran is a shifted block version of the basic Lanczos recurrence relation. The blocking approach to the Lanczos algorithm (working with blocks of p Lanczos vectors simultaneously) enables the method to handle eigenvalues of high multiplicity including shifting in the algorithm which helps to speed the convergence of the method.

In this method, the A matrix is replaced by the sum of the stiffness matrix plus shifted mass matrix, similar to the approach in the modified tridiagonal methods. This allows solution of problems with rigid body modes and generally faster convergence. The shifts (trial roots) are influenced by user input. The user is required to input either a frequency band of interest, a desired number of roots, or a combination of this data.

As an example, suppose that both the lower bound (V1) and upper bound (V2) of the frequency band are defined by the user as well as the number of roots desired (ND). The main objective for the shift strategy is to encompass the region containing the eigenvalues of interest in which all of the eigenvalues have been computed and the number of eigenvalues has been verified with a Sturm sequence check.

The first shift is at V1 to determine the Sturm sequence number. The factor matrix is stored for possible later use. If V1 is not defined by the user, the first shift is made at λ_s. The second shift point is chosen at V2.

After a Lanczos iteration based on the selected shift and the computation of the corresponding Ritz values, some values will be found to be acceptable eigenvalues while other eigenpairs will fail convergence tests. A decision is made as to whether it is more efficient to re-shift or continue with further iteration. The re-shift point is chosen from the existing Ritz values (smaller than V2) or from the stored factor from the shift at V2. At this point, the number of accepted eigenvalues and the Sturm sequence numbers at each end of the region are known.

If iteration with the factor from V2 does not produce all of the roots desired, two more types of shift will be used. If it appears that the missing roots are near the lowest shift, an approximate first mode eigenvalue is used. This is either a nonzero SHFSCL field from the EIGRL entry or the a similar shift term used in the modified tridiagonal methods. If the missing roots are elsewhere, bisection between prior shifts is used. If all requested eigenpairs still cannot be found, a user information message is printed, and all accepted

eigenpairs are output. If some roots have been found, the module exits normally. A fatal error is issued if no roots have been found. If accepted Ritz values are found outside the requested region, they are discarded.

The strategy for selecting block size is to first find the minimum of N/2, 2E, p and MAXSET. N is the problem size, E the number of roots desired, p the number of Lanczos vectors that will fit into memory, and MAXSET the user selection for block size (which has a default of 7).

Another efficiency feature unique to the Lanczos method is selective orthogonalization of the trial eigenvectors. All of those contained in the same block are made orthogonal to one another. Tests are made, at several steps, to determine if further orthogonalization between vectors in different blocks is required. This avoids the cost term cubic on E (the number of eigenvectors calculated) which becomes the dominant term for GDR and the SINV methods as E becomes large.

If the SUPORT entry is used, the $[D_{ir}]$ matrix is merged with an identity matrix $[I_{rr}]$ to form raw rigid body vectors $[D_{ar}]$. These raw vectors are used as initial vectors. If the r-set has been well-chosen, the rigid body modes will converge rapidly. If they have been chosen poorly, the Lanczos iterations will continue until a good set of eigenvectors have been found. The corresponding roots are set to the aesthetically pleasing value of zero rather than to the small numerical zeros likely to be produced by the actual computations.

The Lanczos method is more forgiving than the other methods since it repairs the effects of a poor r-set selection. However, the repeatability of rigid body modes computed by Lanczos with the SUPORT entry is not the same as with other extraction methods. Rigid body modes computed using the SUPORT entry and a non-Lanczos method will produce identical modes, irrespective of the method. If the rigid body modes produced by the Lanczos method with SUPORT entries are compared with those produced by any of the other methods, the Lanczos modes will be a proper linear combination of the modes from the other methods and may be markedly different in appearance. Furthermore, if small changes are made to the stiffness matrix, the Lanczos modes again may be markedly different, although they are again a proper linear combination of the set produced by other methods. This lack of repeatability makes the Lanczos method unusable with the scaled response spectra capability of MSC.Nastran.

The cost for the LAN method is dominated by the decomposition, inverse iteration, and orthogonalization operations at the size of the input matrices N. The number of roots per decomposition varies by problem and is difficult to determine *a priori*.

User Interface for Real Eigenvalue Analysis

The EIGR and EIGRL Bulk Data entries are the heart of the user interface because they define a method and select parameters that control the eigenvalue extraction procedure. The EIGRL entry is used for the LANCZOS method, and the EIGR entries are used for all of the other methods.

The data used for the EIGR entry depend on the method selected. The basic data required is related to the eigenvalue extraction method chosen and to the frequency range or number of required roots. The basic format of the Bulk Data entry is as follows:

1	2	3	4	5	6	7	8	9	10
EIGR	SID	METHOD	F1	F2	NE	ND			+BC
+BC	NORM	GID	CID						

The SID (Field 2) is the Set ID associated with this EIGR entry. A particular EIGR entry is activated in an analysis using the METHOD = SID entry in the Case Control Section. If the Set ID on the METHOD and EIGR match, the eigenvalues will be extracted using the method referenced on that entry.

The METHOD Entry (Field 3) selects the eigenvalue method from the following list:

1. INV   Inverse Power
2. SINV   Sturm Modified Inverse Power
3. GIV   Givens Method
4. HOU   Householder Method
5. MGIV   Modified Givens Method
6. MHOU   Modified Householder Method
7. AGIV   Automatic Givens Method
8. AHOU   Automatic Householder

The F1 Entry (Field 4) is used to specify the lowest frequency of interest in the eigenvalue extraction.

The F2 Entry (Field 5) is used to specify the highest frequency of interest in the eigenvalue extraction.

The NE entry (Field 6) is used by the INV method only. It defines the estimated number of roots in the range. A good estimate will result in a more efficient solution.

The ND entry (Field 7) is used to specify the desired number of roots in the range of interest.

The NORM (Field 2 – continuation) entry on the continuation card is used to specify the method of eigenvector normalization. The choices are:

1. MASS   Mass normalization (Default – if used continuation entry not required)
2. MAX   Normalization to maximum A-set component
3. POINT   Normalization to user-defined DOF

The POINT entry (Field 3 – continuation) is used to specify the point of interest from the analysis set for POINT normalization only.

The CID entry (Field 4 – continuation) is used to specify the component of displacement for

There is an interrelationship between the F1, F2, and ND field on the EIGR entry.

Table A-1 EIGR Input Parameters

	When METHOD = INV or SINV	When METHOD = GIV, MGIV, HOU, or MHOU
F1,F2	Frequency range of interest ($\text{Real} \geq 0.0$). F1 must be input. If METHOD = SINV and ND is blank, then F2 must be input.	Frequency range of interest ($\text{Real} \geq 0.0$; F1 < F2. (If ND is blank, F1 and F2 are ignored. If ND is blank, eigenvectors are found whose natural frequencies lie in the range between F1 and F2.
NE	Estimate of number of roots in range (Required for METHOD = "INV" (Integer > 0). Not used by SINV method.	Not used.
ND	Desired number of roots (Default is 3*NE, INV only) (Integer > 0). If this field is blank and METHOD = SINV, then all roots between F1 and F2 are searched and the limit is 600 roots.	Desired number of eigenvectors (Integer ≥ 0). If ND is zero, the number of eigenvectors is determined from F1 and F2 (Default = 0). If all three are blank, then ND is automatically set to one more than the number of degrees-of-freedom listed on SUPORT entries.

The rules for METHOD = GIV, HOU, MGIV, MHOU, AGIV and AHOU are identical. If any of these methods are selected, MSC.Nastran will find all of the eigenvalues but will compute only the eigenvectors specified by F1 and F2 or those specified by ND (the "desired" number). F1 and F2 specify the lower and upper bounds of the frequency range in which eigenvectors are computed, and ND specifies the number of eigenvectors, starting with the lowest (or the first rigid body mode, if present). If F1, F2, and ND entries are present, ND takes precedence. Note that the default for F1 is 0.0.

The following examples demonstrate the use of the EIGR data entry.

1	2	3	4	5	6	7	8	9	10
EIGR	1	AHOU			10				

In the first example (SID = 1), the automatic Householder method is selected with 10 roots requested. Since the default "MASS" eigenvector normalization is requested, no continuation entry is needed.

EIGR	2	AHOU		100.0					+2
+2	MAX								

For the second example (SID = 2), the same method is requested, but all the roots below 100 cycles per unit time are requested with "MAX" vector normalization.

1	2	3	4	5	6	7	8	9	10
EIGR	3	SINV	0.0	100.0		6			+3
+3	POINT	32	4						

For the third example (SID = 3), the inverse iteration method with Sturm sequence checks is requested for the first six roots in the range specified. The POINT normalization is requested for grid point 32 in the R1 direction.

If METHOD = SINV, the values of F1, F2, and ND determine both the number of eigenvalues and the eigenvectors that will be computed. These entries also provide hints to help MSC.Nastran find the eigenvalues. F1 and F2 specify the frequency range of interest within which MSC.Nastran will search for modes. MSC.Nastran will attempt to find all of the modes in the range F1, F2 or the number specified by ND, whichever is less. If searching stops because ND modes are found, there is no guarantee that they will be the lowest eigenvalues. Iterative methods only guarantee the solution for modes nearest the shift point. If ND modes are not found in the range of interest, SINV will usually find one mode outside the range F1, F2 (or possibly more) before stopping the search.

The inverse power method is particularly efficient when only a small number of eigenvalues and eigenvectors are wanted. Very often only the lowest mode is of interest. The following example illustrates an EIGR entry which will extract only the lowest nonzero eigenvalue.

EIGR	SID	METHOD	F1	F2	NE	ND			
EIGR	13	INV	0.0	.011	1				

It is assumed in the example that the frequency of the lowest mode is greater than 0.01 cycles per unit time. The program will find one eigenvalue outside the range F1, F2 and stop the search. The eigenvalue found is guaranteed to be the lowest non zero eigenvalue (or a member of the lowest closely spaced cluster of eigenvalues in cases with pathologically close roots) provided that there are no negative eigenvalues and that the SUPORT entry has been used to specify the correct number of zero eigenvalues. The NE entry (field 6) is used only by the INV method.

The fields of the EIGRL entry are designed to select and set parameters for the Lanczos method as well as request diagnostics.

EIGRL	SID	V1	V2	ND	MSGL	VL	MAXSET	SHFSCL	
EIGRL	1	0.1	3.2		10				

The V1 field defines the lower frequency bound, the V2 field defines the upper frequency bound, and the ND field defines the number of eigenvalues and eigenvectors desired in the region. The V1 and V2 are expressed in units of cycles per unit time. Examples of the

results of using explicit or default values for the V1, V2, and ND fields are shown in **Table A-2**. The defaults on the EIGRL entry are designed to provide the minimum number of roots in cases where the input is ambiguous.

Table A-2 Model Outputs from EIGRL Input Options

Case	V1	V2	ND	Number and Type of Roots Found
1	V1	V2	ND	Lowest ND or all in range; whichever is smaller
2	V1	V2		All in range
3	V1		ND	Lowest ND in range [V1, +00]
4	V1			Lowest root in range [V1, +00]
5			ND	Lowest ND roots in [-00, +00]
6				Lowest root
7		V2	ND	Lowest ND roots below V2
8		V2		All below V2

The MSGLVL field of the EIGRL entry is used to control the amount of diagnostic output provided by Lanczos. The default value of 0 produces no diagnostic output. The values 1, 2, or 3 provide more output with the higher values providing increasingly more output. Typically, the default value is sufficient. In some cases, higher diagnostics levels may be in order to help resolve difficulties with special modeling problems.

The MAXSET field is used to control the block size, the number of appropriate eigenvectors computed in the outermost iteration loop. The default value of 7 is recommended for most applications. There may be special cases where a larger value may result in quicker convergence of highly multiple roots or a lower value may result in more efficiency when the structure is lightly coupled. However, the default value has been chosen after reviewing results from a wide range of problem types on several different computer types with the goal of minimizing the sum of CPU and I/O cost.

One common occurrence is for the block size to be reset by MSC.Nastran during the run because there is insufficient memory for a block size of 7. Computational efficiency tends to degrade as the block size decreases. It is, therefore, important to examine the EIGENVALUE ANALYSIS SUMMARY output to determine that the program has sufficient memory to use an efficient block size. A smaller block size may be more efficient when only a few roots are requested. The minimum recommended block size is 2.

The SHFSCL field allows a user-designated shift to be used when all other shifting strategies fail. This entry is only used under special circumstances. However, when used, its value should be set to the expected first natural frequency.

The Lanczos method normalizes the computed eigenvectors using the MASS method. The other normalization methods are not available.

Solution Control For Normal Modes

When used as an independent solution, normal modes analysis is available in SOL 103 of the Structured Solution Sequences and SOL 3 and SOL 63 in the Unstructured Solution Sequences. All eigenvalue extraction methods are available in all of these solutions, with one exception. If the Lanczos method is to be used in SOL 3, Rigid Format Alter RF3D83 must also be included. The Executive Control Section can also contain diagnostic DIAG 16 which will print the iteration information used in the INV or SINV methods.

One of the most important entries in the Case Control Section is the METHOD entry. This entry is required. The Set ID referenced by the METHOD entry refers to the Set ID of an EIGR entry or an EIGRL entry in the Bulk Data.

When a modal extraction is performed, the MSC.Nastran output file contains various diagnostic messages and an Eigenvalue Table. Optional grid and element output are available using standard Case Control output requests. These requests are summarized in Table A-3.

Table A-3 Eigenvalue Extraction Output Requests

Grid Output	
DISPLACEMENT (or VECTOR)	Requests the eigenvector (mode shape) for a set of grid points
GPFORCE	Requests the Grid Point Force Balance Table to be computed for each mode
GPSTRESS	Requests grid point stresses to be computed for a set of grid points. This request must be accompanied by the ELSTRESS Case Control request and the definition of Stress Surfaces and/or Stress Volumes in the OUTPUT(POST) section of the Case Control. This request also requires the use of Rigid Format Alter RF3D81 when used in SOL 3.
SPCFORCE	Requests Forces of Single Point Constraint to be computed for a set of grid points for each mode.
Element Output	
ELSTRESS (or STRESS)	Requests the computation of modal stresses for a set of elements for each mode
ESE	Requests the computation of modal element strain energies for a set of elements for each mode
ELFORCE (or FORCE)	Requests the computation of modal element forces for a set of elements for each mode
STRAIN	Requests the computation of the modal element strains for a set of elements
MODES	A special Case Control request which permits selective output requests to be processed on selective modes

In addition to Bulk Data entries required to define the structural model, the only required Bulk Data entry is the eigenvalue selection entry, EIGR or EIGRL. The EIGR entry is used to select the modal extraction parameters for the Givens, Householder, Modified Givens, Modified Householder, Automatic Givens, and Automatic Householder methods. The EIGRL entry is used to select the modal extraction parameters for the Lanczos method.

B

SSSALTER Library For MSC.Nastran

- Overview

- SSSALTER Library for MSC.Nastran Version 69.1

- Alter to Perform Rigid Body Checks, Kinetic Energy Calculation, and Modal Effective Weight Calculation

- References

B.1   Overview

The most current (MSC.Nastran V69.1) SSSALTER filenames and their full descriptions are maintained on the MSC.Software Corporate Web page at

http://www.mscsoftware.com

The SSSALTER files are delivered with MSC.Nastran on the MSC.Nastran delivery media. MSC.Nastran clients may also request specific SSSALTERs from their authorized MSC representative.

B.2   SSSALTER Library for MSC.Nastran Version 69.1

Attached is a brief description of each DMAP delivered with the SSSALTER library in Version 69.1, some of which may be of interest to dynamics engineers.

Each of the DMAP alters was tested for a number of possible applications, but they have not undergone the extensive testing required to be included in MSC.Nastran. It is possible that your application may use a path through the DMAP alter that was not tested, so always review your results carefully. Unlike the RFALTER directory, these DMAP alters were developed independently and it is likely that a conflict will occur if more than one alter is used in a run.

addstata.v691

Adds a static solution onto a transient solution. This is often necessary for structures that have an existing (constant) static loading in addition to the transient load.

alter1ga.v691, alter2ga.v691, alter9ga.v691

These DMAP alters are used to create a reduced model of a component using the Craig-Bampton method of component modal synthesis. A special feature of these files is that they create output transformation matrices (OTM) for displacements, forces, and stresses. They also allow for assembly plots that include a skeleton for the component. This skeleton is based on grid points selected during the processing of the component. The DMAP alters are:

alter1g.v691 (SOL 103) – Creates reduced models (often referred to as Craig-Bampton models) of components using superelements. Includes creation of transformation matrices for output quantities.

alter2g.v691 (SOL 103) – Reads the matrices created by alter1g into MSC.Nastran and stores them as a superelement.

alter9ga.v691 (SOLs 111 and 112) – Calculates the boundary forces for a superelement and calculates the results using transformation matrices (includes sebloada.v691).

appenda.v691

Appends eigenvalue solutions.

checka.v691

Performs mass and stiffness checks in preparation for analysis. Calculates assembly weight when using superelements. In modal solutions, calculates modal effective weight and kinetic energy. If superelements are used, provides the total fractions of effective weight and kinetic energy for each superelement and assembly. Will force Lanczos method to treat a SUPORT entry like the other eigenvalue solution methods.

cova.v691

Computes the variance and standard deviation in response given the user-specified variance in design variables. Calculations are performed by postprocessing design sensitivity results. The following is computed:

$$COVR = S_{(t)} \cdot COVD \cdot S$$

where:

COVR = Response variance

S = Sensitivity coefficient matrix

COVD = Design variable variance

cygyroa.v691

Adds gyroscopic terms to cyclic symmetry analyses.

ddama.v691

Performs dynamic analysis of shipboard equipment using the dynamic design analysis method (DDAM) for response spectra analysis.

delmodea.v691

Allows the user to delete individual modes from the set of system (residual) level modes.

dmigtrna.v691

Transforms the DMIG matrix selected by the K2GG Case Control command from the coordinate system listed on PARAM,XCID to the basic coordinate system. It will then punch this transformed DMIG matrix into the punch file.

dtranra.v691

Allows NOAP restarts in the Structured Solution Sequences.

evdsa.v691, evds103a.v691, evds200a.v691

Computes eigenvector derivatives in design sensitivity analysis.

gdrlana.v691

Incorporates Lanczos into GDR in order to replace the inverse iteration method (IIM).

genela.v691

Calculates the forces resulting from a GENEL element in SOL 112.

glforcea.v691

Calculates superelement interface loads.

iter101.v691, iter106.v691, iter108.v691, iter111.v691, iter24.v691, iter26.v691, iter30.v691, iter66.v691

Use the iterative solver instead of the direct solver in SOL 101, 106, 108, 111, 24, 26, 30, and 66, respectively.

lmt01.v691, lmt03.v691, lmt07.v691, lmt08.v691, lmt09.v691, lmt10.v691, lmt11.v691, lmt12.v691

Use the Lagrange Multiplier technique instead of the conventional method for SOL 101, 103, 107, 108, 109, 110, 111, and 112.

loop8a.v691

Allows for different FREQ requests in separate subcases in direct frequency response.

mfreqea.v691

Calculates the contribution of each mode to the strain energy. These values will help identify which modes contribute to the solution.

mica.v691

Allows the use of initial conditions in a modal transient analysis. This DMAP alter imposes user-specified displacement and velocity initial conditions in a modal transient solution. In order to get a match on the initial conditions, the DMAP appends one or two vectors onto the modes. These vectors represent the amount of the initial conditions which the modes are not capable of representing. (They are automatically orthogonalized to the modes.)

modevala.v691

Determines if the modes obtained are capable of representing the solution to a set of applied loadings. A common practice in modal solutions is to assume that if the modes are capable of representing the static solution to an applied loading, they contain sufficient information to represent the high frequency response of the structure to a dynamic application of the loading. This DMAP alter provides that information without having to perform a dynamic solution.

mtacca.v691

Allows use of modal transient analysis to solve for a structure which has non-zero initial accelerations. This DMAP alter assumes that the initial condition is a steady-state acceleration based on the initial loading. The alter performs a static solution (in modal coordinates) to the initial loading, subtracts the initial loading from all applied loadings, solves the transient analysis, then adds the initial static solution to the results.

mtranea.v691

To calculate the contribution of each mode to the strain energy and kinetic energy of the solution. These values will help identify which modes contribute to the solution.

mtranra.v691

Allows NOAP restarts in the Structured Solution Sequences (SOL 112).

nlgyroa.v691

Adds gyroscopic terms to nonlinear analysis.

norma.v691

Normalizes the output eigenvectors to a maximum of 1.0.

norma.v691

Normalizes the output eigenvectors to a maximum of 1.0.

If a reduction method is used, the eigenvectors are scaled based on the reduced solution set. This DMAP alter scales the eigenvectors based on the largest value in the g-set (excluding the q-set) being set to 1.0.

ortx7a.v691, ortx10a.v691

Scale comlex eigenvectors to produce unit generalized mass matrix.

pchdispa.v691

Creates DMIG entries containing the solution from a static run.

postmaca.v691

Computes the cross-orthogonality between test modes and modes of an MSC.Nastran model.

Two cross-orthogonality checks are made: modal assurance criterion (MAC) and mass orthogonality (ORTHOA).

premaca.v691

Computes the cross-orthogonality between modes of a full model and modes of a reduced model. Three cross-orthogonality checks are made: modal assurance criterion (MAC) and two types of mass orthogonality (ORTHOA and CHECKIT).

propa.v691, propf.for (a FORTRAN program)

Provides the propeller aerodynamic coefficients and wing/nacelle aerodynamic interference loads for aircraft flutter analysis.

raleigh.v691

Includes raleigh damping in SOL 108.

resflexa.v691

Appends static residual vectors onto the eigenvectors in dynamic solutions for improved accuracy. It works at the superelement and the system level. Similar to the mode-acceleration and residual flexibility methods.

rflag.v691

Uses the Lagrange Multiplier technique instead of the conventional method. It incorporates features in lmt01, lmt03, lmt07, lmt08, lmt09, lmt10, lmt11, and lmt12.

rflagb.v691

Uses the Lagrange Multiplier technique for enforced motion, but all other constraints are processed by conventional constraint variable elimination techniques.

ridgyroa.v691

Adds gyroscopic terms to dynamic analysis using the structured solution sequences. These solution sequences include direct and modal frequency response, direct and modal transient response, and direct and modal complex eigenvalue analyses. The alter does not support real eigenvalue analysis.

sebloada.v691

Calculates dynamic superelement interface loads.

sedampa.v691

Allows modal damping on superelement component modes.

segyroa.v691

Adds gyroscopic terms to superelement analysis.

solchk.v691, dcchk.v691, dfchk.v691, dtchk.v691, mfchk.v691, mcchk.v691, mochk.v691, mtchk.v691, sechk.v691

This alter extends the same theory for load epsilon checks long used in static analysis to dynamic analysis. The load residual

$$R \ = \ P - K \cdot DISP - B \cdot VELO - M \cdot ACCEL$$

is computed. The load epsilon EPSM is computed for the first ten solutions.

spc101a.v691

Organizes the calculated SPCForces by the type of constraint placed upon a DOF; e.g., was it a user-induced constraint such as the PS field on the GRID or an SPC card, or was it a DOF constrained by the AUTOSPC function. User has further option of breaking the user-induced constraints into those DOF constrained by the GRID PS field and those on an SPC set. Answers may be independently filtered to remove smaller SPCForces from the printouts. Resultant vectors for SPCForce contributions are also calculated.

spc24a.v691

Organizes the calculated SPCForces by the type of constraint placed upon a DOF; e.g., whether it was a user-induced constraint such as the PS field on the GRID or an SPC card, or whether it was a DOF constrained by the AUTOSPC function. The user has the further option of breaking the user-induced constraints into those DOF constrained by the GRID

PS field and those on an SPC set. Answers may be independently filtered to remove smaller SPCForces from the printouts. Resultant vectors for SPCForce contributions are also calculated.

zfreq.v691

Allows for modeling of frequency-dependent springs and dampers and multiple subcases calling out different FREQi entries in modal frequency response analysis.

B.3   Alter to Perform Rigid Body Checks, Kinetic Energy Calculation, and Modal Effective Weight Calculation

checka.v691

Performs mass and stiffness checks in preparation for analysis. Calculates assembly weight when using superelements. In modal solutions, calculates modal effective weight and kinetic energy. If superelements are used, provides the total fractions of effective weight and kinetic energy for each superelement and assembly. Will force Lanczos method to treat a SUPORT entry like the other eigenvalue solution methods.

SOL 101, 103 (possibly others).

Input

Executive Control

Include 'checka.v691'.

The following parameters affect the operation of this DMAP alter:

GRDPNT (Default = -1). Used by grid point weight generator. This DMAP also uses this grid point for assembly grid point weight generator and as the reference location for rigid-body checks.

CHKSTIF (Default = 1). A positive value causes the DMAP to perform checks on the stiffness as follows:

1 = check KGG, KNN, and KAA.
2 = check KGG and KNN.
3 = check KGG only.

The DMAP performs rigid-body checks on the stiffness matrices by generating geometric rigid-body vectors about GRDPNT and multiplying the stiffness matrix by the vectors.

CHECKTOL (Default = 1.e-05) – Acceptable tolerance on stiffness matrix checks. If the strain energy for all checks of a stiffness matrix is less than this value, a message is printed stating so. If not, then the strain energy and the resulting (normalized) reactions are printed.

CHKMASS (Default = 1) – Similar to CHKSTIF only for the mass matrices. Allows verification that no mass was removed during processing.

KEPRT (Default = 1) – Applicable only in modal solutions. A positive value of this parameter results in the calculation of kinetic energy fractions for the modes (assuming that modes are normalized to unit mass).

EFWGT (Default = 2) – Applicable only in modal solutions. A positive value results in the calculation of the modal effective mass for each mode (once again, assuming modes are normalized to unit mass).

1 = calculates the effective weight and print for each mode.
2 = calculates the effective weight and fraction of the total for each mode and prints the fraction (requires CHKMASSu0).

LANSUP (default = 1) – forces Lanczos method to treat a SUPORT entry in the same manner as the other eigenvalue solution methods.

1 = Lanczos will treat a SUPORT like the other methods
< >1 = > No change from the current way Lanczos handles a SUPORT

Various matrices representing the calculated quantities.

The alter does what is requested by the user. That is, if kinetic energy is requested in a static solution, the DMAP is not smart enough to realize that the solution is static. Therefore, it calculates and prints an incorrect quantity using the static vectors.

check1.dat (SOL 103) – Run to perform stiffness and mass checks plus effective weight and kinetic energy calculations.

B.4 References

JPL, "MSC.Nastran Model Checkout," 1986 MSC World Users' Conference Proceedings, Paper No. 9, March 1986.

T. Rose, "Using Superelements to Identify the Dynamic Properties of a Structure," 1988 MSC World Users' Conference Proceedings, Vol. 1, Paper No. 41, March 1988.

Set Notations

■ Degree-of-Freedom Sets

■ Multipoint Constraints

■ Single Point Constraints

■ Rigid Body Supports

■ Sets for Dynamic Reduction

■ Sets for Aerodynamics

■ Rules of Sets for Undefined Degrees-of-Freedom

■ Output Selection via Set Specification

C.1 Degree-of-Freedom Sets

Structural matrices are initially assembled in terms of all structural points, which excludes only the extra points introduced for dynamic analysis. These matrices are generated with six degrees-of-freedom for each geometric grid point and a single degree-of-freedom for each scalar point. These degrees-of-freedom are partitioned into sets, based on user inputs. The sets are used to successively eliminate variables during the solution process, as described in "**General Operations**" on page 303 of the *MSC.Nastran Reference Manual*.

Degree-of-Freedom Set Definitions

Each degree-of-freedom is a member of one mutually exclusive "set". Set names have the following definitions:

Set Name	Meaning
m	degrees-of-freedom eliminated by <u>m</u>ultipoint constraints.
sb*	deegrees-of-freedom eliminated by <u>s</u>ingle-point constraints that are included in <u>b</u>oundary condition changes and by the AUTOSPC feature.
sg*	degrees-of-freedom eliminated by <u>s</u>ingle-point constraints that are specified on the PS field on <u>G</u>RID Bulk Data entries.
o	degrees-of-freedom <u>o</u>mitted by structural matrix partitioning.
q	generalized degrees-of-freedom for dynamic reduction or component mode synthesis.
r	<u>r</u>eference degrees-of-freedom used to determine free body motion.
c	degrees-of-freedom which are free during component mode synthesis or dynamic reduction.
b	degrees-of-freedom fixed for component mode analysis or dynamic reduction.
e	<u>e</u>xtra degrees-of-freedom introduced in dynamic analysis.
sa	permanently constrained aerodynamic degrees-of-freedom.
k	aerodynamic degrees-of-freedom.

* Strictly speaking, sb and sg are not exclusive with respect to one another. Degrees-of-freedom may exist in both sets simultaneously. Since these sets are not used explicitly in the solution sequences, this need not concern the user. However, those who use these sets in their own DMAPs should avoid redundant specifications when using these sets for partitioning or merging operations. That is, a degree-of-freedom should not be specified on both a PS field of a GRID entry (sg set) and on a selected SPC entry (sb set). Redundant specifications will cause UFM 2120 in the VEC module and behavior listed in the *MSC.Nastran 2001 DMAP Programmer's Guide* for the UPARTN module. These sets are exclusive, however, from other mutually exclusive sets.

Each degree-of-freedom is also a member of one or more combined sets called "supersets." Supersets have the following definitions:
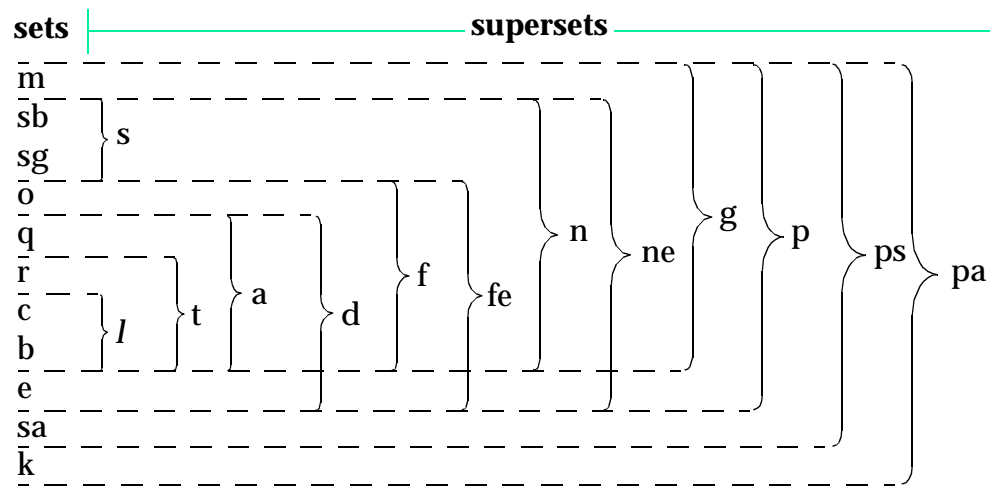
Set Name	Meaning (+ Indicates Union of Two Sets)
$s = sb + sg$	All degrees-of-freedom eliminated by single-point constraints.
$l = b + c$	The structural coordinates remaining after the reference coordinates are removed (degrees-of-freedom left over).
$t = l + r$	The <u>t</u>otal set of physical boundary degrees-of-freedom for superelements.
$a = t + q$	The set <u>a</u>ssembled in superelement analysis.
$d = a + e$	The set used in dynamic analysis by the <u>d</u>irect method.
$f = a + o$	Unconstrained (<u>f</u>ree) structural degrees-of-freedom.
$fe = f + e$	Free structural degrees-of-freedom plus extra degrees-of-freedom.
$n = f + s$	All structural degrees-of-freedom <u>n</u>ot constrained by multipoint constraints.
$ne = n + e$	All structural degrees-of-freedom <u>n</u>ot constrained by multipoint constraints plus <u>e</u>xtra degrees-of-freedom.
$g = n + m$	All structural (<u>g</u>rid) degrees-of-freedom including scalar degrees-of-freedom.
$p = g + e$	All <u>p</u>hysical degrees-of-freedom.
$ps = p + sa$	Physical and constrained aerodynamic degrees-of-freedom.
$pa = ps + k$	<u>P</u>hysical set for <u>a</u>erodynamics.
$fr = o + l$	Statically independent set minus the statically determinate supports $(fr = \underline{f} - q - \underline{r})$.
$v = o + c + r$	The set free to <u>v</u>ibrate in dynamic reduction and component mode

The a-set and o-set are created in the following ways:

1. If only OMITi entries are present, then the o-set consists of degrees-of-freedom listed explicitly on OMITi entries. The remaining f-set degrees-of-freedom are placed in the b-set which is a subset of the a-set.

2. If ASETi or QSETi entries are present, then the a-set consists of all degrees-of-freedom listed on ASETi entries and any entries listing its subsets, such as QSETi, SUPORTi, CSETi, and BSETi entries. Any OMITi entries are redundant. The remaining f-set degrees-of-freedom are placed in the o-set.

3. If there are no ASETi, QSETi, or OMITi entries present but there are SUPORTi, BSETi, or CSETi entries present then the entire f-set is placed in the a-set and the o-set is not created.

4. There must be at least one explicity ASETi, QSETi, or OMITi entry for the o-set to exist, even if the ASETi, QSETi, or OMITi entry is redundant.

In dynamic analysis, additional vector sets are obtained by a modal transformation derived from real eigenvalue analysis of the a-set. These sets are as follows:

ξ_o = rigid body (zero frequency) modal degrees-of-freedom

ξ_f = finite frequency modal degrees-of-freedom

ξ_i = $\xi_o + \xi_f$, the set of all modal degrees-of-freedom

One vector set is defined that combines physical and modal degrees-of-freedom:

u_h = $\xi_i + u_e$, the set of all modal degrees-of-freedom

The membership of each degree of freedom can be printed by use of the Bulk Data entries PARAM,USETPRT and PARAM,USETSEL.

Degree of Freedom Set Bulk Data Entries

Degrees-of-freedom are placed in sets as specified by the user on the following Bulk Data entries:

Name	Bulk Data Entry Name
m	MPC, MPCADD, MPCAX, POlNTAX, RBAR, RBE1, RBE2, RBE3, RROD, RSPLINE, RTRPLT, GMBC, GMSPC*
sb	SPC, SPC1, SPCADD, SPCAX, FLSYM, GMSPC*, BNDGRID, (PARAM,AUTOSPC,YES)
sg	GRID, GRIDB, GRDSET (PS field)
o	OMIT, OMIT1, OMlTAX, GRID (SEID field), SESET
q	QSET,QSET1
r	SUPORT, SUPORT1, SUPAX
c	CSET,CSET1
b	BSET, BSET1
e	EPOINT
sa	CAEROi
k	CAEROi
a	ASET, ASET1, Superelement exterior degrees-of-freedom, CSUPEXT

* Placed in set only if constraints are not specified in the basic coordinate system.

In superelement analysis, the appropriate entry names are preceded by the letters SE, and have a field reserved for the superelement identification number. This identification is used because a boundary (exterior) grid point may be in one mutually exclusive set in one superelement and in a different set in the adjoining superelement. The SE-type entries are internally translated to the following types of entry for the referenced superelement:

Entry Type	Equivalent Type
SEQSETi	QSETi
SESUP	SUPORT
SECSETi	CSETi
SEBSETi	BSETi

C.2   Multipoint Constraints

Each multipoint constraint is described by a single equation that specifies a linear relationship for two or more degrees-of-freedom. In static analysis, multiple sets of multipoint constraints can be provided in the Bulk Data Section, with selections made at execution time by using the subcase structure in Case Control as explained in "**Case Control Section**" on page 9 of the *MSC.Nastran Reference Manual*. Multipoint constraints are also discussed in Sections 3.5.1 of the *MSC.Nastran Reference Manual* and Section 5.4 of *The NASTRAN Theoretical Manual*.

Multipoint constraints are defined on MPC, MPCADD, and MPCAX entries. MPC is the basic entry for defining multipoint constraints. The first component specified on the entry is the dependent degree-of-freedom, i.e., that degree-of-freedom that is removed from the equations of motion. Dependent degrees-of-freedom may appear as independent terms in other equations of the set; however, they may appear as dependent terms in only a single equation. The MPCADD entry defines a union of multipoint constraints. The MPCAX defines multipoint constraints in conical shell problems. Some uses of multipoint constraints are:

- To describe rigid elements and mechanisms such as levers, pulleys, and gear trains. In this application, the degrees-of-freedom associated with the rigid element that are in excess of those needed to describe rigid body motion are eliminated with multipoint constraint equations. Treating very stiff members as rigid elements eliminates the ill-conditioning associated with their treatment as ordinary elastic elements.

- To enforce zero motion in directions other than those corresponding with components of the global coordinate system. In this case, the multipoint constraint will involve only the degrees-of-freedom at a single grid point. The constraint equation relates the displacement in the direction of zero motion to the displacement components in the global system at the grid point.

- To be used with scalar elements to generate nonstandard structural elements and other special effects.

- To describe parts of a structure by local vibration modes. This application is treated in Section 14.1 of *The NASTRAN Theoretical Manual*. The general idea is that the matrix of local eigenvectors represents a set of constraints relating physical coordinates to modal coordinates.

In general, the user must provide the coefficients in the multipoint constraint equations. However, several rigid elements have been introduced which will generate the MPC equations for some applications:

RROD   A pin-ended rod which is rigid in extension.

RBAR   A rigid bending element with six degrees-of-freedom at each end.

RTRPLT   A rigid triangular plate with six degrees-of-freedom at each vertex.

RBE1	A rigid body connected to an arbitrary number of grid points. The independent and dependent degrees-of-freedom can be arbitrarily selected by the user.
RBE2	A rigid body connected to an arbitrary number of grid points. The independent degrees-of-freedom are the six components of motion at a single grid point. The dependent degrees-of-freedom are specified at an arbitrary number of grid points.
RBE3	Defines the motion at a reference grid point as the weighted average of the motions at a set of other grid points.
RSPLINE	Defines multipoint constraints for the interpolation of displacements at grid points.

The rigid elements will always meet equilibrium and continuity requirements, whereas this is a user responsibility for MPC equations.

Multipoint forces of constraint may be output with MPCFORCE Case Control command in SOLution Sequences 101 through 200.

C.3 Single Point Constraints

A single point constraint (SPC) applies a fixed value to a translational or rotational component at a geometric grid point or to a scalar point. Common uses of single point constraints are to specify the boundary conditions of a structural model by fixing the appropriate degrees-of-freedom and to eliminate unwanted degrees-of-freedom with zero stiffness. Multiple sets of single point constraints can be provided in the Bulk Data Section, with selections made at execution time by using the subcase structure in the Case Control Section as explained in "**Case Control Section**" on page 9 of the *MSC.Nastran Reference Manual*. This procedure is particularly useful in the solution of problems having one or more planes of symmetry.

The elements connected to a grid point may not provide resistance to motion in certain directions, causing the stiffness matrix to be singular. Single point constraints are used to remove these degrees-of-freedom from the stiffness matrix. A typical example is a planar structure composed of membrane and extensional elements. The translations normal to the plane and all three rotational degrees-of-freedom must be constrained since the corresponding stiffness matrix terms are all zero. If a grid point has a direction of zero stiffness, the single point constraint needs not be exactly in that direction, but only needs to have a component in that direction. This allows the use of single point constraints for the removal of such singularities regardless of the orientation of the global coordinate system. Although the displacements will depend on the direction of the constraint, the internal forces will be unaffected.

One of the tasks performed by the Grid Point Singularity Processor (GPSP) is to examine the stiffness matrix for singularities at the grid point level. Singularities remaining at this level, following the application of the multipoint and single point constraints, are listed in the Grid Point Singularity Table (GPST), which is automatically printed. The GPST lists all singular degrees-of-freedom, in the global coordinate system, and the ratio of stiffness between the softest and stiffest degree-of-freedom for the grid point. The user may request that single point constraints be generated for all identified singularities by use of the Bulk Data entry PARAM,AUTOSPC,YES.

Single point constraints are defined on SPC, SPC1, SPCADD and SPCAX entries. The SPC entry is the most general way of specifying single point constraints. The SPC1 entry is a less general entry that is more convenient when several grid points have the same components constrained to a zero displacement. The SPCADD entry defines a union of single point constraint sets specified with SPC or SPC1 entries. The SPCAX entry is used only for specifying single point constraints in problems using conical shell elements.

Single point constraints can also be defined on the GRID entry. In this case, however, the points are constrained for all subcases. The default value for enforced displacement on points constrained on GRID entries is zero. The default value can be overridden at the subcase level with SPC entries.

The printed output for single point forces of constraints can be requested in Case Control. All nonzero forces are printed, whether they originate from SPCi entries, the PS field on GRID entries, or by PARAM,AUTOSPC,YES.

C.4 Rigid Body Supports

In the following discussion, a free body is defined as a structure that is capable of motion without internal stress; i.e., it has one or more rigid body degrees-of-freedom. The stiffness matrix for a free body is singular with the defect equal to the number of stress-free, or rigid body modes. A solid three-dimensional body has up to six rigid body modes. Linkages and mechanisms can have a greater number. In order to permit the analysis of mechanisms, no restriction is placed in the program on the number of stress-free modes.

Free-body supports are defined with a SUPORT or SUPORT1 entry. In the case of problems using conical shell elements, the SUPAX entry is used. Free-body supports must be defined in the global coordinate system. The SUPORT1 entry must be selected by the SUPORT1 Case Control command.

In static analysis by the displacement method, the rigid body modes must be restrained in order to remove the singularity of the stiffness matrix. The required constraints may be supplied with single point constraints, multipoint constraints, or free body supports. If free body supports are used, the rigid body characteristics will be calculated and a check will be made on the sufficiency of the supports. Such a check is obtained by calculating the rigid body error ratio and the strain energy as defined in the Rigid Body Matrix Generator operation. This error ratio and the strain energy are automatically printed following the execution of the Rigid Body Matrix Generator. The error ratio and the strain energy should be zero, but may be nonzero for any of the following reasons:

- Round-off error accumulation.
- Insufficient free body supports have been provided.
- Redundant free body supports have been provided.

The redundancy of the supports may be caused by improper use of the free body supports themselves or by the presence of single point or multipoint constraints that constrain the rigid body motions.

Static analysis with inertia relief is necessarily made on a model having at least one rigid body motion. Such rigid body motion must be constrained by the use of free body supports. These supported degrees-of-freedom define a reference system, and the elastic displacements are calculated relative to the motion of the support points. The element stresses and forces will be independent of any valid set of supports.

Rigid body vibration modes are calculated by a separate procedure provided that a set of free body supports is supplied by the user. This is done to improve efficiency and, in some cases, reliability. The determinant method, for example, has difficulty extracting zero frequency roots of high multiplicity, whereas the alternate procedure of extracting rigid body modes is both efficient and reliable. If the user does not specify free body supports (or he specifies an insufficient number of them), the (remaining) rigid body modes will be calculated by the method selected for the finite frequency modes, provided zero frequency is included in the range of interest. If the user does not provide free body supports, and if zero frequency is not included in the range of interest, the rigid body modes will not be calculated.

Free body supports must be specified if the mode acceleration method of solution improvement is used for dynamic problems having rigid body degrees-of-freedom (see "**Rigid-body Modes**" on page 87 of the *MSC.Nastran Basic Dynamic Analysis User's Guide*). This solution improvement technique involves a static solution, and although the dynamic solution can be made on a free body, the static solution cannot be performed without removing the singularities in the stiffness matrix associated with the rigid body motions.

C.5 Sets for Dynamic Reduction

There are several methods for reducing the size of models in dynamic analysis. The method described here uses shpaes derived as generalized functions by static analysis. The same entries may be used in static analysis with the same nomenclature being used internally as in superelement analysis.

The statically independent degrees-of-freedom remaining after constraint elimination are partitioned into two sets. The partitions are defined by listing the degrees-of-freedom for one of the partitions on the ASETi entries. These degrees-of-freedom are referred to as the analysis set. The remaining degrees-of-freedom in the omitted set with the remaining degrees-of-freedom being placed in the analysis set. This is easier if the analysis set is large. In the case of problems using conical shell elements, the OMITAX entry is used.

On of the more important applications of partitioning is Guyan reduction, described in "**Overview**" on page 290 of the *MSC.Nastran Basic Dynamic Analysis User's Guide*. This technique is a means for reducing the number of degrees-of-freedom used in dynamic analysis with minimum loss of accuracy. Its basis is that many fewer grid points are needed to describe the inertia of a structure than are needed to describe it elasticity with comparable accuracy. The error in the approximation is small provided that the set of displacements used for dynamic analysis is judiciously chosen. Its members should be uniformly dispersed throughout the structure, and all large mass items should be connected to grid points that are members of the analysis set.

The use is cautioned to consider the fact that the matrix operations associated with this partitioning procedure tend to create nonzero terms and to fill what were previously very sparse matrices. The partitioning option is most effectively used if the members of the omitted set are either a very large fraction or a very small fraction of the total set. In most of the applications, the omitted set is a large fraction of the total and the matrices used for analysis, while small, are usually full. If the analysis set is not a small fraction of the total, a solution using the large, but sparser, matrices may be more efficient.

The a-set is further partitioned into the q-, r-, c-, and b-sets. The q-set is used to store the coefficients for the generalized coordinates determined by dynamic reduction and/or component mode calculations. The r-set is again used to determine rigid body modes. The c-set contains coordinates considered free to move while computing the generalized coordinate functions. The b-set contains coordinates fixed during this process.

The set used to describe the generalized functions for dynamic reduction and component mode synthesis is the v-set, the union of the o-, r-, and c-sets.

The d-set (dynamic) for direct formulations is formed from the union of the structural degrees-of-freedom in the a-set and the extra points of the e-set. The d-set can be used to input unsymmetric terms into the equations of motion using DMIG and TF Bulk Data entries. In the modal formulations, the h-set is composed of the union of the ξ_i (modal set and the e-set. Again, the DMIG and TF Bulk Data entries are a means to introduce unsymmetric matrix coefficients.

C.6   Sets for Aerodynamics

Aerodynamic calculations are made in a Cartesian aerodynamic coordinate system. By convention, the flow is in the positive x direction. The basic coordinate system was not chosen, since it would place an undesirable restriction upon the description of the structural model. Any MSC.Nastran Cartesian system may be specified, and flow will be defined in the direction of its positive x-axis. All element and aerodynamic grid point data, computed initially in the basic coordinate system, will be converted to the aerodynamic coordinate system. The global (displacement) coordinate system of the aerodynamic grid points will have its T1 direction in the flow direction. T3 is normal to the element for boxes, and parallel to the aerodynamic T3 in the case of bodies. Coordinate system data are generated for the aerodynamic grid points.

The grid points are physically located at the centers of the boxes and body elements. Permanent constraints are generated for the unused degrees-of-freedom. A second set of grid points, used only for undeformed plotting, is located at the element corners. All six degrees-of-freedom associated with each grid point in this second set are permanently constrained. Grid point numbers are generated based upon the element identification number. For any panel, the external grid point numbers for the boxes start with the panel identification number and increase consecutively.

Aerodynamic degrees-of-freedom, along with the extra points, are added after the structural matrices and modes have been determined. This introduces the following displacement sets:

k	Aerodynamic box and body degrees-of-freedom
sa	Permanently constrained degrees-of-freedom associated with aerodynamic grid points
ps	Union of the p-set (physical) and the sa-set
pa	Union of k-set and ps-set (physical and aerodynamic)

C.7 Rules of Sets for Undefined Degrees-of-Freedom

Most of the Bulk Data entries used to list set membership specify mutually exclusive sets. This means that degrees-of-freedom listed on more than one such entry will result in a fatal error. For example, a degree-of-freedom may not be in the m-set on two RBAR entries, or on a selected SPC entry and a SUPORT entry.

The a-set, by contrast, defines a combined set. Degrees-of-freedom listed on Bulk Data entries that define its subsets, the q-, r-, c-, and b-set, may also be listed on ASETi Bulk Data entries, although this is a redundant specification and is not necessary. However, automatic restarts are more reliable if ASETi entries are present for all degrees-of-freedom listed on SUPORT entries.

Bulk Data entries used to define mutually exclusive sets automatically place them in their specified set and any combined set to which they belong. Since the ASETi entries define a combined set, the subsets of the a-set, if not defined, must be placed in a mutually exclusive set by an arbitrary convention. The conventions described below are used because they allow the user to specify these sets with the minimum input for most cases. In superelement analysis, exterior (boundary) degrees-of-freedom are automatically determined and placed in the a-set of the superelement. Exterior degrees-of-freedom for superelements are therefore equivalent to degrees-of-freedom listed on ASETi entries in the discussion below.

The f-set is the union of the mutually exclusive o-, q-, r-, c-, and b-sets and includes the a-set. The o-set exists under two conditions only:

1. If OMITi entries are present, the o-set consists of degrees-of-freedom listed explicitly on OMlTi entries. The remaining f-set degrees-of-freedom are placed in the b-set. They are then also members of the a-set.

2. If ASETi or QSETi entries are present, the a-set consists of all degrees-of-freedom listed on ASETi entries and any entries listing its subsets, such as QSETi, SUPORTi, CSETi, and BSETi entries. The remaining f-set degrees-of-freedom are placed in the o-set. Note, however, there must be at least one explicit ASETi or QSETi entry type present for the o-set to exist, even if it is a redundant specification. If there are no ASETi or QSETi entries present, and SUPORT, BSETi, or CSETi are present, the entire f-set is placed in the a-set; that is, the o-set is not formed.

If both OMITi and ASETi entries are present, the OMITi entries are ignored, so that condition 2, above, applies. Similarly, if ASETi entries are used in conjunction with entries defining its subsets, undefined degrees-of-freedom in the a-set are placed in mutually exclusive sets as shown in the following table (0 = no entry types present; 1 = entry type present):

Set Defined by Entry Type	Case			
	1	2	3	4
c	0	0	1	1
b	0	1	0	1
Undefined a-set placed in	b	c	b	b

C.8 Output Selection via Set Specification

The membership of grid points and their components and scalar points in the various sets is stored in the USET table as digits in a binary number. Some modules use input parameters that are translations of these binary numbers as a shorthand notation. Three formats are used:

Set Name

(DEFUSET, USET and USET1 Bulk Data entries, MATGPR, UPARTN, VEC, UMERGE, UMERGE1, and PARAML (OP = USET) Modules)

The name of the set from the table below (which may be redefined by the DEFUSET entry).

Decimal Equivalent

(TABPRT, MATMOD (Option 17), and MATGEN (Option 11) Modules)

The decimal equivalent of the set is listed below. Several sets can be described by a single number that is the sum of the listed equivalents. For example, to print the m and s sets, the value of 3(1+2) is input to the TABPRT module. The value of -1 will cause the output of all sets.

Bit Position

(VEC Module)

The location of the digit corresponding to the set in the binary number, starting with the left-most digit, can be used to identify one set, as listed in Table C-1.

Table C-1 USET Table: Set Name, Decimal Equivalent, and Bit Position

Set Name	Decimal Equivalent	Bit Position
U1	--	1
U2	--	2
U3	--	3
U4	--	4
U5	--	5
U6	--	6
V	33554432	7
FR	16777216	8
T	8388608	9
O	4194304	10
B	2097152	11

Set Name	Decimal Equivalent	Bit Position
C	1048576	12
PA	524288	13
K	262144	14
SA	131072	15
PS	65536	16
D	32768	17
FE	16384	18
NE	8192	19
P	4096	20
E	2048	21
SB	1024	22
SG	512	23
L	256	24
A	128	25
F	64	26
N	32	27
G	16	28
R	8	29
O	4	30
S	2	31
M	1	32
H,J,...	--	--

The data block naming convention in the solution sequences for matrices related to the sets is based on the set names. For example, the system stiffness matrix $[K_{gg}]$ has the name KGG. Some sets are used that do not appear in the USET table. The h-set, for example, is the set used for modal formulations. Its size is not known until after the USET table is formed, so it does not appear in the table. The j-set, a set synonymous with the g-set, is used in superelement analysis. There are several other sets used that also do not appear in the USET table.

Some names may be used for other purposes. The name H, for example, may be input to the MATGPR module when one wants to label rows or columns of matrices sequentially, rather than by their external sequence numbers. This feature may be used to number vectors in load matrices or in other instances not related to modal analysis, even though H is defined for modal analysis.

APPENDIX
D

Selected Bibliography

1. Miura, H., *MSC/NASTRAN Handbook for Structural Optimization*, The MacNeal-Schwendler Corporation, 1988.

2. Moore, G.J. *MSC/NASTRAN Design Sensitivity and Optimization User's Guide*, Version 67, The MacNeal-Schwendler Corporation, 1992.

3. Moore, G.J. and Nagendra, G.K., "Dynamic Response Sensitivities in MSC/NASTRAN" Proceedings of the MSC 1991 World User's Conference, Paper No. 4, March 1991.

4. Patel, H., "Multidisciplinary Design with Superelements in MSC/NASTRAN," AIAA CP-92-4732, Fourth AIAA/USAF/NASA/OAI Symposium on Multidisciplinary Analysis and Optimization, Cleveland, Ohio, September1992.

5. Johnson, E.H., and Reymond, M.A., "Multidisciplinary Aeroelastic Analysis and Design using MSC/NASTRAN," AIAA CP-91-1097, 32nd SDM Conference, Baltimore, MD, April 1991.

6. Kodiyalam, S., Vanderplaats, G., Miura, H., Nagendra, G. and Wallerstein, D. "Structural Shape Optimization with MSC/NASTRAN," AIAA CP 90-1007, 31st SDM Conference, Long Beach, CA, April 1990.

7. Johnson, E.H., "Disjoint Design Spaces in the Optimization of Harmonically Excited Structures," AIAA Journal, Vol. 14, No. 2, February 1976, pp 259-261.

8. "Introduction to Version 67 of MSC/NASTRAN," The MacNeal-Schwendler Corporation, September 1991.

9. Cassis, J.H., "Optimum Design of Structures Subjected to Dynamic Loads," PhD.

I N D E X

Damping, 17, 212
    critical, 20
    modal, 19
    nonlinear, 21
    structural, 17, 22
    viscuous, 17, 20, 22
Data recovery, 214
    and superelements, 219
    for modal methods, 215
    improving results, 217
Decoupled response solutions, 131
Deformed plots, 60
Design sensitivity, 195, 205
DIAG 10, 33
Direct matrix input (DMIGs), 23, 24
DoubletLattice method, 83, 194
Downwash, 197
Dynamic analysis
    cost factors, 8

E

EFMASS, 54, 56
Elastic rigid coupling matrix (MER), 56
Enforced acceleration, 97
Enforced motion
    with loads, 87
Excitations, 141
Extra points, 152, 200

F

Fluid
    boundaries, 126
    examples, 123
    loads, 145
Fluidstructure analysis, 101
Flutter, 82, 195
Flutter analysis, 83, 195
    PKmethod, 83
Fourier
    coefficients, 105
    transform methods, 176
    transform, inverse, 204
    transformations, 203
    transforms, 240
Free bodies, 51, 190
Free surfaces, 119
Frequency range, 8
Frequency response, 178, 195
    equations for, 95

G

General dynamic reduction, 66
Generalized aerodynamic matrices, 200
Generalized dynamic reduction, 60, 63, 101
Geometric shape methods, 192
Gravity effects, 122
Grid point weight generator, 44
Grid Point Weight Generator (GPWG), 48
Guyan reduction, 54, 63, 66

H

HARMONICS, 107
Hessenberg method, 148, 152
Hydroelastic modeling, 107
    data processing, 111
    sample, 113
    solution sequences, 110
Hysteresis, 22

I

impedance, 70
Inertia relief, 10, 14, 15, 102, 193, 199, 289
Inertial forces
    and rotating coordinate systems, 74
Inertial loads approach, 89
    input data, 90
    recommendations, 91
Initial conditions, 145
Integration matrix, 197
Interation strategies, 174
Inverse Fourier Transform, 204
Inverse power method, 149, 150
Inverse transformation, 178

K

Flutter analysis
    Kmethod, 201
Kmethod, 201
Kinetic and strain energy, 59